ROCK INHIBITION FOR THE PROMOTION

OF SPINAL CORD REGENERATION

by

CARMEN CHAN

B.Sc., The University of British Columbia, 2000

A THESIS SUBMITTED IN PARTIAL FULFILMENT OF THE REQUIREMENTS FOR
THE DEGREE OF

DOCTOR OF PHILOSOPHY

in

THE FACULTY OF GRADUATE STUDIES

(Neuroscience)

THE UNIVERSITY OF BRITISH COLUMBIA

August 2006

Abstract

Axonal regeneration within the injured spinal cord is hampered by multiple inhibitory molecules in the glial scar and in the surrounding disrupted myelin. Of these the chondroitin sulfate proteoglycans (CSPGs) have an important role in the regeneration failure but its signaling is not fully understood. Therefore, the effects of CSPG on neurite growth were analyzed by growing embryonic chick dorsal root ganglion (DRG) explants on aggrecan (a CSPG of the hyalectan family). Aggrecan aggregate, aggrecan monomer, and hyaluronic acid inhibited neurite growth from nerve growth factor- and neurotrophin-3-responsive DRG neurons. Chondroitinase ABC digestion reversed aggrecan inhibition. ROCK inhibition with Y27632 increased neurite growth on some, although not all of the aggrecan components tested, suggesting that some of them activated the Rho/ROCK pathway.

Many of the inhibitory molecules found in the injured spinal cord activate the Rho pathway, providing a strong rationale to target it following spinal cord injuries (SCI). A dorsal column transection model in rats was used to analyze the efficacy of the ROCK inhibitor, Y27632, in stimulating axonal regeneration. Acute treatment with Y27632 stimulated sprouting of corticospinal tract and dorsal column tract axons, and accelerated functional recovery/compensation. However, lower doses of Y27632 appeared to be detrimental, as low dose-treated animals had decreased axonal regrowth and impaired functional recovery.

Y27632 treatment caused negative side effects potentially by acting on the non-neuronal cells in the injured spinal cord. *In vivo* spinal cord tissue and *in vitro* astrocyte cultures were used to test if ROCK inhibition increased axonal growth inhibition by astrocytes. *In vivo*, Y27632 treatment enhanced the upregulation of GFAP and neurocan after SCI. *In vitro*, the ECM derived from Y27632-treated astrocytes contained higher levels of CSPGs, on which neurite growth from cortical neurons was inhibited. The increased expression of inhibitory CSPGs with Y27632 treatment may contribute to the negative side effects observed in the rat model of SCI.

Results here demonstrate that more basic science research must be done to determine the range of dosage of Y27632 that is safe for use in treating SCI, and to design methods for cell specific targeting of ROCK inhibition.

Table of contents

List of tables

List of figures

List of abbreviations

aFGF	acidic fibroblast growth factor
BDNF	Brain-derived neurotrophic factor
CGN	Cerebellar granule neurons
C-domain	Central domain
ChABC	Chondroitinase ABC
CNS	Central nervous system
CRMP	Collapsin response mediator protein
CSPG	Chondroitin sulfate proteoglycan
CS	Chondroitin sulphate
CSF	Cerebrospinal fluid
CST	Corticospinal tract
DCT	Dorsal column tract
DREZ	Dorsal root entry zone
DRG	Dorsal root ganglion
DS	Dermatan sulphate
E	Embryonic day
EGF	Epidermal growth factor
ERM	ezrin-radixin-moesin
F-actin	Filamentous-actin
FGF	Fibroblast growth factor
GAG	Glycosaminoglycan
GAP	GTPase-activating protein
GAP-43	Growth-associated protein-43
GDNF	Glial cell line-derived neurotrophic factor
GDI	Guanine nucleotide dissociation inhibitor
GEF	Guanine nucleotide exchange factor
GFR	GDNF family receptor
HA	Hyaluronic acid
HS	Heparin sulfate
ECM	Extracellular matrix
GFAP	Glial fibrillary acidic protein
KSPG	Keratin sulfate proteoglycan
INF-γ	Interferon-γ
IL	Interleukin
LARG	Leukemia-associated Rho GEF
LIMK	LIM motif-containing protein kinase
LPA	Lysophosphatidic acid
MAG	Myelin associated glycoprotein
MBS	Myosin-binding subunit
mDia	Mammalian Dia
MLC	Myosin light chain
MP	Myosin phosphatase
MT	Microtubule
NGF	Nerve growth factor

MYPT	Myosin phosphatase target subunit
NGF	Nerve growth factor
NT3	Neurotrophin-3
OEC	Oligodendrocyte ensheathing cell
OMgp	Oligodendrocyte myelin glycoprotein
P-domain	Peripheral domain
PDGF	Platelet-derived growth factor
PDL	Poly-D-lysine
PKC	Protein kinase C
PNS	Peripheral nervous system
RB domain	Rho-binding domain
RGC	Retinal ganglion cell
RGM	Repulsive guidance molecule
Rho	Ras-homologous
ROCK	Rho-associated coiled-coil-containing protein kinase
SCI	Spinal cord injury
TGF	Transforming growth factor
TNF	Tumor necrosis factor
Trk	Tropomyosin-related kinase

Acknowledgements

I am indebted to a lot of people ever since I started my PhD study. I would first like to thank Mom, Dad, and my fiancé Eric, for their unfaltering love and support throughout this endeavour. They are always there for me and constantly shower me with love and encouragement.

I thank my supervisor Wolfram Tetzlaff for giving me the opportunity to pursue my PhD degree in his laboratory, the freedom to follow my interest, and for providing guidance throughout my studies. He awes me with his passion for scientific inquiry, experience and knowledge. I would also like to thank the members of my committee, Vanessa Auld, Timothy O'Conner, Clive Roberts, Calvin Roskelley for their guidance, patience, and constructive criticism. They keep my path to graduation less meandering and more fruitful.

I have been very fortunate to be part of a great group of researchers in the Tetzlaff, Kwon, Ramer, and Steeves laboratories. I am very thankful to all these friends and colleagues including, Jaimie Borisoff, Frederic Bretzner, Kevin Chen, Anthony Choo, Brian Kwon, Rene Lane, Jae Lee, Jie Liu, Victoria MacDermid, Christopher McBride, Loren Oschipok, David Pataky, Jason Plemel, Matthew and Leanne Ramer, Simon Sjovold, Joseph Sparling, Egidio Spinelli, Anthea Stammers, John D. Steeves, David Stirling, Darren Sutherland, John Steeves, Angela Scott, Jeremy Toma, Jackie Vanderluit, Angel Wong, and Robert Xie. I am especially thankful to Clarrie Lam, Ward Plunet, John McGraw, and Lowell McPhail for their endless patience, numerous helpful tips for survival in research and in graduate school, and for being so understanding in my time of frustration and disillusion.

Finally, I want to thank Eric's family, the Lok's. They took me in and treated me as family.

No word or phrase can truly express my gratitude towards all these people.

Dedicated to my parents and my sweetheart Eric

Chapter 1: General introduction

Overview

Spinal cord injury (SCI) results in a range of disabilities that, depending on the type and level of injury, includes permanent paralysis, loss of sensation, and loss of control over critical bodily functions such as temperature and blood pressure regulations. According to the Canadian Paraplegic Association, an estimated number of 1,050 new SCI cases occur per year and approximately 36,000 Canadians live with SCI (figures do not include non-deficit or fatal injuries). These patients retain a lifelong handicap, and a large proportion (~80%) of them is below the age of 30. In addition to physical disabilities, they also suffer from economical losses due to lost income and bear considerable psychosocial strain.

Given the dramatic loss in the quality of life, it is imperative that clinical treatments be developed to repair damage to the spinal cord. At present, the immediate treatment given to SCI patients is targeted at preserving remaining neurological function and preventing secondary cell death. In North America, the corticosteroid, methylprednisolone, is regularly used in clinics to reduce inflammation in acute (< 8 hours) SCI. However, in order to achieve full functional recovery, the injured axons must regrow pass the injury site and back to the vicinity of their respective targets, followed by the re-formation of appropriate synapses and reconnection with targets. Attaining this kind of 'axonal regeneration' is the ultimate goal of spinal cord regeneration research.

Unlike neurons of the peripheral nervous system (PNS), central nervous system (CNS) neurons do not readily regenerate their axons after injury. Nonetheless, when presented with a permissive environment, injured CNS neurons can regrow to a certain extent, indicating that adult CNS neurons retain some capacity to regenerate. Several landmark studies by Aguayo, Richardson and colleagues, in which injured CNS axons grew into peripheral nerve grafts inserted into the spinal cord, emphasized that the environment was important for axonal regrowth (Richardson et al., 1980;David and Aguayo, 1981). Later studies by Richardson and colleagues (Richardson and Issa, 1984;Richardson and Verge, 1986) showed that dorsal root ganglion neurons regenerated their central axon if the peripheral branches of their axons was previously injured. Therefore, some kind of cell body response was also important for axonal regeneration.

The failure of adult CNS neurons to regenerate is due to a combination of factors that can be roughly divided into two main categories, (1) limited regenerative capacities (the cell body

responses), and (2) the non-permissive injured CNS environment encountered by the regrowing axons. A neuron's regenerative competence is associated with its expression of regeneration-associated genes (RAGs) (reviewed in Fernandes and Tetzlaff, 2001). These genes encode transcription factors, cytoskeletal proteins, trophic factors and cytokines (including their receptors), ion channels, etc. In the PNS, the expression of these genes is upregulated in a timely and persistent manner until successful regeneration occurs, but the upregulation in CNS neurons is weaker and more transient (reviewed in Plunet et al., 2002).

The post-injury environment in the CNS is much more hostile compared to the PNS. After injury to a peripheral nerve, myelin debris from axonal degeneration is promptly removed. Schwann cells proliferate and undergo phenotypic changes that prepare the local environment for axonal regeneration. Also, trophic factors are available from multiple sources (reviewed in Fu and Gordon, 1997). However, after SCI, a fluid-filled cavity develops and a glial scar forms, which is composed of reactive astrocytes, microglial cells, oligodendrocyte-lineage cells, and meningeal cells. They secrete or express on their surface several axonal growth inhibiting molecules (reviewed in Silver and Miller, 2004). These growth-inhibitory molecules activate signaling pathways in the injured axons that lead to axonal growth arrest. My research focused on interfering with these inhibitory signals in an attempt to stimulate axonal regeneration. I targeted a possible point of convergence in the inhibitory signaling, namely the Rho pathway. A specific and cell permeable drug commonly known as Y27632, was used to inhibit one of Rho's downstream effectors, the Rho kinase called ROCK.

'Regeneration' in a sense encompasses neurogenesis, regrowth of axons to their targets, re-establishment of functional synapses, and recovery of function. However, in this thesis, axonal 'regeneration' is used in a narrower sense, that is synonymous with axonal regrowth.

The non-permissive environment of the injured adult spinal cord

Mechanical injury to the adult mammalian CNS results in the formation of a 'glial scar'. The morphologies and sequence of events of glial scarring in rats, hamsters, cats, monkeys, and humans are similar (Bresnahan et al., 1976;Balentine, 1978a;1978b;Blight, 1983;Noble and Wrathall, 1985;Bunge et al., 1997). The glial scar is an evolving structure with different cell types participating at different times. Within hours of injury, hematogenous macrophages and residential microglia from surrounding tissues arrive at the injury site (Dusart and Schwab,

1994;Popovich et al., 1997). Starting from the next three to five days and persisting for at least two weeks, oligodendrocyte precursor cells are recruited from surrounding tissues (Levine, 1994;McTigue et al., 2001). Eventually, a scar-encapsulated cavity forms, and it is many times the size of the initial wound (Balentine, 1978a). Astrocytes become the predominant cell type in the scar tissue (reviewed in Fawcett and Asher, 1999), and form a barrier between the fluid-filled cavity and normal tissue (Popovich et al., 1997).

Immediately after a SCI, axons are directly damaged, and the mechanical impact destroys neurons and glial cells (microglia, oligodendrocytes, and astrocytes). Within hours to days after the initial injury, a complex cascade of secondary injury processes follows. They include alterations in regional blood flow, electrolyte homeostasis perturbations, edema, free radical generation, excitotoxicity, inflammation, and Wallerian degeneration of the distal cut axons (reviewed in Sekhon and Fehlings, 2001). At the same time, there is necrotic cell death due to the initial mechanical injury (Balentine, 1978a), and necrotic and apoptotic cell death due to the secondary injury (Crowe et al., 1997;Liu et al., 1997). The death of neurons and glial cells and Wallerian degeneration contribute to the activation of microglia/macrophages and of astrocytes (Dusart and Schwab, 1994;Fujiki et al., 1996), which may in turn cause further secondary damage.

Disruption of the blood-brain barrier leads to the recruitment of intrinsic (microglia) and extrinsic (macrophages, lymphocytes, natural killer cells) inflammatory cells. They abundantly release a range of cytokines such as interleukin (IL)-1, IL-6, IL-10, interferon (INF)-γ, transforming growth factor (TGF)-β1, and tumor necrosis factor (TNF)-α (Streit et al., 1998;reviewed in Raivich et al., 1999;Lee et al., 2000b). Most of these cytokines are pro-inflammatory. They initiate or modulate a range of cellular responses including the activation and migration of microglia (Basu et al., 2002;Shaked et al., 2005) and astrocytes (Rostworowski et al., 1997;Herx and Yong, 2001). Some cytokines are anti-inflammatory and they include TGFβ1 and IL-10. They counteract the effects of pro-inflammatory cytokines and may be neuroprotective (Brewer et al., 1999). Currently, the role of inflammation in spinal cord regeneration is under debate. It may facilitate the recovery from SCI by reducing the size of lesion and facilitating wound repair (Dusart and Schwab, 1994;Klusman and Schwab, 1997;Streit et al., 1998). On the other hand, the responses initiated by the pro-inflammatory cytokines, especially the activation of macrophages, exacerbate secondary tissue damage and the

formation of an inhibitory glial scar (Zhang et al., 1997;Fitch et al., 1999;Popovich et al., 1999;Lee et al., 2000a;Popovich et al., 2002). In the absence of significant mechanical injury, inflammation induced by microinjection of zymozan particles into the spinal cord causes secondary injury-like pathologies including progressive cavitation and upregulation of glial scar-associated inhibitory molecules (Fitch et al., 1999).

A cystic cavity filled with fluid and with necrotic tissue forms at the injured site. It extends rostrally and caudally from the original lesion (Zhang et al., 1997), and is surround by scar tissue, which consists of cellular (glial scar: reactive astrocytes, microglia and meningeal fibroblasts) and extracellular components (fibrous scar: extracellular matrix depositions, glial limitans) (Stichel and Muller, 1998;for reviews, see Grimpe and Silver, 2002). One to four weeks after injury, the cavity is gradually isolated from surrounding viable tissue mainly by reactive astrocytes (Popovich et al., 1997). If the injury penetrates the meningeal surfaces of the CNS, meningeal cells migrate into the injury site to recreate the collagenous basement membrane, and interact with astrocytes to reform the glial limitans (Ness and David, 1997;reviewed in Shearer and Fawcett, 2001). Meningeal cells and their production of the collagenous basement membrane are non-permissive substrates for axon regrowth (Stichel et al., 1999a;Stichel et al., 1999b;Shearer et al., 2003). In contrast to the PNS, where hematogenous macrophages are rapidly recruited to remove myelin debris, there is transient and insufficient activation of macrophages in the CNS injury response (reviewed in Stoll and Jander, 1999). As a result, myelin debris accumulates (Perry and Gordon, 1991), and proteins found on myelin inhibit axonal regrowth. Various proteoglycans are expressed on the glial scar and on myelin. Among those the keratan sulfate proteoglycans (KSPGs; Krautstrunk et al., 2002) and chondroitin sulfate proteoglycans (CSPG; covered in later sections) (reviewed in Fawcett and Asher, 1999) significantly inhibit axonal growth.

Santiago Ramon y Cajal (1928) was the first to show that axon regeneration failed at the site of injury, and these axons were dystrophic and displayed abortive sprouting. Enormous progress has been made since then in identifying the scar components that inhibit axonal regeneration. Specific inhibitors are found on myelin, three of which have been well-characterized: 1) Nogo (Chen et al., 2000;GrandPre et al., 2000), 2) myelin associated glycoprotein (MAG) (McKerracher et al., 1994), and 3) oligodendrocyte myelin glycoprotein (OMgp) (Kottis et al., 2002;Wang et al., 2002b). The Nogo proteins (Nogo-A, -B, and -C

isoforms) were first identified as antigens of the monoclonal mouse antibody IN-1 (Rubin et al., 1994;Chen et al., 2000), and treatment with the IN-1 antibody produced significant regeneration/sprouting in the injured CNS (Schnell and Schwab, 1990;Buffo et al., 2000;Bareyre et al., 2002). NogoA is specifically expressed in the CNS, and two separate domains, the Nogo-66 peptide in the extracellular loop and the N-terminal domain (Amino-Nogo), inhibit neurite growth and induce growth cone (GC) collapse *in vitro* (McKerracher et al., 1994;Prinjha et al., 2000;Chen et al., 2000;GrandPre et al., 2000).

MAG is a transmembrane protein that stimulates axonal growth from young neurons, but inhibits growth from mature neurons (McKerracher et al., 1994;Mukhopadhyay et al., 1994;Li et al., 1996). Changes in the endogenous levels of cAMP in neurons may account for such developmental changes. OMgp is a GPI-linked protein highly expressed in CNS myelin (Mikol and Stefansson, 1988). Similar to MAG and Nogo, OMgp is inhibitory to neurite outgrowth *in vitro* (Kottis et al., 2002;Wang et al., 2002b). Surprisingly, all three major myelin-associated inhibitors are ligands of the Nogo receptor, NgR (Fournier et al., 2001;Domeniconi et al., 2002;Liu et al., 2002;Wang et al., 2002b), which interacts with the neurotrophin receptor p75, and together they form a receptor complex mediating axonal inhibition (Wong et al., 2002;Yamashita et al., 2002;Wang et al., 2002a). New inhibitors from myelin are still being identified, and examples of such are repulsive guidance molecule (RGM) (Monnier et al., 2002;Rajagopalan et al., 2004), and Wnt (Yoshikawa et al., 2003;Lyuksyutova et al., 2003).

Some of the guidance molecules and their receptors expressed during CNS development are re-expressed or upregulated after SCI, and they are inhibitory to axonal growth. Examples of such are the semaphorins and their neuropilin/plexin receptors (Pasterkamp et al., 2001), and ephrins and their Eph receptors (Miranda et al., 1999;Benson et al., 2005). These molecules are found on astrocytes (Bundesen et al., 2003;Shearer et al., 2003), on meningeal fibroblasts that migrate into the lesion area (De et al., 2002;Bundesen et al., 2003;Shearer et al., 2003), and also on myelin (Benson et al., 2005). Another class of inhibitory molecules are the CSPGs (reviewed in Carulli et al., 2005). They are expressed by the above-mentioned cell types, and form one of the main impediments to axon regeneration of after SCI (covered in later sections).

Astrocytes, important constituents of the glial scar

Several cell types are found in the glial scar, and they include astrocytes, microglia, oligodendrocyte precursor cells, macrophages, fibroblasts and meningeal cells (reviewed in Fawcett and Asher, 1999). Astrocytes are the most conspicuous cell type, and they produce many of the inhibitory CSPGs in the glial scar.

During development, astrocytes are involved in axon pathfinding (Steindler et al., 1988;Joosten and Gribnau, 1989;reviewed in Powell et al., 1997;Hsu et al., 2005). They release cytokines, trophic factors, proteases, and protease inhibitors (Gloor et al., 1986;Assouline et al., 1987;Mizuno et al., 1994;reviewed in Muller et al., 1995). They also express on their surfaces numerous adhesion molecules (N-cadherin, neural cell adhesion molecule, and integrins; Neugebauer et al., 1988;Tomaselli et al., 1988) and extracellular matrix (ECM) molecules (fibronectin, and laminin; Liesi et al., 1983;Price and Hynes, 1985;Liesi et al., 1986) that positively influence axon growth. On the other hand, they can guide axons by acting as a barrier, via the expression of inhibitory KSPGs, CSPGs and tenascin (Steindler et al., 1989;Grierson et al., 1990;Snow et al., 1990;Geisert, Jr. and Bidanset, 1993;Powell and Geller, 1999). For example, in the spinal cord, astrocytes in the roof plate may contribute to the construction of a barrier which restricts the extension of commissural and dorsal column axons (Snow et al., 1990). These astrocytic boundaries fade and disappear in the adult CNS (reviewed in Steindler, 1993). However, after an injury to the CNS, an astrocytic boundary redevelops, and it has both positive and negative influences on injury recovery.

A prominent consequence of trauma to the adult CNS is astrogliosis, in which astrocytes become 'reactive', i.e. they undergo hypertrophy and hyperplasia, and increase their expression of intermediate filaments including glial fibrillary acidic protein (GFAP), vimentin, and nestin (Topp et al., 1989;Vijayan et al., 1990;Calvo et al., 1991;Frisen et al., 1995). There is also astrocytic migration from the adjacent undamaged parenchyma towards the injured area (Janeczko, 1989). These cells connect with each other through tight and gap junctions along their interdigitated processes (Eng et al., 1987), and are surrounded by ECM (Reier and Houle, 1988;reviewed in Raivich et al., 1999). Astrogliosis occurs shortly, within 3 to 5 days after injury. They are thought to 'wall-off' the damaged tissue from normal tissue, to reestablish the blood-brain barrier, and to restore the structural integrity of injured nervous tissue (reviewed in Reier et al., 1989).

At later stages of the recovery from injury, astrogliosis becomes a significant obstacle to axonal regeneration. Using an *in vitro* model of the glial scar formed by implanting nitrocellulose membranes into rodent cerebral cortex, Silver and colleagues showed that the reactive astrocyte was the major cell type contributing to the highly inhibitory nature of the adult injured CNS environment (Rudge et al., 1989;Rudge and Silver, 1990). The implants contained cellular and extracellular matrix components of the glial scar, and those obtained from neonatal animals were much more permissive to neurite growth than implants obtained from adult animals. Later studies showed that on the scar implants collected from adult rat cortices, astrocytes expressed several ECM molecules, especially the CSPGs, that significantly inhibited neurite growth (McKeon et al., 1991;1995;1999).

A series of astrocytic cell lines has been developed *in vitro* to study the factors important for the inhibition of neurite growth (Grierson et al., 1990;Groves et al., 1993;Smith-Thomas et al., 1994;Fok-Seang et al., 1995). Some of these cell lines were less permissive than others. Similar to results from the scar implant experiments, the inhibitory nature of the nonpermissive cell lines lies in the ECM produced by these cells. Antibodies to tenascin, chondroitinase ABC (ChABC, enzyme which degrades glycosaminoglycan side chains on CSPGs), or inhibitors of proteoglycan synthesis rendered the nonpermissive astrocytes cell lines less inhibitory (Meiners et al., 1995;Smith-Thomas et al., 1995;Powell and Geller, 1999).

The upregulation of GFAP expression is perhaps the best-known hall-mark of reactive astrocytes. *In vitro,* GFAP expression is associated with the astrocytic inhibition to neurite growth. Astrocytes treated with GFAP antisense mRNA, or from GFAP knock-out mice were more permissive for neurite extension than those from wild type animals (Lefrancois et al., 1997;Menet et al., 2000). Analysis of the ECM components showed that the GFAP-deficient astrocytes expressed higher levels of laminin (Lefrancois et al., 1997;Menet et al., 2001). *In vivo,* double null mice for GFAP and vimentin (another intermediate filament expressed by astrocytes) displayed reduced astroglial reactivity after spinal cord lesion (Menet et al., 2003). These mice also had increased sprouting of supraspinal axons and improved functional recovery. In another study, no stimulation was found with the regrowth of corticospinal tract axons in GFAP knockout mice (Wang et al., 1997). However, there was a slight decrease in CSPG expression in the grey matter of these knockouts. Therefore, there may be a link between the expression of GFAP and ECM molecules.

In vitro, the ECM of astrocytes has an important role in its inhibition of neurite extension (Smith-Thomas et al., 1995;scar implants, astrocytic cell lines, and; Canning et al., 1996;Yamada et al., 1997;Snow et al., 2001;Grimpe and Silver, 2004). *In vivo*, analyses of immunoreactivity on injured spinal cord tissue showed colocalization between GFAP and CSPGs, and *in situ* hybridization studies indicated that reactive astrocytes produce CSPGs (Tang et al., 2003;Jones et al., 2003). Among the various CSPGs that are highly upregulated after injury, astrocytes express neurocan and brevican (Yamada et al., 1997;McKeon et al., 1999;Tang et al., 2003;Jones et al., 2003). Although reactive astrocytes increase the expression of both stimulatory and inhibitory ECM molecules, the inhibitory ECM components are more dramatically upregulated (McKeon et al., 1991). Stimulatory ECM molecules such as laminin and fibronectin probably contribute to some axonal regrowth after injury (Zuo et al., 1998;Tom et al., 2004). However, the inhibitory ECM components dominate and counteract the intrinsic potential of the reactive astrocytes to support axonal regeneration (McKeon et al., 1995;Tom et al., 2004).

CSPGs in the glial scar

Various proteoglycans are found in the ECM of the nervous system. Among these a family of highly sulfated proteoglycans, the chondroitin sulfate proteoglycans (CSPGs), have an important role in the failure of CNS axonal regeneration (reviewed in Morgenstern et al., 2002). They consist of a protein core with covalently bound chondroitin sulfate (CS)-substituted glycosaminoglycan (GAG) side chains. GAGs are unbranched polymers composed of repeating disaccharide units, and depending on their structures, they can be grouped under CS, KS, dermatan sulfate (DS), or heparin sulfate (HS). The hyalectan family of CSPGs are important constituents of the nervous system (Milev et al., 1998). They are large aggregating proteoglycans that bind to hyaluronic acid (HA) in the ECM with the aid of a link protein. HA is also a GAG, but different from aforementioned ones for it is non-sulfated. The hyalectan family members include versican, neurocan, brevican, and aggrecan, and they share a common structure consisting of highly similar N- and C- terminals, and poorly conserved GAG-carrying middle region (reviewed in Bandtlow and Zimmermann, 2000). The N-terminal contains immunoglobulin domains followed by HA-binding tandem repeats. In the C-terminal, there are epidermal growth factor-like repeats, a lectin domain, and a complement regulatory protein element.

Even though many different molecules in the lesion area (e.g. myelin-associated inhibitors) are potent inhibitors of axonal growth, the barrier to axonal regeneration may ultimately lie in the presence of CSPGs found in the glial scar. After an *in vivo* CNS injury, there is a rapid and dramatic increase in CSPG expression within the lesion cavity and in the gliotic tissue surrounding the cavity (reviewed in Carulli et al., 2005). Immunostaining and immunoblotting studies have shown that neurocan, brevican, versican, and NG2 are upregulated in the lesion area within a few days after a CNS lesion (Jaworski et al., 1999;Asher et al., 2002;Tang et al., 2003;Jones et al., 2003). Using a microtransplantation technique to minimize damage, dissociated adult sensory (dorsal root ganglion) neurons transplanted into the spinal cord grew for long distances within normal white matter (Davies et al., 1997) and along degenerating white matter in rats (Davies et al., 1999). These vigorously growing axons stopped and became dystrophic when they reached the CSPG-rich reactive glial matrix (Davies et al., 1999). Thus, there was a spatial correlation between the upregulation of CSPGs and the failure of axonal regeneration.

The mechanism of CSPG inhibition on axonal growth is not fully understood. Different *in vitro* models have been developed to analyze the inhibition due to CSPGs. On a homogenous substrate, CSPGs significantly decreased neurite length (Snow et al., 1990;Dou and Levine, 1994;Hynds and Snow, 1999;Niederost et al., 1999;Borisoff et al., 2003). On a 'stripe assay', dorsal root ganglion (DRG) neurites growing on a permissive substrate (laminin only) stopped abruptly when they encountered a 'stripe' containing both laminin and CSPG, or they turned to grow along the border (Snow et al., 1990;Challacombe et al., 1996). On a 'step assay', increasing concentration of CSPG slowed down the rate of neurite growth until at a high enough concentration, the neurite ceased to grow (Snow and Letourneau, 1992). These experiments showed that CSPGs caused growth cone turning or avoidance responses in addition to decreasing neurite length. Also, the presence of stimulatory molecules such as laminin counteracted the inhibition due to CSPGs.

The role of CS-GAG side chains differs for each individual CSPG. The bacterial enzyme, chondroitinase ABC (ChABC), digests the GAG side chains from these proteoglycans (Jandik et al., 1994), and is commonly used to determine the degree to which attached GAG chains contribute to the molecule's inhibitory properties. The non-permissiveness of some CSPGs, such as brevican, depend on their GAG chains as ChABC digestion abolishes brevican inhibition on

neuronal attachment and neurite growth (Yamada et al., 1997). For other CSPGs such as NG2 (Dou and Levine, 1994) and versican (Schmalfeldt et al., 2000), the CS-GAGs are not required for their inhibition. For these CSPGs, the core proteins left behind after ChABC digestion were as inhibitory as the untreated molecules (Dou and Levine, 1994;Schmalfeldt et al., 2000).

Attenuating CSPG inhibition in the glial scar by removing the GAG side chains has been shown to stimulate axonal growth. *In vitro*, degradation of GAGs with ChABC significantly increased neurite growth from embryonic retinal neuron on nitrocellulose membranes that had previously been implanted into the cortex of adult rats (gliotic scar implants mentioned earlier) (McKeon et al., 1995). Also, ChABC digestion increased embryonic chick dorsal root ganglion (DRG) neurite growth on normal and injured spinal cord sections (Zuo et al., 1998). In both studies, function-blocking antibodies to laminin reversed the stimulatory effects of ChABC digestion. Their results pointed to the postulation that growth-promoting and growth-inhibitory molecules coexisted in the adult normal or injured adult CNS, and they antagonize each other. The removal of GAG chains uncovered the neurite-promoting laminin activity, and allowed for robust neurite growth.

In vivo, ChABC enhanced regeneration of nigrostriatal fibers (Moon et al., 2001). After a spinal cord dorsal column crush lesion, ChABC digestion improved regeneration/sprouting of axons in the corticospinal and dorsal ascending tracts (Bradbury et al., 2002). This anatomical regeneration is accompanied by restoration of electrophysiological function and improvement in various behavioral tests of locomotion and proprioception. The growth-promoting effects of ChABC on CNS axons were also demonstrated by several other studies by means of a retinal injury (Tropea et al., 2003), spinal cord contusion (Caggiano et al., 2005) or a spinal cord transection (Yick et al., 2000) model. When used in combination with cell grafts into the SC, ChABC improved the re-entrance of regenerating axons into host tissue (Chau et al., 2004;Ikegami et al., 2005). Despite the provision of a permissive substrate within the lesion cavity with cell transplants, gliotic tissue at the graft-host interface hindered axon crossing from the graft into host spinal cord (Lemons et al., 1999). The growth-promoting effects of ChABC digestion indicated that CSPGs in the gliotic tissue, or their GAG side chains, are important inhibitors of axonal regeneration in the glial scar.

Hyaluronidase is an enzyme that digests HA and releases CSPGs from the ECM. Injection of hyaluronidase into crushed optic nerves resulted in short growth of axons into the

distal stump whereas in saline-injected controls, no regrowth of axons was observed (Tona and Bignami, 1993). Similarly, hyaluronidase treatment to transection lesions of the nigrostriatal tract resulted in reduced immunostaining of HA-binding CSPGs such as neurocan and versican, and in local sprouting of transected dopaminergic nigral axons (Moon et al., 2003). However, long distance regeneration failed in regions with residual HA and HA-binding CSPGs. These studies showed that HA, HA-binding CSPGs, or both, contributed toward the failure of axon regeneration in the injured CNS.

In vitro studies revealed that in addition to masking stimulatory or permissive substrates, CSPGs also directly influence neurite growth by binding to cell surface receptors and initiating intracellular signaling. A cell membrane protein on cerebellar granule neurons (CGN) was identified as a potential NG2 receptor, and it mediated signaling that was dependent on G-proteins, and on intracellular calcium (Ca^{2+}) and cAMP levels (Dou and Levine, 1997). Pharmacological agents that increased Ca^{2+} or cAMP levels reversed the NG2-induced inhibition on neurite growth. Another study showed that in CGNs, conventional protein kinase C's (PKCs), which included PKC-α, -β, and –γ, were activated downstream of CSPGs, and transduced the signals to the Rho GTPase (Sivasankaran et al., 2004). In that study, infusion of a PKC inhibitor intrathecally and acutely after a dorsal hemisection appeared to stimulate regeneration from dorsal column (sensory) axons.

Chapter 2 of this thesis examined the inhibition on neurite growth by the CSPG, aggrecan, using a chick DRG explant model (covered in later sections). Aggrecan is expressed in both the CNS (Popp et al., 2003), and PNS (Pettway et al., 1996). In the embryonic spinal cord, aggrecan is present in areas avoided by migrating neural crest cells and by extending axons (Popp et al., 2003). Also, it is expressed in the DRG, and in the fasciculi gracilis and cuneatus in the spinal cord where the central branches of the DRG axons project (Popp et al., 2003).

Growth cone structure and dynamics

Various inhibitory molecules found in the post-injury environment have been discussed in previous sections. Their effects on the regrowing axons depends on reactions of the growth cone (GC) located at the leading edge of the axons. During development, the GC detects and responds to environmental cues that guide axons to their appropriate targets. These guidance molecules can be attractants (e.g. cytokines and growth factors) or repellents (slit, semaphorins,

ephrins). In some cases, the same molecule can act as both, depending on the receptor expressed by the GC. One example of such is netrin, which acts as an attractant to DCC-expressing axons (Chan et al., 1996;Keino-Masu et al., 1996), and as a repellent to UNC5- and DCC-expressing ones (Hamelin et al., 1993;Chan et al., 1996). The guidance cues can also be contact-mediated or secreted molecules, acting over short or long distances, respectively (for reviews, see Huber et al., 2003;Guan and Rao, 2003). They initiate sequences of signaling events in the GC, and instruct the GC to advance, turn, stall, or even collapse. Axonal regeneration shares significant similarities with axon guidance during development, in that the inhibitory molecules in the post-injury environment guides, repels or collapse GCs in a manner similar to the guidance molecules. Despite their diversity, signaling pathways activated by these molecules eventually lead to changes in the cytoskeletal components within the GC.

The GC consists of the lamellipodia, which contain networks of cross-linked actin filament (F-actin), and multiple filopodia, which contain bundled F-actin that project radially from the GC center (Gordon-Weeks, 1987) (Fig. 1.1A). Actin filaments are helical polymers composed of actin monomers (globular, or G-actin) (reviewed in Dent and Gertler, 2003). Polymerization is favored at the 'barbed end', and dissociation at the 'pointed ends'. The barbed end generally points towards the distal membrane, and the pointed end towards the GC center. In addition to actin filaments, another major constituent of the GC cytoskeleton are microtubules (MTs), which are composed of tubulin dimers assembled into linear arrays (reviewed in Dent and Gertler, 2003). Tubulin dimers consist of one α-tubulin subunit and one β-tubulin subunit, resulting in an α/β dimer. Because these α/β dimers are arranged in a head-to-tail configuration, the MTs are polarized structures, with a "plus" end and a "minus" end. The minus end is where nucleation of new MT occurs. At the plus end, polymerization and shrinkage occur intermittently and rapidly. The control of cytoskeletal polymerization and stability are key regulatory steps in axon growth (thoroughly reviewed by Song and Poo, 1999;Dickson, 2001;Meyer and Feldman, 2002;Luo, 2002;Huber et al., 2003).

The distal GC is generally known as the peripheral, or P-domain (Fig. 1.1A). This is where actin predominates, and actin 'treadmilling' (or recycling) occurs (Fig. 1.1B; reviewed in Suter and Forscher, 1998). Actin recycling involves actin polymerization at the leading edge of filopodia and lamellipodia (at the barbed end of F-actin) (Forscher et al., 1992;Lin and Forscher, 1993), actin depolymerization at the pointed end, and myosin-driven retrograde F-actin flow

(Letourneau, 1983;Forscher and Smith, 1988;Lin and Forscher, 1995;Lin et al., 1996). When actin recycling is coupled with substrate adhesion, there is net forward movement of the GC, and this model of GC advance is termed the 'clutch' hypothesis (reviewed in Suter and Forscher, 1998). Actin filaments interact with cell membrane molecules that in turn bind to the substrate. Examples of such membrane molecules are the integrins, which firmly link the cytoskeleton with the substrate (Gomez et al., 1996;Renaudin et al., 1999). The tension generated by retrograde F-actin flow is thus transduced into forward movement of the GC (Lin and Forscher, 1995). In the absence of adhesion to the substrate, retrograde F-actin flow is inversely correlated with GC advance (Lin and Forscher, 1995).

More than twenty proteins bind directly to F- and/or actin monomers, and have been localized immunocytochemically to the GC. They carry out a wide range of functions in the control of actin dynamics. For examples, cofilin severs F-actin (Meberg et al., 1998), GAP43 stabilizes F-actin by binding to the barbed end (He et al., 1997), and α-actinin anchors F-actin to membrane adhesions (Sobue and Kanda, 1989). They provide means by which extracellular guidance cues can control GC behavior (Aizawa et al., 2001;Gallo et al., 2002;Gehler et al., 2004;reviewed in Gallo and Letourneau, 2004;Hsieh et al., 2006).

In the proximal region of the GC (central, or C-domain), MT predominates, and there is interactions between actin and MTs (Fig. 1.1A; Mallavarapu and Mitchison, 1999). It was originally thought that MTs rarely protruded into the periphery of the GC (Letourneau, 1983;Forscher and Smith, 1988). However, later studies show that MTs can actually extend well into the P-domain and filopodia (Letourneau, 1983;Gordon-Weeks, 1987). Similar to actin filament, MT dynamics are regulated by their associated proteins. Examples of such are the microtubule-associated proteins (MAPs), which in general increase the stability of MTs (Umeyama et al., 1993;Mack et al., 2000), and collapsin response mediator protein-2 (CRMP-2), which promotes MT assembly (Fukata et al., 2002). These proteins are regulated downstream of some of the guidance cues such as netrin (Del Rio et al., 2004), and semaphorin (Goshima et al., 1995;Deo et al., 2004).

Although it was thought that actin was primarily responsible for GC steering while MTs provide the structure needed (Smith, 1988), increasing number of studies have shown that MTs also participate in steering (Sabry et al., 1991;Tanaka et al., 1995;Challacombe et al., 1997;Mack et al., 2000;Buck and Zheng, 2002). MT protrusion into the P-domain of GCs pushes the forward

movement of GCs, and MT stabilization on one side of the GC results in turning response. There is also evidence that actin reorganizations interact with MT dynamics in GC steering. In some conditions, F-actin in the P-domain acted as a barrier against the protrusion of MTs, and depletion of F-actins in that region facilitated MT invasion (Forscher and Smith, 1988). In other circumstances, increased actin polymerization was associated with directed MT stabilization (Zhou et al., 2002). Therefore, efficient GC advance probably depends on the coordinated actions of actin and MTs. The sum actions of microtubule invasion into the GC, and actin recycling thus determine the rate of GC advance.

An important phenomenon that occurs in regrowing neurites is 'GC collapse'. Its definition varies, and it can refer to a general lack of protrusive activity, or as extreme as a total loss of GC morphology. Very often, a GC makes initial contact with a negative guidance molecule with its filopodia, and the guidance molecule steers the GC by inducing partial or localized collapse. Multiple components play roles in this complex process, and they include the cessation of protrusive activity, reorganization of actin filaments, loss of attachment to the substratum, and endocytosis of the plasma membrane (reviewed in Gallo and Letourneau, 2004). The relative importance of each component and the signaling pathway leading to GC collapse is at present not fully understood.

Guidance molecules that cause GC collapse include semaphorins (Jin and Strittmatter, 1997;Campbell et al., 2001), slit (Nguyen Ba-Charvet et al., 2001), and ephrins (Wahl et al., 2000). Most of the neurite growth-inhibitory molecules upregulated after SCI also induce GC collapse. They included the CSPGs, NG2 and versican (Ughrin et al., 2003;Schweigreiter et al., 2004); and also the myelin proteins, MAG, Nogo and OMgp (Bandtlow et al., 1993;Li et al., 1996;Kottis et al., 2002;Niederost et al., 2002;Schweigreiter et al., 2004).

GC collapse is often associated with axon retraction. *In vivo*, damaged axons retract from the edge of injury, while the injury site develops into a highly inhibitory terrain for regrowth (reviewed in Houle and Tessler, 2003). Thus, if axon retraction can be blocked, the axon tips would be at a point of advantage during regeneration. These axons may be able to start regrowing before the development of an inhibitory environment. Therefore, it is of interest to understand the mechanistic basis of axon retraction, and to develop means to suppress it. Retraction can occur through two separate, although not mutually exclusive, mechanisms: passive depolymerization of the axonal cytoskeleton; and active retraction of the cytoskeleton

because of tension developed in the axon. Recent evidence favors the latter mechanism. Retraction requires actin turnover and cytoskeletal motor proteins including the MT-associated motor, dynein, and the actin-associated motor, myosin (Ahmad et al., 2000;Gallo et al., 2002;Wylie and Chantler, 2003;Gallo, 2004). Since the Rho GTPase regulates myosin, it plays an important role in GC collapse, and is discussed in the next section.

The Rho/ROCK signaling pathway

The responses of the GC to guidance/inhibitory molecules rely on rearrangements in its cytoskeleton. An important class of molecules acts as mediators between the guidance/inhibitory molecules and the GC cytoskeleton, and they are the Rho family of small GTPases. The most well-known family members, Rho, Rac, and Cdc42, regulate a wide range of cellular functions, some of which are associated with axonal growth. These functions include axonal initiation (Bito et al., 2000;May et al., 2002;Thies and Davenport, 2003), elongation (Jin and Strittmatter, 1997;Lehmann et al., 1999;Sebok et al., 1999;Bito et al., 2000;Niederost et al., 2002;Fournier et al., 2003), GC turning (Buck and Zheng, 2002;Yuan et al., 2003;Jin et al., 2005), and GC morphology (Luo and Raper, 1994;Jin and Strittmatter, 1997;Bito et al., 2000). *In vitro*, activation of Rac and Cdc42 induces the formation of lamellipodia and filopodia, respectively (Ridley et al., 1992;Nobes and Hall, 1995;Kozma et al., 1995). Rho activation induces stress fiber and focal adhesion formation in non-neuronal cells (Paterson et al., 1990;Maekawa et al., 1999), and neurite retraction or GC collapse in neurons (Hirose et al., 1998;Lehmann et al., 1999;Bito et al., 2000). In general, these studies suggest that axon growth-promoting signaling molecules activate Rac and Cdc42, while inhibitory ones activate Rho (reviewed in Luo, 2000).

The Rho GTPases cycle between active, GTP-bound and inactive, GDP-bound states through the binding and hydrolysis of guanine nucleotides. Their activation states are regulated by the Rho guanine nucleotide exchange factors (GEFs), and GTPase-activating proteins (GAPs). GEFs turn the Rho GTPases 'on' by stimulating the release of GDP and the uptake of GTP (Cherfils and Chardin, 1999). GAPs turn them 'off' by stimulating their intrinsic GTPase activity (reviewed in Lamarche and Hall, 1994;Rittinger et al., 1997). Numerous GEFs (reviewed in Rossman et al., 2005) and GAPs (reviewed in Moon and Zheng, 2003) have been identified. Some of these GEFs (Shamah et al., 2001;Aurandt et al., 2002;Perrot et al., 2002) and GAPs (Lundstrom et al., 2004;Barberis et al., 2005) are regulated by guidance/inhibitory molecules and

their receptors. For example, one component of the semaphorin receptor complex, plexin, associates with two Rho GEFs, the PDZRhoGEF and Leukemia-associated Rho GEF (LARG), which in turn stimulates the activity of Rho (Aurandt et al., 2002;Perrot et al., 2002)..

Rho stands for Ras-homologous, and its gene was first cloned in 1985 from a cDNA library from the abdominal ganglia of *Aplysia* (Madaule and Axel, 1985). It shares 35% amino acid sequence identity with H-ras (Madaule and Axel, 1985). In that same study, three human homologs were found by comparing the gene sequence for *Aplysia* Rho against human DNA. They are now known as RhoA, RhoB, and RhoC. Originally, Rho was thought to be an oncogene, like Ras, and early studies were directed at the effects of RhoA on DNA synthesis (reviewed in Ridley, 2001). However, it was soon noticed that injection of RhoA into fibroblasts dramatically changed cell morphology, which was correlated with an increase in actin stress fibers (Paterson et al., 1990). This discovery ignited a massive amount of research on the signaling and cell functions of Rho, and on the other family members, Rac and Cdc42.

Alan Hall's laboratory was one of the first in this field of study. They showed that the Rho proteins underwent post-translational modifications by geranylgeranylation (Adamson et al., 1992a), and while most of the Rho proteins were found in the cytosol, some were found associated with the plasma membrane (Adamson et al., 1992b). Geranylgeranylation, which is the addition of an isoprenoid lipid at the C-terminal cysteine residue, is important for membrane association and activation of signaling proteins. Stress fiber formation induced by lysophosphatidic acid (LPA) and growth factors such as platelet-derived growth factor (PDGF) is mediated by Rho (Ridley and Hall, 1992). Another Rho family member, Rac, is required for growth factor-induced membrane ruffling (Ridley et al., 1992). From then on, more research has shown the importance of the Rho GTPases in the generation of actin-based morphology and motility (Nobes and Hall, 1995;Kozma et al., 1995;Allen et al., 1998;Gotta et al., 2001;Dong et al., 2003), and they are recognized as signaling proteins that regulates the actin cytoskeleton.

Neurons use similar mechanisms to regulate their cytoskeleton, and the Rho proteins are key regulators of GC morphology and navigation. An important downstream effector of GTP-bound active Rho is the Rho kinase called ROCK, which is best studied in its contribution to neurite retraction and the GC collapse response. Rho-associated coiled-coil-containing protein kinase (ROCK) was identified about a decade ago as as a Rho-activated serine/threonine kinase (Leung et al., 1995;Matsui et al., 1996;Ishizaki et al., 1996). The originally identified kinase was

called ROKα or ROCKII, and later an isoform, ROCKI (ROKβ, or p160ROCK) was found (Nakagawa et al., 1996;Ishizaki et al., 1997). ROCKI is ubiquitously expressed all over the body but it is not found in the brain, while ROCKII is the predominant isoform in the nervous system (Matsui et al., 1996;Ishizaki et al., 1996;Nakagawa et al., 1996). The two isoforms share 64% sequence identity, and they show the highest conservation in their kinase domains (92% identical) (Nakagawa et al., 1996). Their kinase domains are found at the N-terminal, and at resting state, the C-terminal negative regulatory region folds at the central coiled-coil domain over the N-terminal to keep the kinase inactive (Matsui et al., 1996;Nakagawa et al., 1996;Amano et al., 1999). Rho-GTP binds to the Rho-binding (RB) domain in the C-terminus of ROCK, resulting in conformational changes that relieve the kinase domain of its suppression by the regulatory domain. This activates the phosphotransferase activity of ROCK. In subsequent instances in this thesis, 'ROCK' refers to ROCKII, although the two isoforms share many similarities in their regulation and downstream effectors.

ROCK phosphorylates numerous substrates, such as the myosin-binding subunit (MBS or otherwise known as the myosin phosphatase target subunit, MYPT) of myosin phosphatase (MP), myosin light chain (MLC) of myosin II, LIM motif-containing protein kinase (LIMK), and collapsin response mediator protein-2 (CRMP2) (Amano et al., 1996;Kimura et al., 1996;Sumi et al., 1999;Arimura et al., 2000;Ohashi et al., 2000). MLC is the regulatory domain of myosin II, (reviewed in Trybus, 1994), and one of the most well-studied functions of ROCK is modulating MLC phosphorylation (Fig. 1.2). ROCK directly phosphorylates MLC. It also indirectly increases MLC phosphorylation by phosphorylating and thereby inhibiting MP, reducing its ability to de-phosphorylate the very same residues on MLC (Amano et al., 1996;Kimura et al., 1996;Feng et al., 1999). Thus, by two parallel mechanisms, Rho increases the net phosphorylation of MLC. Phosphorylated MLC has increased interaction with actin, which in turn stimulates myosin ATPase activity and myosin contractility (Amano et al., 1996). The increase in myosin activity results in enhanced retrograde F-actin flow and contributes to GC collapse (Schmidt et al., 2002).

LIMKs are serine/threonine kinases. Phosphorylation of LIMK by ROCK enhances the ability of LIMK to phosphorylate cofilin (Maekawa et al., 1999) (Fig. 1.2). Cofilin is an actin-depolymerizing factor, and phosphorylated cofilin loses its actin-depolymerizing activity (Arber et al., 1998;Sumi et al., 1999;reviewed in Gungabissoon and Bamburg, 2003). Therefore, ROCK

inhibits actin disassembly via its activity on LIMK and cofilin, and leads to a net increase in actin stability.

CRMP2 was originally identified as a mediator in semaphorin-induced GC collapse (Goshima et al., 1995). It regulates MT assembly during neurite growth (Gu and Ihara, 2000;Fukata et al., 2002). It is phosphorylated downstream of Rho and ROCK (Arimura et al., 2000;Hall et al., 2001), and this phosphorylation was associated with LPA-induced GC collapse in DRG neurons (Arimura et al., 2000). Later studies have shown that phosphorylation of CRMP2 by ROCK inactivates CRMP2's ability to promote MT assembly (Arimura et al., 2005). Therefore, although this pathway was originally recognized as regulators of the actin cytoskeleton, the Rho/ROCK pathway also controls MT dynamics.

Other downstream effectors of Rho include mDia, which is a mammalian homolog of the *Drosophila* protein, diaphanous (Watanabe et al., 1997). It belongs to a family of formin-related proteins, which are all involved in the regulation of cell structure and polarity (for reviews, see Evangelista et al., 2003;Wallar and Alberts, 2003). mDia binds to and enhances the function of profilin (Fig. 1.2). It was originally thought that profilin sequestered unpolymerized actin in the cytosol, and decrease the pool of free actin monomers available for polymerization (Lassing and Lindberg, 1985). Later studies find that it actually promotes actin polymerization (Mockrin and Korn, 1980;Goldschmidt-Clermont et al., 1992). It accomplishes this mainly by stimulating nucleotide-exchange (ADP to ATP exchange) activity of actin monomers, thereby replenishing the pool of ATP–actin in the cell. ATP-actin-profilin readily interacts with the fast-growing, or barbed, end of actin filaments, and ATP-actin becomes incorporated into filaments.

The activation of Rho and one of its downstream effectors, ROCK, is generally considered to be inhibitory to neurite growth, because this pathway is activated downstream of multiple repulsive guidance cues (Shamah et al., 2001;Hu et al., 2001;Yamashita et al., 2002;Niederost et al., 2002), and it leads to GC collapse (Jalink et al., 1994). It is also involved in signaling downstream of inhibitory molecules found after SCI. For examples, the myelin-associated inhibitory molecules (MAG, Nogo and OMgp) activate Rho via the NgR-p75 receptor complex (Yamashita et al., 2002;Niederost et al., 2002;Madura et al., 2004;Domeniconi et al., 2005). The p75 receptor can act as a Rho displacement factor that relieves Rho suppression by its GDP dissociation inhibitor (Yamashita and Tohyama, 2003).

The activation of Rho after SCI was documented in several studies (Dubreuil et al., 2003;Sung et al., 2003;Madura et al., 2004;Conrad et al., 2005). In uninjured and sham-operated rats, Rho activation is low in the white matter and most of the activated Rho was found in cell bodies in the grey matter (Madura et al., 2004;Conrad et al., 2005). After dorsal spinal cord transection, the level of activated Rho was significantly increased in the injured neurites in the white matter (Madura et al., 2004). The increase in Rho activation started within 1 day after injury and persisted for a month (Conrad et al., 2005). In this study, the cellular source of activated Rho was found to be in immune cells, including polymorphonuclear leukocytes, monocytes and macrophages, and in reactive astrocytes. It was thought that this increase in activated Rho was associated with the facilitation of cell migration (Conrad et al., 2005).

In vitro, different methods have been used to inhibit Rho or ROCK: (1) Clostridium botulium C3 exoenzyme that ribosylates and inactivate Rho (Nishiki et al., 1990;Jalink et al., 1994), (2) dominant-negative Rho mutation through N19TRho-expressing plasmid transfection (Kozma et al., 1997;Kranenburg et al., 1997;Lehmann et al., 1999), and (3) Y27632 which specifically inhibits ROCK (Uehata et al., 1997), and (4) dominant negative ROCK with point mutations in both the kinase and Rho-binding domains (Hirose et al., 1998). These studies demonstrated that ROCK is the necessary and sufficient effector of Rho in signaling leading to neurite retraction and GC collapse. The inactivation of endogenous Rho or ROCK in neurons using one of the above methods significantly reduced inhibition on neurite outgrowth due to MAG, Nogo, or myelin (Jin and Strittmatter, 1997;Lehmann et al., 1999;Yamashita et al., 2002;Dergham et al., 2002;Niederost et al., 2002). Suppression of the Rho signaling pathway also overcomes neurite growth inhibition due to Collapsin-1 (Sema3A), and A5 Ephrins (Jin and Strittmatter, 1997;Wahl et al., 2000).

Recently, several research groups including ourselves (Dergham et al., 2002;Borisoff et al., 2003;Monnier et al., 2003) found that axonal growth inhibition due to some CSPG is at least partially mediated by the Rho/ROCK pathway. We found that *in vitro*, substrate-bound aggrecan stimulated Rho activity in DRG neurons and decreased neurite outgrowth. The specific and cell-permeable ROCK inhibitor Y27632 partially reversed the decrease in outgrowth (Borisoff et al., 2003). Also, the inhibitory activity of a CSPG mixture on retinal ganglion neurons (Monnier et al., 2003) and cortical neurons (Dergham et al., 2002) can be blocked by treatment with either C3 or Y27632.

In vivo, inhibition of Rho/ROCK signaling increased axonal regeneration. For example, in the optic nerve after a microcrush lesion, treatment with C3 dramatically increased the number of axons that cross the crush site (Lehmann et al., 1999). Without C3 treatment, most retinal ganglion cell axons stopped abruptly at the crush site, and characterization of the lesion area suggested that both CSPG and myelin-derived inhibitors contributed to the failure of regeneration (Selles-Navarro et al., 2001). In the spinal cord, C3 or Y27632 application at the lesion site by embedding it in fibrin glue (Dergham et al., 2002) or via osmotic minipump implants (Fournier et al., 2003) increased sprouting of corticospinal axons into and apparently beyond the lesion site.

DRG neurons

Chick and rodents DRGs are widely used in culture to study the development of embryonic neurons in response to trophic factors (Ruit et al., 1992;Williams and Ebendal, 1995;Kucera et al., 1995;Wright and Snider, 1995;Lefcort et al., 1996;reviewed in Ernfors, 2001). They are also used in axon guidance research (Jin and Strittmatter, 1997;Nguyen Ba-Charvet et al., 2001;Dontchev and Letourneau, 2002;Rajagopalan et al., 2004), in characterizing neurite growth-inhibitory molecules (Snow et al., 1991;Snow and Letourneau, 1992;Tang et al., 2001;Yamashita et al., 2002;Snow et al., 2003;Ughrin et al., 2003;Gilbert et al., 2005), and in identifying pharmacological or biological compounds that stimulate neurite growth (Cai et al., 1999;Chen et al., 2000;Fournier et al., 2003;Borisoff et al., 2003).

There are several classes of sensory neurons found in the DRG. In addition to differences in sizes and function, they also have different trophic factor dependencies and receptor expression (Mu et al., 1993;McMahon et al., 1994;Wright and Snider, 1995). Almost all of the large myelinated DRG neurons expresses the tropomyosin-related kinase (Trk) C receptor, and respond to neurotrophin-3 (NT3) (Mu et al., 1993;McMahon et al., 1994). Some of the TrkC-positive neurons co-express TrkB, and are BDNF-responsive (McMahon et al., 1994). The rest of the large DRG neurons are glial-cell-line-derived neurotrophic factor- (GDNF) responsive, and express the GDNF family receptor-α1 (GFRα1) and RET (a receptor tyrosine kinase) (Kashiba et al., 2003). The small unmyelinated DRG neurons express either TrkA (Averill et al., 1995), or GFRα1/2 and RET (Bennett et al., 1998;Kashiba et al., 2003). The former type of neurons responds to nerve growth factor (NGF), and the later one responds to GDNF.

Many of the large DRG neurons (TrkC-expressing) are proprioceptors that provide sensory feedback from muscle spindles and Golgi tendon organs (Ernfors et al., 1994;Wright et al., 1997). Some of the TrkC-expressing neurons are cutaneous mechanoreceptors that convey information on discriminative touch sensations (McMahon et al., 1994;Fundin et al., 1997). The small (all TrkA-expressing and some of the GFR- and RET-expressing) DRG neurons convey information concerning different kinds of noxious stimuli (thermal, chemical, or mechanical) (reviewed in Snider and McMahon, 1998).

Regeneration/sprouting of the DCT and CST axons

Many different strategies of facilitating axonal regeneration have been tested using various rodent models of SCI. The limited regenerative capacity of adult CNS neurons is an important factor in regeneration failure. Therefore, many of these different approaches involve the use of trophic factors to stimulate the neuronal cell body regenerative response (Giehl and Tetzlaff, 1996;Kobayashi et al., 1997;Bregman et al., 1998;Novikova et al., 2000;Kwon et al., 2002). Since the non-permissive post-injury environment also plays a role in regeneration failure, other regeneration-stimulating paradigms make use of cell and tissue grafts (Richardson et al., 1980;David and Aguayo, 1981;Xu et al., 1995;Cheng et al., 1996;Guest et al., 1997;Li et al., 1998;Fernandes et al., 1999;Hiebert et al., 2002), or enzymes (Bradbury et al., 2002) to render the environment less inhibitory. Yet other methods are available, such as the use of pharmacological or molecular agents to alter the signaling initiated in the GCs by axonal growth inhibitors (examples of such are C3 and Y27632 mentioned in the earlier sections). Researchers have also experimented with combinatorial approaches that generate synergistic effects (Tropea et al., 2003;Lu et al., 2004;Fouad et al., 2005).

In this thesis, a dorsal column transection model was used to study simultaneously the regeneration/sprouting of two different spinal cord long projection tract axons (Chapter 3). They were the ascending sensory, or dorsal column tract (DCT), and the descending corticospinal tract (CST). These two tracts are both anatomically and functionally well-defined, and are widely used in regeneration research. They also have the advantage of ease of application of tracers. In the following, the anatomy and regeneration propensity of the DCT and CST are summarized in order to give a general perceptive on these two axonal tracts.

The DCT is composed of axons from the DRGs. DRG axons bifurcate such that the peripheral branches project in the peripheral nerves to the sensory organs in the skin and muscles, while their central branches project through the dorsal roots into the spinal cord. The central projections of TrkC-expressing DRG neurons terminate in the deeper laminae of the dorsal horn, and their axon collaterals form the DCT (McMahon et al., 1994). The DCT runs in the dorsal part of the dorsal columns in the spinal cord, and terminate in the cuneate (for DRG axons from the upper body) and gracile nuclei (from lower body).

Injured peripheral DRG axons spontaneously regenerate and re-innervate their targets (Bisby and Pollock, 1983;Oblinger and Lasek, 1984), indicating that the DRG neurons possess the intrinsic capacity to regrow their axons. However, the central DRG axons display limited regeneration after being injured by a dorsal root rhizotomy, or by a dorsal column lesion. The dorsal root entry zone (DREZ, or known as the transitional zone) is where the dorsal roots join the spinal cord. Rhizotomized dorsal root axons regrow until they reach the DREZ and stop there (Nathaniel and Nathaniel, 1973;Bignami et al., 1984;Liuzzi and Lasek, 1987;Chong et al., 1994;Ramer et al., 2001). In the DCT, axonal regeneration is even less efficient, as these axons do not regrow, but form retraction bulbs at the injury site (Neumann and Woolf, 1999). Interestingly, the abilities of the DRG neurons to mount a cell body response appropriate for regeneration differ for the various types of injuries. Injuries to the peripheral nerve increase the expression of the 43 kDa growth-associated protein (GAP-43) (Hoffman, 1989;Van der Zee et al., 1989;Verge et al., 1990;Ramer et al., 2001). Upregulation of GAP-43 is commonly associated with regeneration success (Hoffman, 1989;Van der Zee et al., 1989;Tetzlaff et al., 1989;Tetzlaff et al., 1991;Doster et al., 1991;Chong et al., 1994;Fernandes et al., 1999). In contrast, injuries of the dorsal root and DCT do not result in such an increase (Schreyer and Skene, 1993;Chong et al., 1994).

Nonetheless, regeneration of the central DRG axons can be stimulated by a 'conditioning lesion' of the peripheral branch. A landmark study by Richardson and Issa (1984) showed that the injured DCT axons could regrow into a peripheral nerve implant in the spinal cord, if the peripheral DRG projections had previously been transected. Such peripheral nerve conditioning lesion also accelerated central axon regeneration in the crushed dorsal roots (Richardson and Verge, 1987). Later it was found that even in the absence of a peripheral nerve graft, a conditioning lesion given 1 or 2 weeks prior to a dorsal column lesion resulted in enhanced DCT

axonal regrowth within CNS tissue (Neumann and Woolf, 1999). The conditioning lesion induced molecular changes in the DRG neurons that favored regeneration of both the peripheral (Bisby and Pollock, 1983;Oblinger and Lasek, 1984) and central axons. The elevation of cAMP likely plays an important role in such growth-potentiating effects, since the cAMP level is dramatically increased within 1 day after the conditioning lesion, and cAMP injection into the DRG cell bodies 1 week prior to an injury produced similar results as measured by the distance regenerated by the DCT axons (Qiu et al., 2002;Neumann et al., 2002).

Neurotrophic factors have diverse functions, one of which is the stimulation of axonal growth (for reviews, see Plunet et al., 2002;Markus et al., 2002). Regeneration across the DREZ can be stimulated by NGF, NT3, and GDNF, but not BDNF (Ramer et al., 2000). Such regeneration was accompanied by the recovery of sensory functions. In the SC, regeneration of the DCT axons can also be stimulated by neurotrophic factors such as NGF and NT3 (Bradbury et al., 1999;Oudega and Hagg, 1999). Intrathecal infusion of NT3 induced sprouting of DCT axons at the lesion site and beyond into rostral tissue after a dorsal column crush lesion (Bradbury et al., 1999). Combined with a peripheral nerve graft, NGF infusion increased the number of regenerated sensory axons within the implant and the distance traveled by these axons (Fernandez et al., 1990). When neurotrophic factors were infused into the spinal cord rostral to a peripheral nerve graft, NGF or NT3 increased the number of regenerated sensory axons that reenter the host spinal cord rostral to the implant (Oudega and Hagg, 1999).

The CST arises from layer V pyramidal cells in the sensorimotor cortex (Hicks and D'Amato, 1977;Leong, 1983;Akintunde and Buxton, 1992), and projects via the internal capsule and cerebral peduncle to the ventral aspect of the brainstem. In rats, most of the CST fibers cross the midline in the pyramidal decussation and turn dorsally to give rise to the contralateral dorsal CST, which reside in the ventromedial aspect of the dorsal funiculus in the spinal cord (Hicks and D'Amato, 1975;Armand, 1982). A minor proportion of the CST axons traverse the spinal cord in the dorsolateral funiculus (Liang et al., 1991). Still some axons remain uncrossed and run in the ipsilateral ventromedial funiculus (Vahlsing and Feringa, 1980;Joosten et al., 1992;Brosamle and Schwab, 1997). Most of the CST fibers terminate in the dorsal and medial grey matter in the spinal cord, and synapse with interneurons, but a small percentage terminate in more ventral regions and synapse directly with motor neurons (Casale et al., 1988;Liang et al., 1991).

Injured CST axons usually do not regrow into tissue implants such as a peripheral nerve graft (Blits et al., 2000;Hiebert et al., 2002) or a Schwann cell graft (Xu et al., 1995;Chen et al., 1996), even with an exogenous supply of neurotrophic factors. This could arguably be due to a lack of retrograde transport of the neurotrophic factor signals when the trophic factors were supplied at the spinal cord injury site. However, with cell body application of BDNF, there was still no regeneration into peripheral nerve transplants inserted into the spinal cord dorsal columns (Hiebert et al., 2002). When the CST fibers did grow into an embryonic spinal cord graft (Schnell and Schwab, 1993;Bregman et al., 1997) or a NT3-supplemented collagen matrix (Houweling et al., 1998), none of these fibers were found to come out of the distal graft/host interface. Nonetheless, these fibers often display terminal or collateral sprouting rostral or caudal to the implants. Similar to DCT axons, transected CST fibers terminally sprouted on contact with microtransplanted Schwann cells (Li and Raisman, 1994). When supplied with NT3, transected CST axons regrow around and below the tissue grafts and there is often significant sprouting in the distal grey matter (Grill et al., 1997;Blits et al., 2000;Tuszynski et al., 2003). Interestingly, if the CST was unilaterally transected at the pyramidal decussation, cell body treatment with BDNF stimulated sprouting of the contralateral, intact CST (Khodarahmi et al., 2001). These collateral sprouts from the intact CST could be observed to cross the midline, and they may have reconnected with denervated neurons in the grey matter.

In contrast, CST axons grew into acidic fibroblast growth factor (aFGF)-supplemented peripheral nerve graft (Cheng et al., 1996). Multiple intercostals nerves that redirected white matter tract fibers into grey matter were implanted into a gap formed by complete spinal cord transection at low thoracic level. CST axons grew into and across the peripheral nerve grafts supplemented with aFGF rather than sprouting into the rostral or caudal cord as seen in the other studies. The discrepancy between Cheng's results and others' is potentially due to the different lesion paradigms. Other researchers, including Hiebert (2002) and Blits (2000), employed the spinal cord partial lesion model, thus part of the grey matter remained intact. Intact spinal cord grey matter may present a more permissive substrate than peripheral nerve grafts. In a later study, CST regeneration in peripheral nerves bridged from grey to white matter (similar to Cheng et al.'s model) was compared to spinal cord anastomosis, in which the transected spinal cord stumps were apposed with pial sutures and peripheral nerves placed around the anastomosis site (Tsai et al., 2005). In both models, CST axons regenerated through the repair sites into the

caudal cord, indicating that circumvention of white matter inhibition was not essential for CST regneration. Rather, it appears that the availability of exogenous aFGF determines CST axonal regeneration.

Other strategies to stimulate DCT or CST regeneration target (1) the inhibitory molecules found on myelin and in the glial scar, or (2) the growth cone-signaling cascades through which these molecules exert their inhibitory effects (mentioned in the last section on Rho/ROCK). One prominent strategy is the usage of the IN-1 antibodies, which recognize several myelin-associated epitopes that are proposed to be the Nogo proteins. CST axons did not readily grow into various tissue grafts, nonetheless, their regenerative ability was facilitated by combining tissue implants with application of the IN-1 antibodies into the motor cortex (Schnell and Schwab, 1993). In fact, IN-1 by itself is also able to increase the regenerating propensity of CST axons into the caudal spinal cord (Schnell and Schwab, 1990;Schnell et al., 1994;Bregman et al., 1995). However, the major effect of the IN-1 antibodies may lie in the stimulation of sprouting rostral or caudal to a cell or tissue graft, rather than producing regeneration within the graft. Intrathecal delivery of a Nogo-66 antagonist peptide, NEP1-40, that competitively bind to the Nogo receptor, NgR, promoted CST sprouting (GrandPre et al., 2002). In contrast, there is no further enhancement on NGF-promoted DCT fibers that grow into a peripheral nerve graft with the IN-1 antibodies, suggesting that the IN-1 antigens do not play a determining role in inhibiting DCT axonal regeneration (Oudega et al., 2000).

Sensorimotor functions and SCI

In Chapter 2, I assessed the axonal regeneration/sprouting of the DCT and CST. Several tests of sensorimotor functions, whose performance depended on these two neural pathways, were used to assess functional recovery in the dorsal column transection model of SCI. Using multiple tests allowed more reliable conclusions to be drawn regarding the integrity of those axon tracts. The behavioral tests used were: (1) the footprint analysis, which assessed the pattern of locomotion on flat surfaces; (2) the footslip test (or the horizontal ladder test) which required precise paw placement on irregularly-spaced rungs on a horizontal ladder, and thus evaluated skilled locomotion; (3) the Whishaw food pellet reaching task which assessed skilled forelimb reaching and retrieval movements; (4) the von Frey hair tests which detected abnormal pain

sensation to mechanical stimuli; and (5) the infra-red test which detected abnormal pain sensation to heat.

Purposeful motor behavior requires the coordinated action of many muscles, and neural circuits within the spinal cord are essential for the coordinated activation of these muscles. For example, networks of interneurons, called the central pattern generators, produce alternating flexion and extension movements that comprise the normal walking pattern (reviewed in MacKay-Lyons, 2002). This pattern is subject to supraspinal and sensory afferent modifications (Cheng et al., 1997). Injuries to the ascending DCT and descending CST would differentially impair walking and other sensorimotor functions.

The DCT carries proprioceptive information (Perry et al., 1991;Ernfors et al., 1994;McMahon et al., 1994;Wright et al., 1997). While the reticulospinal tract is hypothesized to initiate locomotion and may be the most important tract for overground locomotion (Steeves and Jordan, 1980;Loy et al., 2002), Webb and Muir's study (2003) shows that the DCT does contribute to locomotion. With force platforms embedded·in the centre of a runway to assess locomotion on flat surfaces, DCT-injured rats used the limbs on their injured side less frequently and developed an asymmetric gait characterized by impaired braking with the forelimb and reduced weight support by the hindlimb ipsilateral to injury. In addition, DCT lesion significantly increased the number of footslips on a horizontal ladder (Webb and Muir, 2003). The study indicates that the joint and muscle feedback provided by the DCT is important for locomotion and skilled motor functions.

The DCT also contributes to skilled reaching (food pellet reaching), as proprioceptive input plays a role in targeting of the limb towards a food pellet (Schrimsher and Reier, 1993;Whishaw and Gorny, 1994). In addition, the DCT may also carry discriminative touch information, and the presence of food in the paw is thought to initiate grasping (McKenna and Whishaw, 1999;Ballermann et al., 2001). In rodents, the sense of touch is particularly important, as they depend on olfaction and touch rather than vision (as in primates) to guide their reaching movements (reviewed in Whishaw, 2003). A spinal cord lesion that selectively injured the DCT at the cervical level altered the reaching trajectory in retrieving food pellets and the changes persisted over time (McKenna and Whishaw, 1999). The alterations might have resulted from an inability to adjust digit positions and to produce independent, fractionated digit movements (Cooper et al., 1993;Glendinning et al., 1993; cited in McKenna and Whishaw, 1999).

The CST plays a role in locomotion. In rats, unilateral lesions of the CST by pyramidotomy produced locomotory deficits that were revealed by measurements of ground reaction forces as the rats walked across a runway (Muir and Whishaw, 1999). The deficits were transient, and consisted of an asymmetric gait and abnormal braking forces of the impaired forelimbs. Damage to the CST also resulted in long-lasting alterations in the joint angles during walking (Metz et al., 1998). In another study, pyramidotomy increased the angle of outward forepaw rotation of the impaired side in a footprint analysis, and regeneration/sprouting of CST fibers was correlated with normalization of the rotation angle (Thallmair et al., 1998).

The CST is very important in skilled movements. Injuries to the sensorimotor cortex or CST resulted in long-lasting impairment in ladder-crossing and food pellet-reaching, since the cerebral cortex, via the CST, is responsible for gait modification during the adjustments to environmental changes (Drew, 1993). In the horizontal ladder test, a unilateral motor cortex lesion or pyramidotomy increased footslips compared to sham-operated animals (Metz and Whishaw, 2002). Close examination of the stepping movement suggested that these types of injuries impaired aiming movements. For the injured animals, frequent corrections of paw placement were necessary in order to lay the limb on the appropriate rung, and they showed an increased use of the digits/toes or wrist/heel rather than the plantar surface of the foot. Digit flexion, which stabilized the limb's position on the rung, was also impaired by lesions to the CST (Metz and Whishaw, 2002).

Motor cortical neurons displayed a distinctive pattern of activity during reach-to-grasp movements, and periods of changes in neural activity correlated with specific components of the reaching sequence (Hyland, 1998). Motor cortex lesion (Whishaw et al., 1986) and CST injury (Whishaw et al., 1993;Thallmair et al., 1998;Whishaw et al., 1998) impaired food pellet reaching. Rats were still able to reach for and retrieve the food pellet, but apparently they used compensatory strategies to aid in or substitute for deficient limb movements (Whishaw et al., 1993). Similar to the deficits detected in ladder-crossing, damage to the CST caused targeting problems during reaching attempts and dysfunctions in grasping the food pellet (Schrimsher and Reier, 1993;Whishaw et al., 1993;Whishaw et al., 1998). The damage also significantly decreased the rate of successful pellet retrieval.

SCI very often results in different kinds of abnormal pain sensations, one of which is neuropathic pain (reviewed in Siddall et al., 1999;Woolf and Mannion, 1999). Neuropathic pain

has no biological advantage, and causes suffering and distress. There are two common manifestations of neuropathic pain, hyperalgesia and allodynia (reviewed in Zimmermann, 2001). Hyperalgesia is a stronger or earlier than normal withdrawal response than healthy animals to a noxious stimulus. Allodynia is pain that occurs following a stimulus that normally does not cause pain sensation. These abnormal pain sensations can be evoked by different stimuli, which are classified as mechanical, thermal, or chemical. It is unclear why such abnormal sensitivities develop after SCI, but one of the proposed theories states that such pain sensations result from a loss of balance between noxious (mainly the spinothalamic pathways) and non-noxious (the dorsal column-medial lemniscal pathway) sensory inputs at the thalamic level, and the CNS misinterprets the peripheral signals (reviewed in Eide, 1998). In favor of this hypothesis, analysis of the termination patterns of spinothalamic and dorsal column axons showed that they projected to different, but overlapping regions in the thalamus (Ma et al., 1987). The hypothesis predicts that deafferentation of the spinothalamic pathways would cause neuropathic pain. However, damage to either the spinothalamic or dorsal column-medial lemniscal pathways was not directly associated with neuropathic pain (Eide et al., 1996). Nonetheless, in other studies, the dorsal column fibers were implicated in the transmission of abnormal pain sensation to upper brain regions (Palecek et al., 2002;Saade et al., 2002). Therefore lesions to the DCT (and/or drug treatments) can potentially lead to abnormal sensitivity to pain. The von Frey hair test and infra-red test were used in my experiments to detect mechanical and thermal allodynia/hyperalgesia, respectively. These tests are commonly used in rat models of regeneration research to monitor the development of abnormal pain (Christensen et al., 1996;Ramon-Cueto et al., 2000;Ramer et al., 2000;Hains et al., 2001;Tang et al., 2004;Ramer et al., 2004;Fouad et al., 2005;McGraw et al., 2005).

Hypotheses and overviews

In Chapter 2, I used an *in vitro* model to analyze the inhibition by different components of aggrecan on chick DRG neurite growth. The aggrecan components that were tested included aggrecan bound with hyaluronic acid and link protein (as in the ECM), aggrecan monomers, chondroitin sulfate glycosaminoglycan side chains, hyaluronic acid, and chondroitinase-treated aggrecan (core protein with digested carbohydrate stubs). The neurite length and growth cone morphology of NGF- versus NT3-dependent DRG neurites were compared on substrates

containing these various molecules. I also determined whether the ROCK inhibitor, Y27632, reversed the decrease in neurite growth due to the different aggrecan components. These experiments were to test the hypotheses that both the chondroitin sulfate glycosaminoglycan side chains and core protein are important for aggrecan inhibition on neurite growth, and that ROCK suppression with Y27632 overcome inhibition due to each aggrecan component.

In Chapter 3, I hypothesized that pharmacological inhibition of ROCK using Y27632 promoted axonal regeneration and functional recovery *in vivo*. A cervical dorsal column transection model in rats was used to test whether Y27632 stimulated axonal regeneration in the DCT and CST axons. In addition, various behavioral tests for the forelimbs were used to test whether Y27632 accelerated or enhanced the recovery of sensorimotor functions.

In Chapter 4, I hypothesized that non-specific ROCK inhibition affected non-neuronal cells in the SCI environment, resulting in decreased permissiveness of these cells to axonal regeneration. *In vivo*, rats were treated with the Y27632 inhibitor for one week, and their spinal cord tissues were harvested to analyze the expression of GFAP and the CSPG, neurocan. *In vitro*, astrocyte monolayer cultures were established to analyze the effects of Y27632 treatment on the expression of stimulatory ECM molecules, fibronectin and laminin, and of the inhibitory CSPGs. Neuron-astrocyte cocultures were used to test whether Y27632-treated astrocyte were more inhibitory to neurite growth from cortical neurons.

List of hypotheses:

(1) Both the chondroitin sulfate glycosaminoglycan side chains and core protein are important for aggrecan inhibition on neurite growth, and ROCK suppression with Y27632 will overcome inhibition due to each aggrecan component.

(2) Pharmacological inhibition of ROCK using Y27632 will promote axonal regeneration and functional recovery *in vivo*.

(3) Non-specific ROCK inhibition will affect non-neuronal cells in the SCI environment, and will result in decreased permissiveness of these cells to axonal regeneration.
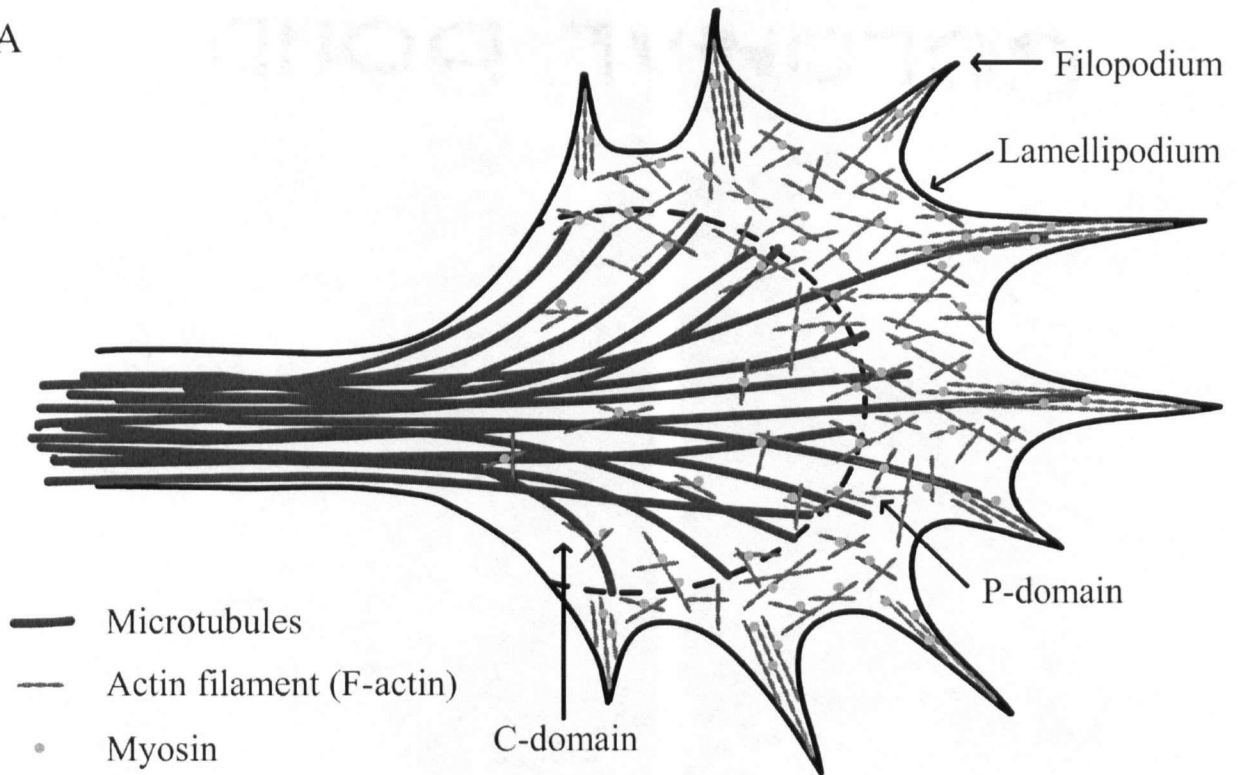
List of objectives:

(1) To use an *in vitro* model in analyzing the inhibition by different components of aggrecan on chick DRG neurite growth.

(2) To apply the Y27632 ROCK inhibitor in an *in vivo* model of SCI in rats and determine if it increases axonal regeneration and stimulates functional recovery.

(3) To analyze *in vitro* and *in vivo* the effects of Y27632 treatment on astrocytes, on their expression of CSPGs and on their permissiveness to neurite growth.

Figure 1.1

(A) Cytoskeletal organization of a growth cone (GC). Microtubules are mostly localized in the central domain (C-domain), but some project more distally towards the filopodia. Actin filaments (or F-actin) dominate in the peripheral domain (P-domain). Filopodia contain bundled F-actin, and in the lamellipodia the actin filaments are cross-linked into a dense meshwork.

(B) Actin recycling (or 'treadmilling) in a filopodia. Actin bundles are polarized with the 'barbed' end pointing outward and 'pointed' end towards the GC center. Actin polymerization occurs at the barbed end, progressing away from the GC center. Depolymerization occurs at the pointed end, and the released actin monomers provide building blocks for polymerization. Retrograde F-actin flow is driven by myosin motors, and tension is generated toward the GC center. If the actin filaments are stabilized by interaction with the substrate, i.e. the 'clutch' is engaged, then the tension pulls the filopodia forward. Cofilin and GAP43 are examples of actin-interacting proteins. Cofilin is an actin-severing protein and is important for actin turnover. GAP43 binds to the barbed end, and stabilize this end of the actin filament.

A

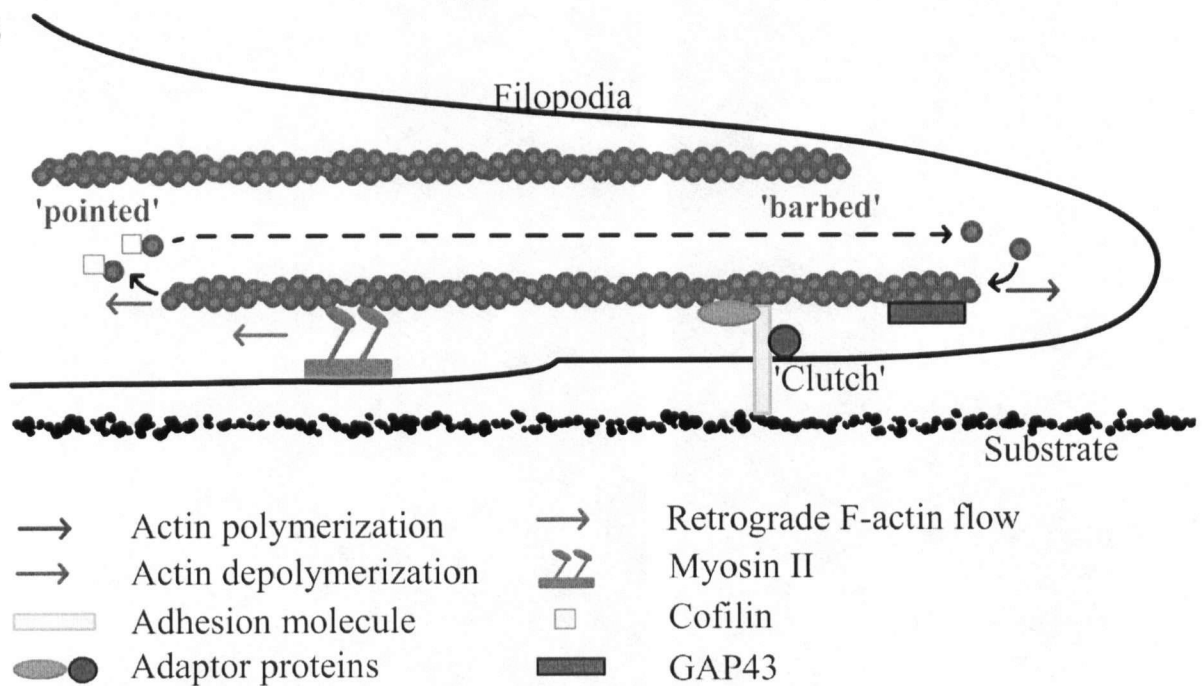

Filopodium

Lamellipodium

P-domain

C-domain

— Microtubules

— Actin filament (F-actin)

• Myosin

B

Filopodia

'pointed'

'barbed'

'Clutch'

Substrate

→ Actin polymerization

→ Actin depolymerization

▭ Adhesion molecule

⬭⬤ Adaptor proteins

→ Retrograde F-actin flow

⋙ Myosin II

▫ Cofilin

▬ GAP43

Figure 1.2

Major elements in the Rho signal-transduction pathway. Numerous guidance/inhibitory molecules activate the Rho pathway. ROCK is one of the downstream effectors of Rho, and it can be inhibited by a specific and membrane-permeable drug, Y27632. ROCK phosphorylates myosin light chain and also myosin phosphatase. This leads to increased association between actin and myosin, and increased contraction of the actin-myosin network. ROCK also phosphorylates LIM kinase, which in turn phosphorylates and inactivates the actin depolymerizing factor, cofilin. mDia (mammalian Dia) is another downstream effect of Rho. mDia binds to and enhances the function of profilin, which promotes actin polymerization.
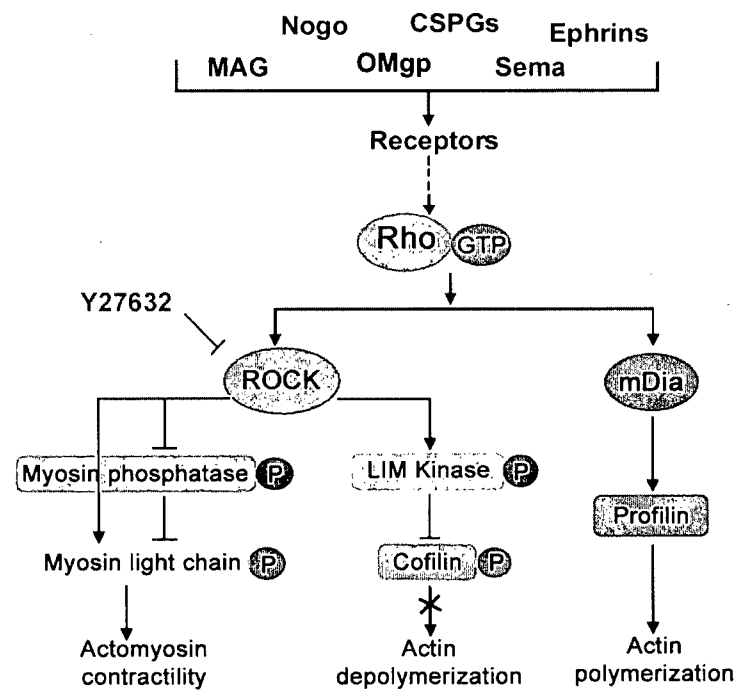
References

Adamson P, Marshall CJ, Hall A, Tilbrook PA (1992a) Post-translational modifications of p21rho proteins. J Biol Chem 267:20033-20038.

Adamson P, Paterson HF, Hall A (1992b) Intracellular localization of the P21rho proteins. J Cell Biol 119:617-627.

Ahmad FJ, Hughey J, Wittmann T, Hyman A, Greaser M, Baas PW (2000) Motor proteins regulate force interactions between microtubules and microfilaments in the axon. Nat Cell Biol 2:276-280.

Aizawa H, Wakatsuki S, Ishii A, Moriyama K, Sasaki Y, Ohashi K, Sekine-Aizawa Y, Sehara-Fujisawa A, Mizuno K, Goshima Y, Yahara I (2001) Phosphorylation of cofilin by LIM-kinase is necessary for semaphorin 3A- induced growth cone collapse. Nat Neurosci 4:367-373.

Akintunde A, Buxton DF (1992) Differential sites of origin and collateralization of corticospinal neurons in the rat: a multiple fluorescent retrograde tracer study. Brain Res 575:86-92.

Allen WE, Zicha D, Ridley AJ, Jones GE (1998) A role for Cdc42 in macrophage chemotaxis. J Cell Biol 141:1147-1157.

Amano M, Chihara K, Nakamura N, Kaneko T, Matsuura Y, Kaibuchi K (1999) The COOH terminus of Rho-kinase negatively regulates rho-kinase activity. J Biol Chem 274:32418-32424.

Amano M, Ito M, Kimura K, Fukata Y, Chihara K, Nakano T, Matsuura Y, Kaibuchi K (1996) Phosphorylation and activation of myosin by Rho-associated kinase (Rho- kinase). J Biol Chem 271:20246-20249.

Arber S, Barbayannis FA, Hanser H, Schneider C, Stanyon CA, Bernard O, Caroni P (1998) Regulation of actin dynamics through phosphorylation of cofilin by LIM-kinase. Nature 393:805-809.

Arimura N, Inagaki N, Chihara K, Menager C, Nakamura N, Amano M, Iwamatsu A, Goshima Y, Kaibuchi K (2000) Phosphorylation of collapsin response mediator protein-2 by Rho-kinase. Evidence for two separate signaling pathways for growth cone collapse. J Biol Chem 275:23973-23980.

Arimura N, Menager C, Kawano Y, Yoshimura T, Kawabata S, Hattori A, Fukata Y, Amano M, Goshima Y, Inagaki M, Morone N, Usukura J, Kaibuchi K (2005) Phosphorylation by Rho kinase regulates CRMP-2 activity in growth cones. Mol Cell Biol 25:9973-9984.

Armand J (1982) The origin, course and terminations of corticospinal fibers in various mammals. Prog Brain Res 57:329-360.

Asher RA, Morgenstern DA, Shearer MC, Adcock KH, Pesheva P, Fawcett JW (2002) Versican is upregulated in CNS injury and is a product of oligodendrocyte lineage cells. J Neurosci 22:2225-2236.

Assouline JG, Bosch P, Lim R, Kim IS, Jensen R, Pantazis NJ (1987) Rat astrocytes and Schwann cells in culture synthesize nerve growth factor-like neurite-promoting factors. Brain Res 428:103-118.

Aurandt J, Vikis HG, Gutkind JS, Ahn N, Guan KL (2002) The semaphorin receptor plexin-B1 signals through a direct interaction with the Rho-specific nucleotide exchange factor, LARG. Proc Natl Acad Sci U S A 99:12085-12090.

Averill S, McMahon SB, Clary DO, Reichardt LF, Priestley JV (1995) Immunocytochemical localization of trkA receptors in chemically identified subgroups of adult rat sensory neurons. Eur J Neurosci 7:1484-1494.

Balentine JD (1978a) Pathology of experimental spinal cord trauma. I. The necrotic lesion as a function of vascular injury. Lab Invest 39:236-253.

Balentine JD (1978b) Pathology of experimental spinal cord trauma. II. Ultrastructure of axons and myelin. Lab Invest 39:254-266.

Ballermann M, McKenna J, Whishaw IQ (2001) A grasp-related deficit in tactile discrimination following dorsal column lesion in the rat. Brain Res Bull 54:237-242.

Bandtlow CE, Schmidt MF, Hassinger TD, Schwab ME, Kater SB (1993) Role of intracellular calcium in NI-35-evoked collapse of neuronal growth cones. Science 259:80-83.

Bandtlow CE, Zimmermann DR (2000) Proteoglycans in the developing brain: new conceptual insights for old proteins. Physiol Rev 80:1267-1290.

Barberis D, Casazza A, Sordella R, Corso S, Artigiani S, Settleman J, Comoglio PM, Tamagnone L (2005) p190 Rho-GTPase activating protein associates with plexins and it is required for semaphorin signalling. J Cell Sci 118:4689-4700.

Bareyre FM, Haudenschild B, Schwab ME (2002) Long-lasting sprouting and gene expression changes induced by the monoclonal antibody IN-1 in the adult spinal cord. J Neurosci 22:7097-7110.

Basu A, Krady JK, Enterline JR, Levison SW (2002) Transforming growth factor beta1 prevents IL-1beta-induced microglial activation, whereas TNFalpha- and IL-6-stimulated activation are not antagonized. Glia 40:109-120.

Bennett DL, Michael GJ, Ramachandran N, Munson JB, Averill S, Yan Q, McMahon SB, Priestley JV (1998) A distinct subgroup of small DRG cells express GDNF receptor components and GDNF is protective for these neurons after nerve injury. J Neurosci 18:3059-3072.

Benson MD, Romero MI, Lush ME, Lu QR, Henkemeyer M, Parada LF (2005) Ephrin-B3 is a myelin-based inhibitor of neurite outgrowth. Proc Natl Acad Sci U S A 102:10694-10699.

Bignami A, Chi NH, Dahl D (1984) Regenerating dorsal roots and the nerve entry zone: an immunofluorescence study with neurofilament and laminin antisera. Exp Neurol 85:426-436.

Bisby MA, Pollock B (1983) Increased regeneration rate in peripheral nerve axons following double lesions: enhancement of the conditioning lesion phenomenon. J Neurobiol 14:467-472.

Bito H, Furuyashiki T, Ishihara H, Shibasaki Y, Ohashi K, Mizuno K, Maekawa M, Ishizaki T, Narumiya S (2000) A critical role for a Rho-associated kinase, p160ROCK, in determining axon outgrowth in mammalian CNS neurons. Neuron 26:431-441.

Blight AR (1983) Cellular morphology of chronic spinal cord injury in the cat: analysis of myelinated axons by line-sampling. Neuroscience 10:521-543.

Blits B, Dijkhuizen PA, Boer GJ, Verhaagen J (2000) Intercostal nerve implants transduced with an adenoviral vector encoding neurotrophin-3 promote regrowth of injured rat corticospinal tract fibers and improve hindlimb function. Exp Neurol 164:25-37.

Borisoff JF, Chan CC, Hiebert GW, Oschipok L, Robertson GS, Zamboni R, Steeves JD, Tetzlaff W (2003) Suppression of Rho-kinase activity promotes axonal growth on inhibitory CNS substrates. Mol Cell Neurosci 22:405-416.

Bradbury EJ, Khemani S, Von R, King, Priestley JV, McMahon SB (1999) NT-3 promotes growth of lesioned adult rat sensory axons ascending in the dorsal columns of the spinal cord. Eur J Neurosci 11:3873-3883.

Bradbury EJ, Moon LD, Popat RJ, King VR, Bennett GS, Patel PN, Fawcett JW, McMahon SB (2002) Chondroitinase ABC promotes functional recovery after spinal cord injury. Nature 416:636-640.

Bregman BS, Broude E, McAtee M, Kelley MS (1998) Transplants and neurotrophic factors prevent atrophy of mature CNS neurons after spinal cord injury. Exp Neurol 149:13-27.

Bregman BS, Kunkel-Bagden E, Schnell L, Dai HN, Gao D, Schwab ME (1995) Recovery from spinal cord injury mediated by antibodies to neurite growth inhibitors. Nature 378:498-501.

Bregman BS, McAtee M, Dai HN, Kuhn PL (1997) Neurotrophic factors increase axonal growth after spinal cord injury and transplantation in the adult rat. Exp Neurol 148:475-494.

Bresnahan JC, King JS, Martin GF, Yashon D (1976) A neuroanatomical analysis of spinal cord injury in the rhesus monkey (Macaca mulatta). J Neurol Sci 28:521-542.

Brewer KL, Bethea JR, Yezierski RP (1999) Neuroprotective effects of interleukin-10 following excitotoxic spinal cord injury. Exp Neurol 159:484-493.

Brosamle C, Schwab ME (1997) Cells of origin, course, and termination patterns of the ventral, uncrossed component of the mature rat corticospinal tract. J Comp Neurol 386:293-303.

Buck KB, Zheng JQ (2002) Growth cone turning induced by direct local modification of microtubule dynamics. J Neurosci 22:9358-9367.

Buffo A, Zagrebelsky M, Huber AB, Skerra A, Schwab ME, Strata P, Rossi F (2000) Application of neutralizing antibodies against NI-35/250 myelin- associated neurite growth inhibitory proteins to the adult rat cerebellum induces sprouting of uninjured purkinje cell axons. J Neurosci 20:2275-2286.

Bundesen LQ, Scheel TA, Bregman BS, Kromer LF (2003) Ephrin-B2 and EphB2 regulation of astrocyte-meningeal fibroblast interactions in response to spinal cord lesions in adult rats. J Neurosci 23:7789-7800.

Bunge RP, Puckett WR, Hiester ED (1997) Observations on the pathology of several types of human spinal cord injury, with emphasis on the astrocyte response to penetrating injuries. Adv Neurol 72:305-315.

Caggiano AO, Zimber MP, Ganguly A, Blight AR, Gruskin EA (2005) Chondroitinase ABCI Improves Locomotion and Bladder Function following Contusion Injury of the Rat Spinal Cord. J Neurotrauma 22:226-239.

Cai D, Shen Y, De Bellard M, Tang S, Filbin MT (1999) Prior exposure to neurotrophins blocks inhibition of axonal regeneration by MAG and myelin via a cAMP-dependent mechanism. Neuron 22:89-101.

Calvo JL, Carbonell AL, Boya J (1991) Co-expression of glial fibrillary acidic protein and vimentin in reactive astrocytes following brain injury in rats. Brain Res 566:333-336.

Campbell DS, Regan AG, Lopez JS, Tannahill D, Harris WA, Holt CE (2001) Semaphorin 3A elicits stage-dependent collapse, turning, and branching in Xenopus retinal growth cones. J Neurosci 21:8538-8547.

Canning DR, Hoke A, Malemud CJ, Silver J (1996) A potent inhibitor of neurite outgrowth that predominates in the extracellular matrix of reactive astrocytes. Int J Dev Neurosci 14:153-175.

Carulli D, Laabs T, Geller HM, Fawcett JW (2005) Chondroitin sulfate proteoglycans in neural development and regeneration. Curr Opin Neurobiol 15:116-120.

Casale EJ, Light AR, Rustioni A (1988) Direct projection of the corticospinal tract to the superficial laminae of the spinal cord in the rat. J Comp Neurol 278:275-286.

Challacombe JF, Snow DM, Letourneau PC (1996) Actin filament bundles are required for microtubule reorientation during growth cone turning to avoid an inhibitory guidance cue. J Cell Sci 109 (Pt 8):2031-2040.

Challacombe JF, Snow DM, Letourneau PC (1997) Dynamic microtubule ends are required for growth cone turning to avoid an inhibitory guidance cue. J Neurosci 17:3085-3095.

Chan SS, Zheng H, Su MW, Wilk R, Killeen MT, Hedgecock EM, Culotti JG (1996) UNC-40, a C. elegans homolog of DCC (Deleted in Colorectal Cancer), is required in motile cells responding to UNC-6 netrin cues. Cell 87:187-195.

Chau CH, Shum DK, Li H, Pei J, Lui YY, Wirthlin L, Chan YS, Xu XM (2004) Chondroitinase ABC enhances axonal regrowth through Schwann cell-seeded guidance channels after spinal cord injury. FASEB J 18:194-196.

Chen A, Xu XM, Kleitman N, Bunge MB (1996) Methylprednisolone administration improves axonal regeneration into Schwann cell grafts in transected adult rat thoracic spinal cord. Exp Neurol 138:261-276.

Chen MS, Huber AB, van der Haar ME, Frank M, Schnell L, Spillmann AA, Christ F, Schwab ME (2000) Nogo-A is a myelin-associated neurite outgrowth inhibitor and an antigen for monoclonal antibody IN-1. Nature 403:434-439.

Cheng H, Almstrom S, Gimenez-Llort L, Chang R, Ove OS, Hoffer B, Olson L (1997) Gait analysis of adult paraplegic rats after spinal cord repair. Exp Neurol 148:544-557.

Cheng H, Cao Y, Olson L (1996) Spinal cord repair in adult paraplegic rats: partial restoration of hind limb function. Science 273:510-513.

Cherfils J, Chardin P (1999) GEFs: structural basis for their activation of small GTP-binding proteins. Trends Biochem Sci 24:306-311.

Chong MS, Reynolds ML, Irwin N, Coggeshall RE, Emson PC, Benowitz LI, Woolf CJ (1994) GAP-43 expression in primary sensory neurons following central axotomy. J Neurosci 14:4375-4384.

Christensen MD, Everhart AW, Pickelman JT, Hulsebosch CE (1996) Mechanical and thermal allodynia in chronic central pain following spinal cord injury. Pain 68:97-107.

Conrad S, Schluesener HJ, Trautmann K, Joannin N, Meyermann R, Schwab JM (2005) Prolonged lesional expression of RhoA and RhoB following spinal cord injury. J Comp Neurol 487:166-175.

Cooper BY, Glendinning DS, Vierck CJ, Jr. (1993) Finger movement deficits in the stumptail macaque following lesions of the fasciculus cuneatus. Somatosens Mot Res 10:17-29.

Crowe MJ, Bresnahan JC, Shuman SL, Masters JN, Beattie MS (1997) Apoptosis and delayed degeneration after spinal cord injury in rats and monkeys. Nat Med 3:73-76.

David S, Aguayo AJ (1981) Axonal elongation into peripheral nervous system "bridges" after central nervous system injury in adult rats. Science 214:931-933.

Davies SJ, Fitch MT, Memberg SP, Hall AK, Raisman G, Silver J (1997) Regeneration of adult axons in white matter tracts of the central nervous system. Nature 390:680-683.

Davies SJ, Goucher DR, Doller C, Silver J (1999) Robust regeneration of adult sensory axons in degenerating white matter of the adult rat spinal cord. J Neurosci 19:5810-5822.

De WF, Oudega M, Lankhorst AJ, Hamers FP, Blits B, Ruitenberg MJ, Pasterkamp RJ, Gispen WH, Verhaagen J (2002) Injury-induced class 3 semaphorin expression in the rat spinal cord. Exp Neurol 175:61-75.

Del Rio JA, Gonzalez-Billault C, Urena JM, Jimenez EM, Barallobre MJ, Pascual M, Pujadas L, Simo S, La TA, Wandosell F, Avila J, Soriano E (2004) MAP1B is required for Netrin 1 signaling in neuronal migration and axonal guidance. Curr Biol 14:840-850.

Dent EW, Gertler FB (2003) Cytoskeletal dynamics and transport in growth cone motility and axon guidance. Neuron 40:209-227.

Deo RC, Schmidt EF, Elhabazi A, Togashi H, Burley SK, Strittmatter SM (2004) Structural bases for CRMP function in plexin-dependent semaphorin3A signaling. EMBO J 23:9-22.

Dergham P, Ellezam B, Essagian C, Avedissian H, Lubell WD, McKerracher L (2002) Rho signaling pathway targeted to promote spinal cord repair. J Neurosci 22:6570-6577.

Dickson BJ (2001) Rho GTPases in growth cone guidance. Curr Opin Neurobiol 11:103-110.

Domeniconi M, Cao Z, Spencer T, Sivasankaran R, Wang K, Nikulina E, Kimura N, Cai H, Deng K, Gao Y, He Z, Filbin M (2002) Myelin-associated glycoprotein interacts with the Nogo66 receptor to inhibit neurite outgrowth. Neuron 35:283-290.

Domeniconi M, Zampieri N, Spencer T, Hilaire M, Mellado W, Chao MV, Filbin MT (2005) MAG Induces Regulated Intramembrane Proteolysis of the p75 Neurotrophin Receptor to Inhibit Neurite Outgrowth. Neuron 46:849-855.

Dong Y, Pruyne D, Bretscher A (2003) Formin-dependent actin assembly is regulated by distinct modes of Rho signaling in yeast. J Cell Biol 161:1081-1092.

Dontchev VD, Letourneau PC (2002) Nerve growth factor and semaphorin 3A signaling pathways interact in regulating sensory neuronal growth cone motility. J Neurosci 22:6659-6669.

Doster SK, Lozano AM, Aguayo AJ, Willard MB (1991) Expression of the growth-associated protein GAP-43 in adult rat retinal ganglion cells following axon injury. Neuron 6:635-647.

Dou CL, Levine JM (1997) Identification of a neuronal cell surface receptor for a growth inhibitory chondroitin sulfate proteoglycan (NG2). J Neurochem 68:1021-1030.

Dou CL, Levine JM (1994) Inhibition of neurite growth by the NG2 chondroitin sulfate proteoglycan. J Neurosci 14:7616-7628.

Drew T (1993) Motor cortical activity during voluntary gait modifications in the cat. I. Cells related to the forelimbs. J Neurophysiol 70:179-199.

Dubreuil CI, Winton MJ, McKerracher L (2003) Rho activation patterns after spinal cord injury and the role of activated Rho in apoptosis in the central nervous system. J Cell Biol 162:233-243.

Dusart I, Schwab ME (1994) Secondary cell death and the inflammatory reaction after dorsal hemisection of the rat spinal cord. Eur J Neurosci 6:712-724.

Eide PK (1998) Pathophysiological mechanisms of central neuropathic pain after spinal cord injury. Spinal Cord 36:601-612.

Eide PK, Jorum E, Stenehjem AE (1996) Somatosensory findings in patients with spinal cord injury and central dysaesthesia pain. J Neurol Neurosurg Psychiatry 60:411-415.

Eng LF, Reier PJ, Houle JD (1987) Astrocyte activation and fibrous gliosis: glial fibrillary acidic protein immunostaining of astrocytes following intraspinal cord grafting of fetal CNS tissue. Prog Brain Res 71:439-455.

Ernfors P (2001) Local and target-derived actions of neurotrophins during peripheral nervous system development. Cell Mol Life Sci 58:1036-1044.

Ernfors P, Lee KF, Kucera J, Jaenisch R (1994) Lack of neurotrophin-3 leads to deficiencies in the peripheral nervous system and loss of limb proprioceptive afferents. Cell 77:503-512.

Evangelista M, Zigmond S, Boone C (2003) Formins: signaling effectors for assembly and polarization of actin filaments. J Cell Sci 116:2603-2611.

Fawcett JW, Asher RA (1999) The glial scar and central nervous system repair. Brain Res Bull 49:377-391.

Feng J, Ito M, Ichikawa K, Isaka N, Nishikawa M, Hartshorne DJ, Nakano T (1999) Inhibitory phosphorylation site for Rho-associated kinase on smooth muscle myosin phosphatase. J Biol Chem 274:37385-37390.

Fernandes KJ, Fan DP, Tsui BJ, Cassar SL, Tetzlaff W (1999) Influence of the axotomy to cell body distance in rat rubrospinal and spinal motoneurons: differential regulation of GAP-43, tubulins, and neurofilament-M. J Comp Neurol 414:495-510.

Fernandes KJ, Tetzlaff W (2001) Gene expression in axotomized neurons: Identifying the intrinsic determinants of axonal growth. In: Axonal regeneration in the central nervous system (Ingoglia N, Murray M, eds), pp 219-266. New York: Marcel Dekker.

Fernandez E, Pallini R, Mercanti D (1990) Effects of topically administered nerve growth factor on axonal regeneration in peripheral nerve autografts implanted in the spinal cord of rats. Neurosurgery 26:37-42.

Fitch MT, Doller C, Combs CK, Landreth GE, Silver J (1999) Cellular and molecular mechanisms of glial scarring and progressive cavitation: in vivo and in vitro analysis of inflammation-induced secondary injury after CNS trauma. J Neurosci 19:8182-8198.

Fok-Seang J, Smith-Thomas LC, Meiners S, Muir E, Du JS, Housden E, Johnson AR, Faissner A, Geller HM, Keynes RJ, . (1995) An analysis of astrocytic cell lines with different abilities to promote axon growth. Brain Res 689:207-223.

Forscher P, Lin CH, Thompson C (1992) Novel form of growth cone motility involving site-directed actin filament assembly. Nature 357:515-518.

Forscher P, Smith SJ (1988) Actions of cytochalasins on the organization of actin filaments and microtubules in a neuronal growth cone. J Cell Biol 107:1505-1516.

Fouad K, Schnell L, Bunge MB, Schwab ME, Liebscher T, Pearse DD (2005) Combining Schwann cell bridges and olfactory-ensheathing glia grafts with chondroitinase promotes locomotor recovery after complete transection of the spinal cord. J Neurosci 25:1169-1178.

Fournier AE, GrandPre T, Strittmatter SM (2001) Identification of a receptor mediating Nogo-66 inhibition of axonal regeneration. Nature 409:341-346.

Fournier AE, Takizawa BT, Strittmatter SM (2003) Rho kinase inhibition enhances axonal regeneration in the injured CNS. J Neurosci 23:1416-1423.

Frisen J, Johansson CB, Torok C, Risling M, Lendahl U (1995) Rapid, widespread, and longlasting induction of nestin contributes to the generation of glial scar tissue after CNS injury. J Cell Biol 131:453-464.

Fu SY, Gordon T (1997) The cellular and molecular basis of peripheral nerve regeneration. Mol Neurobiol 14:67-116.

Fujiki M, Zhang Z, Guth L, Steward O (1996) Genetic influences on cellular reactions to spinal cord injury: activation of macrophages/microglia and astrocytes is delayed in mice carrying a mutation (WldS) that causes delayed Wallerian degeneration. J Comp Neurol 371:469-484.

Fukata Y, Itoh TJ, Kimura T, Menager C, Nishimura T, Shiromizu T, Watanabe H, Inagaki N, Iwamatsu A, Hotani H, Kaibuchi K (2002) CRMP-2 binds to tubulin heterodimers to promote microtubule assembly. Nat Cell Biol 4:583-591.

Fundin BT, Silos-Santiago I, Ernfors P, Fagan AM, Aldskogius H, DeChiara TM, Phillips HS, Barbacid M, Yancopoulos GD, Rice FL (1997) Differential dependency of cutaneous mechanoreceptors on neurotrophins, trk receptors, and P75 LNGFR. Dev Biol 190:94-116.

Gallo G (2004) Myosin II activity is required for severing-induced axon retraction in vitro. Exp Neurol 189:112-121.

Gallo G, Letourneau PC (2004) Regulation of growth cone actin filaments by guidance cues. J Neurobiol 58:92-102.

Gallo G, Yee HF, Jr., Letourneau PC (2002) Actin turnover is required to prevent axon retraction driven by endogenous actomyosin contractility. J Cell Biol 158:1219-1228.

Gehler S, Shaw AE, Sarmiere PD, Bamburg JR, Letourneau PC (2004) Brain-derived neurotrophic factor regulation of retinal growth cone filopodial dynamics is mediated through actin depolymerizing factor/cofilin. J Neurosci 24:10741-10749.

Geisert EE, Jr., Bidanset DJ (1993) A central nervous system keratan sulfate proteoglycan: localization to boundaries in the neonatal rat brain. Brain Res Dev Brain Res 75:163-173.

Giehl KM, Tetzlaff W (1996) BDNF and NT-3, but not NGF, prevent axotomy-induced death of rat corticospinal neurons in vivo. Eur J Neurosci 8:1167-1175.

Gilbert RJ, McKeon RJ, Darr A, Calabro A, Hascall VC, Bellamkonda RV (2005) CS-4,6 is differentially upregulated in glial scar and is a potent inhibitor of neurite extension. Mol Cell Neurosci.

Glendinning DS, Vierck CJ, Jr., Cooper BY (1993) The effect of fasciculus cuneatus lesions on finger positioning and long-latency reflexes in monkeys. Exp Brain Res 93:104-116.

Gloor S, Odink K, Guenther J, Nick H, Monard D (1986) A glia-derived neurite promoting factor with protease inhibitory activity belongs to the protease nexins. Cell 47:687-693.

Goldschmidt-Clermont PJ, Furman MI, Wachsstock D, Safer D, Nachmias VT, Pollard TD (1992) The control of actin nucleotide exchange by thymosin beta 4 and profilin. A potential regulatory mechanism for actin polymerization in cells. Mol Biol Cell 3:1015-1024.

Gomez TM, Roche FK, Letourneau PC (1996) Chick sensory neuronal growth cones distinguish fibronectin from laminin by making substratum contacts that resemble focal contacts. J Neurobiol 29:18-34.

Gordon-Weeks PR (1987) The cytoskeletons of isolated, neuronal growth cones. Neuroscience 21:977-989.

Goshima Y, Nakamura F, Strittmatter P, Strittmatter SM (1995) Collapsin-induced growth cone collapse mediated by an intracellular protein related to UNC-33. Nature 376:509-514.

Gotta M, Abraham MC, Ahringer J (2001) CDC-42 controls early cell polarity and spindle orientation in C. elegans. Curr Biol 11:482-488.

GrandPre T, Li S, Strittmatter SM (2002) Nogo-66 receptor antagonist peptide promotes axonal regeneration. Nature 417:547-551.

GrandPre T, Nakamura F, Vartanian T, Strittmatter SM (2000) Identification of the Nogo inhibitor of axon regeneration as a Reticulon protein. Nature 403:439-444.

Grierson JP, Petroski RE, Ling DS, Geller HM (1990) Astrocyte topography and tenascin cytotactin expression: correlation with the ability to support neuritic outgrowth. Brain Res Dev Brain Res 55:11-19.

Grill R, Murai K, Blesch A, Gage FH, Tuszynski MH (1997) Cellular delivery of neurotrophin-3 promotes corticospinal axonal growth and partial functional recovery after spinal cord injury. J Neurosci 17:5560-5572.

Grimpe B, Silver J (2004) A novel DNA enzyme reduces glycosaminoglycan chains in the glial scar and allows microtransplanted dorsal root ganglia axons to regenerate beyond lesions in the spinal cord. J Neurosci 24:1393-1397.

Grimpe B, Silver J (2002) The extracellular matrix in axon regeneration. Prog Brain Res 137:333-349.

Groves AK, Entwistle A, Jat PS, Noble M (1993) The characterization of astrocyte cell lines that display properties of glial scar tissue. Dev Biol 159:87-104.

Gu Y, Ihara Y (2000) Evidence that collapsin response mediator protein-2 is involved in the dynamics of microtubules. J Biol Chem 275:17917-17920.

Guan KL, Rao Y (2003) Signalling mechanisms mediating neuronal responses to guidance cues. Nat Rev Neurosci 4:941-956.

Guest JD, Rao A, Olson L, Bunge MB, Bunge RP (1997) The ability of human Schwann cell grafts to promote regeneration in the transected nude rat spinal cord. Exp Neurol 148:502-522.

Gungabissoon RA, Bamburg JR (2003) Regulation of growth cone actin dynamics by ADF/cofilin. J Histochem Cytochem 51:411-420.

Hains BC, Yucra JA, Hulsebosch CE (2001) Reduction of pathological and behavioral deficits following spinal cord contusion injury with the selective cyclooxygenase-2 inhibitor NS-398. J Neurotrauma 18:409-423.

Hall C, Brown M, Jacobs T, Ferrari G, Cann N, Teo M, Monfries C, Lim L (2001) Collapsin response mediator protein switches RhoA and Rac1 morphology in N1E-115 neuroblastoma cells and is regulated by Rho kinase. J Biol Chem 276:43482-43486.

Hamelin M, Zhou Y, Su MW, Scott IM, Culotti JG (1993) Expression of the UNC-5 guidance receptor in the touch neurons of C. elegans steers their axons dorsally. Nature 364:327-330.

He Q, Dent EW, Meiri KF (1997) Modulation of actin filament behavior by GAP-43 (neuromodulin) is dependent on the phosphorylation status of serine 41, the protein kinase C site. J Neurosci 17:3515-3524.

Herx LM, Yong VW (2001) Interleukin-1 beta is required for the early evolution of reactive astrogliosis following CNS lesion. J Neuropathol Exp Neurol 60:961-971.

Hicks SP, D'Amato CJ (1975) Motor-sensory cortex-corticospinal system and developing locomotion and placing in rats. Am J Anat 143:1-42.

Hicks SP, D'Amato CJ (1977) Locating corticospinal neurons by retrograde axonal transport of horseradish peroxidase. Exp Neurol 56:410-420.

Hiebert GW, Khodarahmi K, McGraw J, Steeves JD, Tetzlaff W (2002) Brain-derived neurotrophic factor applied to the motor cortex promotes sprouting of corticospinal fibers but not regeneration into a peripheral nerve transplant. J Neurosci Res 69:160-168.

Hirose M, Ishizaki T, Watanabe N, Uehata M, Kranenburg O, Moolenaar WH, Matsumura F, Maekawa M, Bito H, Narumiya S (1998) Molecular dissection of the Rho-associated protein kinase (p160ROCK)- regulated neurite remodeling in neuroblastoma N1E-115 cells. J Cell Biol 141:1625-1636.

Hoffman PN (1989) Expression of GAP-43, a rapidly transported growth-associated protein, and class II beta tubulin, a slowly transported cytoskeletal protein, are coordinated in regenerating neurons. J Neurosci 9:893-897.

Houle JD, Tessler A (2003) Repair of chronic spinal cord injury. Exp Neurol 182:247-260.

Houweling DA, Lankhorst AJ, Gispen WH, Bar PR, Joosten EA (1998) Collagen containing neurotrophin-3 (NT-3) attracts regrowing injured corticospinal axons in the adult rat spinal cord and promotes partial functional recovery. Exp Neurol 153:49-59.

Hsieh SH, Ferraro GB, Fournier AE (2006) Myelin-associated inhibitors regulate cofilin phosphorylation and neuronal inhibition through LIM kinase and Slingshot phosphatase. J Neurosci 26:1006-1015.

Hsu JY, Stein SA, Xu XM (2005) Temporal and spatial distribution of growth-associated molecules and astroglial cells in the rat corticospinal tract during development. J Neurosci Res 80:330-340.

Hu H, Marton TF, Goodman CS (2001) Plexin B mediates axon guidance in Drosophila by simultaneously inhibiting active Rac and enhancing RhoA signaling. Neuron 32:39-51.

Huber AB, Kolodkin AL, Ginty DD, Cloutier JF (2003) Signaling at the Growth Cone: Ligand-Receptor Complexes and the Control of Axon Growth and Guidance. Annu Rev Neurosci.

Hyland B (1998) Neural activity related to reaching and grasping in rostral and caudal regions of rat motor cortex. Behav Brain Res 94:255-269.

Hynds DL, Snow DM (1999) Neurite outgrowth inhibition by chondroitin sulfate proteoglycan: stalling/stopping exceeds turning in human neuroblastoma growth cones. Exp Neurol 160:244-255.

Ikegami T, Nakamura M, Yamane J, Katoh H, Okada S, Iwanami A, Watanabe K, Ishii K, Kato F, Fujita H, Takahashi T, Okano HJ, Toyama Y, Okano H (2005) Chondroitinase ABC

combined with neural stem/progenitor cell transplantation enhances graft cell migration and outgrowth of growth-associated protein-43-positive fibers after rat spinal cord injury. Eur J Neurosci 22:3036-3046.

Ishizaki T, Maekawa M, Fujisawa K, Okawa K, Iwamatsu A, Fujita A, Watanabe N, Saito Y, Kakizuka A, Morii N, Narumiya S (1996) The small GTP-binding protein Rho binds to and activates a 160 kDa Ser/Thr protein kinase homologous to myotonic dystrophy kinase. EMBO J 15:1885-1893.

Ishizaki T, Naito M, Fujisawa K, Maekawa M, Watanabe N, Saito Y, Narumiya S (1997) p160ROCK, a Rho-associated coiled-coil forming protein kinase, works downstream of Rho and induces focal adhesions. FEBS Lett 404:118-124.

Jalink K, van Corven EJ, Hengeveld T, Morii N, Narumiya S, Moolenaar WH (1994) Inhibition of lysophosphatidate- and thrombin-induced neurite retraction and neuronal cell rounding by ADP ribosylation of the small GTP-binding protein Rho. J Cell Biol 126:801-810.

Jandik KA, Gu K, Linhardt RJ (1994) Action pattern of polysaccharide lyases on glycosaminoglycans. Glycobiology 4:289-296.

Janeczko K (1989) Spatiotemporal patterns of the astroglial proliferation in rat brain injured at the postmitotic stage of postnatal development: a combined immunocytochemical and autoradiographic study. Brain Res 485:236-243.

Jaworski DM, Kelly GM, Hockfield S (1999) Intracranial injury acutely induces the expression of the secreted isoform of the CNS-specific hyaluronan-binding protein BEHAB/brevican. Exp Neurol 157:327-337.

Jin M, Guan CB, Jiang YA, Chen G, Zhao CT, Cui K, Song YQ, Wu CP, Poo MM, Yuan XB (2005) Ca2+-dependent regulation of rho GTPases triggers turning of nerve growth cones. J Neurosci 25:2338-2347.

Jin Z, Strittmatter SM (1997) Rac1 mediates collapsin-1-induced growth cone collapse. J Neurosci 17:6256-6263.

Jones LL, Margolis RU, Tuszynski MH (2003) The chondroitin sulfate proteoglycans neurocan, brevican, phosphacan, and versican are differentially regulated following spinal cord injury. Exp Neurol 182:399-411.

Joosten EA, Gribnau AA (1989) Astrocytes and guidance of outgrowing corticospinal tract axons in the rat. An immunocytochemical study using anti-vimentin and anti-glial fibrillary acidic protein. Neuroscience 31:439-452.

Joosten EA, Schuitman RL, Vermelis ME, Dederen PJ (1992) Postnatal development of the ipsilateral corticospinal component in rat spinal cord: a light and electron microscopic anterograde HRP study. J Comp Neurol 326:133-146.

Kashiba H, Uchida Y, Senba E (2003) Distribution and colocalization of NGF and GDNF family ligand receptor mRNAs in dorsal root and nodose ganglion neurons of adult rats. Brain Res Mol Brain Res 110:52-62.

Keino-Masu K, Masu M, Hinck L, Leonardo ED, Chan SS, Culotti JG, Tessier-Lavigne M (1996) Deleted in Colorectal Cancer (DCC) encodes a netrin receptor. Cell 87:175-185.

Khodarahmi K, Tetzlaff W, Hiebert GW (2001) BDNF infusion into the motor cortex promotes sprouting of intact corticospinal fibers within the cervical spinal cord.

Kimura K, Ito M, Amano M, Chihara K, Fukata Y, Nakafuku M, Yamamori B, Feng J, Nakano T, Okawa K, Iwamatsu A, Kaibuchi K (1996) Regulation of myosin phosphatase by Rho and Rho-associated kinase (Rho-kinase). Science 273:245-248.

Klusman I, Schwab ME (1997) Effects of pro-inflammatory cytokines in experimental spinal cord injury. Brain Res 762:173-184.

Kobayashi NR, Fan DP, Giehl KM, Bedard AM, Wiegand SJ, Tetzlaff W (1997) BDNF and NT-4/5 prevent atrophy of rat rubrospinal neurons after cervical axotomy, stimulate GAP-43 and Talpha1-tubulin mRNA expression, and promote axonal regeneration. J Neurosci 17:9583-9595.

Kottis V, Thibault P, Mikol D, Xiao ZC, Zhang R, Dergham P, Braun PE (2002) Oligodendrocyte-myelin glycoprotein (OMgp) is an inhibitor of neurite outgrowth. J Neurochem 82:1566-1569.

Kozma R, Ahmed S, Best A, Lim L (1995) The Ras-related protein Cdc42Hs and bradykinin promote formation of peripheral actin microspikes and filopodia in Swiss 3T3 fibroblasts. Mol Cell Biol 15:1942-1952.

Kozma R, Sarner S, Ahmed S, Lim L (1997) Rho family GTPases and neuronal growth cone remodelling: relationship between increased complexity induced by Cdc42Hs, Rac1, and acetylcholine and collapse induced by RhoA and lysophosphatidic acid. Mol Cell Biol 17:1201-1211.

Kranenburg O, Poland M, Gebbink M, Oomen L, Moolenaar WH (1997) Dissociation of LPA-induced cytoskeletal contraction from stress fiber formation by differential localization of RhoA. J Cell Sci 110 (Pt 19):2417-2427.

Krautstrunk M, Scholtes F, Martin D, Schoenen J, Schmitt AB, Plate D, Nacimiento W, Noth J, Brook GA (2002) Increased expression of the putative axon growth-repulsive extracellular matrix molecule, keratan sulphate proteoglycan, following traumatic injury of the adult rat spinal cord. Acta Neuropathol (Berl) 104:592-600.

Kucera J, Fan G, Jaenisch R, Linnarsson S, Ernfors P (1995) Dependence of developing group Ia afferents on neurotrophin-3. J Comp Neurol 363:307-320.

Kwon BK, Liu J, Messerer C, Kobayashi NR, McGraw J, Oschipok L, Tetzlaff W (2002) Survival and regeneration of rubrospinal neurons 1 year after spinal cord injury. Proc Natl Acad Sci U S A 99:3246-3251.

Lamarche N, Hall A (1994) GAPs for rho-related GTPases. Trends Genet 10:436-440.

Lassing I, Lindberg U (1985) Specific interaction between phosphatidylinositol 4,5-bisphosphate and profilactin. Nature 314:472-474.

Lee YB, Yune TY, Baik SY, Shin YH, Du S, Rhim H, Lee EB, Kim YC, Shin ML, Markelonis GJ, Oh TH (2000a) Role of tumor necrosis factor-alpha in neuronal and glial apoptosis after spinal cord injury. Exp Neurol 166:190-195.

Lee YL, Shih K, Bao P, Ghirnikar RS, Eng LF (2000b) Cytokine chemokine expression in contused rat spinal cord. Neurochem Int 36:417-425.

Lefcort F, Clary DO, Rusoff AC, Reichardt LF (1996) Inhibition of the NT-3 receptor TrkC, early in chick embryogenesis, results in severe reductions in multiple neuronal subpopulations in the dorsal root ganglia. J Neurosci 16:3704-3713.

Lefrancois T, Fages C, Peschanski M, Tardy M (1997) Neuritic outgrowth associated with astroglial phenotypic changes induced by antisense glial fibrillary acidic protein (GFAP) mRNA in injured neuron-astrocyte cocultures. J Neurosci 17:4121-4128.

Lehmann M, Fournier A, Selles-Navarro I, Dergham P, Sebok A, Leclerc N, Tigyi G, McKerracher L (1999) Inactivation of Rho signaling pathway promotes CNS axon regeneration. J Neurosci 19:7537-7547.

Lemons ML, Howland DR, Anderson DK (1999) Chondroitin sulfate proteoglycan immunoreactivity increases following spinal cord injury and transplantation. Exp Neurol 160:51-65.

Leong SK (1983) Localizing the corticospinal neurons in neonatal, developing and mature albino rat. Brain Res 265:1-9.

Letourneau PC (1983) Differences in the organization of actin in the growth cones compared with the neurites of cultured neurons from chick embryos. J Cell Biol 97:963-973.

Leung T, Manser E, Tan L, Lim L (1995) A novel serine/threonine kinase binding the Ras-related RhoA GTPase which translocates the kinase to peripheral membranes. J Biol Chem 270:29051-29054.

Levine JM (1994) Increased expression of the NG2 chondroitin-sulfate proteoglycan after brain injury. J Neurosci 14:4716-4730.

Li M, Shibata A, Li C, Braun PE, McKerracher L, Roder J, Kater SB, David S (1996) Myelin-associated glycoprotein inhibits neurite/axon growth and causes growth cone collapse. J Neurosci Res 46:404-414.

Li Y, Field PM, Raisman G (1998) Regeneration of adult rat corticospinal axons induced by transplanted olfactory ensheathing cells. J Neurosci 18:10514-10524.

Li Y, Raisman G (1994) Schwann cells induce sprouting in motor and sensory axons in the adult rat spinal cord. J Neurosci 14:4050-4063.

Liang FY, Moret V, Wiesendanger M, Rouiller EM (1991) Corticomotoneuronal connections in the rat: evidence from double-labeling of motoneurons and corticospinal axon arborizations. J Comp Neurol 311:356-366.

Liesi P, Dahl D, Vaheri A (1983) Laminin is produced by early rat astrocytes in primary culture. J Cell Biol 96:920-924.

Liesi P, Kirkwood T, Vaheri A (1986) Fibronectin is expressed by astrocytes cultured from embryonic and early postnatal rat brain. Exp Cell Res 163:175-185.

Lin CH, Espreafico EM, Mooseker MS, Forscher P (1996) Myosin drives retrograde F-actin flow in neuronal growth cones. Neuron 16:769-782.

Lin CH, Forscher P (1993) Cytoskeletal remodeling during growth cone-target interactions. J Cell Biol 121:1369-1383.

Lin CH, Forscher P (1995) Growth cone advance is inversely proportional to retrograde F-actin flow. Neuron 14:763-771.

Liu BP, Fournier A, GrandPre T, Strittmatter SM (2002) Myelin-associated glycoprotein as a functional ligand for the Nogo-66 receptor. Science 297:1190-1193.

Liu XZ, Xu XM, Hu R, Du C, Zhang SX, McDonald JW, Dong HX, Wu YJ, Fan GS, Jacquin MF, Hsu CY, Choi DW (1997) Neuronal and glial apoptosis after traumatic spinal cord injury. J Neurosci 17:5395-5406.

Liuzzi FJ, Lasek RJ (1987) Astrocytes block axonal regeneration in mammals by activating the physiological stop pathway. Science 237:642-645.

Loy DN, Talbott JF, Onifer SM, Mills MD, Burke DA, Dennison JB, Fajardo LC, Magnuson DS, Whittemore SR (2002) Both dorsal and ventral spinal cord pathways contribute to overground locomotion in the adult rat. Exp Neurol 177:575-580.

Lu P, Yang H, Jones LL, Filbin MT, Tuszynski MH (2004) Combinatorial therapy with neurotrophins and cAMP promotes axonal regeneration beyond sites of spinal cord injury. J Neurosci 24:6402-6409.

Lundstrom A, Gallio M, Englund C, Steneberg P, Hemphala J, Aspenstrom P, Keleman K, Falileeva L, Dickson BJ, Samakovlis C (2004) Vilse, a conserved Rac/Cdc42 GAP mediating Robo repulsion in tracheal cells and axons. Genes Dev 18:2161-2171.

Luo L (2000) Rho GTPases in neuronal morphogenesis. Nat Rev Neurosci 1:173-180.

Luo L (2002) Actin cytoskeleton regulation in neuronal morphogenesis and structural plasticity. Annu Rev Cell Dev Biol 18:601-635.

Luo Y, Raper JA (1994) Inhibitory factors controlling growth cone motility and guidance. Curr Opin Neurobiol 4:648-654.

Lyuksyutova AI, Lu CC, Milanesio N, King LA, Guo N, Wang Y, Nathans J, Tessier-Lavigne M, Zou Y (2003) Anterior-posterior guidance of commissural axons by Wnt-frizzled signaling. Science 302:1984-1988.

Ma W, Peschanski M, Ralston HJ, III (1987) The differential synaptic organization of the spinal and lemniscal projections to the ventrobasal complex of the rat thalamus. Evidence for convergence of the two systems upon single thalamic neurons. Neuroscience 22:925-934.

Mack TG, Koester MP, Pollerberg GE (2000) The microtubule-associated protein MAP1B is involved in local stabilization of turning growth cones. Mol Cell Neurosci 15:51-65.

MacKay-Lyons M (2002) Central pattern generation of locomotion: a review of the evidence. Phys Ther 82:69-83.

Madaule P, Axel R (1985) A novel ras-related gene family. Cell 41:31-40.

Madura T, Yamashita T, Kubo T, Fujitani M, Hosokawa K, Tohyama M (2004) Activation of Rho in the injured axons following spinal cord injury. EMBO Rep 5:412-417.

Maekawa M, Ishizaki T, Boku S, Watanabe N, Fujita A, Iwamatsu A, Obinata T, Ohashi K, Mizuno K, Narumiya S (1999) Signaling from Rho to the actin cytoskeleton through protein kinases ROCK and LIM-kinase. Science 285:895-898.

Mallavarapu A, Mitchison T (1999) Regulated actin cytoskeleton assembly at filopodium tips controls their extension and retraction. J Cell Biol 146:1097-1106.

Markus A, Patel TD, Snider WD (2002) Neurotrophic factors and axonal growth. Curr Opin Neurobiol 12:523-531.

Matsui T, Amano M, Yamamoto T, Chihara K, Nakafuku M, Ito M, Nakano T, Okawa K, Iwamatsu A, Kaibuchi K (1996) Rho-associated kinase, a novel serine/threonine kinase, as a putative target for small GTP binding protein Rho. EMBO J 15:2208-2216.

May V, Schiller MR, Eipper BA, Mains RE (2002) Kalirin Dbl-homology guanine nucleotide exchange factor 1 domain initiates new axon outgrowths via RhoG-mediated mechanisms. J Neurosci 22:6980-6990.

McGraw J, Gaudet AD, Oschipok LW, Steeves JD, Poirier F, Tetzlaff W, Ramer MS (2005) Altered primary afferent anatomy and reduced thermal sensitivity in mice lacking galectin-1. Pain 114:7-18.

McKenna JE, Whishaw IQ (1999) Complete compensation in skilled reaching success with associated impairments in limb synergies, after dorsal column lesion in the rat. J Neurosci 19:1885-1894.

McKeon RJ, Hoke A, Silver J (1995) Injury-induced proteoglycans inhibit the potential for laminin-mediated axon growth on astrocytic scars. Exp Neurol 136:32-43.

McKeon RJ, Jurynec MJ, Buck CR (1999) The chondroitin sulfate proteoglycans neurocan and phosphacan are expressed by reactive astrocytes in the chronic CNS glial scar. J Neurosci 19:10778-10788.

McKeon RJ, Schreiber RC, Rudge JS, Silver J (1991) Reduction of neurite outgrowth in a model of glial scarring following CNS injury is correlated with the expression of inhibitory molecules on reactive astrocytes. J Neurosci 11:3398-3411.

McKerracher L, David S, Jackson DL, Kottis V, Dunn RJ, Braun PE (1994) Identification of myelin-associated glycoprotein as a major myelin- derived inhibitor of neurite growth. Neuron 13:805-811.

McMahon SB, Armanini MP, Ling LH, Phillips HS (1994) Expression and coexpression of Trk receptors in subpopulations of adult primary sensory neurons projecting to identified peripheral targets. Neuron 12:1161-1171.

McTigue DM, Wei P, Stokes BT (2001) Proliferation of NG2-positive cells and altered oligodendrocyte numbers in the contused rat spinal cord. J Neurosci 21:3392-3400.

Meberg PJ, Ono S, Minamide LS, Takahashi M, Bamburg JR (1998) Actin depolymerizing factor and cofilin phosphorylation dynamics: response to signals that regulate neurite extension. Cell Motil Cytoskeleton 39:172-190.

Meiners S, Powell EM, Geller HM (1995) A distinct subset of tenascin/CS-6-PG-rich astrocytes restricts neuronal growth in vitro. J Neurosci 15:8096-8108.

Menet V, Gimenez YR, Sandillon F, Privat A (2000) GFAP null astrocytes are a favorable substrate for neuronal survival and neurite growth. Glia 31:267-272.

Menet V, Prieto M, Privat A, Ribotta M (2003) Axonal plasticity and functional recovery after spinal cord injury in mice deficient in both glial fibrillary acidic protein and vimentin genes. Proc Natl Acad Sci U S A 100:8999-9004.

Menet V, Ribotta M, Chauvet N, Drian MJ, Lannoy J, Colucci-Guyon E, Privat A (2001) Inactivation of the glial fibrillary acidic protein gene, but not that of vimentin, improves neuronal survival and neurite growth by modifying adhesion molecule expression. J Neurosci 21:6147-6158.

Metz GA, Dietz V, Schwab ME, van de MH (1998) The effects of unilateral pyramidal tract section on hindlimb motor performance in the rat. Behav Brain Res 96:37-46.

Metz GA, Whishaw IQ (2002) Cortical and subcortical lesions impair skilled walking in the ladder rung walking test: a new task to evaluate fore- and hindlimb stepping, placing, and co-ordination. J Neurosci Methods 115:169-179.

Meyer G, Feldman EL (2002) Signaling mechanisms that regulate actin-based motility processes in the nervous system. J Neurochem 83:490-503.

Mikol DD, Stefansson K (1988) A phosphatidylinositol-linked peanut agglutinin-binding glycoprotein in central nervous system myelin and on oligodendrocytes. J Cell Biol 106:1273-1279.

Milev P, Maurel P, Chiba A, Mevissen M, Popp S, Yamaguchi Y, Margolis RK, Margolis RU (1998) Differential regulation of expression of hyaluronan-binding proteoglycans in developing brain: aggrecan, versican, neurocan, and brevican. Biochem Biophys Res Commun 247:207-212.

Miranda JD, White LA, Marcillo AE, Willson CA, Jagid J, Whittemore SR (1999) Induction of Eph B3 after spinal cord injury. Exp Neurol 156:218-222.

Mizuno T, Sawada M, Suzumura A, Marunouchi T (1994) Expression of cytokines during glial differentiation. Brain Res 656:141-146.

Mockrin SC, Korn ED (1980) Acanthamoeba profilin interacts with G-actin to increase the rate of exchange of actin-bound adenosine 5'-triphosphate. Biochemistry 19:5359-5362.

Monnier PP, Sierra A, Macchi P, Deitinghoff L, Andersen JS, Mann M, Flad M, Hornberger MR, Stahl B, Bonhoeffer F, Mueller BK (2002) RGM is a repulsive guidance molecule for retinal axons. Nature 419:392-395.

Monnier PP, Sierra A, Schwab JM, Henke-Fahle S, Mueller BK (2003) The Rho/ROCK pathway mediates neurite growth-inhibitory activity associated with the chondroitin sulfate proteoglycans of the CNS glial scar. Mol Cell Neurosci 22:319-330.

Moon LD, Asher RA, Fawcett JW (2003) Limited growth of severed CNS axons after treatment of adult rat brain with hyaluronidase. J Neurosci Res 71:23-37.

Moon LD, Asher RA, Rhodes KE, Fawcett JW (2001) Regeneration of CNS axons back to their target following treatment of adult rat brain with chondroitinase ABC. Nat Neurosci 4:465-466.

Moon SY, Zheng Y (2003) Rho GTPase-activating proteins in cell regulation. Trends Cell Biol 13:13-22.

Morgenstern DA, Asher RA, Fawcett JW (2002) Chondroitin sulphate proteoglycans in the CNS injury response. Prog Brain Res 137:313-332.

Mu X, Silos-Santiago I, Carroll SL, Snider WD (1993) Neurotrophin receptor genes are expressed in distinct patterns in developing dorsal root ganglia. J Neurosci 13:4029-4041.

Muir GD, Whishaw IQ (1999) Complete locomotor recovery following corticospinal tract lesions: measurement of ground reaction forces during overground locomotion in rats. Behav Brain Res 103:45-53.

Mukhopadhyay G, Doherty P, Walsh FS, Crocker PR, Filbin MT (1994) A novel role for myelin-associated glycoprotein as an inhibitor of axonal regeneration. Neuron 13:757-767.

Muller HW, Junghans U, Kappler J (1995) Astroglial neurotrophic and neurite-promoting factors. Pharmacol Ther 65:1-18.

Nakagawa O, Fujisawa K, Ishizaki T, Saito Y, Nakao K, Narumiya S (1996) ROCK-I and ROCK-II, two isoforms of Rho-associated coiled-coil forming protein serine/threonine kinase in mice. FEBS Lett 392:189-193.

Nathaniel EJ, Nathaniel DR (1973) Regeneration of dorsal root fibers into the adult rat spinal cord. Exp Neurol 40:333-350.

Ness R, David S (1997) Leptomeningeal cells modulate the neurite growth promoting properties of astrocytes in vitro. Glia 19:47-57.

Neugebauer KM, Tomaselli KJ, Lilien J, Reichardt LF (1988) N-cadherin, NCAM, and integrins promote retinal neurite outgrowth on astrocytes in vitro. J Cell Biol 107:1177-1187.

Neumann S, Bradke F, Tessier-Lavigne M, Basbaum AI (2002) Regeneration of sensory axons within the injured spinal cord induced by intraganglionic cAMP elevation. Neuron 34:885-893.

Neumann S, Woolf CJ (1999) Regeneration of dorsal column fibers into and beyond the lesion site following adult spinal cord injury. Neuron 23:83-91.

Nguyen Ba-Charvet KT, Brose K, Ma L, Wang KH, Marillat V, Sotelo C, Tessier-Lavigne M, Chedotal A (2001) Diversity and specificity of actions of Slit2 proteolytic fragments in axon guidance. J Neurosci 21:4281-4289.

Niederost B, Oertle T, Fritsche J, McKinney RA, Bandtlow CE (2002) Nogo-A and myelin-associated glycoprotein mediate neurite growth inhibition by antagonistic regulation of RhoA and Rac1. J Neurosci 22:10368-10376.

Niederost BP, Zimmermann DR, Schwab ME, Bandtlow CE (1999) Bovine CNS myelin contains neurite growth-inhibitory activity associated with chondroitin sulfate proteoglycans. J Neurosci 19:8979-8989.

Nishiki T, Narumiya S, Morii N, Yamamoto M, Fujiwara M, Kamata Y, Sakaguchi G, Kozaki S (1990) ADP-ribosylation of the rho/rac proteins induces growth inhibition, neurite outgrowth and acetylcholine esterase in cultured PC-12 cells. Biochem Biophys Res Commun 167:265-272.

Nobes CD, Hall A (1995) Rho, rac, and cdc42 GTPases regulate the assembly of multimolecular focal complexes associated with actin stress fibers, lamellipodia, and filopodia. Cell 81:53-62.

Noble LJ, Wrathall JR (1985) Spinal cord contusion in the rat: morphometric analyses of alterations in the spinal cord. Exp Neurol 88:135-149.

Novikova LN, Novikov LN, Kellerth JO (2000) Survival effects of BDNF and NT-3 on axotomized rubrospinal neurons depend on the temporal pattern of neurotrophin administration. Eur J Neurosci 12:776-780.

Oblinger MM, Lasek RJ (1984) A conditioning lesion of the peripheral axons of dorsal root ganglion cells accelerates regeneration of only their peripheral axons. J Neurosci 4:1736-1744.

Ohashi K, Nagata K, Maekawa M, Ishizaki T, Narumiya S, Mizuno K (2000) Rho-associated kinase ROCK activates LIM-kinase 1 by phosphorylation at threonine 508 within the activation loop. J Biol Chem 275:3577-3582.

Oudega M, Hagg T (1999) Neurotrophins promote regeneration of sensory axons in the adult rat spinal cord. Brain Res 818:431-438.

Oudega M, Rosano C, Sadi D, Wood PM, Schwab ME, Hagg T (2000) Neutralizing antibodies against neurite growth inhibitor NI-35/250 do not promote regeneration of sensory axons in the adult rat spinal cord. Neuroscience 100:873-883.

Palecek J, Paleckova V, Willis WD (2002) The roles of pathways in the spinal cord lateral and dorsal funiculi in signaling nociceptive somatic and visceral stimuli in rats. Pain 96:297-307.

Pasterkamp RJ, Anderson PN, Verhaagen J (2001) Peripheral nerve injury fails to induce growth of lesioned ascending dorsal column axons into spinal cord scar tissue expressing the axon repellent Semaphorin3A. Eur J Neurosci 13:457-471.

Paterson HF, Self AJ, Garrett MD, Just I, Aktories K, Hall A (1990) Microinjection of recombinant p21rho induces rapid changes in cell morphology. J Cell Biol 111:1001-1007.

Perrot V, Vazquez-Prado J, Gutkind JS (2002) Plexin B Regulates Rho through the Guanine Nucleotide Exchange Factors Leukemia-associated Rho GEF (LARG) and PDZ-RhoGEF. J Biol Chem 277:43115-43120.

Perry MJ, Lawson SN, Robertson J (1991) Neurofilament immunoreactivity in populations of rat primary afferent neurons: a quantitative study of phosphorylated and non-phosphorylated subunits. J Neurocytol 20:746-758.

Perry VH, Gordon S (1991) Macrophages and the nervous system. Int Rev Cytol 125:203-244.

Pettway Z, Domowicz M, Schwartz NB, Bronner-Fraser M (1996) Age-dependent inhibition of neural crest migration by the notochord correlates with alterations in the S103L chondroitin sulfate proteoglycan. Exp Cell Res 225:195-206.

Plunet W, Kwon BK, Tetzlaff W (2002) Promoting axonal regeneration in the central nervous system by enhancing the cell body response to axotomy. J Neurosci Res 68:1-6.

Popovich PG, Guan Z, McGaughy V, Fisher L, Hickey WF, Basso DM (2002) The neuropathological and behavioral consequences of intraspinal microglial/macrophage activation. J Neuropathol Exp Neurol 61:623-633.

Popovich PG, Guan Z, Wei P, Huitinga I, van RN, Stokes BT (1999) Depletion of hematogenous macrophages promotes partial hindlimb recovery and neuroanatomical repair after experimental spinal cord injury. Exp Neurol 158:351-365.

Popovich PG, Wei P, Stokes BT (1997) Cellular inflammatory response after spinal cord injury in Sprague-Dawley and Lewis rats. J Comp Neurol 377:443-464.

Popp S, Andersen JS, Maurel P, Margolis RU (2003) Localization of aggrecan and versican in the developing rat central nervous system. Dev Dyn 227:143-149.

Powell EM, Geller HM (1999) Dissection of astrocyte-mediated cues in neuronal guidance and process extension. Glia 26:73-83.

Powell EM, Meiners S, DiProspero NA, Geller HM (1997) Mechanisms of astrocyte-directed neurite guidance. Cell Tissue Res 290:385-393.

Price J, Hynes RO (1985) Astrocytes in culture synthesize and secrete a variant form of fibronectin. J Neurosci 5:2205-2211.

Prinjha R, Moore SE, Vinson M, Blake S, Morrow R, Christie G, Michalovich D, Simmons DL, Walsh FS (2000) Inhibitor of neurite outgrowth in humans. Nature 403:383-384.

Qiu J, Cai D, Dai H, McAtee M, Hoffman PN, Bregman BS, Filbin MT (2002) Spinal axon regeneration induced by elevation of cyclic AMP. Neuron 34:895-903.

Raivich G, Bohatschek M, Kloss CU, Werner A, Jones LL, Kreutzberg GW (1999) Neuroglial activation repertoire in the injured brain: graded response, molecular mechanisms and cues to physiological function. Brain Res Brain Res Rev 30:77-105.

Rajagopalan S, Deitinghoff L, Davis D, Conrad S, Skutella T, Chedotal A, Mueller BK, Strittmatter SM (2004) Neogenin mediates the action of repulsive guidance molecule. Nat Cell Biol 6:756-762.

Ramer LM, Borisoff JF, Ramer MS (2004) Rho-kinase inhibition enhances axonal plasticity and attenuates cold hyperalgesia after dorsal rhizotomy. J Neurosci 24:10796-10805.

Ramer MS, Duraisingam I, Priestley JV, McMahon SB (2001) Two-tiered inhibition of axon regeneration at the dorsal root entry zone. J Neurosci 21:2651-2660.

Ramer MS, Priestley JV, McMahon SB (2000) Functional regeneration of sensory axons into the adult spinal cord. Nature 403:312-316.

Ramon y Cajal S (1928) Degeneration and regeneration of the nervous system. New York: Hafner.

Ramon-Cueto A, Cordero MI, Santos-Benito FF, Avila J (2000) Functional recovery of paraplegic rats and motor axon regeneration in their spinal cords by olfactory ensheathing glia. Neuron 25:425-435.

Reier PJ, Houle JD (1988) The glial scar: its bearing on axonal elongation and transplantation approaches to CNS repair. Adv Neurol 47:87-138.

Reier PJ, L.F.Eng, Jakeman L (1989) Reactive astrocyte and axonal outgrowth in the injured CNS: Is gliosis really an impediment to regeneration? In: Neural Regeneration and Transplantation. (Seil FJ, ed), pp 183-209. New York: Alan R. Liss, Inc.

Renaudin A, Lehmann M, Girault J, McKerracher L (1999) Organization of point contacts in neuronal growth cones. J Neurosci Res 55:458-471.

Richardson PM, Issa VM (1984) Peripheral injury enhances central regeneration of primary sensory neurones. Nature 309:791-793.

Richardson PM, McGuinness UM, Aguayo AJ (1980) Axons from CNS neurons regenerate into PNS grafts. Nature 284:264-265.

Richardson PM, Verge VM (1986) The induction of a regenerative propensity in sensory neurons following peripheral axonal injury. J Neurocytol 15:585-594.

Richardson PM, Verge VM (1987) Axonal regeneration in dorsal spinal roots is accelerated by peripheral axonal transection. Brain Res 411:406-408.

Ridley AJ (2001) Rho family proteins: coordinating cell responses. Trends Cell Biol 11:471-477.

Ridley AJ, Hall A (1992) The small GTP-binding protein rho regulates the assembly of focal adhesions and actin stress fibers in response to growth factors. Cell 70:389-399.

Ridley AJ, Paterson HF, Johnston CL, Diekmann D, Hall A (1992) The small GTP-binding protein rac regulates growth factor-induced membrane ruffling. Cell 70:401-410.

Rittinger K, Walker PA, Eccleston JF, Smerdon SJ, Gamblin SJ (1997) Structure at 1.65 A of RhoA and its GTPase-activating protein in complex with a transition-state analogue. Nature 389:758-762.

Rossman KL, Der CJ, Sondek J (2005) GEF means go: turning on RHO GTPases with guanine nucleotide-exchange factors. Nat Rev Mol Cell Biol 6:167-180.

Rostworowski M, Balasingam V, Chabot S, Owens T, Yong VW (1997) Astrogliosis in the neonatal and adult murine brain post-trauma: elevation of inflammatory cytokines and the lack of requirement for endogenous interferon-gamma. J Neurosci 17:3664-3674.

Rubin BP, Dusart I, Schwab ME (1994) A monoclonal antibody (IN-1) which neutralizes neurite growth inhibitory proteins in the rat CNS recognizes antigens localized in CNS myelin. J Neurocytol 23:209-217.

Rudge JS, Silver J (1990) Inhibition of neurite outgrowth on astroglial scars in vitro. J Neurosci 10:3594-3603.

Rudge JS, Smith GM, Silver J (1989) An in vitro model of wound healing in the CNS: analysis of cell reaction and interaction at different ages. Exp Neurol 103:1-16.

Ruit KG, Elliott JL, Osborne PA, Yan Q, Snider WD (1992) Selective dependence of mammalian dorsal root ganglion neurons on nerve growth factor during embryonic development. Neuron 8:573-587.

Saade NE, Baliki M, El Khoury C, Hawwa N, Atweh SF, Apkarian AV, Jabbur SJ (2002) The role of the dorsal columns in neuropathic behavior: evidence for plasticity and non-specificity. Neuroscience 115:403-413.

Sabry JH, O'Connor TP, Evans L, Toroian-Raymond A, Kirschner M, Bentley D (1991) Microtubule behavior during guidance of pioneer neuron growth cones in situ. J Cell Biol 115:381-395.

Schmalfeldt M, Bandtlow CE, Dours-Zimmermann MT, Winterhalter KH, Zimmermann DR (2000) Brain derived versican V2 is a potent inhibitor of axonal growth. J Cell Sci 113 (Pt 5):807-816.

Schmidt JT, Morgan P, Dowell N, Leu B (2002) Myosin light chain phosphorylation and growth cone motility. J Neurobiol 52:175-188.

Schnell L, Schneider R, Kolbeck R, Barde YA, Schwab ME (1994) Neurotrophin-3 enhances sprouting of corticospinal tract during development and after adult spinal cord lesion. Nature 367:170-173.

Schnell L, Schwab ME (1990) Axonal regeneration in the rat spinal cord produced by an antibody against myelin-associated neurite growth inhibitors. Nature 343:269-272.

Schnell L, Schwab ME (1993) Sprouting and regeneration of lesioned corticospinal tract fibres in the adult rat spinal cord. Eur J Neurosci 5:1156-1171.

Schreyer DJ, Skene JH (1993) Injury-associated induction of GAP-43 expression displays axon branch specificity in rat dorsal root ganglion neurons. J Neurobiol 24:959-970.

Schrimsher GW, Reier PJ (1993) Forelimb motor performance following dorsal column, dorsolateral funiculi, or ventrolateral funiculi lesions of the cervical spinal cord in the rat. Exp Neurol 120:264-276.

Schweigreiter R, Walmsley AR, Niederost B, Zimmermann DR, Oertle T, Casademunt E, Frentzel S, Dechant G, Mir A, Bandtlow CE (2004) Versican V2 and the central inhibitory domain of Nogo-A inhibit neurite growth via p75NTR/NgR-independent pathways that converge at RhoA. Mol Cell Neurosci 27:163-174.

Sebok A, Nusser N, Debreceni B, Guo Z, Santos MF, Szeberenyi J, Tigyi G (1999) Different roles for RhoA during neurite initiation, elongation, and regeneration in PC12 cells. J Neurochem 73:949-960.

Sekhon LH, Fehlings MG (2001) Epidemiology, demographics, and pathophysiology of acute spinal cord injury. Spine 26:S2-12.

Selles-Navarro I, Ellezam B, Fajardo R, Latour M, McKerracher L (2001) Retinal ganglion cell and nonneuronal cell responses to a microcrush lesion of adult rat optic nerve. Exp Neurol 167:282-289.

Shaked I, Tchoresh D, Gersner R, Meiri G, Mordechai S, Xiao X, Hart RP, Schwartz M (2005) Protective autoimmunity: interferon-gamma enables microglia to remove glutamate without evoking inflammatory mediators. J Neurochem 92:997-1009.

Shamah SM, Lin MZ, Goldberg JL, Estrach S, Sahin M, Hu L, Bazalakova M, Neve RL, Corfas G, Debant A, Greenberg ME (2001) EphA receptors regulate growth cone dynamics through the novel guanine nucleotide exchange factor ephexin. Cell 105:233-244.

Shearer MC, Fawcett JW (2001) The astrocyte/meningeal cell interface--a barrier to successful nerve regeneration? Cell Tissue Res 305:267-273.

Shearer MC, Niclou SP, Brown D, Asher RA, Holtmaat AJ, Levine JM, Verhaagen J, Fawcett JW (2003) The astrocyte/meningeal cell interface is a barrier to neurite outgrowth which can be overcome by manipulation of inhibitory molecules or axonal signalling pathways. Mol Cell Neurosci 24:913-925.

Siddall PJ, Taylor DA, McClelland JM, Rutkowski SB, Cousins MJ (1999) Pain report and the relationship of pain to physical factors in the first 6 months following spinal cord injury. Pain 81:187-197.

Silver J, Miller JH (2004) Regeneration beyond the glial scar. Nat Rev Neurosci 5:146-156.

Sivasankaran R, Pei J, Wang KC, Zhang YP, Shields CB, Xu XM, He Z (2004) PKC mediates inhibitory effects of myelin and chondroitin sulfate proteoglycans on axonal regeneration. Nat Neurosci 7:261-268.

Smith SJ (1988) Neuronal cytomechanics: the actin-based motility of growth cones. Science 242:708-715.

Smith-Thomas LC, Fok-Seang J, Stevens J, Du JS, Muir E, Faissner A, Geller HM, Rogers JH, Fawcett JW (1994) An inhibitor of neurite outgrowth produced by astrocytes. J Cell Sci 107 (Pt 6):1687-1695.

Smith-Thomas LC, Stevens J, Fok-Seang J, Faissner A, Rogers JH, Fawcett JW (1995) Increased axon regeneration in astrocytes grown in the presence of proteoglycan synthesis inhibitors. J Cell Sci 108 (Pt 3):1307-1315.

Snider WD, McMahon SB (1998) Tackling pain at the source: new ideas about nociceptors. Neuron 20:629-632.

Snow DM, Lemmon V, Carrino DA, Caplan AI, Silver J (1990) Sulfated proteoglycans in astroglial barriers inhibit neurite outgrowth in vitro. Exp Neurol 109:111-130.

Snow DM, Letourneau PC (1992) Neurite outgrowth on a step gradient of chondroitin sulfate proteoglycan (CS-PG). J Neurobiol 23:322-336.

Snow DM, Mullins N, Hynds DL (2001) Nervous system-derived chondroitin sulfate proteoglycans regulate growth cone morphology and inhibit neurite outgrowth: a light, epifluorescence, and electron microscopy study. Microsc Res Tech 54:273-286.

Snow DM, Smith JD, Cunningham AT, McFarlin J, Goshorn EC (2003) Neurite elongation on chondroitin sulfate proteoglycans is characterized by axonal fasciculation. Exp Neurol 182:310-321.

Snow DM, Watanabe M, Letourneau PC, Silver J (1991) A chondroitin sulfate proteoglycan may influence the direction of retinal ganglion cell outgrowth. Development 113:1473-1485.

Sobue K, Kanda K (1989) Alpha-actinins, calspectin (brain spectrin or fodrin), and actin participate in adhesion and movement of growth cones. Neuron 3:311-319.

Song HJ, Poo MM (1999) Signal transduction underlying growth cone guidance by diffusible factors. Curr Opin Neurobiol 9:355-363.

Steeves JD, Jordan LM (1980) Localization of a descending pathway in the spinal cord which is necessary for controlled treadmill locomotion. Neurosci Lett 20:283-288.

Steindler DA (1993) Glial boundaries in the developing nervous system. Annu Rev Neurosci 16:445-470.

Steindler DA, Cooper NG, Faissner A, Schachner M (1989) Boundaries defined by adhesion molecules during development of the cerebral cortex: the J1/tenascin glycoprotein in the mouse somatosensory cortical barrel field. Dev Biol 131:243-260.

Steindler DA, O'Brien TF, Cooper NG (1988) Glycoconjugate boundaries during early postnatal development of the neostriatal mosaic. J Comp Neurol 267:357-369.

Stichel CC, Hermanns S, Luhmann HJ, Lausberg F, Niermann H, D'Urso D, Servos G, Hartwig HG, Muller HW (1999a) Inhibition of collagen IV deposition promotes regeneration of injured CNS axons. Eur J Neurosci 11:632-646.

Stichel CC, Muller HW (1998) The CNS lesion scar: new vistas on an old regeneration barrier. Cell Tissue Res 294:1-9.

Stichel CC, Niermann H, D'Urso D, Lausberg F, Hermanns S, Muller HW (1999b) Basal membrane-depleted scar in lesioned CNS: characteristics and relationships with regenerating axons. Neuroscience 93:321-333.

Stoll G, Jander S (1999) The role of microglia and macrophages in the pathophysiology of the CNS. Prog Neurobiol 58:233-247.

Streit WJ, Semple-Rowland SL, Hurley SD, Miller RC, Popovich PG, Stokes BT (1998) Cytokine mRNA profiles in contused spinal cord and axotomized facial nucleus suggest a beneficial role for inflammation and gliosis. Exp Neurol 152:74-87.

Sumi T, Matsumoto K, Takai Y, Nakamura T (1999) Cofilin phosphorylation and actin cytoskeletal dynamics regulated by rho- and Cdc42-activated LIM-kinase 2. J Cell Biol 147:1519-1532.

Sung JK, Miao L, Calvert JW, Huang L, Louis HH, Zhang JH (2003) A possible role of RhoA/Rho-kinase in experimental spinal cord injury in rat. Brain Res 959:29-38.

Suter DM, Forscher P (1998) An emerging link between cytoskeletal dynamics and cell adhesion molecules in growth cone guidance. Curr Opin Neurobiol 8:106-116.

Tanaka E, Ho T, Kirschner MW (1995) The role of microtubule dynamics in growth cone motility and axonal growth. J Cell Biol 128:139-155.

Tang S, Qiu J, Nikulina E, Filbin MT (2001) Soluble myelin-associated glycoprotein released from damaged white matter inhibits axonal regeneration. Mol Cell Neurosci 18:259-269.

Tang X, Davies JE, Davies SJ (2003) Changes in distribution, cell associations, and protein expression levels of NG2, neurocan, phosphacan, brevican, versican V2, and tenascin-C during acute to chronic maturation of spinal cord scar tissue. J Neurosci Res 71:427-444.

Tang XQ, Tanelian DL, Smith GM (2004) Semaphorin3A inhibits nerve growth factor-induced sprouting of nociceptive afferents in adult rat spinal cord. J Neurosci 24:819-827.

Tetzlaff W, Alexander SW, Miller FD, Bisby MA (1991) Response of facial and rubrospinal neurons to axotomy: changes in mRNA expression for cytoskeletal proteins and GAP-43. J Neurosci 11:2528-2544.

Tetzlaff W, Zwiers H, Lederis K, Cassar L, Bisby MA (1989) Axonal transport and localization of B-50/GAP-43-like immunoreactivity in regenerating sciatic and facial nerves of the rat. J Neurosci 9:1303-1313.

Thallmair M, Metz GA, Z'Graggen WJ, Raineteau O, Kartje GL, Schwab ME (1998) Neurite growth inhibitors restrict plasticity and functional recovery following corticospinal tract lesions. Nat Neurosci 1:124-131.

Thies E, Davenport RW (2003) Independent roles of Rho-GTPases in growth cone and axonal behavior. J Neurobiol 54:358-369.

Tom VJ, Doller CM, Malouf AT, Silver J (2004) Astrocyte-associated fibronectin is critical for axonal regeneration in adult white matter. J Neurosci 24:9282-9290.

Tomaselli KJ, Neugebauer KM, Bixby JL, Lilien J, Reichardt LF (1988) N-cadherin and integrins: two receptor systems that mediate neuronal process outgrowth on astrocyte surfaces. Neuron 1:33-43.

Tona A, Bignami A (1993) Effect of hyaluronidase on brain extracellular matrix in vivo and optic nerve regeneration. J Neurosci Res 36:191-199.

Topp KS, Faddis BT, Vijayan VK (1989) Trauma-induced proliferation of astrocytes in the brains of young and aged rats. Glia 2:201-211.

Tropea D, Caleo M, Maffei L (2003) Synergistic effects of brain-derived neurotrophic factor and chondroitinase ABC on retinal fiber sprouting after denervation of the superior colliculus in adult rats. J Neurosci 23:7034-7044.

Trybus KM (1994) Role of myosin light chains. J Muscle Res Cell Motil 15:587-594.

Tsai EC, Krassioukov AV, Tator CH (2005) Corticospinal regeneration into lumbar grey matter correlates with locomotor recovery after complete spinal cord transection and repair with peripheral nerve grafts, fibroblast growth factor 1, fibrin glue, and spinal fusion. J Neuropathol Exp Neurol 64:230-244.

Tuszynski MH, Grill R, Jones LL, Brant A, Blesch A, Low K, Lacroix S, Lu P (2003) NT-3 gene delivery elicits growth of chronically injured corticospinal axons and modestly improves functional deficits after chronic scar resection. Exp Neurol 181:47-56.

Uehata M, Ishizaki T, Satoh H, Ono T, Kawahara T, Morishita T, Tamakawa H, Yamagami K, Inui J, Maekawa M, Narumiya S (1997) Calcium sensitization of smooth muscle mediated by a Rho-associated protein kinase in hypertension. Nature 389:990-994.

Ughrin YM, Chen ZJ, Levine JM (2003) Multiple regions of the NG2 proteoglycan inhibit neurite growth and induce growth cone collapse. J Neurosci 23:175-186.

Umeyama T, Okabe S, Kanai Y, Hirokawa N (1993) Dynamics of microtubules bundled by microtubule associated protein 2C (MAP2C). J Cell Biol 120:451-465.

Vahlsing HL, Feringa ER (1980) A ventral uncrossed corticospinal tract in the rat. Exp Neurol 70:282-287.

Van der Zee CE, Nielander HB, Vos JP, Lopes dS, Verhaagen J, Oestreicher AB, Schrama LH, Schotman P, Gispen WH (1989) Expression of growth-associated protein B-50 (GAP43) in dorsal root ganglia and sciatic nerve during regenerative sprouting. J Neurosci 9:3505-3512.

Verge VM, Tetzlaff W, Richardson PM, Bisby MA (1990) Correlation between GAP43 and nerve growth factor receptors in rat sensory neurons. J Neurosci 10:926-934.

Vijayan VK, Lee YL, Eng LF (1990) Increase in glial fibrillary acidic protein following neural trauma. Mol Chem Neuropathol 13:107-118.

Wahl S, Barth H, Ciossek T, Aktories K, Mueller BK (2000) Ephrin-A5 induces collapse of growth cones by activating Rho and Rho kinase. J Cell Biol 149:263-270.

Wallar BJ, Alberts AS (2003) The formins: active scaffolds that remodel the cytoskeleton. Trends Cell Biol 13:435-446.

Wang KC, Kim JA, Sivasankaran R, Segal R, He Z (2002a) p75 interacts with the Nogo receptor as a co-receptor for Nogo, MAG and OMgp. Nature 420:74-78.

Wang KC, Koprivica V, Kim JA, Sivasankaran R, Guo Y, Neve RL, He Z (2002b) Oligodendrocyte-myelin glycoprotein is a Nogo receptor ligand that inhibits neurite outgrowth. Nature 417:941-944.

Wang X, Messing A, David S (1997) Axonal and nonneuronal cell responses to spinal cord injury in mice lacking glial fibrillary acidic protein. Exp Neurol 148:568-576.

Watanabe N, Madaule P, Reid T, Ishizaki T, Watanabe G, Kakizuka A, Saito Y, Nakao K, Jockusch BM, Narumiya S (1997) p140mDia, a mammalian homolog of Drosophila diaphanous, is a target protein for Rho small GTPase and is a ligand for profilin. EMBO J 16:3044-3056.

Webb AA, Muir GD (2003) Unilateral dorsal column and rubrospinal tract injuries affect overground locomotion in the unrestrained rat. Eur J Neurosci 18:412-422.

Whishaw IQ (2003) Did a change in sensory control of skilled movements stimulate the evolution of the primate frontal cortex? Behav Brain Res 146:31-41.

Whishaw IQ, Gorny B (1994) Arpeggio and fractionated digit movements used in prehension by rats. Behav Brain Res 60:15-24.

Whishaw IQ, Gorny B, Sarna J (1998) Paw and limb use in skilled and spontaneous reaching after pyramidal tract, red nucleus and combined lesions in the rat: behavioral and anatomical dissociations. Behav Brain Res 93:167-183.

Whishaw IQ, O'Connor WT, Dunnett SB (1986) The contributions of motor cortex, nigrostriatal dopamine and caudate-putamen to skilled forelimb use in the rat. Brain 109 (Pt 5):805-843.

Whishaw IQ, Pellis SM, Gorny B, Kolb B, Tetzlaff W (1993) Proximal and distal impairments in rat forelimb use in reaching follow unilateral pyramidal tract lesions. Behav Brain Res 56:59-76.

Williams R, Ebendal T (1995) Neurotrophin receptor expression during development of the chick spinal sensory ganglion. Neuroreport 6:2277-2282.

Wong ST, Henley JR, Kanning KC, Huang KH, Bothwell M, Poo MM (2002) A p75(NTR) and Nogo receptor complex mediates repulsive signaling by myelin-associated glycoprotein. Nat Neurosci 5:1302-1308.

Woolf CJ, Mannion RJ (1999) Neuropathic pain: aetiology, symptoms, mechanisms, and management. Lancet 353:1959-1964.

Wright DE, Snider WD (1995) Neurotrophin receptor mRNA expression defines distinct populations of neurons in rat dorsal root ganglia. J Comp Neurol 351:329-338.

Wright DE, Zhou L, Kucera J, Snider WD (1997) Introduction of a neurotrophin-3 transgene into muscle selectively rescues proprioceptive neurons in mice lacking endogenous neurotrophin-3. Neuron 19:503-517.

Wylie SR, Chantler PD (2003) Myosin IIA drives neurite retraction. Mol Biol Cell 14:4654-4666.

Xu XM, Guenard V, Kleitman N, Aebischer P, Bunge MB (1995) A combination of BDNF and NT-3 promotes supraspinal axonal regeneration into Schwann cell grafts in adult rat thoracic spinal cord. Exp Neurol 134:261-272.

Yamada H, Fredette B, Shitara K, Hagihara K, Miura R, Ranscht B, Stallcup WB, Yamaguchi Y (1997) The brain chondroitin sulfate proteoglycan brevican associates with astrocytes ensheathing cerebellar glomeruli and inhibits neurite outgrowth from granule neurons. J Neurosci 17:7784-7795.

Yamashita T, Higuchi H, Tohyama M (2002) The p75 receptor transduces the signal from myelin-associated glycoprotein to Rho. J Cell Biol 157:565-570.

Yamashita T, Tohyama M (2003) The p75 receptor acts as a displacement factor that releases Rho from Rho-GDI. Nat Neurosci 6:461-467.

Yick LW, Wu W, So KF, Yip HK, Shum DK (2000) Chondroitinase ABC promotes axonal regeneration of Clarke's neurons after spinal cord injury. Neuroreport 11:1063-1067.

Yoshikawa S, McKinnon RD, Kokel M, Thomas JB (2003) Wnt-mediated axon guidance via the Drosophila Derailed receptor. Nature 422:583-588.

Yuan XB, Jin M, Xu X, Song YQ, Wu CP, Poo MM, Duan S (2003) Signalling and crosstalk of Rho GTPases in mediating axon guidance. Nat Cell Biol 5:38-45.

Zhang Z, Krebs CJ, Guth L (1997) Experimental analysis of progressive necrosis after spinal cord trauma in the rat: etiological role of the inflammatory response. Exp Neurol 143:141-152.

Zhou FQ, Waterman-Storer CM, Cohan CS (2002) Focal loss of actin bundles causes microtubule redistribution and growth cone turning. J Cell Biol 157:839-849.

Zimmermann M (2001) Pathobiology of neuropathic pain. Eur J Pharmacol 429:23-37.

Zuo J, Neubauer D, Dyess K, Ferguson TA, Muir D (1998) Degradation of chondroitin sulfate proteoglycan enhances the neurite-promoting potential of spinal cord tissue. Exp Neurol 154:654-662.

Chapter 2

Differential effects of aggrecan components on dorsal root ganglion neurite growth and growth cone morphology.

Introduction

Chondroitin sulfate proteoglycans (CSPGs) consist of a protein core with covalently attached chondroitin sulfate-substituted glycosaminoglycan side chains. The hyalectan family, which includes aggrecan, versican, neurocan, and brevican, are aggregating CSPGs that bind to hyaluronic acid in the extracellular matrix (ECM). In the nervous system, these CSPGs function in axonal guidance during development (Popp et al., 2003;Landolt et al., 1995), and in structural stabilization of the mature CNS (Yamada et al., 1997). After spinal cord injury (SCI), CSPGs of the hyalectan family are upregulated in the gliotic tissue bordering and surrounding the lesion cavity, and are found in association with immune cells, fibroblasts, astrocytes and other glial cells (Jones et al., 2003;Tang et al., 2003). These proteoglycans, along with inhibitors found on myelin (Caroni et al., 1988;Tang et al., 2001;Bandtlow and Schwab, 2000;Wang et al., 2002;Monnier et al., 2002), contribute to the failure of axonal regeneration (Fitch and Silver, 1997;Lemons et al., 1999;McKeon et al., 1995;reviewed in Morgenstern et al., 2002).

Aggrecan is commonly found in the ECM of cartilage (Doege et al., 1991), and also of the central nervous system (CNS) (Asher et al., 1995). In the CNS, it is one of the major CSPGs expressed during development (Milev et al., 1998;Popp et al., 2003) and the expression persists to adulthood (Asher et al., 1995;Lemons et al., 2001). Aggrecan core protein is composed of two N-terminal globular domains, G_1 and G_2, followed by a long central glycosaminoglycan attachment region, and a C-terminal globular domain, G_3 (Kiani et al., 2002). Aggrecan monomer interacts through the G1 domain with hyaluronic acid and link protein to form large molecular weight aggregates in the ECM (Kiani et al., 2002). *In vitro*, aggrecan potently inhibits neurite growth (Condic et al., 1999;Johnson et al., 2002;Snow et al., 1990;Borisoff et al., 2003;Snow and Letourneau, 1992;Tom et al., 2004). However, the signaling pathways activated downstream of aggrecan and of CSPGs in general and the importance of the chondroitin sulfate-glycosaminoglycan side chains in CSPG inhibition are less clear. The bacterial enzyme, chondroitinase ABC (ChABC), digests the glycosaminoglycan side chains from these proteoglycans (Jandik et al., 1994), and is commonly used to determine the degree to which attached glycosaminoglycan chains contribute to the molecule's inhibitory properties.

In vitro, chick dorsal root ganglions (DRGs) are widely used in axonal guidance studies in which a potentially inhibitory molecule is presented to DRG neurites either as a substrate or in

solution to test whether it suppresses neurite growth (Jin and Strittmatter, 1997;Fournier et al., 2003;Dontchev and Letourneau, 2003). In each DRG, there is a heterogeneous population of cells, and during embryogenesis these neurons depend on different trophic factors for survival and neurite extension. They are differentially responsive to glial cell line-derived neurotrophic factor (GDNF), and to members of the neurotrophin family including nerve growth factor (NGF), brain-derived neurotrophic factor (BDNF), and neurotrophin-3 (NT3) (Buj-Bello et al., 1995;Gaese et al., 1994;Lefcort et al., 1996;reviewed in Ernfors, 2001). In culture, between embryonic (E) day 6 and E12 of chick development, the DRGs extend neurites in response to NGF, BDNF, or NT3 (Buchman and Davies, 1993).

In this study, we determined whether each component of 'aggrecan', including aggrecan aggregate (aggrecan bound to hyaluronic acid and link protein), aggrecan monomer, chondroitin sulfate, hyaluronic acid, or chondroitinase-treated aggrecan (protein core with chondroitin sulfate stubs), was inhibitory to neurite outgrowth from E9 chick DRG neurons. Although the mechanism of signaling downstream of CSPGs is not well-characterized, various researchers, including our lab, have found that similar to other guidance molecules, CSPGs signal through the Rho GTPases (Monnier et al., 2003;Borisoff et al., 2003). Therefore we also tested whether ROCK inhibition with Y27632 reversed the decrease in neurite growth due to individual aggrecan components. By supplying one of the various neurotrophic factors in the medium, one specific group of neurons can be stimulated to extend neurites. In this study, we compared the growth of neurites stimulated by NGF and NT3 on substrates containing each of the aggrecan components.

Materials and methods

DRG explant culture

Whole DRG explants were removed from the lumbar spinal cord of embryonic day (E) 9 chicks. They were maintained in Neurobasal medium supplemented with B27 nutrients, 0.5 mM glutamine, and 100 units/mL penicillin/strepmycin, and on 8-chamber glass slides (Nunc, Rochester, NY) that were pre-coated with 0.01% poly-D-lysine (Sigma, St. Louis, MO). Media were also supplemented with 2 ng/mL Nerve Growth Factor (NGF) or Neurotrophin-3 (NT-3) (kindly provided by Regeneron Pharmaceuticals Inc.). The slides were further treated with solutions containing 25 μg/mL aggrecan aggregate (aggrecan monomers bound with hyaluronic

acid with the aid of link protein), aggrecan monomer, chondroitin sulfate, or hyaluronic acid for 2 hours at 37°C. For chondroitinase-treated aggrecan aggregate, slides were further incubated with 1 U/ml chondroitinase (Seikagaku Kogyo Co., Tokyo, Japan) for 1 hour at 37°C. It was then inactivated by heat (on hot plate for 30 seconds) and washed off with sterile water. DRGs were incubated for 24 hours under humidified conditions in 95% air and 5% CO_2 at 37°C before fixing in formalin.

Immunohistochemistry and Immunofluorescence Microscopy

DRGs on glass slides were fixed with 4% formalin in 0.01 M PBS for 15 minutes at room temperature. They were washed in PBS, and incubated overnight at room temperature with the primary antibodies in PBS with 0.1% Triton X. Primary antibodies used included polyclonal rabbit anti-neurofilament H (1/400; Serotec, Oxford, UK) or monoclonal mouse anti-tubulin III (1/400; Covance, Berkeley, CA) antibodies. Although in rats only large diameter (NT3-responsive) sensory axons express neurofilament H (Averill et al., 1995;Molliver et al., 1995), we found that the polyclonal anti-neurofilament H antibodies also stained the small diameter, NGF-responsive neurites from our chick DRGs. Some DRG neurite outgrowth was immunostained with both antibodies, and similar neurite lengths were recorded from each immunostaining. After blocking with the appropriate normal serum for ½ hour, the DRGs were immediately stained with fluorescence-conjugated secondary antibodies for 1 hour at room temperature. Cells were washed between steps with 0.01 M PBS.

For visualizing growth cones, the DRG cultures were immunostained with anti-tubulin and anti-actin antibodies (MP Biomedicals, Montreal, Quebec; 1/200). The DRG cell bodies were microdissected away using a 26-gauge needle, allowing glass cover slips to be mounted onto the 8-chamber glass slides on which the DRG were grown. Images of the growth cones were captured under high magnification (40x objective, 10x eyepiece) on a Zeiss Axioplan microscope (Thornwood, NY), using a Q-imaging camera (Burnaby, BC) with the aid of the Northern Eclipse software (Empix Imaging, Mississauga, ON)

Quantification of neurite growth

Images of the DRG explants were captured under a 10x objective. The neurite growth around each DRG explants was quantified using a macro written for Northern Eclipse (Fig. 2.1). First, the mean radius (in μm) of the DRG explant was determined by picking a central reference

point (C) on the collection of DRG cell bodies, and manually tracing around the perimeter (P) of the cell bodies. Second, the mean distance of the neurite ends to the central reference point was calculated by the software after manually tracing along the neurite ends (N). To calculate 'DRG outgrowth' (in μm), the mean DRG radius was subtracted from the mean distance of the neurite ends to the central reference point (N minus P).

The differences in growth cone morphologies on the various substrates were analyzed by measuring growth cone sizes and filopodial numbers. On captured images of the growth cones, the area of each growth cone (enlarged area distal to the initial spraying of the axon) was selected using the trace mode in SigmaScan Pro5 software to give growth cone sizes in pixels. 16 pixels equalled 1 μm^2 on the captured images (captured using 40x objective, 10x eyepiece), and the growth cone sizes were expressed in μm^2. The number of filopodia for each growth cone was counted on the captured images. At least 30 growth cones on each substrate were included in these analyses.

Statistics

All data were reported as the mean ± SEM. The DRG outgrowth on different substrates were analysed for statistical significance using the Kruskal-Wallis One Way Analysis of Variance on Ranks followed by the post-hoc Dunn's Test for comparison with control (PDL only). Outgrowth in the presence of Y27632 was compared to that without using the student's t-test or Mann-Whitney Rank Sum Test, depending on whether the distribution of data was normal. In all analyses, statistical significance was accepted at a p value less than 0.05.

Results

DRG outgrowth was inhibited by aggrecan aggregate, aggrecan monomer, and hyaluronic acid

To determine how each component of aggrecan affect neurite growth, whole DRGs from E9 chick were explanted onto substrates containing different components of 'aggrecan': aggrecan aggregate (aggrecan bound to hyaluronic acid and link protein), aggrecan monomer, chondroitin sulfate, hyaluronic acid, or chondroitinase-treated aggrecan (protein core with chondroitin sulfate stubs). The DRGs were grown in serum-free media supplemented with 2ng/ml NGF or NT3. After 18-24 hours in culture, a halo of axonal growth formed around the DRG cell bodies (NGF-responsive neurites shown in Fig. 2.2A-F). 'Neurite outgrowth' was

quantified as outlined in the methods section, and on control (PDL-treated) substrate it was 135 ± 10 μm (Fig. 2.2A, G).

NGF was supplied in the culture medium to stimulate neurite growth from TrkA-expressing DRG neurons. Outgrowth on aggrecan aggregate (aggrecan bound with hyaluronic acid and link protein; 37.5 ± 6.9 μm; Fig. 2.2B, G), or on aggrecan monomer (50.7 ± 8.9 μm; Fig. 2.2C, G) was only about one-third of that on PDL. Chondroitin sulfate by itself did not inhibit neurite growth (128 ± 7 μm; Fig. 2.2D, G). Hyaluronic acid, which was also a glycosaminoglycan but non-sulfated, significantly inhibited outgrowth (54.8 ± 6.4 μm; Fig. 2.2E, G). Outgrowth on ChABC-treated aggrecan aggregate was not different from control (115 ± 20 μm, Fig. 2.2F, G). Kruskal-Wallis One Way Analysis of Variance on Ranks followed by the post-hoc Dunn's Test for comparison with control (PDL only) showed that neurite lengths on aggrecan aggregate, aggrecan monomer, and hyaluronic acid were significantly different from neurite length on PDL ($p < 0.001$).

Since chondroitin sulfate-treated glass did not inhibit growth, we determined if chondroitin sulfate adhered to the PDL-treated glass slides by immunostaining with the CS56 antibodies. Similar intensities of immunostaining were seen for chondroitin sulfate and aggrecan aggregate (data not shown). This confirmed the presence of chondroitin sulfate on glass slides and the permissive nature of chondroitin sulfate when presented by itself, without the aggrecan core protein.

Although neurite growth on aggrecan aggregate was not significantly different from growth on aggrecan monomer, the presence of hyaluronic acid in the former substrate may contribute to its inhibition of neurite growth. Up to about 100 aggrecan monomers bind to one hyaluronic acid (reviewed in Dudhia, 2005). Since we used a 25μg/ml solution of aggrecan aggregate to coat the glass slides, there should be approximately 0.25-0.5 μg/ml hyaluronic acid in the solution. We used a serial dilution of hyaluronic acid solutions to coat the glass slides. Between 0.1 to 0.25μg/ml hyaluronic acid, growth was not inhibited at all compared to growth on control PDL (all at approx. 134 μm; Fig. 2.3A, B, E). Concentrations of 0.5μg/ml and higher were inhibitory to neurite growth (Fig. 2.3; $p < 0.001$). At 0.5μg/ml, neurite growth was decreased by half (76.9 ± 12.9 μm; Fig. 2.3C, E). At 10μg/ml and above, neurite length was further decreased to approximately 40-50μm (Fig. 2.3D, E). This suggested that hyaluronic acid contributed to the inhibition on DRG neurite growth due to aggrecan aggregate.

NT3 was supplied in the culture medium to stimulate growth from TrkC-expressing DRG neurons, which are a different population from the NGF-responsive ones. Neurite extension on PDL in the presence of NT3 (192 ± 15 μm; Fig. 2.4A, F) was 42% longer than growth with NGF (compare Fig.2.4 with Fig.2.2). The NT3-dependent neurite growth on aggrecan aggregate (45.5 ± 7.4 μm; Fig. 2.4B, F) was significantly reduced (p<0.001 by the Kruskal-Wallis One Way Analysis of Variance on Ranks followed by post-hoc Dunn's test) to one-quarter of the growth on PDL. Hyaluronic acid was also inhibitory and reduced growth to one-third (59.4 ± 10.5 μm; Fig. 2.4D, F) of control (p<0.001). Similar to neurite growth in NGF, chondroitin sulfate (Fig. 2.4C, F) and ChABC-treated aggrecan (Fig. 2.4E, F) did not reduce growth, although neurite length on ChABC-treated aggrecan (137 ± 18 μm) appeared slightly shorter compared to on control PDL.

Growth cones had very different morphologies on the various 'aggrecan' substrates

We next examined how each aggrecan component affected growth cone morphology. In the presence of NGF, growth cones growing on control PDL substrate had a fan-like, extended shape (Fig. 2.5A). Microtubules were present in the neurite shaft and in the central domain of the lamellipodia. Actin levels were highest in the peripheral domain of the lamellipodia and in filopodia. Numerous filopodia were found protruding from the lamellipodia and from the distal axon shaft. In stark contrast, growth cones growing on aggrecan aggregate were smaller (Fig. 2.5B, F) and many of them were pestle-shaped (arrow in Fig. 2.5B). They were devoid of filopodia (Fig. 2.5B, G). Such morphologies were suggestive of growth cone collapse. Branching of growth cones (arrowhead in Fig. 2.5B) could be found among neurites growing on this substrate.

Interestingly, although chondroitin sulfate did not reduce neurite length, it altered growth cone morphology, which was larger than the growth cones on PDL and had slightly (not significant) more filopodia (Fig. 2.5C, F, G). On hyaluronan, neurites had atypical growth cones (Fig. 2.5D) that were similar to those on aggrecan. The growth cones were small and had few filopodia (Fig. 2.5F, G), suggestive of total growth cone collapse. On ChABC-treated aggrecan, there appeared to be partial growth cone collapse (Fig. 2.5E). Growth cone sizes were slightly smaller than on PDL control substrate (Fig. 2.5F), and had significantly fewer filopodia (Fig. 2.5G).

For NT3-responsive neurite, the differences in growth cone morphologies on the various aggrecan substrates mirrored those of NGF-responsive ones. But on chondroitin sulfate, NT3-dependent neurite growth cones (Fig. 2.6A) were even larger than the growth cones from NGF-responsive neurites (Fig. 2.5C). On aggrecan, HA and ChABC-treated aggrecan, growth cones were significantly smaller and had fewer filopodia than on PDL (Fig. 2.6B, C).

Y27632 stimulated neurite growth on the different 'aggrecan' substrates

In our previous experiments (Borisoff et al., 2003), the Y27632 ROCK inhibitor promoted the growth of DRG neurites on a substrate containing aggrecan aggregate and laminin. In this study, we tested the whether Y27632 (25µM) stimulated neurite growth on each individual aggrecan components (Fig. 2.7; DRG cultures with and without Y27632 were performed concurrently. Neurite outgrowth without Y27632 (grey columns) were the same data as shown in Figures 2.2 and 2.4).

For NGF-dependent neurites (Fig. 2.7A), the presence of Y27632 in the culture medium stimulated NGF-dependent neurite growth in general, except for growth on hyaluronic acid. On PDL, the 'mean maximum neurite length' with Y27632 was 195 ± 16 µm, which was 44% higher than growth without Y27632 (p<0.001). On aggrecan aggregate (79.0 ± 12.1 µm; p<0.005) and aggrecan monomer (111 ± 9 µm; p<0.001), growth with Y27632 treatment was double that without ROCK inhibition. On chondroitin sulfate, ROCK inhibition resulted in 76% increase in growth (225 ± 13 µm; p<0.001). On ChABC-treated aggrecan, growth was increased by 68% (193 ± 26 µm; p<0.05). Neurite growth on the hyaluronic acid substrate was unchanged with Y27632 treatment (45.7 ± 6.9 µm).

In contrast to NGF-dependent neurite growth, the presence of Y27632 in the culture medium only slightly increased the growth of NT3-responsive neurites on control PDL, but the increase was not significant (Fig. 2.7B). On aggrecan aggregate, Y27632 significantly stimulated neurite growth by 61% (73.4 ± 9.8 µm; p<0.05). On chondroitin sulfate, neurite growth with Y27632 was 276 ± 17 µm, representing an increase of 47% (p<0.005). Another difference between NT3-and NGF-dependent neurite growth was that Y27632 increased NT3-dependent growth on hyaluronic acid to 126 ± 17 µm, which was double the length without Y27632 (p<0.05). A third difference between NGF- and NT3-responsive neurites was that NT3-responsive neurite growth on ChABC-treated aggrecan was not enhanced by Y27632 as for

NGF-responsive neurites. In the presence of Y27632, NT3-dependent growth on this substrate was 158 ± 20 μm, which was similar to growth without Y27632.

Interestingly, on hyaluronic acid, 25μM Y27632 treatment had no effect on NGF-neurite outgrowth, but significantly increased NT3-dependent neurite length. Therefore we further analysed neurite growth on hyaluronic acid at different concentrations of Y27632 (1 to 25μM). With NGF in the culture medium, neurite outgrowth slightly increased (although not significantly) with Y27632 treatment up to 5μM. At concentrations above 5μM, neurite length decreased and became slightly shorter than that in the absence of Y27632. NGF-dependent neurite growth was 54.8 ± 6.4μm in the absence of Y27632, 74.4 ± 12.3μm at 5μM Y27632, and 46.9 ± 6.9μm at 25μM Y27632. With NT3 in the medium, neurite outgrowth displayed a similar trend as NGF-dependent neurite growth at the different concentrations of Y27632 treatment. However, at all concentrations tested, Y27632 significantly increased neurite outgrowth ($p < 0.01$ by Kruskal Wallis ranked sum test followed by post-hoc Dunn's test). Neurite length in the absence of Y27632 was 59.4 ± 10.4μm, and maximum growth occurred at 5μM Y27632 (171 ± 40μm). At 25μM Y27362, neurite outgrowth was 126 ± 18μm.

Discussion

In the present study, we examined differences in neurite behaviour on various components of aggrecan, including aggrecan aggregate, aggrecan monomers, chondroitin sulfate, hyaluronic acid, and ChABC-treated aggrecan. Substrates containing aggrecan aggregate, aggrecan monomer, or hyaluronic acid inhibited neurite growth from NGF- and NT3-responsive DRG neurons. Chondroitin sulfate-glycosaminoglycan side chains did not decrease neurite length, but it induced atypical growth cone morphology with large lamellipodial veil. ChABC-treated aggrecan, i.e. aggrecan core protein with chondroitin sulfate stubs, also did not decrease neurite length, but it appeared to cause a partial collapse of growth cones. Hyaluronic acid, which was also a glycosaminoglycan but with no sulphated side group, dramatically inhibited neurite growth. It also appeared to cause total growth cone collapse. The Y27632 ROCK inhibitor stimulated neurite growth on most, but not all substrates. For NGF-responsive neurites, Y27632 treatment increased neurite length on all substrates tested, except on hyaluronic acid. For NT3-responsive neurites, it increased growth on aggrecan aggregate, chondroitin sulfate, and hyaluronic acid.

Aggrecan aggregate decreased the length of NGF- and NT3-responsive DRG neurites, as expected from our previous findings (Borisoff et al., 2003) and from work of others (Condic et al., 1999;Johnson et al., 2002;Snow et al., 1990;Snow and Letourneau, 1992;Tom et al., 2004). However, growth cone morphology on this substrate was different from that observed previously, which had relatively large lamellipodia and numerous filopodia (Borisoff et al., 2003). Growth cones, also from embryonic chick DRG, on laminin mixed with non-neural CSPGs (Snow et al., 1996) or with nervous system-derived CSPGs (Snow et al., 2001) did not collapse, but displayed a more streamlined morphology with many filopodia. Close examination of the growth cones revealed that their filopodia constantly sampled the laminin/CSPG border (Snow et al., 1996;2001). The substrate used in this experiment differed from those in others by the absence of the stimulatory molecule laminin. In this experiment, many of the growth cones on aggrecan aggregate were pestle-shaped and devoid of filopodia, and resembled the 'dystrophic' growth cones from adult rat DRGs on aggrecan/laminin (Tom et al., 2004). Therefore, whether the growth cone collapses on CSPGs may be dependent on age or species, and in the absence of a stimulatory molecule, CSPGs cause at least partial growth cone collapse.

The importance of chondroitin sulfate-glycosaminoglycan side chains in CSPG inhibition have been topics of debate. *In vitro*, glycosaminoglycan substrates can stimulate (Dou and Levine, 1995;Clement et al., 1998) or inhibit (Carbonetto et al., 1983;Verna et al., 1989;Snow et al., 1996) neurite growth, and the inhibition is affected by cell type and other molecules that coexisted with glycosaminoglycans in the substrate, such as collagen, laminin, or L1. On discontinuously coated substrates, growth of E8 DRG neurites on the side with type I collagen only was straight and profuse, while neurite growth were shorter and convoluted on the side with both collagen and chondroitin sulfate (Verna et al., 1989). The presence of chondroitin sulfate-glycosaminoglycan bound to type I collagen appeared to restrict neurites in their path of elongation. In our experiments, chondroitin sulfate-glycosaminoglycan on its own neither stimulated nor inhibited neurite growth. Thus, it appeared that neurite growth in response to chondroitin sulfate was dependent on the presence of other substrate molecules.

In this study, ChABC treatment abolished aggrecan inhibition on neurite growth, indicating that the chondroitin sulfate-glycosaminoglycan side chains were critical for aggrecan inhibition. And since chondroitin sulfate by itself was not inhibitory, the effect of intact aggrecan appeared to result from the chondroitin sulfate-glycosaminoglycan side chains being held in a

particular conformation, or anchored by the protein core. The increase in neurite growth with ChABC digestion is in agreement with results from the *in vitro* 'turning assay' in which a significantly higher number of DRG neurites crossed from laminin onto ChABC-treated intervertebral disc aggrecan, compared to untreated aggrecan (Johnson et al., 2002). Our results also agreed with those obtained by Snow and colleagues (1990;1991), who found that a cartilage CSPG, most probably aggrecan, was repulsive to embryonic DRG and retinal ganglion cell (RGC) neurites, but ChABC treatment partially reversed its non-permissiveness. In these other studies, since aggrecan was mixed with laminin, it was uncertain whether ChABC reversed the inhibition directly by cleaving the inhibitory glycosaminoglycan chains, or indirectly through unmasking of the laminin epitopes that interact with integrin receptors on the growth cones (McKeon et al., 1995). Since there was no stimulatory molecule present in the substrates used in this experiments, our results supported the former explanation.

The Rho/ROCK pathway is activated downstream of CSPGs (Borisoff et al., 2003;Monnier et al., 2003;Sivasankaran et al., 2004). In our previous study, the ROCK inhibitor Y27632 stimulated chick DRG outgrowth on a substrate with aggrecan and laminin (Borisoff et al., 2003). Others have shown that Y27632 increased neurite outgrowth on CSPGs other than aggrecan (Monnier et al., 2003;Sivasankaran et al., 2004). Results from Borisoff et al. (2003) and Schweigreiter et al. (2004) indicated that aggrecan and versican, respectively, increased RhoA activation. In the present study, Y27632 increased neurite growth on most of the aggrecan component, in agreement with Rho/ROCK signaling being associated with inhibitory signaling. However, NGF-dependent neurite growth on hyaluronic acid was unchanged with Y27632 treatment. On ChABC-digested aggrecan, there was no stimulation of NT3-dependent neurite growth with Y27632. One possibility was that the Rho/ROCK pathway was not activated on these substrates in the respective neurites. Furthermore, since Y27632 increased neurite growth on neutral PDL, it was possible that such treatment increased the general growth propensity of DRG neurites, rather than specifically overcome aggrecan inhibition. Therefore, additional experiments are needed to determine the exact signaling mechanism activated by the different aggrecan components, especially by hyaluronic acid and aggrecan core protein.

Hyaluronic acid significantly decreased neurite length from both NGF- and NT3-responsive DRG neurites, and appeared to induce total growth cone collapse. The signaling activated by hyaluronic acid in neurons is largely unknown. In non-neuronal cells, CD44 is a

major cell surface receptor for hyaluronic acid (Underhill et al., 1987). In these cells, CD44 activates Rho via Rho guanine nucleotide exchange factor (GEF) (Bourguignon et al., 2003), and this receptor also interacts directly with ROCK (Singleton and Bourguignon, 2002;Bourguignon et al., 1999). Moreover, Rho and ROCK facilitate the interaction between CD44 and focal adhesion molecules, ankyrin and the ERM (ezrin-radixin-moesin) proteins (Hirao et al., 1996;Bourguignon et al., 1999). Since the CD44 receptor is expressed by DRG neurons (Ikeda et al., 1996), we hypothesize that hyaluronic acid activated the Rho/ROCK pathway in these neurons via the CD44 receptor. And since Rho and ROCK activation often result in neurite retraction and growth cone collapse (Bito et al., 2000;Lehmann et al., 1999;Hirose et al., 1998), the knowledge of CD44 expression could help to explain how hyaluronic acid induced such responses from the DRG neurites.

Both NGF- and NT3-neurites displayed a trend with neurite length increasing at low Y27632 concentrations up to 5μM, but decreasing as concentrations of Y27632 increased from 5 to 25 μM. Such decrease in neurite length with higher Y27362 treatment may be explained by considering the mechanics behind growth cone dynamics. A well-accepted theory of growth cone advance hypothesizes that three factors: actin polymerization, engagement–disengagement between actin cytoskeleton and substrate (the 'clutch'), and retrograde flow of F-actin, determine whether the growth cone extends, retracts, or remains stationary (Suter and Forscher, 1998;Mitchison and Kirschner, 1988). Rho/ROCK signaling is involved in all three factors of growth cone advance (Amano et al., 1996;Ohashi et al., 2000;Renaudin et al., 1999). Inhibition of ROCK facilitates actin turnover (Bito et al., 2000), disengagement of 'clutch' (Woo and Gomez, 2006), and attenuates retrograde F-actin flow (Schmidt et al., 2002), thus the net result of Rho/ROCK inhibition in general favours growth cone advance and neurite extension. In this experiment, for neurite growth on aggrecan components where Y27632 increased growth (aggrecan aggregate, glycosaminoglycan, and aggrecan core protein), suppression of Rho/ROCK appeared to drive the growth cone toward a more optimal state for growth cone advance. On hyaluronic acid, the 'growth cones' were dramatically disrupted, resulting in very small structures that could hardly be identified as growth cones. We hypothesize that ROCK inhibition might have limited the formation or stabilization of focal adhesions in the NGF growth cones on this substrate to such a degree that growth cone advance was confounded. A recent paper by Woo and Gomez (2006) lends support to this hypothesis. Although Rho/ROCK activation

generally led to growth cone collapse and neurite retraction, a modest level of Rho/ROCK activity was necessary for the formation of stable point contacts (Woo and Gomez, 2006). Therefore, low concentrations of the ROCK inhibitor increased growth, but extreme inhibition of ROCK with high concentrations of Y27632 limited growth.

In this study, we investigated the effects of different components of aggrecan on neurite growth without the co-existence of any stimulatory molecule in the substrate. Some of the aggrecan components, including aggrecan aggregate and hyaluronic acid, decreased the length of NGF- and NT3-responsive neurites. Chondroitin sulfate-glycosaminoglycan side chains on aggrecan are critical to the inhibition on neurite growth, as ChABC treatment abolished aggrecan inhibition. However, chondroitin sulfate by itself was not inhibitory, indicating that these side chains must be held in specific conformation by the core protein in order to be active. ROCK inhibition with Y27632 increased neurite growth on most, but not all, of the substrates, suggesting that not all aggrecan components signalled through the Rho/ROCK pathway. In future experiments, it would be interesting to determine whether the aggrecan core protein and chondroitin sulfate-glycosaminoglycan side chains activate different downstream signaling pathways in growth cones, thus resulting in the differences in growth cone morphologies. Also, since hyaluronic acid appears to be a significant inhibitor of neurite growth and is abundant in the CNS ECM (Margolis et al., 1975), it may contribute to the failure of axonal regeneration after spinal cord injury.

Figure 2.1

Quantification of neurite outgrowth from E9 chick dorsal root ganglion (DRG) explants. The neurites were immunostained with anti-neurofilament antibodies, and digital images of the explant were captured on a fluorescent microscope connected to a Q-imaging camera. Using a macro within the Northern Eclipse software, a central reference point (C) on the DRG cell bodies was denoted by the crosshair. Then a line (P) was traced around the perimeter of the cell bodies to calculate the mean radius of the DRG, with reference to the cross hair. Another line (N) was traced around the neurite ends to calculate the mean distance between the neurite ends and the central reference point. Finally, the mean DRG radius was subtracted from the mean distance of the neurite ends to calculate the 'mean maximum neurite length' (in μm). Scale bar, 250μm.
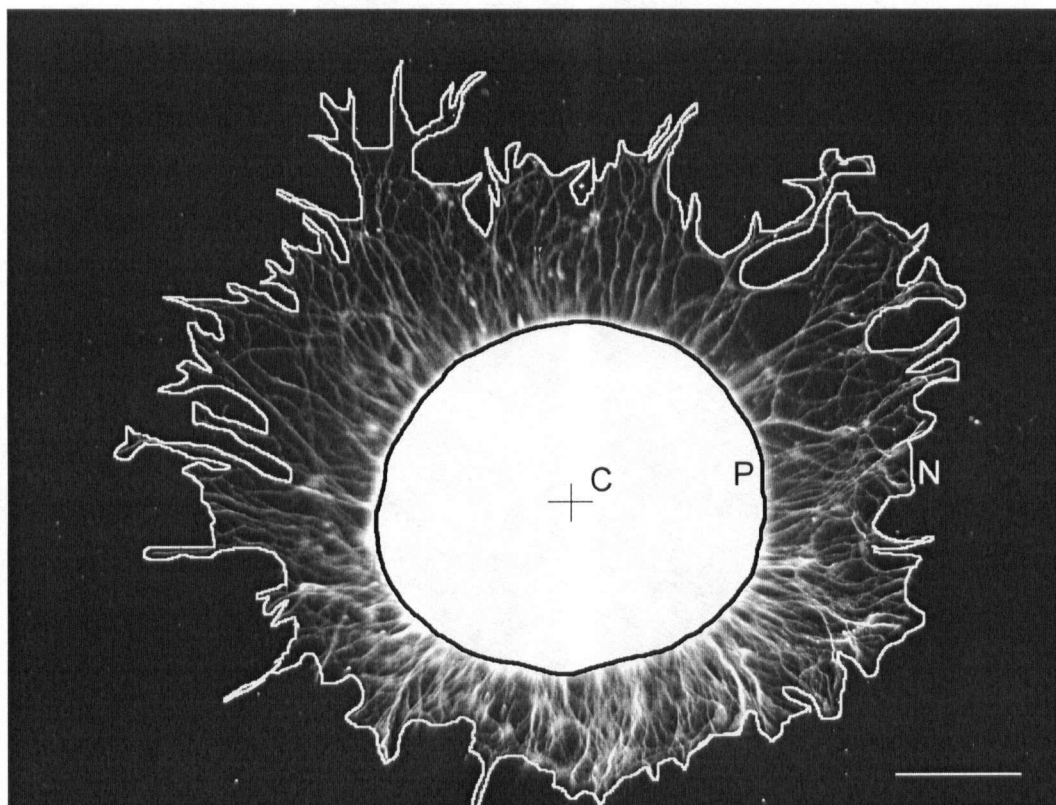
Figure 2.2

NGF-dependent neurite outgrowth on poly-D-lysine (PDL) and various components of aggrecan. A) E9 chick DRG explants in the lumbar spinal cord region were harvested and plated on control PDL substrate (A), and on PDL with subsequent treatment with aggrecan bound with hyaluronic acid (B), aggrecan monomer (C), chondroitin sulfate glycosaminoglycan side chains (D), hyaluronic acid (E), or with chondroitinase ABC (ChABC)-treated aggrecan with hyaluronic acid (F). The DRGs were grown in Neurobasal medium with B27 nutrient, and 2 ng/ml NGF. (G) Neurite length was quantified using the Northern Eclipse software. Aggrecan aggregate, aggrecan monomer, and hyaluronic acid were inhibitory to neurite growth compared to growth on control PDL. *, $p < 0.001$ by Kruskal-Wallis One Way Analysis of Variance on Ranks followed by post-hoc Dunn's test. Scale bar, 250μm.

A PDL

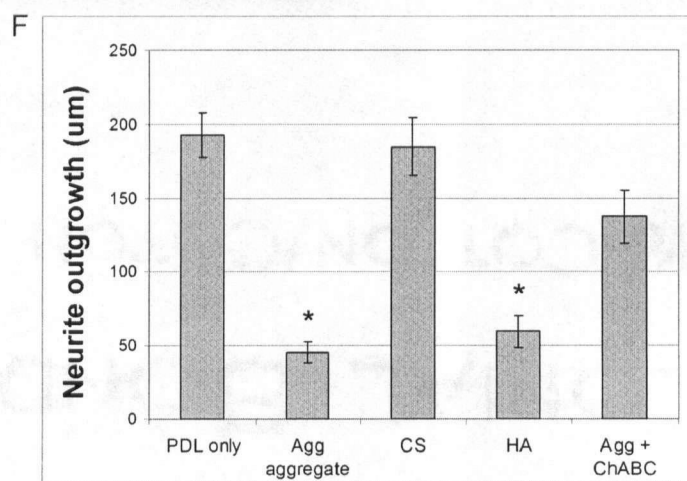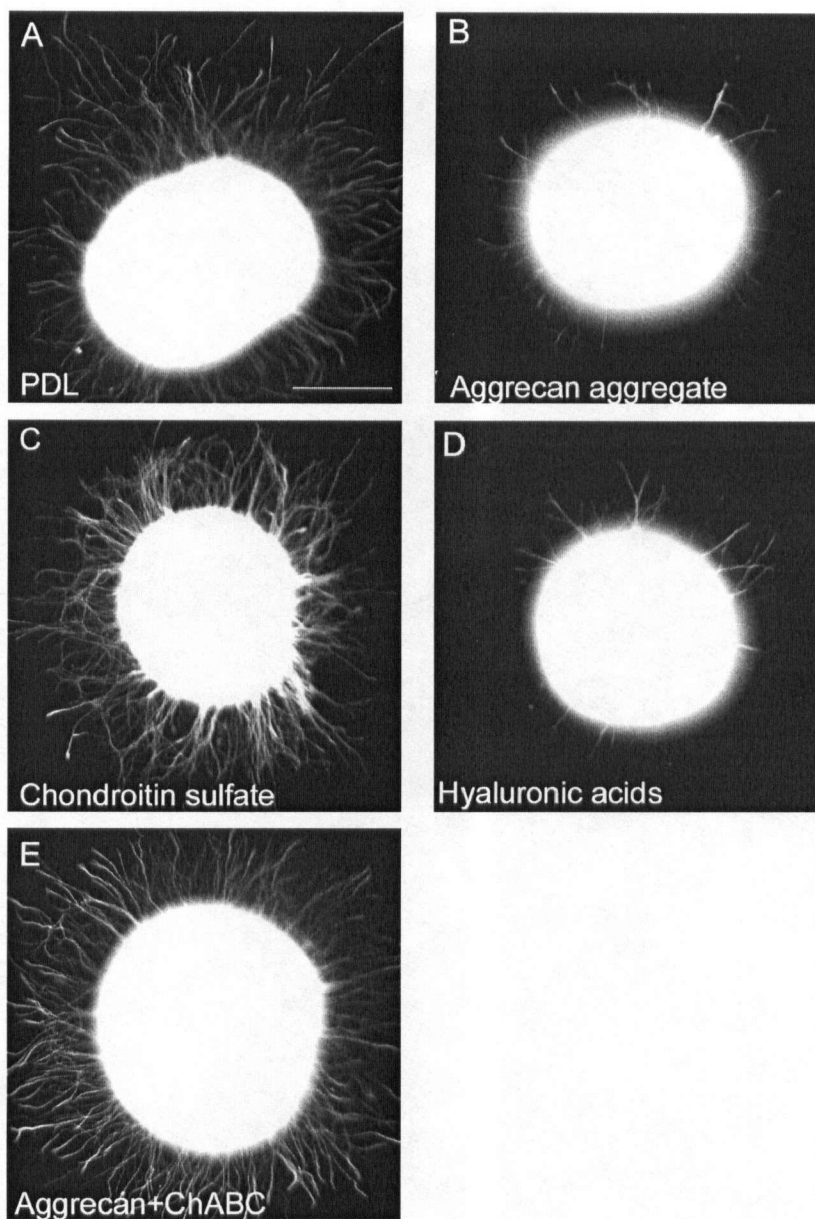B Aggrecan aggregate

C Aggrecan monomer

D Chondroitin sulfate

E Hyaluronic acid

F Aggrecan+ChABC

G
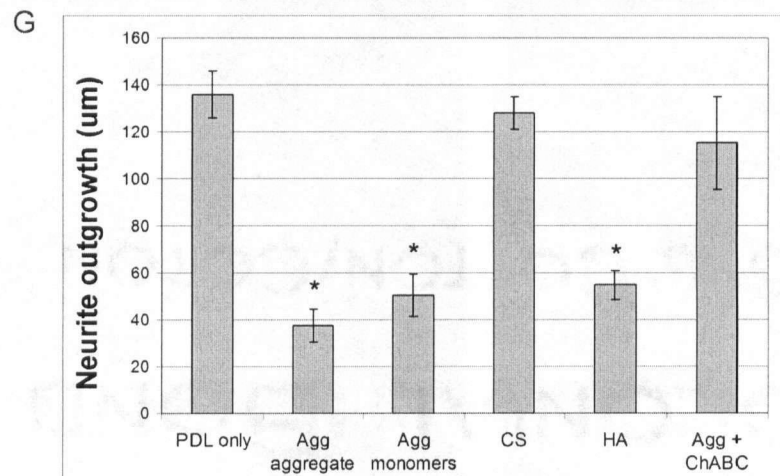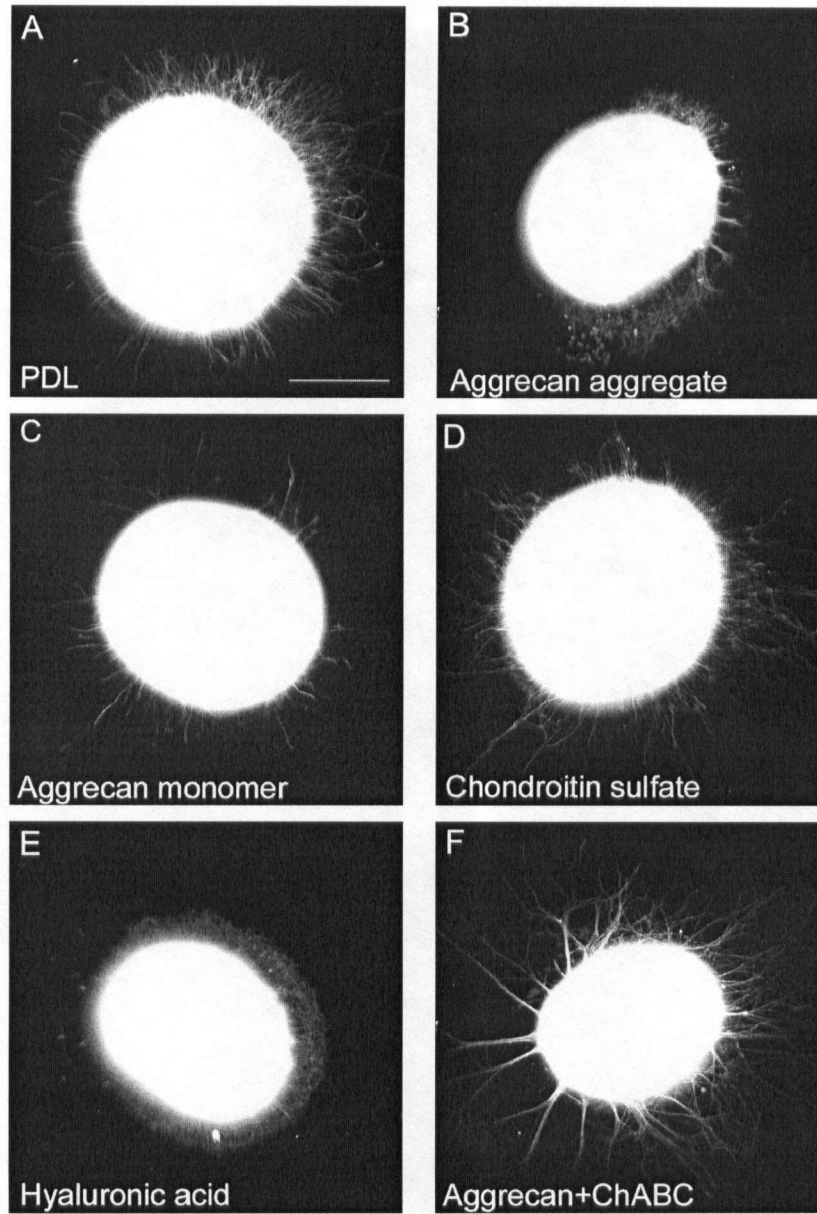
Figure 2.3

Hyaluronic acid (HA) inhibited DRG neurite outgrowth in a dose-dependent manner. When low concentrations of hyaluronic acid solution was used to coat the PDL-treated glass slides, neurite outgrowth was not inhibited. For example, when 0.1 (A) and 0.25 μM (B) hyaluronic acid solutions were used to coat glass slides, neurite growth was as robust as on PDL control. At concentrations of 0.5 μg/ml and higher (C and D), growth was significantly inhibited. (E) Quantification of neurite outgrowth. *, p<0.001. Scale bar, 250μm.
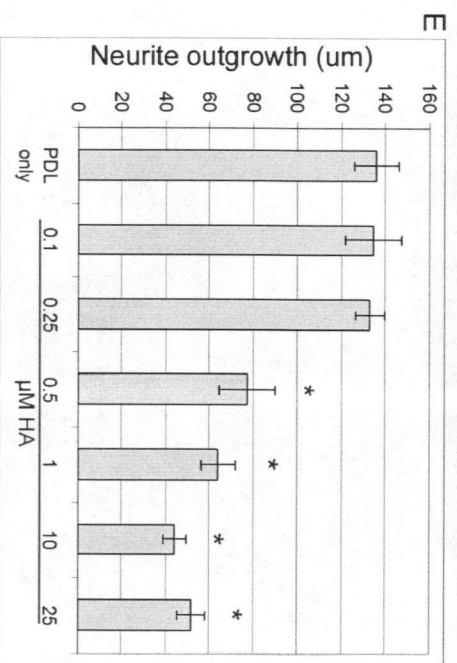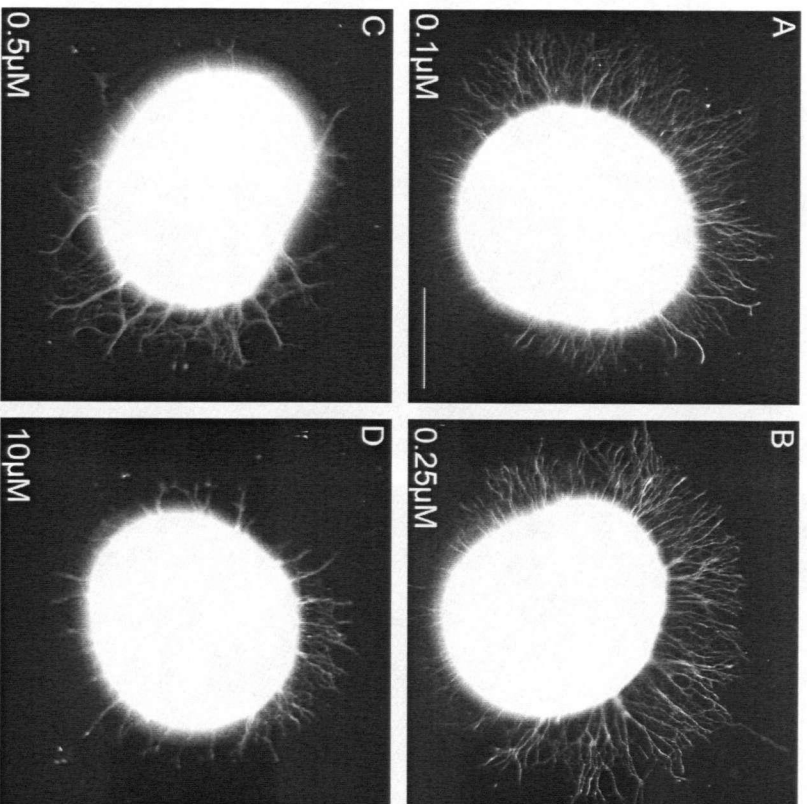
Figure 2.4

NT3-dependent neurite outgrowth was inhibited on aggrecan aggregate and on hyaluronic acid. The DRGs were grown in Neurobasal medium with B27 nutrient, and 2 ng/ml NT3. (A) E9 chick DRG outgrowth on control PDL substrate. (B) Growth on aggrecan bound with hyaluronic acid and link protein was inhibited compared to that on control PDL. (C) Growth on chondroitin sulfate side chains was as robust as on PDL control. (D) Growth on hyaluronic acid was inhibited. (E) Growth on ChABC-treated aggrecan was not inhibited. (F) Neurite length was quantified using the Northern Eclipse software. *, $p<0.001$ by Kruskal-Wallis One Way Analysis of Variance on Ranks followed by post-hoc Dunn's test. Scale bar, 250μm.

A PDL

B Aggrecan aggregate

C Chondroitin sulfate

D Hyaluronic acids

E Aggrecan+ChABC

F

Neurite outgrowth (um)

PDL only | Agg aggregate | CS | HA | Agg + ChABC

Figure 2.5

Different growth cone morphologies as NGF-responsive neurites grew on various aggrecan substrates. DRG cultures were immunostained with anti-actin antibodies (red), and with anti-βIII-tubulin antibodies to label microtubules (green). (A) Growth cone on PDL control substrate, with lamellipodia and numerous filopodia. (B) Growth cones on aggrecan (agg) aggregate were small and devoid of filopodia. One growth cone had a pestle shape (arrow), and another one displayed growth cone branching (arrowhead). (C) A growth cone on chondroitin sulfate glycosaminoglycan (CS), which had large lamellipodial veil. (D) Neurites on hyaluronan (HA) were short and had very small 'growth cone'. (E) Growth cones on ChABC-treated aggrecan (Agg+ChABC) were slightly smaller than on PDL control, and had significantly fewer filopodia. (F) Quantification of growth cone sizes. (G) Quantification of filopodial number per growth cone. Scale bar, 25μm. *, $p < 0.01$.
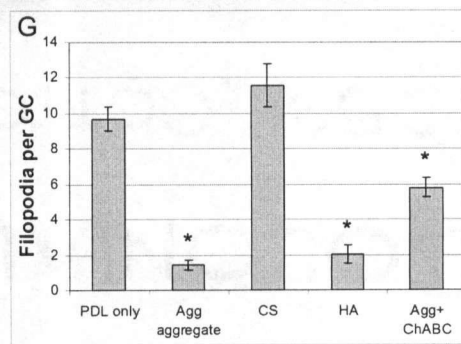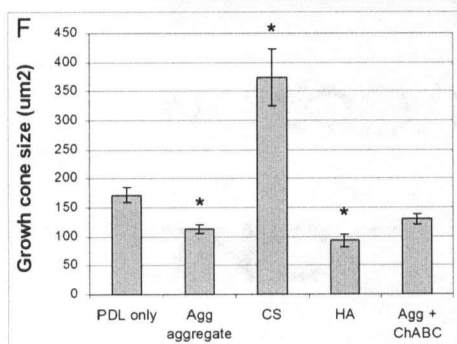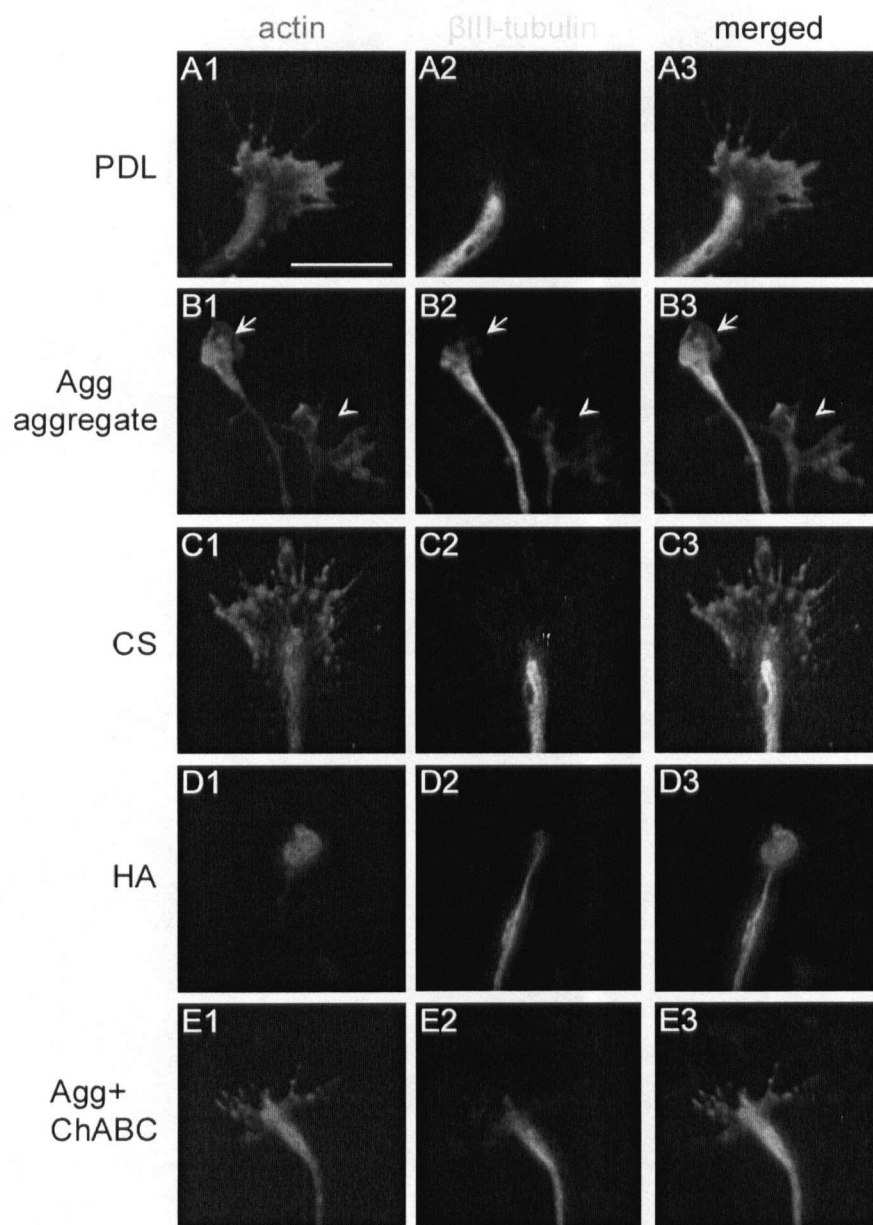
Figure 2.6

(A) A growth cone from NT3-responsive neurite on chondroitin sulfate glycosaminoglycan. It was immunostained with anti-actin antibodies (red) and with anti-βIII-tubulin antibodies to label microtubules (green). (B) Quantification of growth cone sizes. (C) Quantification of filopodial number per growth cone. Scale bar, 25μm. *, $p < 0.05$.
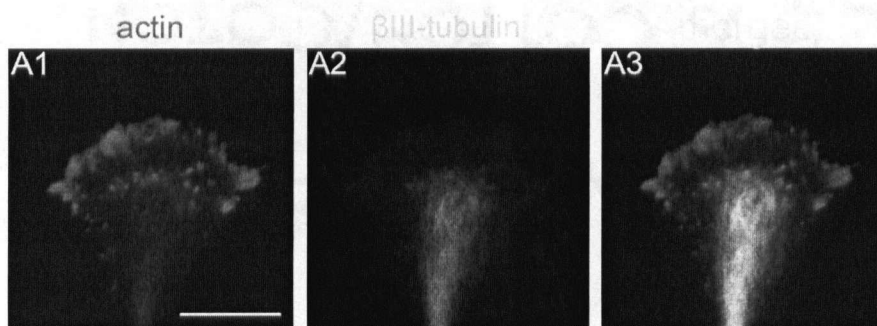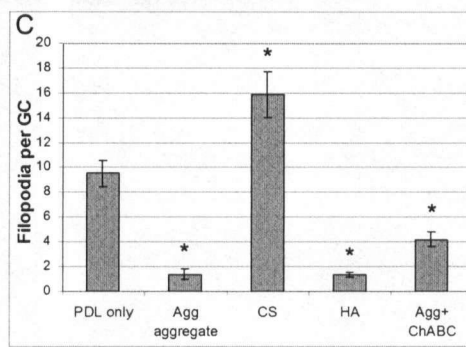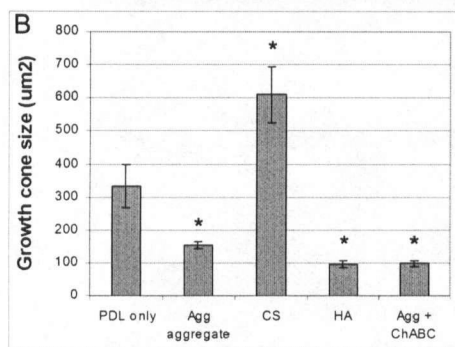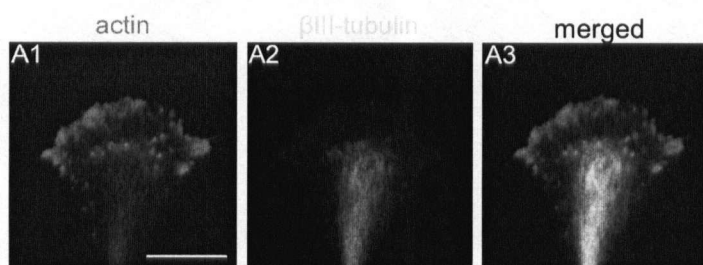
actin   βIII-tubulin   merged

A1   A2   A3

B

Growth cone size (um2)

*

*

*

*

PDL only | Agg aggregate | CS | HA | Agg + ChABC

C

Filopodia per GC

*

*

*

*

PDL only | Agg aggregate | CS | HA | Agg+ ChABC

actin   βIII-tubulin

A1   A2   A3

Figure 2.7

Effects of ROCK inhibition with Y27632 on neurite length. (A) The presence of 25µM Y27632 in the culture medium stimulated NGF-responsive neurite growth on control PDL and on most of the different 'aggrecan' substrates. On hyaluronic acid, neurite length was unchanged. (B) For NT3-responsive neurites, Y27632 treatment stimulated growth on aggrecan aggregate, chondroitin sulfate glycosaminoglycan and hyaluronic acid. DRG cultures with and without Y27632 were performed concurrently. Neurite outgrowth without Y27632 (grey columns) were the same data as shown in figures 2 and 4. *, $p<0.05$; **, $p<0.005$; ***, $p<0.001$. Scale bar, 250µm.

B NT3

Neurite outgrowth (um)

PDL only

Agg aggregate

CS

HA

Agg + ChABC

* ** *

No Y
With Y25

A NGF

Neurite outgrowth (um)

PDL only

Agg aggregate monomers

Agg

CS

HA

Agg + ChABC

*** ** *** *** *

No Y
With Y25
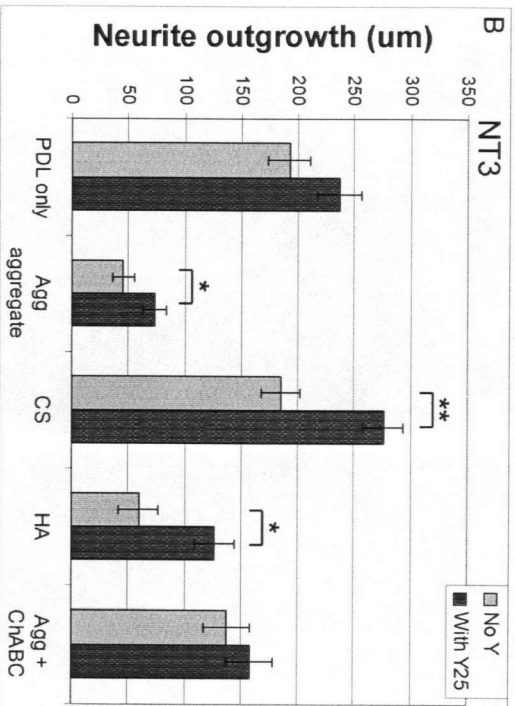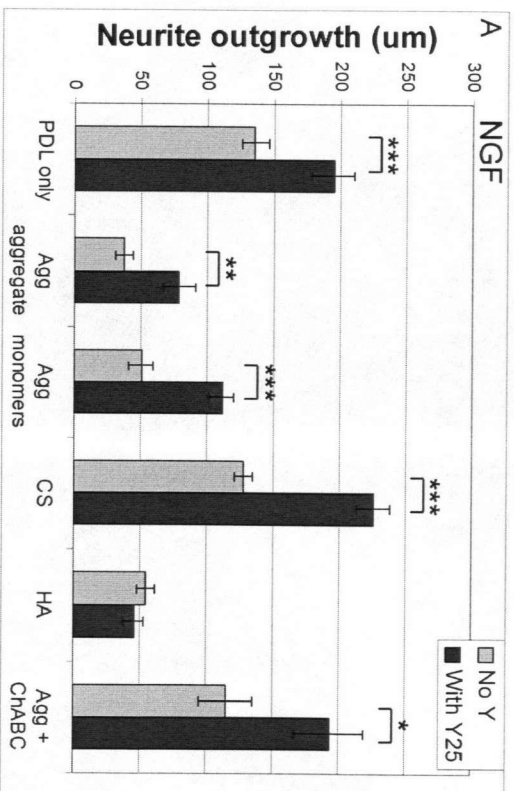
Figure 2.8.

Neurite outgrowth on hyaluronic acid at different concentrations of Y27632 treatment. With NGF in the culture medium (white bars), neurite outgrowth slightly increased (although not significantly) with Y27632 treatment up to 5μM. At concentrations above 5μM, neurite length decreased and became slightly shorter than that in the absence of Y27632 (not significant). With NT3 in the medium, neurite outgrowth (grey bars) displayed a similar trend as NGF-neurite growth with the maximum growth occurring at 5μM Y27632. At all concentrations tested, Y27632 significantly increased neurite outgrowth. *, $p < 0.01$ by ANOVA followed by post-hoc Dunn's test.
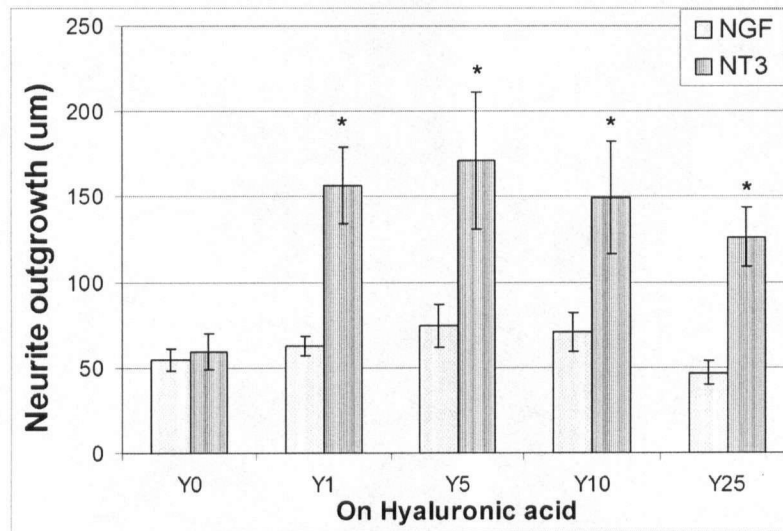
References

Amano M, Ito M, Kimura K, Fukata Y, Chihara K, Nakano T, Matsuura Y, Kaibuchi K (1996) Phosphorylation and activation of myosin by Rho-associated kinase (Rho- kinase). J Biol Chem 271:20246-20249.

Asher RA, Scheibe RJ, Keiser HD, Bignami A (1995) On the existence of a cartilage-like proteoglycan and link proteins in the central nervous system. Glia 13:294-308.

Averill S, McMahon SB, Clary DO, Reichardt LF, Priestley JV (1995) Immunocytochemical localization of trkA receptors in chemically identified subgroups of adult rat sensory neurons. Eur J Neurosci 7:1484-1494.

Bandtlow CE, Schwab ME (2000) NI-35/250/nogo-a: a neurite growth inhibitor restricting structural plasticity and regeneration of nerve fibers in the adult vertebrate CNS. Glia 29:175-181.

Bito H, Furuyashiki T, Ishihara H, Shibasaki Y, Ohashi K, Mizuno K, Maekawa M, Ishizaki T, Narumiya S (2000) A critical role for a Rho-associated kinase, p160ROCK, in determining axon outgrowth in mammalian CNS neurons. Neuron 26:431-441.

Borisoff JF, Chan CC, Hiebert GW, Oschipok L, Robertson GS, Zamboni R, Steeves JD, Tetzlaff W (2003) Suppression of Rho-kinase activity promotes axonal growth on inhibitory CNS substrates. Mol Cell Neurosci 22:405-416.

Bourguignon LY, Singleton PA, Zhu H, Diedrich F (2003) Hyaluronan-mediated CD44 interaction with RhoGEF and Rho kinase promotes Grb2-associated binder-1 phosphorylation and phosphatidylinositol 3-kinase signaling leading to cytokine (macrophage-colony stimulating factor) production and breast tumor progression. J Biol Chem 278:29420-29434.

Bourguignon LY, Zhu H, Shao L, Zhu D, Chen YW (1999) Rho-kinase (ROK) promotes CD44v(3,8-10)-ankyrin interaction and tumor cell migration in metastatic breast cancer cells. Cell Motil Cytoskeleton 43:269-287.

Buchman VL, Davies AM (1993) Different neurotrophins are expressed and act in a developmental sequence to promote the survival of embryonic sensory neurons. Development 118:989-1001.

Buj-Bello A, Buchman VL, Horton A, Rosenthal A, Davies AM (1995) GDNF is an age-specific survival factor for sensory and autonomic neurons. Neuron 15:821-828.

Carbonetto S, Gruver MM, Turner DC (1983) Nerve fiber growth in culture on fibronectin, collagen, and glycosaminoglycan substrates. J Neurosci 3:2324-2335.

Caroni P, Savio T, Schwab ME (1988) Central nervous system regeneration: oligodendrocytes and myelin as non- permissive substrates for neurite growth. Prog Brain Res 78:363-370.

Clement AM, Nadanaka S, Masayama K, Mandl C, Sugahara K, Faissner A (1998) The DSD-1 carbohydrate epitope depends on sulfation, correlates with chondroitin sulfate D motifs, and is sufficient to promote neurite outgrowth. J Biol Chem 273:28444-28453.

Condic ML, Snow DM, Letourneau PC (1999) Embryonic neurons adapt to the inhibitory proteoglycan aggrecan by increasing integrin expression. J Neurosci 19:10036-10043.

Doege KJ, Sasaki M, Kimura T, Yamada Y (1991) Complete coding sequence and deduced primary structure of the human cartilage large aggregating proteoglycan, aggrecan. Human-specific repeats, and additional alternatively spliced forms. J Biol Chem 266:894-902.

Dontchev VD, Letourneau PC (2003) Growth cones integrate signaling from multiple guidance cues. J Histochem Cytochem 51:435-444.

Dou CL, Levine JM (1995) Differential effects of glycosaminoglycans on neurite growth on laminin and L1 substrates. J Neurosci 15:8053-8066.

Dudhia J (2005) Aggrecan, aging and assembly in articular cartilage. Cell Mol Life Sci 62:2241-2256.

Ernfors P (2001) Local and target-derived actions of neurotrophins during peripheral nervous system development. Cell Mol Life Sci 58:1036-1044.

Fitch MT, Silver J (1997) Activated macrophages and the blood-brain barrier: inflammation after CNS injury leads to increases in putative inhibitory molecules. Exp Neurol 148:587-603.

Fournier AE, Takizawa BT, Strittmatter SM (2003) Rho kinase inhibition enhances axonal regeneration in the injured CNS. J Neurosci 23:1416-1423.

Gaese F, Kolbeck R, Barde YA (1994) Sensory ganglia require neurotrophin-3 early in development. Development 120:1613-1619.

Hirao M, Sato N, Kondo T, Yonemura S, Monden M, Sasaki T, Takai Y, Tsukita S, Tsukita S (1996) Regulation mechanism of ERM (ezrin/radixin/moesin) protein/plasma membrane association: possible involvement of phosphatidylinositol turnover and Rho-dependent signaling pathway. J Cell Biol 135:37-51.

Hirose M, Ishizaki T, Watanabe N, Uehata M, Kranenburg O, Moolenaar WH, Matsumura F, Maekawa M, Bito H, Narumiya S (1998) Molecular dissection of the Rho-associated protein kinase (p160ROCK)- regulated neurite remodeling in neuroblastoma N1E-115 cells. J Cell Biol 141:1625-1636.

Ikeda K, Nakao J, Asou H, Toya S, Shinoda J, Uyemura K (1996) Expression of CD44H in the cells of neural crest origin in peripheral nervous system. Neuroreport 7:1713-1716.

Jandik KA, Gu K, Linhardt RJ (1994) Action pattern of polysaccharide lyases on glycosaminoglycans. Glycobiology 4:289-296.

Jin Z, Strittmatter SM (1997) Rac1 mediates collapsin-1-induced growth cone collapse. J Neurosci 17:6256-6263.

Johnson WE, Caterson B, Eisenstein SM, Hynds DL, Snow DM, Roberts S (2002) Human intervertebral disc aggrecan inhibits nerve growth in vitro. Arthritis Rheum 46:2658-2664.

Jones LL, Margolis RU, Tuszynski MH (2003) The chondroitin sulfate proteoglycans neurocan, brevican, phosphacan, and versican are differentially regulated following spinal cord injury. Exp Neurol 182:399-411.

Kiani C, Chen L, Wu YJ, Yee AJ, Yang BB (2002) Structure and function of aggrecan. Cell Res 12:19-32.

Landolt RM, Vaughan L, Winterhalter KH, Zimmermann DR (1995) Versican is selectively expressed in embryonic tissues that act as barriers to neural crest cell migration and axon outgrowth. Development 121:2303-2312.

Lefcort F, Clary DO, Rusoff AC, Reichardt LF (1996) Inhibition of the NT-3 receptor TrkC, early in chick embryogenesis, results in severe reductions in multiple neuronal subpopulations in the dorsal root ganglia. J Neurosci 16:3704-3713.

Lehmann M, Fournier A, Selles-Navarro I, Dergham P, Sebok A, Leclerc N, Tigyi G, McKerracher L (1999) Inactivation of Rho signaling pathway promotes CNS axon regeneration. J Neurosci 19:7537-7547.

Lemons ML, Howland DR, Anderson DK (1999) Chondroitin sulfate proteoglycan immunoreactivity increases following spinal cord injury and transplantation. Exp Neurol 160:51-65.

Lemons ML, Sandy JD, Anderson DK, Howland DR (2001) Intact aggrecan and fragments generated by both aggrecanse and metalloproteinase-like activities are present in the developing and adult rat spinal cord and their relative abundance is altered by injury. J Neurosci 21:4772-4781.

Margolis RU, Margolis RK, Chang LB, Preti C (1975) Glycosaminoglycans of brain during development. Biochemistry 14:85-88.

McKeon RJ, Hoke A, Silver J (1995) Injury-induced proteoglycans inhibit the potential for laminin-mediated axon growth on astrocytic scars. Exp Neurol 136:32-43.

Milev P, Maurel P, Chiba A, Mevissen M, Popp S, Yamaguchi Y, Margolis RK, Margolis RU (1998) Differential regulation of expression of hyaluronan-binding proteoglycans in developing brain: aggrecan, versican, neurocan, and brevican. Biochem Biophys Res Commun 247:207-212.

Mitchison T, Kirschner M (1988) Cytoskeletal dynamics and nerve growth. Neuron 1:761-772.

Molliver DC, Radeke MJ, Feinstein SC, Snider WD (1995) Presence or absence of TrkA protein distinguishes subsets of small sensory neurons with unique cytochemical characteristics and dorsal horn projections. J Comp Neurol 361:404-416.

Monnier PP, Sierra A, Macchi P, Deitinghoff L, Andersen JS, Mann M, Flad M, Hornberger MR, Stahl B, Bonhoeffer F, Mueller BK (2002) RGM is a repulsive guidance molecule for retinal axons. Nature 419:392-395.

Monnier PP, Sierra A, Schwab JM, Henke-Fahle S, Mueller BK (2003) The Rho/ROCK pathway mediates neurite growth-inhibitory activity associated with the chondroitin sulfate proteoglycans of the CNS glial scar. Mol Cell Neurosci 22:319-330.

Morgenstern DA, Asher RA, Fawcett JW (2002) Chondroitin sulphate proteoglycans in the CNS injury response. Prog Brain Res 137:313-332.

Ohashi K, Nagata K, Maekawa M, Ishizaki T, Narumiya S, Mizuno K (2000) Rho-associated kinase ROCK activates LIM-kinase 1 by phosphorylation at threonine 508 within the activation loop. J Biol Chem 275:3577-3582.

Popp S, Andersen JS, Maurel P, Margolis RU (2003) Localization of aggrecan and versican in the developing rat central nervous system. Dev Dyn 227:143-149.

Renaudin A, Lehmann M, Girault J, McKerracher L (1999) Organization of point contacts in neuronal growth cones. J Neurosci Res 55:458-471.

Schmidt JT, Morgan P, Dowell N, Leu B (2002) Myosin light chain phosphorylation and growth cone motility. J Neurobiol 52:175-188.

Schweigreiter R, Walmsley AR, Niederost B, Zimmermann DR, Oertle T, Casademunt E, Frentzel S, Dechant G, Mir A, Bandtlow CE (2004) Versican V2 and the central inhibitory domain of Nogo-A inhibit neurite growth via p75NTR/NgR-independent pathways that converge at RhoA. Mol Cell Neurosci 27:163-174.

Singleton PA, Bourguignon LY (2002) CD44v10 interaction with Rho-kinase (ROK) activates inositol 1,4,5-triphosphate (IP3) receptor-mediated Ca2+ signaling during hyaluronan (HA)-induced endothelial cell migration. Cell Motil Cytoskeleton 53:293-316.

Sivasankaran R, Pei J, Wang KC, Zhang YP, Shields CB, Xu XM, He Z (2004) PKC mediates inhibitory effects of myelin and chondroitin sulfate proteoglycans on axonal regeneration. Nat Neurosci 7:261-268.

Snow DM, Brown EM, Letourneau PC (1996) Growth cone behavior in the presence of soluble chondroitin sulfate proteoglycan (CSPG), compared to behavior on CSPG bound to laminin or fibronectin. Int J Dev Neurosci 14:331-349.

Snow DM, Lemmon V, Carrino DA, Caplan AI, Silver J (1990) Sulfated proteoglycans in astroglial barriers inhibit neurite outgrowth in vitro. Exp Neurol 109:111-130.

Snow DM, Letourneau PC (1992) Neurite outgrowth on a step gradient of chondroitin sulfate proteoglycan (CS-PG). J Neurobiol 23:322-336.

Snow DM, Mullins N, Hynds DL (2001) Nervous system-derived chondroitin sulfate proteoglycans regulate growth cone morphology and inhibit neurite outgrowth: a light, epifluorescence, and electron microscopy study. Microsc Res Tech 54:273-286.

Snow DM, Watanabe M, Letourneau PC, Silver J (1991) A chondroitin sulfate proteoglycan may influence the direction of retinal ganglion cell outgrowth. Development 113:1473-1485.

Suter DM, Forscher P (1998) An emerging link between cytoskeletal dynamics and cell adhesion molecules in growth cone guidance. Curr Opin Neurobiol 8:106-116.

Tang S, Qiu J, Nikulina E, Filbin MT (2001) Soluble myelin-associated glycoprotein released from damaged white matter inhibits axonal regeneration. Mol Cell Neurosci 18:259-269.

Tang X, Davies JE, Davies SJ (2003) Changes in distribution, cell associations, and protein expression levels of NG2, neurocan, phosphacan, brevican, versican V2, and tenascin-C during acute to chronic maturation of spinal cord scar tissue. J Neurosci Res 71:427-444.

Tom VJ, Steinmetz MP, Miller JH, Doller CM, Silver J (2004) Studies on the development and behavior of the dystrophic growth cone, the hallmark of regeneration failure, in an in vitro model of the glial scar and after spinal cord injury. J Neurosci 24:6531-6539.

Underhill CB, Green SJ, Comoglio PM, Tarone G (1987) The hyaluronate receptor is identical to a glycoprotein of Mr 85,000 (gp85) as shown by a monoclonal antibody that interferes with binding activity. J Biol Chem 262:13142-13146.

Verna JM, Fichard A, Saxod R (1989) Influence of glycosaminoglycans on neurite morphology and outgrowth patterns in vitro. Int J Dev Neurosci 7:389-399.

Wang KC, Koprivica V, Kim JA, Sivasankaran R, Guo Y, Neve RL, He Z (2002) Oligodendrocyte-myelin glycoprotein is a Nogo receptor ligand that inhibits neurite outgrowth. Nature 417:941-944.

Woo S, Gomez TM (2006) Rac1 and RhoA promote neurite outgrowth through formation and stabilization of growth cone point contacts. J Neurosci 26:1418-1428.

Yamada H, Fredette B, Shitara K, Hagihara K, Miura R, Ranscht B, Stallcup WB, Yamaguchi Y (1997) The brain chondroitin sulfate proteoglycan brevican associates with astrocytes ensheathing cerebellar glomeruli and inhibits neurite outgrowth from granule neurons. J Neurosci 17:7784-7795.

Chapter 3

Dose-dependent beneficial and detrimental effects of ROCK inhibitor Y27632 on axonal sprouting and functional recovery after rat spinal cord injury.

Introduction

Axonal regeneration after spinal cord injury (SCI) is hampered by several inhibitory molecules associated with myelin, e.g. Nogo (Chen et al., 2000), myelin associated glycoprotein (MAG; McKerracher et al., 1994), and oligodendrocyte myelin glycoprotein (OMgp; Wang et al., 2002). In addition, the scar tissue that forms after injury is rich in chondroitin sulfate proteoglycans (McKeon et al., 1999;CSPGs; Chen et al., 2002;Jones et al., 2003), semaphorins (Pasterkamp et al., 2001), and ephrins (Miranda et al., 1999;Bundesen et al., 2003) that can be inhibitory to axonal growth. It is difficult to predict how many and which of these molecules need to be suppressed in order to achieve successful regeneration. However, many of the above mentioned inhibitors activate Rho GTPase and its downstream effectors, such as ROCK (Rho-kinase) (Yamashita et al., 1999;Aurandt et al., 2002;Niederost et al., 2002;Borisoff et al., 2003;Monnier et al., 2003). Hence one possible method to overcome the inhibitors of CNS regeneration would be to interfere with their downstream intracellular signaling pathways, many of which converge on the Rho pathway (Lehmann et al., 1999).

Many of the Rho-dependent activities are mediated by ROCK (Hirose et al., 1998;Bito et al., 2000). Rho and ROCK exert their growth inhibitory effects through regulation of the actin-myosin network (reviewed in Amano et al., 2000;Dickson, 2001). Upon activation by Rho, ROCK stimulates actin-myosin contractility by phosphorylating myosin light chain and inhibiting myosin phosphatase (Amano et al., 1996;Feng et al., 1999;Schmidt et al., 2002). It also stabilizes the actin meshwork through activation of LIM kinase (LIMK), which inactivates the actin depolymerizing factor, cofilin (Maekawa et al., 1999). *In vitro*, activation of Rho and ROCK induces neurite retraction or GC collapse (Wahl et al., 2000;Neumann et al., 2002;Yamashita et al., 2002). Several methods have been used to inhibit the Rho pathway, such as the *Clostridium botulium* (C3) exoenzyme that ribosylates and inactivates Rho (Lehmann et al., 1999), dominant-negative Rho (N19TRho) (Lehmann et al., 1999), or Y27632 which specifically inhibits ROCK (Ishizaki et al., 2000). Such treatments reversed the inhibition of neurite outgrowth on MAG, Nogo, or myelin substrates (Lehmann et al., 1999;Yamashita et al., 2002;Dergham et al., 2002;Niederost et al., 2002). In addition, we and others have shown that Y27632 treatment can, at least partially, reverse the CSPG-mediated inhibition of dorsal root ganglion (DRG) neurite outgrowth *in vitro* (Borisoff et al., 2003;Monnier et al., 2003).

In the rodent spinal cord, suppression of Rho/ROCK signaling resulted in divergent findings with regards to corticospinal tract (CST) regeneration/sprouting after thoracic dorsal hemisection (Dergham et al., 2002;Fournier et al., 2003). Here, we used a cervical dorsal column transection model in rats to examine the effects of ROCK inhibition using Y27632 on axonal regeneration/sprouting in the ascending dorsal column tract (DCT), and to examine its effects on cervical CST regeneration/sprouting. In addition, various behavioral tests for forelimb function were used to assess sensory and motor functions in these animals.

Materials and methods

Animal surgeries

All experiments were conducted in accordance with the University of BC Animal Care Ethics Committee, and adhered to guidelines of the Canadian Council on Animal Care. Adult male Sprague Dawley rats were anesthetized with an intraperitoneal injection of a mixture of ketamine hydrochloride (72 mg/kg; Bimeda-MTC, Cambridge, ON) and xylazine hydrochloride (9 mg/kg; Bayer Inc., Etobicoke, ON). The animals were placed in a stereotaxic frame and the spinal cord was exposed at the cervical C4 – C5 level. A wire knife (model 120; David Kopf Instruments, Tujunga, CA) was used to produce the dorsal column transection. It was secured onto the stereotaxic frame and moved 0.9 mm lateral to midline on the animal's right side. After a prepuncture of the dura mater with a fine needle, the knife was lowered 1.1 mm into the dorsal horn between the dorsal roots of C4 and C5. The wire knife blade (1.8 mm curvature length) was then extended into the spinal cord through the pre-puncture to a further depth of 0.5 mm (total 1.6 mm). The wire knife was drawn up while gently pushing the dorsal columns down with a cotton swab. To ensure that all axons in the dorsal column were cut, a scalpel blade (11) was introduced to sever all axons against the wire knife.

Y27632 administration

Y27632 (Tocris Cookson Ltd., Avonmouth, Bristol, UK) was dissolved in sterile 0.01 Phosphate buffered saline (PBS) with penicillin/streptomycin, and loaded into two-week osmotic minipumps (0.5μl/hour, Alzet 2002; Durect Corp., Cupertino, CA) according to manufacturer's instructions. Two different concentrations of Y27632 pumps were used: low dose (2 mM; 160 μg per animal over two weeks), and high dose (20 mM; 1600 μg per animal over two weeks). Control pumps contained PBS with penicillin/streptomycin only.

Rats were randomly assigned into three groups: 18 control, 15 low dose, and 20 high dose animals, and a total of 53 animals were used in these experiments. Immediately after the spinal cord lesion, the osmotic minipumps were implanted into the subcutaneous space at the back of the neck. A catheter (0.3 mm O.D., polyethylene) connected to the minipump and looping through the cisterna magna delivered the drug-containing or control solution into the intrathecal space close to the lesion site (catheter opens into C2/3 level). The skin incision was closed with silk sutures.

Assessment of the efficacy of Y27632 and presence of drug in CSF and spinal cord tissue
ROCK activity assay

A commercially available ROCK Activity Assay kit (Upstate Biotechnology, Lake Placid, NY) was used to assess the efficacy of Y27632 on ROCK activity, according to the manufacturer's protocol. This test was used to verify drug activity after 13 days within the minipump at body temperature, and to detect the presence of ROCK inhibitory activity within the cerebrospinal fluid (CSF) of drug-treated animals. The pumps were taken from animals used in the anatomical and behavioral experiments of this project. For the CSF analysis, a separate set of animals was used. These animals received a C6/7 dorsal column transection lesion (instead of a C4/5 lesion) and the catheter looped through the intervertebral space between C1 and C2 (instead of through the cisterna magna) to open into C4/5 level. This left the cisterna magna available for CSF withdrawal on days 3, 7 or 13 after injury.

Phosphorylation of myosin phosphatase and cofilin

A third set of spinal cord injured rats (see above) was treated either with control or Y27632, and protein extracts from spinal cord tissues were analyzed for the effects of ROCK inhibition on the downstream effectors, i.e. myosin phosphatase (MYPT) and cofilin. MYPT is phosphorylated directly by ROCK, and for cofilin, indirectly with LIMK as an intermediate (Maekawa et al., 1999;Feng et al., 1999;Schmidt et al., 2002). Two or four days after dorsal column lesion and osmotic pump implantation, this group of rats was deeply anesthetized with an intraperitoneal injection of chloral hydrate (1 g/kg body weight; BDH Chemicals, Toronto, ON) and decapitated. From each rat, a spinal cord segment (1cm) centered at the lesion area was dissected and washed in ice-cold phosphate buffered saline (PBS). It was transferred to 0.5 ml ice-cold homogenization buffer (50 mM Tris-HCl (pH 7.4), 1% Triton x-100, 0.25% SDS, 150

mM NaCl, 1 mM Na_3VO_4, 1mM NaF, and protease inhibitor cocktail (Roche, Germany) and homogenized. Equal amounts of total protein from different animals were loaded onto each lane of a SDS gel. Proteins were transferred onto an Immobilon-P membrane, and Western Blot was performed using phospho-specific anti-MYPT1 (1/1000; Upstate), LIMK (1/500; Cell Signaling Technology, Beverly, MA), or cofilin (1/250; Upstate) antibodies. Then the membrane was incubated with horseradish peroxidase-conjugated secondary antibodies and protein bands were visualized by Chemiluminescence (Amersham Biosciences, New Jersey). Afterwards, the membranes were stripped and restained with non-phospho-specific antibodies: anti-myosin phosphatase (1/10,000; Covance Research Products, Berkeley, CA), anti-LIMK (1/500; Cell Signaling), or anti-cofilin (1/500; Upstate).

Labeling of the spinal cord long projection tracts

To unilaterally label the DCT, cholera toxin B subunit (CTB; 2 μl 10% solution; List Biological Lab, CA, USA) was injected into the right sciatic nerve six or seven days before the animals were to be sacrificed. CTB preferentially labels large myelinated A fibers in the dorsal column (Shehab et al., 2003). To label the CST, the anterograde tracer biotin dextran amine (BDA; Molecular Probes, Eugene, OR) was injected into the right sensorimotor cortex. A burr hole overlaying the right side of cortex was made to access the cell bodies of the corticospinal neurons. 0.2 μl of 10% BDA was injected into each of eight sites at 1.5 mm depth from the cortical surface to produce effective labeling.

Immunohistochemistry and Immunofluorescence Microscopy

Two months after injury, animals were overdosed with chloral hydrate, and were transcardially perfused with phosphate-buffered saline (PBS) followed by 4% paraformaldehyde (PFA). The spinal cord segments containing the lesion were dissected, post-fixed in PFA overnight, and cryoprotected in increasing concentrations of sucrose solution (12%, 18%, 24%). Each spinal cord was divided into three blocks, a 10 mm lesion block centered at the lesion site ('lesion block'), and two 5 mm blocks at either ends of the lesion block ('rostral' and 'caudal' blocks). The lesion block was cryostat sectioned in a parasagittal orientation at a thickness of 20 μm, while the rostral block (-10 to -5 mm) and caudal block (+5 to +10 mm) were sectioned at traverse orientation, i.e. cross section. The spinal cord sections were collected onto Superfrost Plus slides (Fisher Scientific, Houston, TX).

To visualize the CTB-labeled DCT fibers, the sections were incubated overnight with goat anti-CTB (List Biological) primary antibodies (1/1000) in PBS with 0.1% Triton X-100 (Sigma-Aldrich, Oakville, ON). Then they were incubated with the appropriate normal serum for 30 minutes to block non-specific binding, and were stained with Alexa-488 donkey anti-goat secondary (1:200; Molecular Probes) antibodies for two hours at room temperature. For the BDA-labeled CST fibers, sections were incubated with Cy3-conjugated strepavidin (Jackson ImmunoResearch) for 2 hours at room temperature. Sections were washed between steps with PBS.

Spinal cord sections were viewed on a Zeiss fluorescent microscope (Thornwood, NY), and photographed with a Q-imaging camera (Burnaby, BC) using the Northern Eclipse software (Empix Imaging, Mississauga, ON).

Quantification of lesion size

To approximate the size of the lesion cavity, the edge of the cavity was manually traced on three parasagittal spinal cord sections per animal. The area enclosed by the trace was quantified in pixels using the Photoshop 7.0 software (Adobe).

Quantification of DCT and CST regeneration/sprouting

The lesion block was immunostained for CTB and to assess DCT regeneration/sprouting, three measurements were made. First, in every subject in a series of one in two CTB-labeled parasagittal sections, the distance traveled by the longest axonal sprout (the 'longest distance' measurement) in each animal was measured from the point where the bulk of the traced DCT axons ended. Second, sections from each animal were visually inspected on the microscope and the four best sections (containing the most labeled fibers) were selected. The distances of all axonal sprouts from the end of the labeled tract (same as above) were measured (this was referred to the 'average distance' measurement). Since it was possible that the injured DCT axons retracted to different degrees in control and treated animals, the distances of the axonal sprouts grown beyond the middle of the lesion cavity were also measured. The 'longest distance from center' and 'average distance from center' measurements were generated using this later reference point.

The rostral and caudal spinal cord blocks, which were taken at 5 mm from the lesion center, were used to assess CST sprouting. The tracer-filled axon profiles in the grey matter

ipsilateral to BDA labeling (these were the terminal arborization of the ventral CST) and caudal to the lesion were digitally retraced by hand using the Photoshop 7.0 software (Adobe), and quantified using the Northern Eclipse software (Empix Imaging; Mississauga, ON). To account for different tracing efficiency across animals, the number of axon profiles was normalized to the number of BDA-labeled fibers in the ventral CST tract seen in the rostral cross sections. Four rostral and four caudal sections from each animal were used in this quantification.

Behavioral analyses

Animals were placed on a restricted diet to motivate them to perform the various behavioral tests. According to our observation, when not restricted, each rat ate approximately 20 to 26g of food (regular large rodent food pellet; LabDiet 5001, Missoula, MT) depending on body weight. On the restricted diet, each rat received 13g of food pellets per day. They were given additional food pellets (BioServ, NJ) as rewards while performing the various behavioral tests (approximately 3-5 g per day). At the end of the behavioral testing period (6 weeks after injury), the animals gained 25 ± 3 % of their original body weight (before-injury) body weight.

Walking tract footprint analysis was modified from de Medinaceli et al. (1982). The rats were trained to walk across a narrow wooden beam (7 cm wide and approximately 1 m in length) from a brightly illuminated temporary holding box toward a darkened box containing their familiar housing mates. Two marks were placed 70 cm apart, centered between the two boxes, to exclude analysis of footprints made during the beginning (acceleration) and ending (deceleration) of the movement. During the recording sessions, the animals' forepaws were dipped in green dye (food coloring and non-toxic) and the hind paws in red dye. For each animal, three sets of footprints were generated from three separate traverses of the track. A series of at least six sequential steps was analyzed to determine the mean values of, (1) forelimb base of support; and (2) forelimb outward paw rotation angles. The forepaw base of support was measured as the core to core distance of the central pads of the forepaws. The outward forepaw rotation angle was defined by the degree to which the paw was pointing deviated from the direction of walking. It was measured by the angle formed by the intersection of two lines: one was drawn through the point right between the third and fourth toes, and the central pad (print representing the metatarsophalangeal joint); the other one was drawn through the central pad parallel to the walking direction. Data from the left and right forepaws were pooled to correct for the slight changes in walking direction since occasionally the animals walked slightly off to one side.

In the footslip test, which was modified from Metz and Whishaw (2002), the rats walked along a horizontal ladder with variable rung spacing. The ladder consisted of side walls made of clear Plexiglas and metal rungs (2 mm diameter), and it was 100 cm long and 13 cm wide, with a platform on each end. The distances between the metal rungs were irregular (1.8 to 3.8 cm) and the patterns were different depending on whether the animals were walking from left to right or the other way round. This was to prevent the animals from learning the pattern and anticipating the position of the rungs. A mirror was placed right under that ladder at an angle of 45°, so that when videotaped from the lateral view, the stepping motion of each limb could be observed. The middle portion (approximately 48cm) of the tract was videotaped and footslips that occurred within this part of the tract were recorded. The number of footslips by each forelimb was divided by the total number of steps taken to determine the 'footslip frequency'.

The food pellet-reaching task was modified from Whishaw et al. (1993). The rats were trained to reach through a 1 cm wide opening in the wall of a clear plexiglass box in order to grasp a 190 mg food pellet (Bioserv, NJ) placed in a dimple on a stage 2 cm outside the opening. Once the rat has reached for a food pellet, a 45 mg pellet was dropped into the back of the box to encourage the rat to leave the reaching area. This ensured the rat approached the opening with a new stance on every reach. The rat was filmed from the front and lateral perspectives during reaching. The best 25 of 30 attempts were included in the analysis. The number of times that the rat successfully grasped and retrieved the food pellet was divided by the number of attempts (25 pellets) to give the 'success rate' of that animal.

The reaching behavior was also scored using a 10-point scale developed in our laboratory, since there was evidence that success scores and the qualitative aspects of movements might be dissociated (Whishaw, 2000;Whishaw et al., 2003). We were unable to apply the scale developed by Whishaw et al. (1993) for Long-Evans Hooded rats, since Sprague Dawley rats display much less elaborate qualitative features of their reaching movement (Whishaw et al., 2003). In fact, Sprague Dawley rats have been considered "impaired" (Whishaw et al., 2003) despite the fact that they are equally successful as Long Evans rats in this test. Therefore, our 10-point scale reflects the scoring of the successful execution of sequential aspects of the reach: 1) the reaching through the slot onto the stage and aiming for the food pellet, 2) the grasping of the pellet and 3) the retrieval of the pellet. The possibility that the rat does this with corrective movements or alternative strategies is hereby taken into consideration. Hence rats that failed to reach onto the

stage scored lower than those that were able to reach through the opening but failed to grasp, which in turn scored lower that those animals successfully reaching and grasping (for details see table 1).

To determine whether Y27632 treatment affects the animal's sensitivity to painful or mechanical stimuli, they were subject to tests of sensory functions. Thermal hyperalgesia was evaluated using a Plantar test apparatus (Ugo Basile, Italy), which consisted of a movable infrared generator underneath an elevated glass plane (Hargreaves et al., 1988). The infrared beam intensity was set at 50 units (mid point of the emission range). After the rats settled in, the infrared beam was focused onto the forepaw and the latency time of response in seconds was recorded. The test was performed twice for each paw. A maximum cut-off point of 30 sec. was set to prevent injury.

Mechanical allodynia in unrestrained rats was evaluated with von Frey hairs (Levin et al., 1978;Bell-Krotoski and Tomancik, 1987;Bell-Krotoski et al., 1995). For each rat, calibrated von Frey filaments (North Coast Medical, Inc. San Jose, CA) of ascending target forces: 1, 1.4, 2, 4, 6, 8, 10, 15, 26, 60, and 100 g were sequentially applied to the plantar surface of the forepaw until a withdrawal response was elicited. After a brief resting period (3 to 5 minutes) the paw would be retested with the same hair. Response threshold was defined as the lowest force that consistently produced withdrawal responses on three consecutive filament applications. A target force of 100 g was the largest measurement recorded as this hair size would physically displace the paw.

The animals were trained and tested before the injury, and tested once every week afterwards until week 6 post-injury. Some of the data were expressed as 'relative change', which were determined by the formula [(Value after injury – Value before injury)/Value before injury]. Footslip data were expressed as absolute 'change in footslip frequency' (Value after injury – Value before injury), since the 'value before injury' in many animals equaled to 0. For the reaching test, presurgical baseline and after-injury data were shown as is, since the animals showed large variability in success rate and reaching score.

Statistics

Statistical analysis was performed using the JMPIN software (SAS Institute Inc., Cary, NC). Data were compared among groups using ANOVA and in the cases where the requirements of parametric analysis were not satisfied, the non-parametric Kruskal Wallis ranked sum test was

used. The data were further analyzed using the post-hoc Tukey test. Differences with $p < 0.05$ were considered significant. Pair-wise comparison (t-test, or the non-parametric Wilcoxon test) was also performed between control and any one of the drug-treated groups, or between data sets of the same group at different time points.

Results

Drug stability and in vivo ROCK inhibition by Y27632

First, we determined whether Y27632 was stable for at least 13 days in minipump implants and whether ROCK inhibitory activity was present in the CSF and spinal cord tissues of Y27632-treated animals. We used an *in vitro* assay of the phosphorylation of the synthetic myosin phosphatase (MYPT) peptide by ROCK in order to test the activity of Y27632 (see methods). Phosphorylation level of the MYPT peptide decreased with the inclusion of fresh Y27632 (25 μM), as well as with the drug solution from the minipumps (Y27632, 2 mM or 20 mM) that had been used *in vivo* for 13 days (Fig. 3.1A). The concentration of the pump solution was diluted to 25 μM (low dose pump) or 250 μM (high dose pump) for this assay, demonstrating the Y27632 was still active (compare lane 3 versus 5 or 6 in Fig. 3.1A) following 13 days at body temperature. In addition, on day 7 of drug infusion we tested the CSF of the drug-treated animals for ROCK inhibitory activity using this assay. The inclusion of 20 μl of CSF from both low dose- and high dose- treated rats produced a marked reduction of MYPT phosphorylation, indicating drug levels in excess of 10 μM in the CSF (compare lane 3 versus 5 or 6 in Fig. 3.1B). Thus ROCK inhibitory activity was present in the CSF of these Y27632-treated animals.

Proteins were extracted from the injured spinal cord tissues of control or drug-treated animals and then analyzed for the phosphorylation level of endogenous MYPT and cofilin. There was no difference in the phosphorylation level of MYPT, while there was a decrease in cofilin phosphorylation with high dose Y27632 treatment (Fig. 3.1C). We were unsuccessful in our attempt to examine LIMK phosphorylation using a commercial antibody to phospho-LIMK.

ROCK inhibition promoted DCT sprouting in the lesion cavity

Only animals verified to possess a complete transection of the descending dorsal CST and ascending sensory tracts and with effective labeling of the CNS tracts of interest were included in the analyses. Eight controls, seven low dose, and eight high dose animals were

included in the assessment of DCT sprouting/regeneration. In the transected DCT, CTB labeled axonal end bulbs along with a short section of preceding axon shafts (Fig. 3.2A, B, C). In all experimental groups, the DCT axonal sprouts were seen coursing through thin bridges of reactive (scar) tissue that connect the rostral and caudal ends of the lesion (Fig. 3.2A, C). In most animals, no axons were found beyond the confines of the reactive tissue at the lesion site. However, in one 20 mM Y27632-treated rat, a few axonal sprouts were found at some distance rostral to the lesion or in the rostral spinal cord/lesion interface terminating in an end bulb (Fig. 3.2C, D).

Using a high power lens we saw only rare sprouts originating as collaterals from the axonal shafts. On the other hand, we frequently encountered axonal sprouts that seemed to originate from the terminal swelling of the cut axons of the dorsal ascending fibers (Fig. 3.2E, F). In addition, near the end of the labeled tract, we occasionally found axons that turned away from the injury site, forming loops (Fig. 3.2G). However, a detailed analysis of the fine axonal morphology did not seem warranted at 8 weeks because these animals were treated with the ROCK inhibitor only for 2 weeks and survived for another 6 weeks. The morphology of the axons sprouts would most likely no longer reflect the actual effect of ROCK inhibition.

Quantitative analysis revealed that high dose Y27632 significantly increased the distance of the longest axon compared to controls when measured from the end of the labeled DCT tract (by one-way ANOVA, $p < 0.01$; followed by post-hoc Tukey test; Fig. 3.3A). The absolute longest distance found in the high-dose treated animals was 2.6 mm from the end of the labeled tract, compared to 1.4 mm in control animals, and 1.2 mm in the low dose-treated group. As a whole group, the average 'longest distance' traveled by axonal sprouts in control animals was 1.0 ± 0.1 mm from the end of the labeled tract, 0.9 ± 0.1 mm in low dose, and 1.6 ± 0.2 mm in high dose animals (Fig. 3.3A).

The 'average distance' traveled by all axonal sprouts with reference to the end of the labeled DCT was also measured. Using this measurement, high dose treatment significantly increased the 'average distance' traveled by axonal sprouts in the lesion cavity (0.62 ± 0.07 mm) compared to controls (0.43 ± 0.04 mm), while low dose had no effect (0.43 ± 0.02 mm) (by one-way ANOVA, $p < 0.05$; followed by post-hoc Tukey test; Fig. 3.3B).

Although there was no significant difference in lesion cavity sizes among the three groups (data not shown), given that the end of the labeled tract might have been influenced by possible neuroprotective properties of the drug, we also used the lesion center as an anatomical

reference point to measure the axonal sprouts. The 'longest distance from center' (rostral to the lesion center) traveled by axonal sprouts in control animals was 0.29 ± 0.06 mm, 0.30 ± 0.09 mm in low dose, and 0.73 ± 0.02 mm in high dose animals (Fig. 3.3C). Thus, high dose treatment significantly increased the distance traveled by axonal sprouts ($p < 0.05$ by ANOVA). The 'average distance from center' of all axonal sprouts traveled beyond the lesion center was 0.19 ± 0.04 mm in control animals, 0.19 ± 0.07 mm in low dose animals, and 0.38 ± 0.08 in high dose animals. No significant difference was found among the groups ($p = 0.3$; Fig. 3.3D).

ROCK inhibition promoted CST sprouting into the distal grey matter

In the assessment of CST sprouting, 8 control, 8 low dose, and 10 high dose animals were included, while poor labeling in several animals precluded the analysis of axonal sprouting. Using parasagittal spinal cord sections of the lesion epicenter taken 8 weeks after injury, the axons of the dorsal CST terminated in enlarged end bulbs at approximately 200 μm from the rostral edge of the lesion cavity, or 650 ± 150 μm from the center of lesion cavity (Fig. 3.4A). No CST fibers had visibly grown into or around the lesion cavity in any of the three experimental groups.

There was evidence that ventral CST axons collaterally sprout into the grey matter after injury to the dorsal CST (Weidner et al., 2001). To determine whether ROCK inhibition enhanced collateral sprouting from spared ventral CST fibers, the tracer-filled axon profiles in the distal grey matter ipsilateral to BDA injection (the ventral CST is uncrossed) were digitally drawn and quantified on 4 spinal cord cross sections from each animal taken 5 mm below the injury (Fig. 3.4C,D). Since BDA labeling efficiency differed among individual animals, the summed length of axon profiles (number of pixels) in each animal was normalized to the number of labeled ventral CST fibers counted on 4 rostral spinal cord cross sections (Fig. 3.4B, boxed area). 'Normalized total axon profiles' in controls was 17 ± 4 arbitrary units, 9 ± 1 in low dose animals, and 35 ± 8 in high dose animals (Fig. 3.4E). A non-parametric Kruskal Wallis test revealed significant differences among the 3 treatment groups ($p<0.05$). In pair-wise comparisons high dose-treated animals showed more sprouting in the distal grey matter compared to controls (non-parametric Wilcoxon, $p<0.05$), and in contrast, low dose drug treatment depressed CST sprouting compared to controls ($p<0.05$, Wilcoxon test). Accordingly, low and high dose groups were found to be significantly different from each other (by Kruskal Wallis and post-hoc Tukey, $p<0.01$).

Behavioral testings

The behavioral tests used were: (1) the footprint analysis, which assessed the pattern of paw placement on flat surfaces during locomotion; (2) the footslip test which evaluated skilled walking across a horizontal ladder with irregular pegs; (3) a modified Whishaw food pellet reaching task which assessed skilled forelimb movements; and (4) two sensory tests, von Frey hair and plantar IR tests which detected abnormal sensory function.

In the footprint analysis of the forepaws, the core to core distance of the left versus right central pads (base of support) increased by 73% in control animals at one week after injury and gradually returned to normal, uninjured animal values over the next 5 weeks of observation (Fig. 3.5A, clear columns). Similarly, animals with high dose treatment showed a transient increase of 49% in the first week that normalized within the following 3 weeks (Fig. 3.5A, dark grey columns). There was no statistically significant difference between the control and high dose groups at any time-point. In contrast, rats with low dose treatment showed an elevation of the base of support of their forepaws by 136% and this remained significantly elevated over the entire observation period (Fig. 3.5A, light grey columns). Hence, the low dose animals continued to walk with a significantly wider gait compared to the other groups (p < 0.05 by ANOVA and post-hoc Tukey, or by pair-wise t-test).

The rotation angle of the forepaw, as defined by the angle between the forepaw orientation and the direction of walking (see methods), increased in control rats by 280% by one week after injury; at 6 weeks this rotation angle was still increased by 180% (Fig. 3.5B, clear columns). Similarly, this angle was found to increase by 330% in low dose-treated rats and remained elevated by 240% at the end of the observation period (Fig. 3.5B, light grey columns). Interestingly, the forelimb rotation angles revealed only a 180% increase at 1 week post-injury in rats receiving high dose ROCK inhibitor (Fig. 3.5B, dark grey columns). At the end of the observation period, rotation angles in these animals declined significantly (p < 0.05) when compared to one week following injury, although values were still double that of the pre-lesion baseline (i.e. they were still increased by 100%).

In the horizontal ladder test (counting footslips by the forelimbs), uninjured rats revealed a footslip frequency of 5% on average. 1 week after injury, vehicle-treated rats showed a footslip frequency of approximately 39%, with the frequency dropping to 28% by 6 weeks (Fig. 3.6A, clear columns). Low dose-treated rats showed a footslip average of 38% at week 1 and this

declined to 26% at 6 weeks, similar to controls (Fig. 3.6A, light grey columns). In contrast, high dose-treated rats started with a failure rate of 31% and declined to 15% at 6 weeks (Fig. 3.6A, dark grey columns). At week 6, all animals recovered significantly and had reduced footslip frequency compared to 1 week after surgery ($p < 0.05$ by Wilcoxon; Fig. 3.6A). Statistical analysis showed that both high and low dose Y27632 significantly reduced ($p < 0.05$ by ANOVA) the number of footslips compared to control rats at week 3. However, at weeks 1, 3, 4, and 6, only the high dose regiment effectively reduced footslip frequency ($p < 0.05$ using Kruskal Wallis test followed by post-hoc Tukey test, or using pair–wise comparisons ; Fig. 3.6A).

In the food pellet reaching test, before injury the average success rate of all rats was 0.70 (Fig. 3.7A). Each control or treatment group included rats that had low and high success rates, and there was no difference in the average success rate among the three groups. One week after injury, the success rates of control (0.31) and low dose (0.37) groups, but not the high dose group (0.48), were significantly lower than presurgical levels ($p < 0.05$ by Wilcoxon; Fig. 3.7A). At 5 weeks, both high dose (0.79) and control (0.61) groups recovered their success rates to pre-injury levels (not significantly different from presurgical baseline). In contrast, the low dose-treated rats failed to recover. Their average success rate (0.30) remained significantly reduced at week 5 compared to the presurgical baseline ($p < 0.05$ by Wilcoxon), and also to the high dose group ($p < 0.05$ by Kruskal Wallis test; Fig. 3.7A, light grey columns).

We obtained similar results when we scored the sequential success of the reaching movements using a 10-point scale developed in our laboratory (Table 1). Before surgery, the three groups of rats attained average scores of 7.4, 7.7, and 8.6 (not significantly different) respectively. One week after injury, the control and low dose groups achieved an average score of 4.9 while the high dose group scored 5.9. In agreement with the total 'success rate' measurement, quantification using the 10-point scale indicated that at week 5 after injury both control (6.7) and high dose (8.0) groups recovered to baseline performance while the low dose group (4.9) remained impaired ($p < 0.05$ by Wilcoxon; Fig. 3.7B).

The animals were tested with infrared beam (Plantar IR test) and von Frey hairs for abnormal sensitivities to noxious heat and mechanical stimuli, respectively. In the Plantar IR test, the high dose group withdrawal times were significantly longer compared to controls ($p < 0.05$ by pair wise comparison) and had returned to the uninjured pre-lesion levels by 4 weeks after

injury (Fig. 3.6B, dark grey columns). At all other time points tested, these longer reaction times in the high dose group did not reach significance (e.g. $p = 0.09$ at week 6).

Using the von Frey hair test, there were no significant differences among the three groups over the time period tested (data not shown). Thus no evidence for heightened sensitivity to mechanical stimuli was found with Y27632 treatment.

Discussion

Here we tested whether the suppression of Rho-kinase (ROCK) promoted regeneration and functional recovery after rat spinal cord injury. We applied two different concentrations of the ROCK inhibitor, Y27632, to rats with dorsal column lesions and found that the high dose (20mM ROCK solution in minipump, 12 µl/day, 14 days) regimen stimulated regenerative sprouting of both CST and DCT axons. The high dose regimen also accelerated the recovery/compensation of motor function as revealed by some aspects of footprint analysis, as well as food pellet reaching and skilled locomotion across a horizontal ladder. In contrast, the low dose (2mM, 12 µl/day, 14 days, totally 160ug) regimen either had no effect on or even decreased axonal regrowth, and impaired functional recovery/compensation in some behavioral tests, i.e. foot pellet reaching and the base of support in the footprint analysis.

To confirm that our pharmacological drug regimen reached its target we used a commercially available ROCK activity assay. We determined that Y27632 was stable for at least 13 days at rodent body temperatures and that ROCK inhibitory activity was present in the CSF of treated animals, both at low and high doses. In addition, Western blot analysis of spinal cord protein extracts indicated that the phosphorylation level of one downstream effector of ROCK, cofilin, decreased with the high dose, but not the low dose, regimen of Y27632. Interestingly, the phosphorylation of another effector, myosin phosphatase (MYPT) did not change at any dose of Y27632. Even though the Y27632 concentration in the CSF was sufficiently high to inhibit the phosphorylation of the MYPT synthetic peptide in the *in vitro* assay, the failure to inhibit endogenous MYPT phosphorylation *in vivo* might be due to the its sustained phosphorylation by other enzymes such as MYPT1 kinase and integrin-linked kinase (reviewed in Ito et al., 2004). Hence, the *in vivo* application of Y27632 mediated only partial blockade of the downstream signaling targets of the Rho/ROCK pathway, and our low dose regimen may not yield effective or lasting *in vivo* inhibitions downstream of ROCK.

Our data extend earlier reports by others using inhibition of the Rho/ROCK pathway with either *Clostridium botulium* C3 exoenzyme that ribosylates and inactivates Rho, or the same ROCK inhibitor Y27632 (Dergham et al., 2002;Fournier et al., 2003;Sung et al., 2003;Ramer et al., 2004). Dergham et al. (Dergham et al., 2002) has shown that fibrin glue-mediated application of C3, and to a lesser extent, Y27632 to a thoracic spinal cord dorsal hemisection site increased regeneration/sprouting of mouse CST axons into and beyond the injury site, and produced an early recovery of locomotor function. The fast time course of recovery, which was within 1 day after lesion, was indicative of neuroprotective effects and further studies from this laboratory confirmed this interpretation (Dubreuil et al., 2003). However, other groups have shown that in rats, C3 application by either osmotic minipump infusion (Fournier et al., 2003) or gelform implant at the injury site (Sung et al., 2003) was detrimental after dorsal hemisection (Fournier et al., 2003) or weight-drop injury (Sung et al., 2003). The spinal cords of these C3-treated rats appeared atrophic (Fournier et al., 2003), and some rats were severely emaciated after 1 week post-injury (Sung et al., 2003). In contrast, infusion of Y27632 via osmotic minipump at 340 µg/rat/2 wks resulted in a transient acceleration in the recovery of the open field locomotion (BBB) score, and increased the number of CST axon profiles distal to the site of spinal cord injury (Fournier et al., 2003). In the present study, using a cervical injury model, we observed a similar increase in CST sprouting with our high dose regimen (20 mM; equivalent to 1680 µg/rat/2 wks) that was 5 times higher than the dose used by Fournier *et al* (2003). In addition, we found regenerative sprouting of sensory (DCT) fibers and normalized heat withdrawal times in the high dose Y27632 group. Interestingly, this alleviation of sensitivity to noxious stimulus correlated with a recent study showing that Y27632 (336 µg/rat/7 days) stimulated sprouting of intact supraspinal monoaminergic (serotonin- and tyrosine hydroxylase-positive) axons after dorsal rhizotomy and attenuated cold hyperalgesia (Ramer et al., 2004).

The enhanced functional recovery/compensation observed in high dose Y29632-treated animals correlated with sprouting in the CST. While we did not detect CST regeneration, there were more CST profiles in the grey matter distal to the site of injury indicative of collateral sprouting from ventral, spared CST axons. Such short distance axonal growth might be sufficient for recovering some function due to reinnervation of spinal interneurons or motoneurons (Weidner et al., 2001) located just distal to the lesion. However, the observed degree of axonal regeneration/sprouting in this study was unlikely the sole contributor to the functional

improvements. The reorganization or plasticity of spared pathways, such as other descending motor pathways (rubrospinal, brainstem spinal) or propriospinal pathways and segmental circuitries might also be critical (Raineteau et al., 2002;Bareyre et al., 2004). In addition, the early recovery of some of our behavioral parameters indicates that neuroprotective properties of ROCK may also play an important role. While inhibition of Rho with C3 has recently been shown to be neuroprotective (Dubreuil et al., 2003), a similar effect remains to be demonstrated for inhibition of ROCK.

Although we failed to detect unequivocal regeneration of either tract through and beyond the injury site, ROCK inhibition with high dose Y27632 produced a significant increase in the length of DCT axonal sprouts that grew beyond the lesion center compared to vehicle (PBS)-treated animals. This limited, although significant, growth of axons beyond the center of the lesion site suggests that ROCK inhibition disrupts the signaling of several inhibitory molecules in the lesion site but fails to promote the re-entry through the distal lesion interface. Diverse classes of axonal growth inhibitors associated with myelin (Nogo, MAG and OMgp) as well as the glial scar (CSPGs, semaphorins, and ephrins), which are present after CNS injury, pose an obstacle to regeneration (reviewed in Sandvig et al., 2004). Rho/ROCK activity has been implicated in the inhibition due to myelin (Yamashita et al., 2002;Niederost et al., 2002), CSPGs (Borisoff et al., 2003;Monnier et al., 2003;Jain et al., 2004), semaphorins (Aurandt et al., 2002), and ephrins (Wahl et al., 2000;Shamah et al., 2001). The significant increase in the length of DCT axonal sprouts in high dose Y27632-treated animals correlated with previous *in vitro* studies showing that ROCK inhibition enhanced DRG axon outgrowth on the above mentioned inhibitory substrates (Wahl et al., 2000;Dergham et al., 2002;Niederost et al., 2002;Borisoff et al., 2003;Monnier et al., 2003;Jain et al., 2004). However, the lack of a dramatic regeneration response *in vivo* argues that other inhibitory factors (molecular or physical) and inhibitory signaling pathways are likely involved. Furthermore, the inhibition of ROCK might also affect growth cone motility and steering (Yuan et al., 2003) which could be disadvantageous in the 3-dimensional setting of the *in vivo* injury site.

It is very likely that Y27632 treatments also affected other cell types which in turn affect axon sprouting/regeneration. For example, a recent study has shown that the Rho/ROCK pathway was involved in the generation of reactive astrogliosis (John et al., 2004). Via deactivation of the Rho/ROCK pathway, the proinflammatory cytokine interleukin-1β (IL-1β)

induced the reorganization of actin accompanied by disruption of focal adhesion complexes and deactivation of non-muscle myosin in astrocytes (John et al., 2004). This resulted in the reactive astrocyte phenotype. Since injury to the adult CNS induces the recruitment of inflammatory cells that release diffusible cytokine products including IL-1β, the infusion of Y27632 into the lesion area may further deactivate ROCK and enhance the progress of astrogliosis. It remains controversial whether the process of astrocyte reactivity is beneficial or detrimental to CNS recovery after injury. Astrogliosis may be the result of the adult CNS's attempt to seal off the damaged area from the external environment, reestablish the blood brain barrier and reconstruct the damaged tissue (reviewed in McGraw et al., 2001). However, this process involves deposition of inhibitory substrates and inhibition of axonal growth (Liuzzi and Lasek, 1987;Rudge and Silver, 1990;Fitch et al., 1999;reviewed in McGraw et al., 2001). Since in our experiments the ROCK inhibitor was infused intrathecally, relatively higher drug concentrations might have reached the lesion site with its reactive astrocytes compared to the axonal growth cones in the spinal cord parenchyma. This might explain why low dose Y27632 treatment depressed axon sprouting rather than stimulated it, as it might have worsened the undesirable effects of astrogliosis; yet the concentration might not have been high enough to reach the growth cones in order to overcome this inhibitory milieu. The failure to inhibit cofilin phosphorylation by low dose treatment lends further support to this speculation. However, it is too early to come up with a comprehensive model to explain the inhibitory effects of low doses of Y27632 on sprouting and behavioral recovery.

In addition to depressed sprouting, our low dose (168 μg/rat/2 wks) Y27632-treated rats also showed delayed functional recovery as measured by the forepaw base of support and outward forepaw rotation angle during locomotion on flat surfaces, and by the food-pellet reaching test. Interestingly, results from Sung et al.'s (2003) study also indicated that Y27632 (10 mg/kg/day for 10 days) given orally delayed functional recovery as measured by the BBB score. It is difficult to determine whether their drug treatment regimen results in similar drug concentration in the spinal cord parenchyma as in our regimen. However, the fact that Y27632 treatment was detrimental rather than beneficial further supports the speculation that ROCK inhibition may cause undesirable effects on the non-neuronal cell population to exacerbate the conditions in the injured spinal cord.

Taken together, we have shown that after SCI, acute treatment with the ROCK inhibitor Y27632 stimulated sprouting of long projection axons (CST and DCT axons) in the spinal cord, and accelerated functional recovery/compensation. The enhanced functional recovery in high dose-treated animals might be a result of augmented regeneration/sprouting in these tracts, and possibly of reorganization in other axonal pathways. However, low doses of ROCK inhibition appeared to be detrimental. This underscores a novel concept in the injured spinal cord of adverse versus beneficial drug effects by revealing an inversed relation to the drug dose administered: detrimental at low doses and beneficial at higher doses. Such dose response in the injured spinal cord calls for caution in applying this drug to humans with SCI.

Table 3.1

10-point scale for grading food pellet reaching movements.

Score	Description
0	Rat unable to lift hand or move hand.
1	Rat lifts hand and hits wall.
2	Rat gets fingers on to stage.
3	Rat makes several attempts before touching and fails to grasp.
4	Rat reaches through slot, touches the food immediately but fails to grasp.
5	Rat reaches through slot, makes several attempts to reach/touch the food and ultimately grasps pellet but drops it.
6	Rat reaches through slot, grasps the pellet (immediately) but drops it.
7	Rat reaches through slot, makes several (> 2 corrective movements), grasps the pellet and retrieves it successfully.
8	Rat reaches through, makes only 1 corrective movement and retrieves it successfully.
9	Rat reaches through, grasps pellet on first touch, but has apparent difficulty in retrieving it.
10	Rat reaches through, grasps pellet and retrieves it without hestitation or difficulty.

Figure 3.1

Y27632 was stable for at least 13 days within osmotic minipump implants (A), and ROCK inhibitory activity was present in the CSF (B) and spinal cord tissue (C) of drug-treated animals. (A) On day 13, the minipumps were surgically removed from the rats and the solution left inside the pumps were used in the ROCK activity assays. The *in vitro* phosphorylation mixture consisted of synthetic active ROCK and MYPT peptide (60 KDa, *arrow*) in the presence or absence of fresh Y27632 (25μM), or an aliquot from the pump solution (vehicle control (Con), 2mM low dose pump diluted 80x (Low) or high dose pump diluted 80x (High)). Phosphorylated MYPT peptides were resolved by Western blots using antibodies against phosphorylated MYPT. (B) CSF was withdrawn from the animals at day 3 and tested for ROCK inhibitory activity (same assay as above). 20μL CSF from each rat treated with vehicle control (con), low (Low) or high (High) dose Y27632 was used in each reaction mixture. (C) Endogenous MYPT and cofilin phosphorylation in protein extracts of injured spinal cord tissues. There was no significant difference in MYPT phosphorylation level among the three groups, but there was a decrease in cofilin phosphorylation with high dose Y27632 treatment. *p-MYPT and p-cofilin*, phosphorylated forms; *MYPT and cofilin*, non-phospho-specific bands. Results were representative of 4 sets of control, low dose-, and high dose-treated animals (i.e. total of 12 rats).
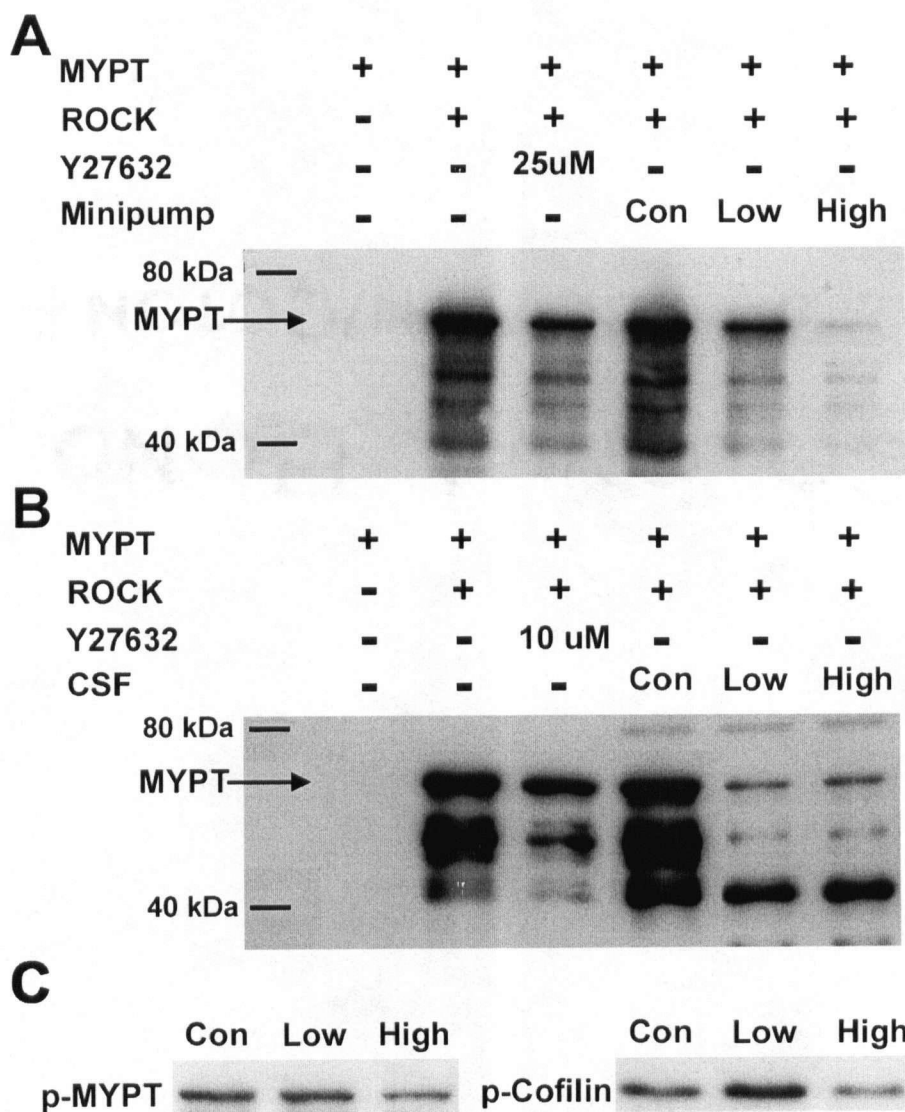
Figure 3.2

DCT axonal sprouts around lesion cavity. DCT axons were labeled by CTB injection into the right sciatic nerve and visualized by immunostaining with fluorescence-conjugated antibodies. (A) Parasagittal spinal cord section of a control animal at low magnification with rostral (Ros) to the right, caudal (Cau) to the left, and dorsal to the top. Most of the cut axons terminated close to the caudal cut edge (*arrowhead*) and the cut ends were swollen into termination bulbs. Within the lesion wall, axon sprouts (manually highlighted) traveled along the strip of scar tissue that connected the caudal and rostral edges of the lesion. (B) Higher magnification (boxed area in (A)) showed the termination bulbs of injured axons. (C) Parasagittal spinal cord section of a high dose-treated rat. (D) Higher magnification of boxed area in (C) showed an axon sprout that had traveled across scar tissue and attempted to re-enter spinal cord tissue at the rostral end of the lesion. (E, F, G) High power images taken from high dose-treated animals, close to the end of the labeled tract. (E and F) Terminal sprouts of injured axons (*arrows*). (G) Some axons turned away from the injury site, forming loops (*arrows*). *Arrowheads*, ends of labeled track; *, center of lesion cavity. *Scale bars: A and C, 250μm; B and D, 50μm; E, F and G, 25 μm.*
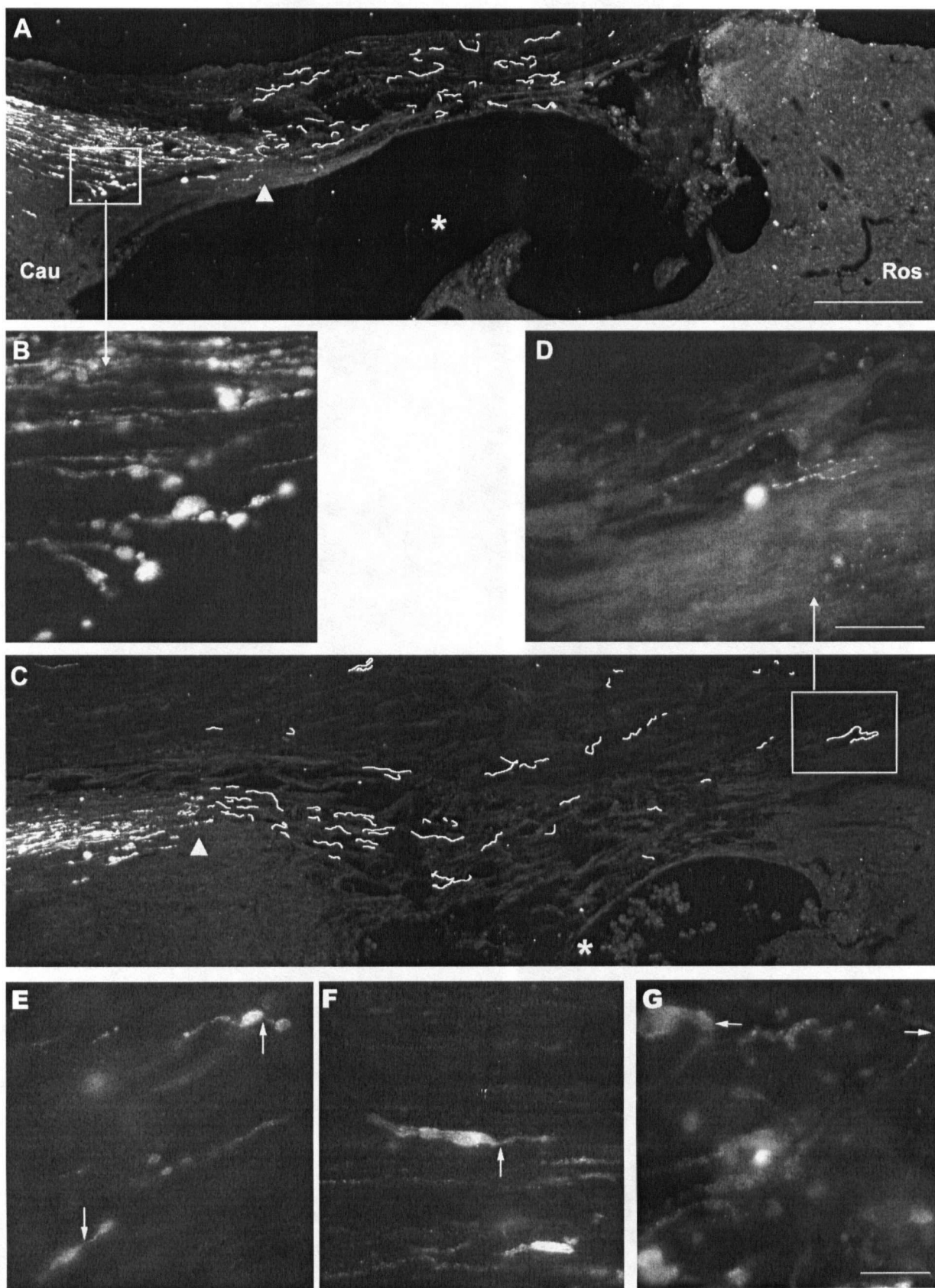
Figure 3.3

ROCK inhibition stimulated sprouting of DCT axons. (A,B) On parasagittal spinal cord sections centered around the lesion area, the distances of the axonal sprouts found in the lesion area were measured from the end of the labeled DCT (see Fig. 3.2). (A) In each animal, the distance of the longest axonal sprout was measured. High dose Y27632 significantly increased the distance of the longest axon compared to controls. (B) On 4 selected parasagittal sections, distances of all axonal sprouts were recorded and averaged for each animal. Again, 20 mM Y27632 significantly increased the distance traveled by the axonal sprouts. (C, D) The distances of the axonal sprouts were measured from the lesion center. C) High dose Y27632 significantly increased the distance of the longest axon compared to controls. D) On 4 selected parasagittal sections, distances of all axonal sprouts were recorded and averaged for each animal. *, $p < 0.05$; **, $p < 0.01$ by ANOVA.

A

Longest distance (mm)

B

Average distance (mm)

C

Longest distance from center (mm)

D

Average distance from center (mm)
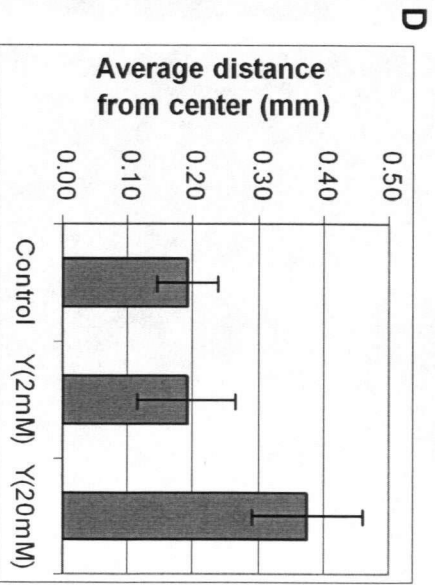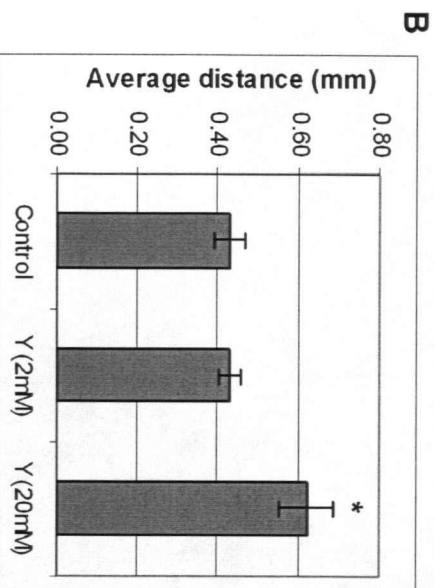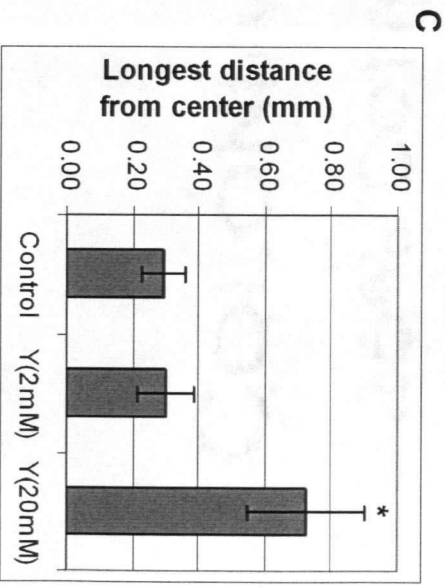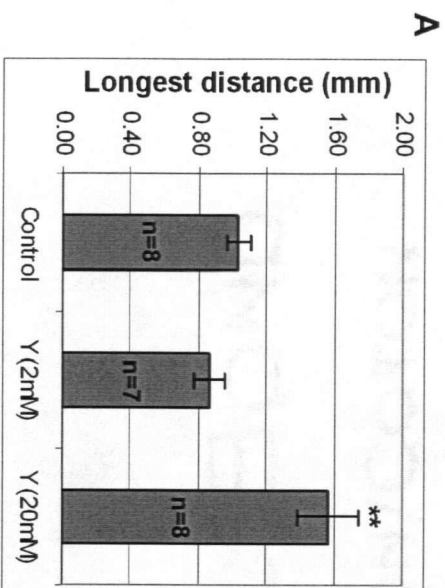
Figure 3.4

ROCK inhibition stimulated CST sprouting in the distal grey matter. (A) Transected CST axons on a parasagittal spinal cord section. Rostral is to the right and dorsal to the top. CST axons were labeled by BDA injection into the right sensorimotor cortex and visualized by fluorescence-conjugated strepavidin staining. Injured CST axons terminated close to the edge of the lesion cavity. (B) Spinal cord cross section showing the labeled CST rostral to injury. The majority of the axons resided in the dorsal column, and minor CST axon groups were found dorsolaterally and ventrally (boxed area). (C) Distal cross section of a control animal. (D) Distal cross section of a high dose-treated animal. (E) Axon fragments in the distal grey matter were manually traced and quantified using the Northern Eclipse software to give the summed lengths (in pixels) of all axon fragments on 4 cross sections per rat. To account for different BDA-labelling efficiencies in different animals, the total axon length was normalized to the number of labeled ventral CST fibers rostral to lesion. Low dose Y27632-treated animals had decreased sprouting in the distal grey matter compared to controls, while high dose-treated animals showed more sprouting. *, $p <$ 0.05 by pair-wise comparison using the Wilcoxon test; **, $p < 0.01$ by Kruskal Wallis followed by post-hoc Tukey test. Ros, rostral to injury; Cau; caudal to injury; *Scale bars: 250μm.*
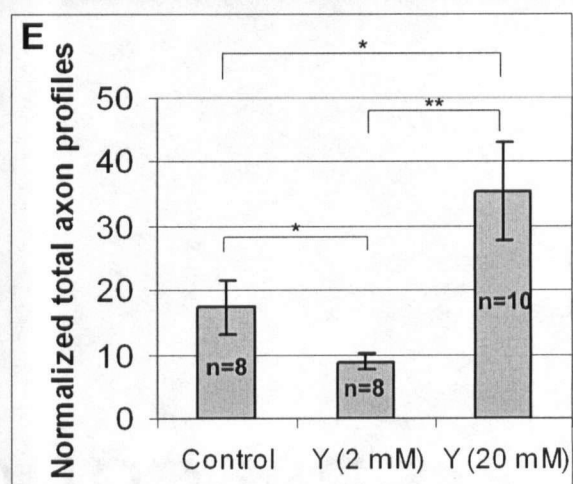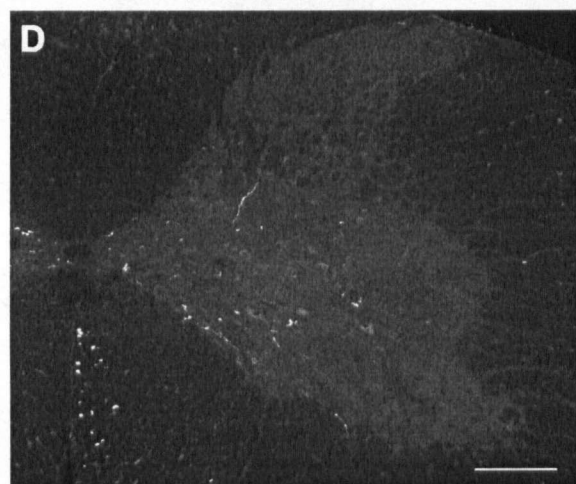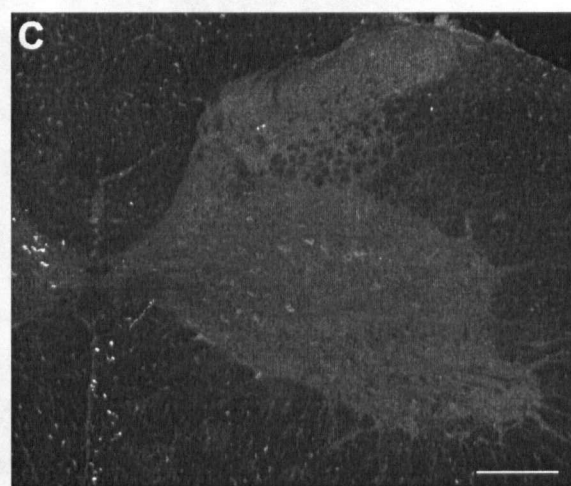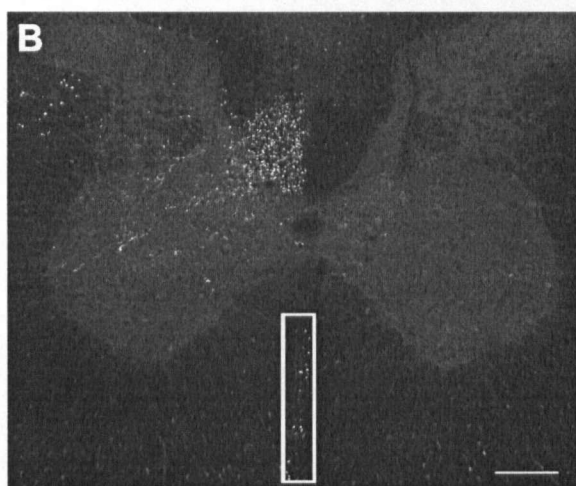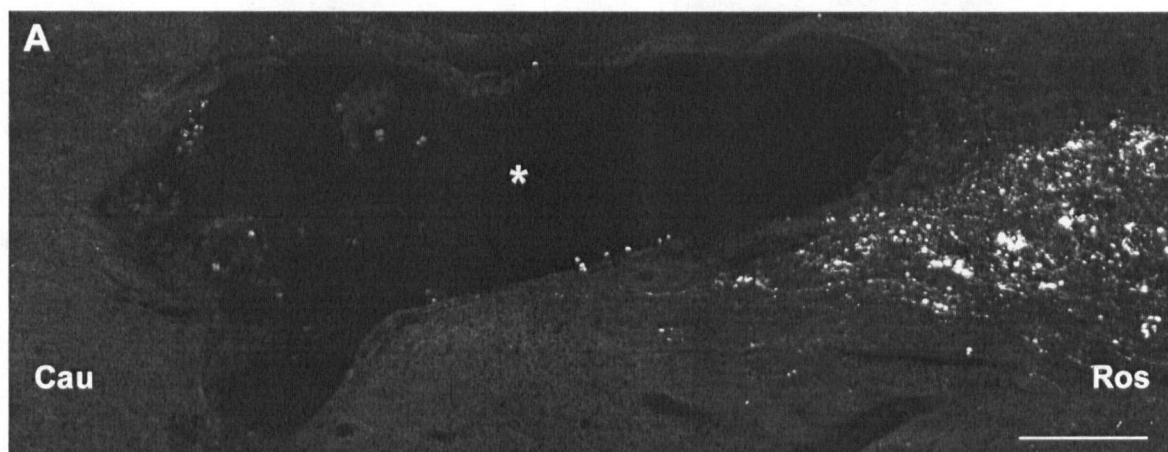
Cau

Ros

*

A

B

C

D

E

Figure 3.5

Footprint analysis after Y27632 treatment indicated that recovery of locomotor functions was inhibited in the low dose treatment group. (A) By the sixth week after injury, the base of support was normalized in control and high dose-treated animals, but not in the low dose animals, whose base of support values were dramatically higher than the other two groups throughout the entire observation period. (B) For the forepaw outward rotation angles, only the high dose group showed significant recovery toward presurgical level at 6 weeks after injury. *Relative change = (Value after injury – Value before injury)/ Value before injury.* *, $p < 0.05$ by ANOVA and post-hoc Tukey test as compared with control or otherwise indicated group; +, $p < 0.05$ by pair-wise comparison with control group; #, week 6 data points significantly different from week 1 data points, $p < 0.05$ by Wilcoxon test.
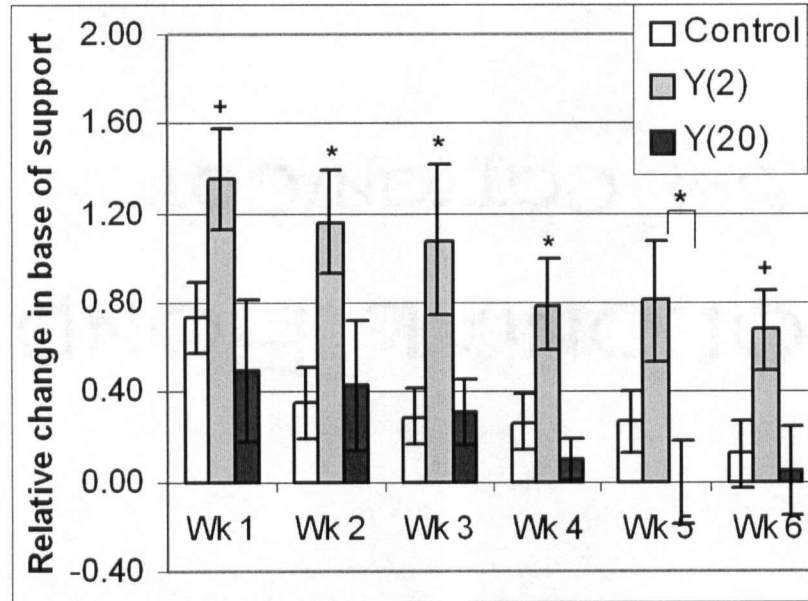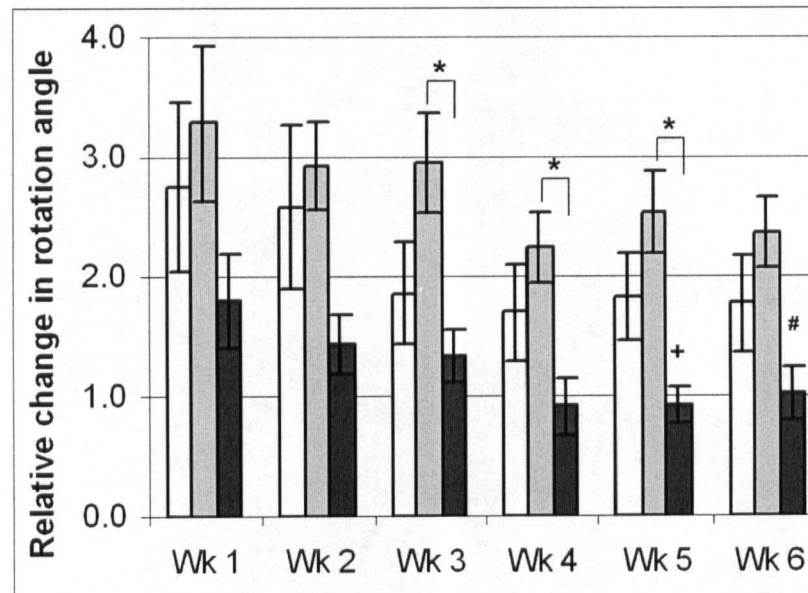
Figure 3.6

(A) Footslip test results indicated that high dose Y27632 accelerated the recovery of skilled locomotory function. At week 3, both high and low dose Y27632 significantly reduced the number of footslips compared to control rats. However, at weeks 1, 4, and 6, only the high dose regiment was more effective than control in reducing footslip frequency. Nonetheless at week 6, all animals had significant recovery and had reduced footslip frequency compared to 1 week after surgery. *Change in footslip frequency (Absolute change) = Value after injury – Value before injury.* (B) There was no sign of hypersensitivity to noxious heat stimulus in drug-treated animals compared to control animals. Using the Plantar IR apparatus, an infrared beam was targeted onto the forepaw and the latency time of response in seconds was recorded. The high dose group showed a longer tolerance compared to control at 4 weeks after injury. Paw withdrawal to noxious heat = Reaction time after injury – Reaction time before injury. *, $p < 0.05$ by ANOVA or Kruskal Wallis test; +, $p<0.05$ by pair-wise comparison.
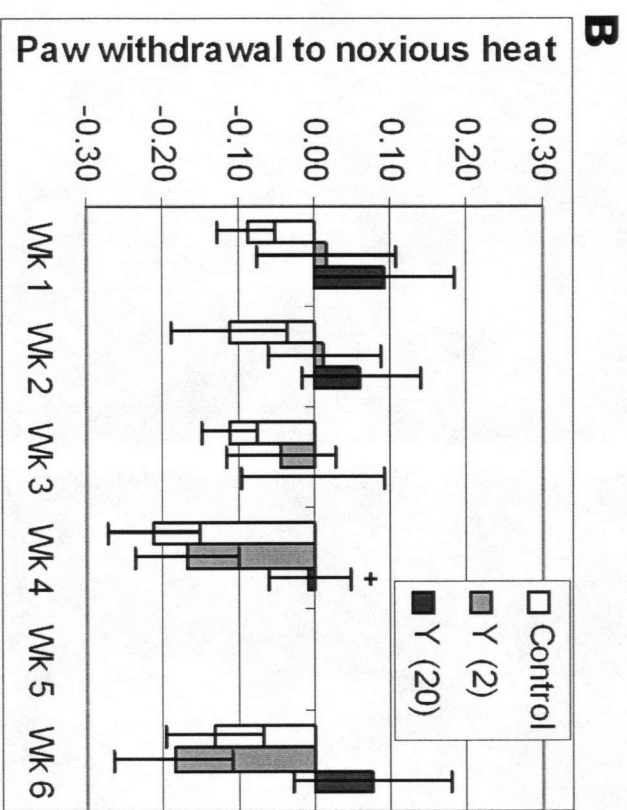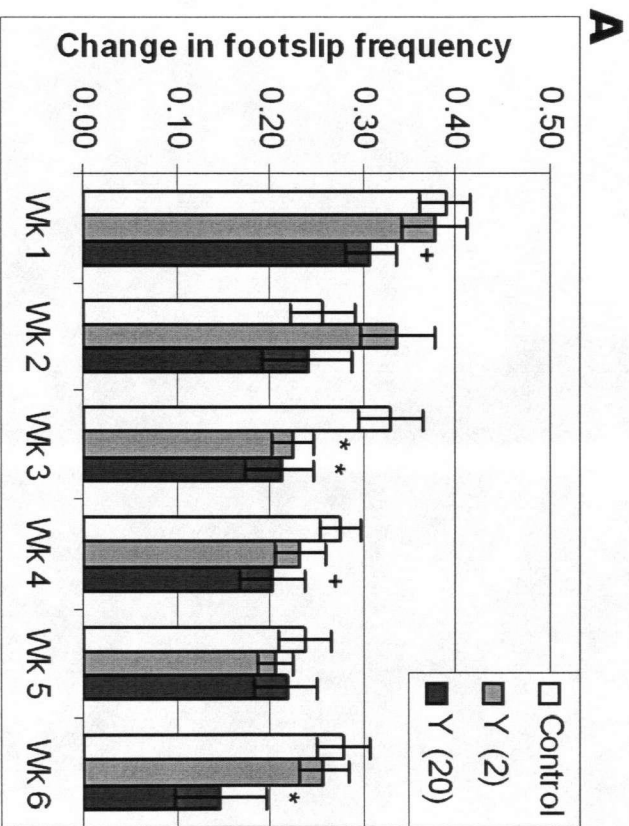
A

Change in footslip frequency

B

Paw withdrawal to noxious heat

□ Control
■ Y (2)
■ Y (20)

Figure 3.7

Food pellet reaching test results indicated that low dose Y27632 treatment worsen the recovery of skilled forelimb movements while high dose accelerated recovery. (A) Success rate as calculated by the number of successful pellet retrieval divided by the number of attempts (25 pellets). (B) Reaching success scores based on the 10-point scale (Table 1). Both quantifications indicated that 1 week after injury, control and low dose groups were significantly impaired while the high dose group retained presurgical reaching success. At week 6, control and high dose-treated animals reached at presurgical levels while the low dose group remained impaired. *, $p < 0.05$ by Kruskal Wallis test; #, significantly different from presurgical baseline values.
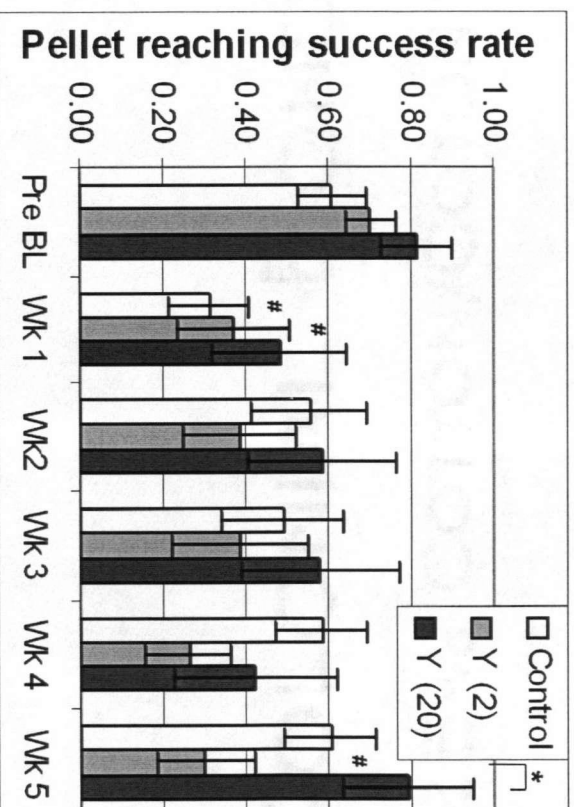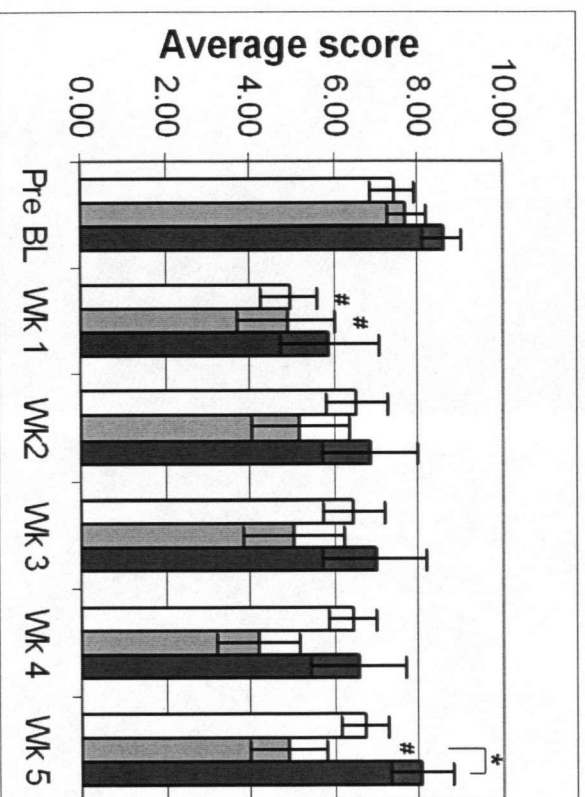
References

Amano M, Fukata Y, Kaibuchi K (2000) Regulation and functions of Rho-associated kinase. Exp Cell Res 261:44-51.

Amano M, Ito M, Kimura K, Fukata Y, Chihara K, Nakano T, Matsuura Y, Kaibuchi K (1996) Phosphorylation and activation of myosin by Rho-associated kinase (Rho- kinase). J Biol Chem 271:20246-20249.

Aurandt J, Vikis HG, Gutkind JS, Ahn N, Guan KL (2002) The semaphorin receptor plexin-B1 signals through a direct interaction with the Rho-specific nucleotide exchange factor, LARG. Proc Natl Acad Sci U S A 99:12085-12090.

Bareyre FM, Kerschensteiner M, Raineteau O, Mettenleiter TC, Weinmann O, Schwab ME (2004) The injured spinal cord spontaneously forms a new intraspinal circuit in adult rats. Nat Neurosci 7:269-277.

Bell-Krotoski J, Tomancik E (1987) The repeatability of testing with Semmes-Weinstein monofilaments. J Hand Surg [Am] 12:155-161.

Bell-Krotoski JA, Fess EE, Figarola JH, Hiltz D (1995) Threshold detection and Semmes-Weinstein monofilaments. J Hand Ther 8:155-162.

Bito H, Furuyashiki T, Ishihara H, Shibasaki Y, Ohashi K, Mizuno K, Maekawa M, Ishizaki T, Narumiya S (2000) A critical role for a Rho-associated kinase, p160ROCK, in determining axon outgrowth in mammalian CNS neurons. Neuron 26:431-441.

Borisoff JF, Chan CC, Hiebert GW, Oschipok L, Robertson GS, Zamboni R, Steeves JD, Tetzlaff W (2003) Suppression of Rho-kinase activity promotes axonal growth on inhibitory CNS substrates. Mol Cell Neurosci 22:405-416.

Bundesen LQ, Scheel TA, Bregman BS, Kromer LF (2003) Ephrin-B2 and EphB2 regulation of astrocyte-meningeal fibroblast interactions in response to spinal cord lesions in adult rats. J Neurosci 23:7789-7800.

Chen MS, Huber AB, van der Haar ME, Frank M, Schnell L, Spillmann AA, Christ F, Schwab ME (2000) Nogo-A is a myelin-associated neurite outgrowth inhibitor and an antigen for monoclonal antibody IN-1. Nature 403:434-439.

Chen ZJ, Ughrin Y, Levine JM (2002) Inhibition of axon growth by oligodendrocyte precursor cells. Mol Cell Neurosci 20:125-139.

de Medinaceli L, Freed WJ, Wyatt RJ (1982) An index of the functional condition of rat sciatic nerve based on measurements made from walking tracks. Exp Neurol 77:634-643.

Dergham P, Ellezam B, Essagian C, Avedissian H, Lubell WD, McKerracher L (2002) Rho signaling pathway targeted to promote spinal cord repair. J Neurosci 22:6570-6577.

Dickson BJ (2001) Rho GTPases in growth cone guidance. Curr Opin Neurobiol 11:103-110.

Dubreuil CI, Winton MJ, McKerracher L (2003) Rho activation patterns after spinal cord injury and the role of activated Rho in apoptosis in the central nervous system. J Cell Biol 162:233-243.

Feng J, Ito M, Ichikawa K, Isaka N, Nishikawa M, Hartshorne DJ, Nakano T (1999) Inhibitory phosphorylation site for Rho-associated kinase on smooth muscle myosin phosphatase. J Biol Chem 274:37385-37390.

Fitch MT, Doller C, Combs CK, Landreth GE, Silver J (1999) Cellular and molecular mechanisms of glial scarring and progressive cavitation: in vivo and in vitro analysis of inflammation-induced secondary injury after CNS trauma. J Neurosci 19:8182-8198.

Fournier AE, Takizawa BT, Strittmatter SM (2003) Rho kinase inhibition enhances axonal regeneration in the injured CNS. J Neurosci 23:1416-1423.

Hargreaves K, Dubner R, Brown F, Flores C, Joris J (1988) A new and sensitive method for measuring thermal nociception in cutaneous hyperalgesia. Pain 32:77-88.

Hirose M, Ishizaki T, Watanabe N, Uehata M, Kranenburg O, Moolenaar WH, Matsumura F, Maekawa M, Bito H, Narumiya S (1998) Molecular dissection of the Rho-associated protein kinase (p160ROCK)- regulated neurite remodeling in neuroblastoma N1E-115 cells. J Cell Biol 141:1625-1636.

Ishizaki T, Uehata M, Tamechika I, Keel J, Nonomura K, Maekawa M, Narumiya S (2000) Pharmacological properties of Y-27632, a specific inhibitor of rho- associated kinases. Mol Pharmacol 57:976-983.

Ito M, Nakano T, Erdodi F, Hartshorne DJ (2004) Myosin phosphatase: structure, regulation and function. Mol Cell Biochem 259:197-209.

Jain A, Brady-Kalnay SM, Bellamkonda RV (2004) Modulation of Rho GTPase activity alleviates chondroitin sulfate proteoglycan-dependent inhibition of neurite extension. J Neurosci Res 77:299-307.

John GR, Chen L, Rivieccio MA, Melendez-Vasquez CV, Hartley A, Brosnan CF (2004) Interleukin-1beta induces a reactive astroglial phenotype via deactivation of the Rho GTPase-Rock axis. J Neurosci 24:2837-2845.

Jones LL, Margolis RU, Tuszynski MH (2003) The chondroitin sulfate proteoglycans neurocan, brevican, phosphacan, and versican are differentially regulated following spinal cord injury. Exp Neurol 182:399-411.

Lehmann M, Fournier A, Selles-Navarro I, Dergham P, Sebok A, Leclerc N, Tigyi G, McKerracher L (1999) Inactivation of Rho signaling pathway promotes CNS axon regeneration. J Neurosci 19:7537-7547.

Levin S, Pearsall G, Ruderman RJ (1978) Von Frey's method of measuring pressure sensibility in the hand: an engineering analysis of the Weinstein-Semmes pressure aesthesiometer. J Hand Surg [Am] 3:211-216.

Liuzzi FJ, Lasek RJ (1987) Astrocytes block axonal regeneration in mammals by activating the physiological stop pathway. Science 237:642-645.

Maekawa M, Ishizaki T, Boku S, Watanabe N, Fujita A, Iwamatsu A, Obinata T, Ohashi K, Mizuno K, Narumiya S (1999) Signaling from Rho to the actin cytoskeleton through protein kinases ROCK and LIM-kinase. Science 285:895-898.

McGraw J, Hiebert GW, Steeves JD (2001) Modulating astrogliosis after neurotrauma. J Neurosci Res 63:109-115.

McKeon RJ, Jurynec MJ, Buck CR (1999) The chondroitin sulfate proteoglycans neurocan and phosphacan are expressed by reactive astrocytes in the chronic CNS glial scar. J Neurosci 19:10778-10788.

McKerracher L, David S, Jackson DL, Kottis V, Dunn RJ, Braun PE (1994) Identification of myelin-associated glycoprotein as a major myelin- derived inhibitor of neurite growth. Neuron 13:805-811.

Metz GA, Whishaw IQ (2002) Cortical and subcortical lesions impair skilled walking in the ladder rung walking test: a new task to evaluate fore- and hindlimb stepping, placing, and co-ordination. J Neurosci Methods 115:169-179.

Miranda JD, White LA, Marcillo AE, Willson CA, Jagid J, Whittemore SR (1999) Induction of Eph B3 after spinal cord injury. Exp Neurol 156:218-222.

Monnier PP, Sierra A, Schwab JM, Henke-Fahle S, Mueller BK (2003) The Rho/ROCK pathway mediates neurite growth-inhibitory activity associated with the chondroitin sulfate proteoglycans of the CNS glial scar. Mol Cell Neurosci 22:319-330.

Neumann H, Schweigreiter R, Yamashita T, Rosenkranz K, Wekerle H, Barde YA (2002) Tumor necrosis factor inhibits neurite outgrowth and branching of hippocampal neurons by a rho-dependent mechanism. J Neurosci 22:854-862.

Niederost B, Oertle T, Fritsche J, McKinney RA, Bandtlow CE (2002) Nogo-A and myelin-associated glycoprotein mediate neurite growth inhibition by antagonistic regulation of RhoA and Rac1. J Neurosci 22:10368-10376.

Pasterkamp RJ, Anderson PN, Verhaagen J (2001) Peripheral nerve injury fails to induce growth of lesioned ascending dorsal column axons into spinal cord scar tissue expressing the axon repellent Semaphorin3A. Eur J Neurosci 13:457-471.

Raineteau O, Fouad K, Bareyre FM, Schwab ME (2002) Reorganization of descending motor tracts in the rat spinal cord. Eur J Neurosci 16:1761-1771.

Ramer LM, Borisoff JF, Ramer MS (2004) Rho-kinase inhibition enhances axonal plasticity and attenuates cold hyperalgesia after dorsal rhizotomy. J Neurosci 24:10796-10805.

Rudge JS, Silver J (1990) Inhibition of neurite outgrowth on astroglial scars in vitro. J Neurosci 10:3594-3603.

Sandvig A, Berry M, Barrett LB, Butt A, Logan A (2004) Myelin-, reactive glia-, and scar-derived CNS axon growth inhibitors: expression, receptor signaling, and correlation with axon regeneration. Glia 46:225-251.

Schmidt JT, Morgan P, Dowell N, Leu B (2002) Myosin light chain phosphorylation and growth cone motility. J Neurobiol 52:175-188.

Shamah SM, Lin MZ, Goldberg JL, Estrach S, Sahin M, Hu L, Bazalakova M, Neve RL, Corfas G, Debant A, Greenberg ME (2001) EphA receptors regulate growth cone dynamics through the novel guanine nucleotide exchange factor ephexin. Cell 105:233-244.

Shehab SA, Spike RC, Todd AJ (2003) Evidence against cholera toxin B subunit as a reliable tracer for sprouting of primary afferents following peripheral nerve injury. Brain Res 964:218-227.

Sung JK, Miao L, Calvert JW, Huang L, Louis HH, Zhang JH (2003) A possible role of RhoA/Rho-kinase in experimental spinal cord injury in rat. Brain Res 959:29-38.

Wahl S, Barth H, Ciossek T, Aktories K, Mueller BK (2000) Ephrin-A5 induces collapse of growth cones by activating Rho and Rho kinase. J Cell Biol 149:263-270.

Wang KC, Koprivica V, Kim JA, Sivasankaran R, Guo Y, Neve RL, He Z (2002) Oligodendrocyte-myelin glycoprotein is a Nogo receptor ligand that inhibits neurite outgrowth. Nature 417:941-944.

Weidner N, Ner A, Salimi N, Tuszynski MH (2001) Spontaneous corticospinal axonal plasticity and functional recovery after adult central nervous system injury. Proc Natl Acad Sci U S A 98:3513-3518.

Whishaw IQ (2000) Loss of the innate cortical engram for action patterns used in skilled reaching and the development of behavioral compensation following motor cortex lesions in the rat. Neuropharmacology 39:788-805.

Whishaw IQ, Gorny B, Foroud A, Kleim JA (2003) Long-Evans and Sprague-Dawley rats have similar skilled reaching success and limb representations in motor cortex but different movements: some cautionary insights into the selection of rat strains for neurobiological motor research. Behav Brain Res 145:221-232.

Whishaw IQ, Pellis SM, Gorny B, Kolb B, Tetzlaff W (1993) Proximal and distal impairments in rat forelimb use in reaching follow unilateral pyramidal tract lesions. Behav Brain Res 56:59-76.

Yamashita T, Higuchi H, Tohyama M (2002) The p75 receptor transduces the signal from myelin-associated glycoprotein to Rho. J Cell Biol 157:565-570.

Yamashita T, Tucker KL, Barde YA (1999) Neurotrophin binding to the p75 receptor modulates Rho activity and axonal outgrowth. Neuron 24:585-593.

Yuan XB, Jin M, Xu X, Song YQ, Wu CP, Poo MM, Duan S (2003) Signalling and crosstalk of Rho GTPases in mediating axon guidance. Nat Cell Biol 5:38-45.

Chapter 4

ROCK inhibition with Y27632 activates astrocytes and increases their expression of chondroitin sulfate proteoglycan

Introduction

The Rho/ROCK pathway is involved in the signaling of multiple molecules inhibitory to neurite/axonal growth, such as myelin-associated glycoprotein (MAG), Nogo, oligodendrocyte myelin glycoprotein (OMgp), and chondroitin sulfate proteoglycans (CSPG) (Borisoff et al., 2003;Dergham et al., 2002;Fournier et al., 2003;Monnier et al., 2003;Niederost et al., 2002;Sivasankaran et al., 2004). *In vivo*, inhibition of Rho or ROCK have been shown to stimulate axonal regeneration/sprouting in various models of CNS injury (Dergham et al., 2002;Fournier et al., 2003;Lehmann et al., 1999). After spinal cord dorsal column transection, inhibition of Rho with C3 and ROCK with Y27632 promoted growth of long projection tract axons (corticospinal CST; dorsal column tract DCT), and accelerated functional recovery/ compensation (Chan et al., 2005;Dergham et al., 2002;Fournier et al., 2003). However, in our hands long distance regeneration of these axons was not observed with ROCK inhibition with Y27632 (Chan et al., 2005) and low doses of Y27632 were detrimental to functional recovery. In our study, the axons typically failed to reenter the normal spinal cord after crossing the lesion site, possibly due to the astrocytic barrier forming at the edge of the lesion. Therefore, we hypothesized that in addition to its effects on the growth cones of cut axons, Y27632 treatment might have also affected the non-neuronal cells in the injured spinal cord, resulting in undesirable side effects. More specifically, we hypothesized that the ROCK inhibitor acted on astrocytes at the lesion site and surrounding parenchyma.

Although in the developing brain, astrocytes may serve as guides for the growth of axons (Smith et al., 1986;Steindler et al., 1988;Hsu et al., 2005;Joosten and Gribnau, 1989), reactive astrocytes found at the adult CNS injury sites contribute to reactive gliosis, which is non-permissive to axon regrowth (Fitch et al., 1999;Liuzzi and Lasek, 1987;reviewed in McGraw et al., 2001;Rudge and Silver, 1990;McKeon et al., 1991;McKeon et al., 1999). Major changes occur in activated astrocytes such as hypertrophy and hyperplasia, accompanied by increased synthesis of the cytoskeletal protein, glial fibrillary acidic protein (GFAP) (reviewed in Eng and Ghirnikar, 1994;reviewed in Pekny and Nilsson, 2005). In addition, astroglial activation is associated with an increase in the expression of inhibitory extracellular matrix (ECM) molecules including CSPGs and tenascin (McKeon et al., 1991;McKeon et al., 1999;Canning et al., 1996), thus contributing to the gliosis-mediated regenerative failure of CNS axons.

In culture, non-stimulated astrocytes typically exhibit a flattened, polygonal morphology which is similar to fibroblasts (Hatten, 1985). Activated astrocytes have multiple processes with rounded cell bodies (Shain et al., 1987), and this morphology is termed 'stellation'. These activated, or stellate, astrocytes are inhibitory to axonal growth (Lefrancois et al., 1997). Astrocyte stellation is regulated by the Rho pathway. Stellation due to interleukin-1β (IL-1β) (John et al., 2004), cAMP (Ramakers and Moolenaar, 1998), or manganese (Chen et al., 2005) is dependent on the inactivation of Rho, while increases in Rho activation due to lysophosphatidic acid (LPA) (Manning, Jr. et al., 1998;Ramakers and Moolenaar, 1998), or to the cell adhesion molecule, Thy-1 (Avalos et al., 2004), result in astrocyte spreading and stress fibre formation.

In the present study, we tested the hypothesis that Y27632 treatment increased axonal growth inhibition by astrocytes. We analysed the *in vivo* effects of ROCK inhibition with Y27632 on the expression of GFAP, and of the CSPG neurocan. Secondly, we studied *in vitro* the expression of GFAP and ECM molecules (including fibronectin, laminin, CSPGs and neurocan) in cultured astrocytes. We tested the effects of Rho-pathway inhibition in astrocytes on their neurite outgrowth promoting properties using cortical neurons.

Materials and methods

Animal experiments

All experiments were conducted in accordance with the University of BC Animal Care Ethics Committee, and adhered to guidelines of the Canadian Council on Animal Care. Animal surgeries were conducted as described previously (Chan et al., 2005). Briefly, adult male Sprague Dawley rats were anesthetized with an intraperitoneal injection of a mixture of ketamine hydrochloride (72 mg/kg; Bimeda-MTC, Cambridge, ON) and xylazine hydrochloride (9 mg/kg; Bayer Inc., Etobicoke, ON). The animals were placed in a stereotaxic frame and the spinal cord was exposed at the cervical C4/5 level. A wire knife (model 120; David Kopf Instruments, Tujunga, CA) was used to produce the dorsal column transection. Rats were randomly assigned into three groups: control group that received no treatment (vehicle solution), and another two groups that each received one of two doses of Y27632 (Tocris Cookson Ltd., Avonmouth, Bristol, UK). The vehicle or drug solution was delivered into the rats via 7-day osmotic minipumps (0.5μl/hour, Alzet 1007D; Durect Corp., Cupertino, CA) according to manufacturer's instructions. The two different concentrations of Y27632 pumps were: low dose (2 mM; 160 μg

per animal over two weeks), and high dose (20 mM; 1600 µg per animal over two weeks). 4 controls, 5 low dose Y27632-treated, and 5 high dose-treated rats were included in this study. Immediately after the spinal cord lesion, the osmotic minipumps were implanted into the subcutaneous space at the back of the neck and a catheter delivered the drug-containing or control solution into the intrathecal space close to the lesion site (catheter opens into C2/3 level). The skin incision was closed with metal clips. The animals were euthanized 1 week after injury by overdosing with chloral hydrate, followed by perfusion with paraformaldehyde.

Astrocyte Culture

Astrocytes were obtained from P1 to P3 Sprague Dawley rats. The pups were decapitated and the cortices were dissected out. After removing the mengines, the cortices were finely minced in chilled cation-free Hank's balanced salt solution (HBSS; Invitrogen, San Diego, CA), and treated with 0.25% trypsin for 15 minutes at 37°C. The tissue was rinsed in serum-containing medium to inactivate trypsin and triturated to dissociate into single-cell suspension. The cells were resuspended in minimal essential medium (MEM) with 10% fetal bovine serum (FBS), 0.36% glucose, 2 mM glutamine, 100 units/mL penicillin/streptomycin, and plated at 1,600,000 cells per T75 tissue culture flask (West Chester, PA). After 8 to 12 days in culture, the astrocytes reached confluence and formed a monolayer with other cells on top, which are mostly oligodendrocytes and some are microglia (McCarthy and de Vellis, 1980). The flasks were shaken at 110 rpm overnight to remove these contaminating cells, which lifted off from the astrocyte monolayer after shaking and were discarded. The astrocytes were gently trypsinized from the surface of the flasks, rinsed in fresh medium with FBS, and plated on poly-D-lysine (Sigma, St. Louis, MO)-coated 8-chamber glass slides (Nunc, Rochester, NY) at 100,000 cells per well.

Cortical neuron dissociation

Cortical neurons were obtained from P5 to P7 Sprague Dawley rats using a modified method of Brewer (1997b). After dissecting out the cortices and removing the meninges, the cortices were finely minced in chilled Neurobasal A (NBA), and incubated in papain (2 mg/mL; Worthington, Freehold, NJ) for 30 minutes at 37°C. The tissue was rinsed in NBA with supplement (B27, 0.5 mM glutamine, and 100 units/mL penicillin/strepmycin), and gently triturated. The single-cell suspension was applied to a four-step Percoll (Sigma) gradient (36, 25,

20 and 13%) in NBA/B27 and centrifuged at 1900 rpm for 20 min. Fraction at and below the 25/36% interface was enriched in neurons (Brewer, 1997a). It was collected, rinsed in NBA/B27, and resuspended in NBA with supplement.

Treating astrocytes with Y27632 or C3

After the astrocytes reached confluence on 8-well glass slides, they were serum-starved overnight in NBA with supplement. For the Y27632 group, some of the wells were treated with different concentrations (0 to 50 μM) of Y27632. For the C3 group, some of the wells were treated with 0.2 μg C3. C3 was used with Chariot (Active Motif, Carlsbad, CA) to facilitate cell entry, following instructions from manufacturer. Briefly, 0.2 μg C3 in PBS was mixed with Chariot diluted in sterile water, and incubated for 30 min at room temperature. Then the mixture, together with NBA with supplement, was added to the astrocyte cultures. The next day, the cells were rinsed in HBSS, and the cells were supplied with fresh medium.

Preparation of astrocyte extracellular matrix (ECM)

Untreated, or drug-treated astrocytes were incubated in sterile water and 0.2% Triton for 30 min to lyses cells by hypotonicity (Smith-Thomas et al., 1994). The cellular debris was then washed away with sterile water.

Some of chambers containing astrocyte ECM were treated with chondroitinase ABC (ChABC; Seikagaku Kogyo Co., Tokyo, Japan). They were incubated with 0.1 U/ml ChABC for 2 hours at 37°C. Afterwards, the slides were washed with sterile water and heated briefly on a hot plate to inactivate the enzyme.

Neuron/Astrocyte co-culture

The cortical neurons were seeded onto the astroglial monolayer at 12,000 cells per well. The neurons were added at the same time as Y27632. These neurons were allowed to grow neurites overnight before fixing in formalin.

Neurons growing on astrocyte ECM or in conditioned medium

Neurons were seeded at 50,000 cells per well onto astrocyte ECM. In the case of neurite growth in astrocyte conditioned medium (CM), neurons were seeded onto glass slides treated with PDL only. CM was collected from untreated, Y27632, or C3-treated astrocytes. For the Y27632 group, the CM was collected from untreated or Y27632-treated astrocytes 1 day after the addition of Y27632. Y27632 remained in the collected medium. For the C3 group, the wells

were replenished with fresh medium 1 day after the addition of C3 and chariot. CM was collected 2 days after the addition. Thus the CM did not contain C3.

Western blots

For astrocyte cultures, cells grown on 6cm culture plates were scrapped off using a rubber policeman and collected in 100µl ice-cold homogenization buffer (50 mM Tris-HCl (pH 7.4), 1% Triton x-100, 0.25% SDS, 150 mM NaCl, 1 mM Na_3VO_4, 1mM NaF, and protease inhibitor cocktail (Roche, Germany). A protein assay (BCA Protein Assay, Pierce Biotechnology, Rockford, IL) was performed to estimate the amount of protein in different samples. They were then subject to ChABC treatment for 1 hr at 37°C. Equal amounts of total protein from different samples were loaded onto each lane of a SDS polyacrylamide gel. Proteins were transferred onto an Immobilon-P membrane (Millopore, Billerica, MA), and Western Blot was performed using antibodies to GFAP (1/2000), actin (1/4000), fibronectin (1/400), laminin (1/500), and neurocan (1/1000). Then the membrane was incubated with horseradish peroxidase-conjugated secondary antibodies and protein bands were visualized by Chemiluminescence (Amersham Biosciences, New Jersey). The membranes were stripped and re-stained with anti-actin antibodies (1/4000) as a loading control.

Immunohistochemistry and Immunofluorescence Microscopy

For spinal cord tissues, immunohistochemistry was performed on 20 µm parasaggital sections that were prefixed in 4% paraformaldehyde and cryoprotected in increasing concentrations (12%, 18%, and 24%) of sucrose solution. The sections were incubated overnight with primary antibodies in PBS with 0.1% Triton X-100 (Sigma-Aldrich, Oakville, ON). Then they were incubated with the appropriate normal serum for 30 minutes to block non-specific binding, and were stained with fluorescence-conjugated secondary antibodies for two hours at room temperature. Spinal cord sections were viewed on a fluorescent microscope (Thornwood, NY), and photographed with a Q-imaging camera (Burnaby, BC) using the Northern Eclipse software (Empix Imaging, Mississauga, ON).

Cells grown on glass slides were fixed with 4% formalin or paraformaldehyde in 0.01 M PBS for 15 minutes at room temperature. They were solubilized in PBS with 0.1% Triton X, and incubated overnight at room temperature with primary antibodies. After blocking with the

appropriate normal serum for 30 min, they were immediately stained with fluorescence-conjugated secondary antibodies. Cells were washed between steps with 0.01 M PBS.

Primary antibodies used for immunohistochemistry included: rabbit anti-fibronectin (1/200; Dako, Glostrup, Denmark); rabbit anti-laminin (1/200; Sigma); monoclonal mouse anti-CSPG (CS56 antibody; 1/200; Sigma); rabbit anti-GFAP (1/400; Dako); monoclonal mouse anti-GFAP (1/400; Sigma); monoclonal mouse anti-Neurocan (1F6 antibody; 1/100; Developmental Studies Hybridoma Bank); and rabbit anti-βIII tubulin (1/400; Covance, Berkeley, CA).

Quantification of immunoreactivity

After immunostaining with anti-GFAP and anti-neurocan antibodies, the intensity of immunoreactivities were quantified, utilizing the SigmaScan software (Systat Software, Point Richmond, CA) on digital images of parasagittal spinal cord sections. The 'trace tool' in SigmaScan was used to select a thin band of spinal cord tissue (50μm) along the entire edge of the lesion cavity, where the intensity of immunostaining was recorded (Fig. 1). Average intensity was normalized to background intensity, as measured in a separate area of tissue at least 4 mm away from the lesion edge. Three spinal cord sections per animal were quantified for each antigen, and the sections were approximately 100μm apart, with the first section harboring the central canal.

For *in vitro* astrocyte cultures, anti-GFAP, anti-fibronectin, anti-laminin, and anti-CSPG immunoreactivities were quantified using similar methods. The intensity of immunostaining was recorded along three bars placed at the top, middle, and bottom of each digital image. Three digital images were used at each Y27632 concentration.

Quantification of neurite growth

Neurons were visualized by anti-βIII tubulin immunostaining and under the fluorescence microscope. Digital images were taken with the 20x objective. Cells with one long and slender process that exceeded the length of any other of its processes were included in the quantification. The longest neurite of each neuron were digitally retraced by hand using the Photoshop 7.0 software (Adobe), and quantified using Northern Eclipse. Data were collected from at least 3 independent experiments, and more than 350 neurons were included in the quantification.

Statistics

Data were reported as the mean ± SEM. Immunostaining intensity at each 100μm intervals of the three groups of rats were compared using ANOVA, and in the cases where the requirements of parametric analysis were not satisfied, the non-parametric Kruskal Wallis ranked sum test. The data were further analyzed using the post-hoc Holm-Sidak method against the control group. *In vitro*, neurite lengths of each treatment group were compared to that of control group using the student's t-test. In all analyses, statistical significance was accepted at a P-value < 0.05.

Results

Y27632 treatment upregulated GFAP and neurocan expression

Dorsal column transection induced the upregulation of GFAP around the lesion cavity in untreated control (Fig.2a) and Y27632-treated (Fig.2b,c) rats. In animals intrathecally infused with low dose (2 mM) and high dose (20 mM) Y27632 (at a rate of 12 μL/day for 7 days), the intensity of GFAP immunostaining along the edge of the lesion cavity was significantly higher than in saline controls (p<0.05; Fig. 2d).

Failure of axonal regeneration in the spinal cord results in part from an upregulation of CSPGs surrounding the lesion (Bradbury et al., 2002; Davies et al., 1999). Neurocan is one of the upregulated CSPGs and is expressed by astrocytes (Jones et al., 2003; McKeon et al., 1999; Tang et al., 2003). Quantification of neurocan immunolabeling revealed that the post-injury level of neurocan was significantly higher in both high dose and low dose Y27632-treated rats (p<0.001; Fig. 3d).

Y27632 induced astrocyte stellation in vitro

To observe morphological changes in astrocytes due to ROCK inhibition, we established cell cultures from P2/3 rat cortices. Astrocytes dominated in the culture, and were identified by their immunoreactivity to antibodies recognizing their intermediate filament component GFAP (Bignami et al., 1972). Consistent with previous results (Hatten, 1985;Abe and Misawa, 2003), most astrocytes are flattened and polygonal, and did not display processes in control cultures with no Y27632 treatment (Fig. 4.4A). Addition of Y27632 induced astrocyte stellation and

condensation of GFAP immunoreactivity (Fig. 4.4B-F; Abe and Misawa, 2003). Effects of Y27632 were evident within 30 minutes and continued for at least 48 hours. Increasing concentrations (1 to 50μM) of Y27632 resulted in progressively enhanced stellation (Fig.4.4B-F), and this effect saturated at a concentration of 25 μM (Fig. 4.4E). Increasing Y27632 concentration to 50 μM (Fig. 4.4F) did not appear to result in any higher degree of stellation. Morphological changes associated with Y27632 treatment were reversible, as stellate astrocytes reverted back to the flattened phenotype within one hour after removal of Y27632 from the culture medium. Quantification of GFAP immunoreactivity did not show any difference in the level of expression (data not shown). Western blots using cell lysates from control and astrocytes treated for 24 hours with Y27632 revealed that Y27632-treated and untreated astrocytes expressed a major GFAP band at 50kDa (Fig. 4.4G), and when normalized to actin, there was no difference between the treatment groups (quantitative data not shown).

Y27632 modified the expression of astrocytic ECM molecules

We examined the expression of various components of the astrocytic extracellular matrix (ECM) induced by Y27632 treatment of astrocytes *in vitro*. Specifically, we analysed the immunostaining of permissive/stimulatory ECM molecules, including laminin and fibronectin, and of inhibitory CSPGs. These molecules are known to be expressed by astrocytes (Jones et al., 2003;Liesi et al., 1983;Liesi et al., 1986;Price and Hynes, 1985;Tang et al., 2003). The patterns of fibronectin (Fig. 4.5A,B) and laminin (Fig. 4.5C,D) expression by Y27632-treated astrocyte were slightly more condensed compared to untreated astrocytes, while the levels of fibronectin expression did not differ between Y27632-treated and untreated astrocytes. However, for laminin, the expression by Y27632-treated (25μM) astrocytes was significantly higher (approximately 40%) than that by untreated cells (p<0.005, Fig. 4.5E).

Subsequently we studied the expression of inhibitory substrates like CSPGs by Y27632-treated astrocytes using immunostaining with the CS56 antibody, which recognizes a wide spectrum of CSPGs. In unstimulated astrocyte cultures, CSPG expression was mainly found in the ECM, and hardly any CSPGs were associated with the cells (Fig. 4.6A). In astrocyte cultures treated with Y27632 for 24 hours, CSPG expression was encountered both extracellularly and associated with the cells (Fig. 4.6B). Quantification of CSPG immunoreactivity showed that the level of expression by Y27632-treated cells was approximately 50% higher than that of untreated

astrocytes (p<0.005, Fig. 4.6C). Unfortunately, immunostaining of the *in vitro* cultures using the 1F6 mouse monoclonal antibody to the N-terminal of neurocan failed in our hands.

For the quantification of neurocan protein expression, western blots were run using cell lysates treated with chondroitinase ABC (ChABC) for 2 hours prior to loading onto the gels. ChABC treatment was needed because most CSPGs, including neurocan, with their chondroitin sulphate (CS) side chains attached, are very large molecules that otherwise fail to run properly on polyacrylamide gels. This precluded the use of the CS56 antibody that only recognized intact CSPGs. With the 1F6 antibody directed to the N-terminal of the neurocan protein core, 2 bands at approximately 245, and 130 kDa were detected (Fig. 4.6D). The 245kDa band corresponded to the full length neurocan core protein, and the 130kDa band was the N-terminal fragment (neurocan-N) after internal cleavage (Asher et al., 2000;Meyer-Puttlitz et al., 1995;Tang et al., 2003). After quantifying the immunoreactive bands and normalizing to actin, treated astrocytes displayed increases in the expression of the 245 and 130 kDa bands (Fig. 4.6E). This indicated that there were increases in the amount of full length and neurocan-N associated with the astrocytes with Y27632 treatment.

Astrocytes pre-treated with Y27632 were inhibitory to neurite growth

To test how Y27632-treated astrocytes influence neurite growth, the length of neurites immunostained for βIII-tubulin was quantified in a series of astrocyte/neuron cocultures (Fig. 4.7A-C). To facilitate comparison across different experiments, neurite lengths were normalized to the average neurite length on untreated (Y0) astrocytes. When the ROCK inhibitor was added at the same time as the cortical neurons are seeded onto the astrocyte monolayer and incubated overnight, there was no significant difference in neurite length compared to growth on untreated astrocytes. Neurite growth was equally robust on control and treated astrocytes. It was slightly increased at 10μM Y27632, but the increase did not reach significance (p= 0.06; Fig. 4.7C). Since Y27632 treatment increased the expression of presumed inhibitory CSPGs by astrocytes but failed to inhibit neurite outgrowth, we surmised that growth promoting as well as inhibitory effects of ROCK inhibition might have been involved in these co-cultures. We had previously shown that ROCK inhibition promoted DRG neurite outgrowth on the CSPG, aggrecan (Borisoff et al., 2003). To single out the effect of ROCK inhibition on astrocytes, cortical neurons were cocultured with astrocytes that had been pre-treated with Y27632 (Fig. 4.7D-F). The astrocytes were incubated with various concentrations of Y27632 for 24 hours. On the next day, the

astrocytes were washed with PBS, and medium was exchanged with no Y27632 present when the neurons were seeded. With Y27632 pre-treatment, neurite length was significantly decreased to 84% of control, however, that was observed only at 25µM Y27632 (p<0.01; Fig.4.7F).

The extracellular matrix produced byY27632-treated astrocytes inhibited neurite growth

The inhibitory CSPGs were constituents of the astrocyte-derived ECM. In order to isolate the effects of astrocyte-derived ECM on neurite growth, the astrocytes were lysed with sterile water and 0.2% triton after overnight treatment with Y27632. The P5/6 cortical neurons were grown on the ECM that was left behind on the PDL-treated glass slides (Fig. 4.8A,B). The ECM produced by Y27632-treated astrocytes, at all concentrations tested, was inhibitory to neurite growth (Fig. 4.8C, p<0.01). Neurite length on Y27632-treated astrocyte ECM (e.g. neurite growth on 25µM Y27632-treated astrocyte-derived ECM in Fig.4.8B) was approximately 70-80% of neurite length on untreated astrocyte-derived ECM (Fig. 4.8A).

To determine if the decrease in neurite growth was due to CSPGs and their respective carbohydrate side chains, the astrocyte-derived ECM was digested with ChABC. Neurite growth on ChABC-digested ECM derived from astrocytes with or without Y27632 treatment (Fig. 4.8D and E), was significantly different from that on control ECM, i.e. ECM produced by untreated astrocytes and not ChABC-digested (Fig. 4.8A; p<0.01; quantification in Fig. 4.8F). On ECM from astrocytes not treated with Y27632, ChABC digestion significantly increased neurite length (p<0.01) by 12% (compare Fig.4.8A and D). This increase was 30% on Y27632 (25µM)-treated astrocyte-derived ECM after ChABC digestion (compare Fig. 4.8B and E). In the latter case, on ChABC-digested ECM from Y27632-treated astrocytes, neurite length reached similar levels as on ECM from untreated astrocytes, indicating that the growth-inhibitory effects were mediated by carbohydrate side chains from CSPGs.

The conditioned medium (CM) from Y27632-treated astrocytes stimulates neurite growth

Since Y27632-treated astrocytes were not inhibitory or only slightly inhibitory to neurite growth of cortical neurons (Fig. 4.7C) while their ECM was significantly inhibitory (Fig. 4.8C), we hypothesized that secreted factors might also affect growth. To test this hypothesis, cortical neurons were grown on PDL-treated glass slides in the presence of medium conditioned by untreated or Y27632-treated astrocytes (Fig. 4.9A and 9B, respectively). For the latter, astrocytes were treated with Y27632, and this medium was collected the next day to be used in neuronal

cultures. Neurite growth was 50% longer in conditioned medium (CM) from astrocytes treated with 1 and 5μM Y27632 (Fig. 4.9C; p<0.001). This effect was even more pronounced (>2fold) at higher concentrations of Y27632 (p<0.001).

In order to eliminate the possibility that Y27632 present in the CM acted as a stimulatory factor, neurite growth on PDL-glass slides in fresh medium with Y27632 was compared with that without Y27632. The range of Y27632 used in this experiment (1 to 50μM) did not stimulate cortical neurite growth on PDL-glass slides (data not shown). As another control, Y27632 was added to untreated astrocyte-CM and this medium was used in dissociated cortical neuronal culture. Y27632 did not increase neurite growth in untreated astrocyte-CM (data not shown).

One possibility of the better neurite growth in Y27632-treated astrocyte-CM was the absence, or a lower concentration of an inhibitory factor compared to untreated astrocyte-CM. Since there was an increase in the level of CSPGs found on the astrocytes and in their ECM with Y27632 treatment (Fig. 4.6), we hypothesized that there was a corresponding decrease in the amount of CSPG released into the CM. Western blot of the astrocyte CM support this hypothesis (Fig. 4.9G). There was a decrease in the level of the 130kDa neurocan with Y27632 treatment, while the 245 band was not visible (not shown).

Our data indicated an increase in the amount of neurocan associated with astrocytes treated with increasing concentrations of Y27632, while the amount of neurocan in the Y27632-treated astrocyte-CM decreased. Neurocan and other CSPGs in the astrocyte-CM could also modify neurite length. Therefore, astrocyte-CM from untreated and Y27632-treated cells was incubated with ChABC and the ChABC heat inactivated 2 hours later, before growing the neurons in this CM. ChABC digestion of CM from untreated astrocytes almost doubled (1.8 times) neurite length (compare Fig. 4.9A and D; p<0.001, quantification in Fig. 4.9F), indicating that CSPGs in the astrocyte-CM were inhibiting neurite growth. The cortical neurons growing in CM from Y27632-treated astrocytes did not show any further increase in neurite length after ChABC digestion of the CM (compare Fig. 4.9B and E), indicating that ROCK inhibition of astrocytes effectively lowered the amount of CSPGs in their CM (as evidenced by neurocan in western blots. Fig. 4.9G).

C3 treatment mimicked the effects of Y27632

Since Y27632 may also inhibit other kinases such as protein kinase C δ (PKCδ) and protein kinase C related kinase (PRK) (Davies et al., 2000), we attempted to confirm that the effects of Y27632 on astrocytes was indeed mediated by the Rho pathway. We repeated some of the experiments with C3 exoenzyme, which specifically inhibited Rho by ADP-ribosylating the GTP-binding site (Jalink et al., 1994). Similar to Y27632 treatment, C3-treated astrocyte ECM was inhibitory compared to untreated astrocyte ECM (Fig. 4.10A). Neurite length on C3-astrocyte-ECM was 74% of that on control ECM ($p < 0.001$). In addition, neurite length in C3-treated astrocyte-CM was longer than in control astrocyte-CM (Fig. 4.10B), although the difference in neurite length was not as dramatic as that for Y27632 treatment (compare with Fig. 4.9). Neurite length in the Y27632-treated astrocyte-CM was 1.4 times of that in the control CM ($p < 0.001$).

Discussion

In the present study, we examined the *in vivo* and *in vitro* effects of the ROCK inhibitor, Y27632, on astrocytes. *In vivo*, dorsal column transection lesions were induced in rats, and they were sacrificed one week after injury. Rats with Y27632 treatment showed enhanced upregulation of GFAP and of the CSPG, neurocan around the lesion site. *In vitro*, we cultured astrocytes from early postnatal rat cortices, and Y27632 treatment increased the levels of laminin and CSPGs immunoreactivities. These Y27632-treated astrocytes had an increase in the level of CSPGs associated with the cells and in the secreted ECM. Western blot analysis with the 1F6 anti-neurocan N-terminal antibody indicated increases of the amount of full length and neurocan-N associated with the astrocytes with Y27632 treatment. Dissociated cortical neurons had reduced neurite growth on the ECM produced by Y27632-treated astrocytes. This decrease was reversed with ChABC digestion, indicating that CSPGs, or more specifically their GAG side chains, in the ECM were inhibitory. Astrocyte-CM had decreased levels of neurocan-N (by western blot) with Y27632 treatment, and untreated astrocyte-CM was inhibitory to neurite growth compared to Y27632-treated astrocyte-CM. ChABC digestion increased neurite length in untreated astrocyte-CM, showing that the presence of CSPGs (or their GAG side chains) in the CM were responsible for the inhibition.

Our results agreed with those of Abe and Misawa (2003) who also showed that inhibiting ROCK with Y27632 induced astrocyte stellation *in vitro*. The expression of dominant negative Rho in primary hippocampal astrocytes also resulted in stellation (Kalman et al., 1999). Moreover, astrocyte stellation induced by neuronal surface antigen Thy-1 (Avalos et al., 2004), cAMP (Ramakers and Moolenaar, 1998), and manganese (Chen et al., 2005) have been shown to involve an inactivation of the Rho pathway. Such *in vitro* evidence suggested that inactivation of the Rho pathway is also important for astrogliosis after injury *in vivo*. Interleukin-1β (IL-1β), a cytokine critical for the induction of reactive astrogliosis in the injured CNS (Giulian et al., 1988;Herx and Yong, 2001), deactivated the Rho/ROCK pathway *in vitro* (John et al., 2004). IL-1β resulted in the dephosphorylation of MLC and of the regulatory subunit of myosin phosphatase (MYPT). The phosphorylation states of these molecules are exquisitely sensitive to the level of Rho/ROCK activation (Feng et al., 1999;Amano et al., 1996). Therefore, astrocyte stellation and response to IL-1β depend on the deactivation of the Rho pathway (Abe and Misawa, 2003;Chen et al., 2005;John et al., 2004). Our study confirms and extents these data by showing that also *in vivo*, the astrogliosis in the injured spinal cord is enhanced by ROCK inhibition.

Our *in vitro* results with cortical neuron/astrocyte cocultures was interesting in that Y27632-treated astrocytes were as permissive as untreated astrocytes, although the ECM produced by treated astrocytes was more inhibitory. The answer to this apparent paradox lied in the observation that their CM was less inhibitory compared to untreated astrocytes. As a result, the effects on neurite growth exerted by the ECM and the CM might have cancelled each other, and the differences in neurite length could only be detected when each component was examined on its own. When neurons were grown on Y27632-treated astrocyte ECM, there was a decrease in neurite length, which was due to an increase in CSPGs (CS56 immunoreactivity) including neurocan expression that was ChABC-sensitive. Neurocan inhibition is at least partially dependent on its chondroitin sulfate glycosaminoglycan side chains (Sango et al., 2003). Although laminin expression also increased, the inhibitory effects of increased CSPG expression dominated over the permissive effects of increased laminin. In contrast, when cortical neurons were grown in Y27632-treated astrocyte-CM, there was an increase in neurite length. This correlated with a decline in neurocan level in the CM of these Y27632-treated astrocytes. Therefore, we hypothesized that the differences in neurite growth were largely due to the

presence of CSPGs in the astrocyte ECM and CM. This hypothesis was supported by the observation that ChABC removed the inhibitory effect on neurite growth by Y27632-treated astrocyte ECM. Conversely, ChABC increased neurite length in control astrocyte-CM, while there was no further stimulation in Y27632-treated astrocytes-CM.

Neurocan undergoes proteolytic cleavage in astrocyte cultures, giving rise to the C-terminal fragment known as Neurocan-C, and in two N-terminal fragments, Neurocan-130 and Neurocan-90 (Asher et al., 2000). All fragments carry chondroitin sulfates. The processed forms, neurocan-C and neurocan-130, are released into the CM (Asher et al., 2000;Asher et al., 2000;Oohira et al., 1994). Neurocan is usually found in the substrate around and under astrocytes, but not on the cells (Asher et al., 2000). The 1F6 antibody recognizes an epitope in the N-terminal half of neurocan and reacts with neurocan-130. (Asher et al., 2000;Meyer-Puttlitz et al., 1995). In our experiments, it was unfortunate that the 1F6 immunostaining of the astrocyte cultures failed in our hands. Nonetheless, the pattern of immunostaining with the CS56 antibodies agreed with that described for neurocan in astrocyte cultures, with most of the staining being extracellular. On the western blot, there was a very low level of the 245 and 130 kDa neurocan from the cell lysate of control astrocytes. This was indicative of the inability of astrocytes to retain neurocan on their cell surfaces. However, Y27632 treatment (5 to 50μM) increased the levels of these two neurocan bands, indicating that an increased amount of neurocan was associated with the cells after ROCK inhibition. Also, we detected the presence of Neurocan-130 in the CM, whose levels decreased with increasing Y27632 concentration. These results suggest that ROCK inhibition with Y27632 increased neurocan deposition onto the ECM, and at the same time decreased its release into the medium.

The Rho pathway may be associated with the degradation of CSPGs by proteases. Several matrix metalloproteinases (MMPs), such as MMP-2 and MMP-9, degrade CSPGs in the ECM (Ferguson and Muir, 2000;Zuo et al., 1998;Asher et al., 2005). Neurocan was identified as a MMP-2 substrate by comparing the amino acid sequence surrounding the processing site with a MMP cleavage site database (Turk et al., 2001). In smooth muscle cells, inhibition of ROCK with Y27632 prevented the phorbol ester (TPA)- or trophic factor-induced MMP-9 mRNA expression (Turner et al., 2005). Conversely, an increase in Rho activity contributes to cytokine-medicated upregulation of membrane type MMPs (MT1-MMP) expression (Bartolome et al., 2006). MT1-MMP is an activator of pro-MMP2 in coordination with tissue inhibitor of

metalloproteinase-2 (TIMP-2) (Banerji et al., 2005). Since astrocytes express MMPs including MMP-2 and -9 (Costa et al., 2002;Pagenstecher et al., 1998;Rathke-Hartlieb et al., 2000;Ahmed et al., 2005), the increase in CSPGs found in the astrocytic ECM after Y27632 treatment might be a result of suppressed MMP activities. In addition, MMP-2 digested other ECM proteins including laminin and fibronectin (Okada et al., 1990). The downregulation of MMPs by ROCK inhibition might also explain the increase in laminin immunoreactivity in Y27632-treated astrocyte cultures (Fig. 4.5).

We therefore hypothesize a model in which the cleavage of CSPGs, including neurocan, by the MMPs is suppressed by the Y27632 ROCK inhibitor (Fig. 4.11). Normally, MMPs digests CSPGs in the ECM. *In vitro* and in the case of neurocan, MMP digestion produces the N- and C-terminal fragments, which are incorporated into the ECM or released into the culture medium. In our study, western blot results from the 1F6 antibody indicated that neurocan-N was present in the astrocyte-CM, but we were uncertain if it could also be found in the ECM. It remains to be determined whether the C-terminal fragment is released into the medium or incorporated into the ECM. Full length neurocan and its fragments all appeared to be inhibitory to neurite growth, as shown in the literature and since in our experiments, astrocyte-CM (containing neurocan-N) decreased neurite length from cortical neurons. We propose that treating the astrocyte cultures with the Y27632 ROCK inhibitor suppresses MMP activities, thus most of the CSPGs remain intact and much smaller amounts of CSPG fragments are released into the medium. Rather, they are incorporated into the ECM, or associated with the astrocytes. Therefore, there is a net increase in the levels of inhibitory CSPGs in the ECM, but a net decrease in the culture medium.

Although Y27632 is a relatively selective inhibitor of ROCK, it also inhibits protein kinase C (PKC) and cyclic AMP-dependent protein kinase (PKA) at higher concentrations. The K_i value for ROCK is 0.14 µM, which is two orders of magnitude less than the K_i's for PKC (26 µM) and PKA (25 µM) (Uehata et al., 1997). Some of the higher Y27632 concentrations used in this experiment (concentrations above 25µM) most likely also inhibited kinases other than ROCK. Nonetheless, C3-exoenzyme, which specifically inactivates Rho by ADP-ribosylating an asparagine residue in the Rho effector domain (Dillon and Feig, 1995), produced similar results as Y27632. The ECM of C3-treated astrocytes was more inhibitory to neurite growth, while their CM was less inhibitory. Therefore, the effects on astrocytes were most likely mediated through

the Rho pathway. However, Y27632 also inhibits PRK2 (a protein kinase C-related protein kinase), and with a potency similar to that for ROCK (Davies et al., 2000). Since PRK2 is also a downstream effector of Rho, its contribution to astrocyte activation and CSPG expression cannot be distinguished from that of ROCK.

In this study, the higher increase in neurocan expression *in vivo* with Y27632 treatment may have contributed to this drug's negative side effects found in our previous experiment (Chan et al., 2005). In *in vitro* neuron-astrocyte cocultures, the increase in CSPG in the Y27632-treated astrocyte ECM was functionally compensated by a decrease in CSPG in the CM. The discrepancy might be a result of the inherent differences between *in vivo* tissue and tissue culture model in which only one major cell type was isolated and studied. The cleaved CSPG found in the CM *in vitro* corresponds to those found in the interstitial fluid *in vivo*, where they may be rapidly cleared by further proteinases degradation and by other cells. An alternative, but not mutually exclusive explanation is that in the three-dimensional (3D) environment *in vivo*, the axonal growth cones are in contact with CSPGs in the ECM on all surfaces. Thus CSPGs in a 3D environment are more effective in inhibiting axonal growth. This was similar to the condition *in vitro* where purified primary astrocytes were packed into 3D culture tubes (Fawcett et al., 1989). These astrocytes were much less permissive compared to astrocyte monolayers, and displayed similar axon regeneration-blocking activity as *in vivo*. In either case, the growth-inhibitory effects of CSPGs bound by the ECM dominate over free-floating CSPGs.

In conclusion, the dosage-dependent beneficial and detrimental effects of Y27632 (Chan et al., 2005), and the increase in CSPG expression with Y27632 treatment shown in this experiment call for caution in applying this drug in clinical research for the treatment of human SCI. More basic science research must be done to determine the range of dosage that is safe for use in treating SCI, and to design methods for cell specific targeting of ROCK inhibition.

Figure 4.1

Quantification of GFAP and neurocan immunostaining intensity. The intensity of immunoreactivities was measured along a thin band (50μm) of tissue around the entire lesion cavity (covered by grey strip). The intensity at each pixel was measured and one average value was recorded for each parasagittal spinal cord section. Average intensity was normalized to background intensity, as measured in a separate area of tissue at least 4 mm away from the lesion edge (grey bar). *Scale bars, 500μm.*
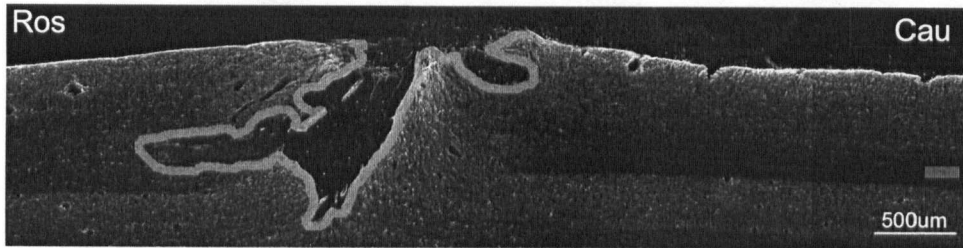
Ros   Cau

500um

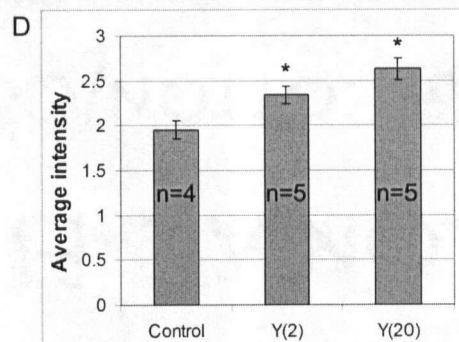**Figure 4.2**

Y27632-treated animals had enhanced upregulation of GFAP. Parasagittal spinal cord sections from control (A, A'), low dose Y27632-treated (B, B'), and high dose-treated (C,C') rats immunostained with anti-GFAP antibodies. Pictures on the right are higher magnification of the boxed areas on the left. Tissues were collected 1 week after C4/5 dorsal column transection and drug infusion. GFAP immunostaining was found at the injury site, at the edge of the lesion and in the perilesion area. D) Quantification of the intensity of immunoreactivities along a 50μm band of spinal cord tissue surrounding the lesion cavity. The upregulation of GFAP was significantly higher in both low dose- and high dose-treated rats. *, p<0.05. *Scale bar, 500μm.*
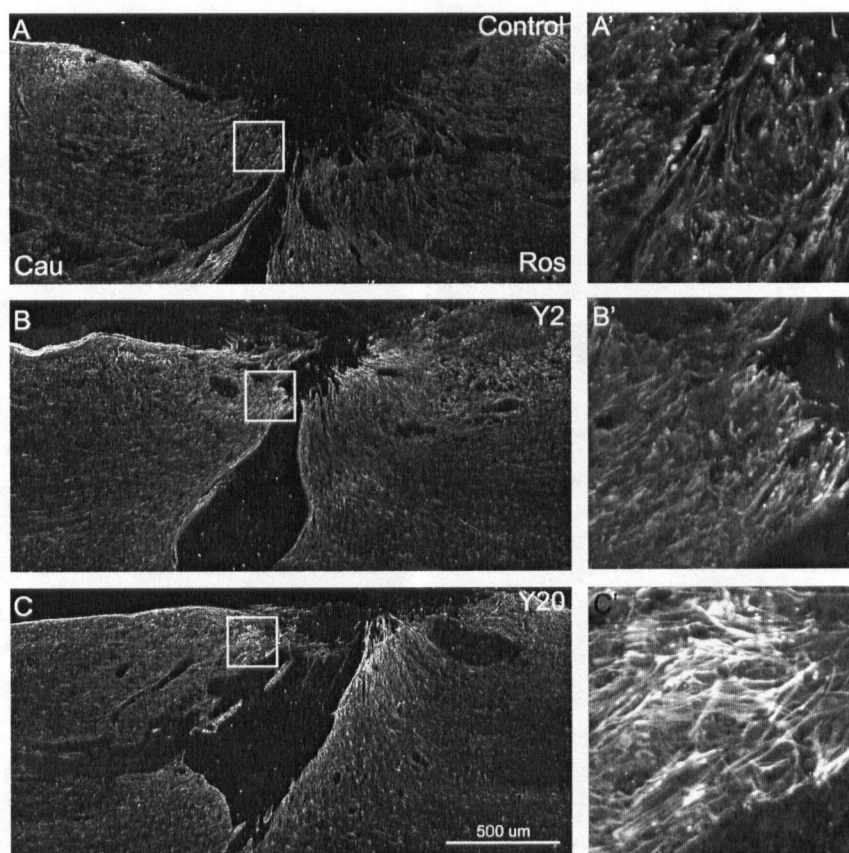
A Control
Cau Ros
A'

B Y2
B'

C Y20
C'
500 um

D

Figure 4.3

Y27632-treated animals had enhanced upregulation of neurocan expression. Parasagittal spinal cord sections from control (A, A'), low dose Y27632-treated (B, B'), and high dose-treated (C, C') rats immunostained with the 1F6 monoclonal anti-neurocan antibody. Pictures on the right are higher magnification of the boxed areas on the left. (D) The upregulation of neurocan along the lesion edge was significantly higher in Y27632-treated animals. **, $p < 0.001$.
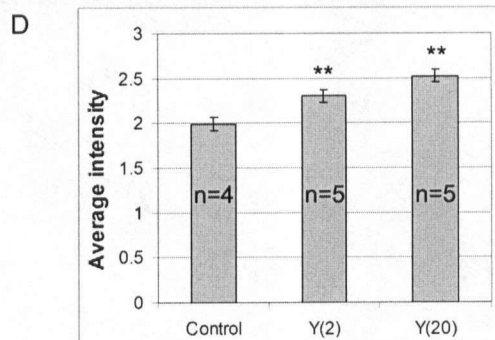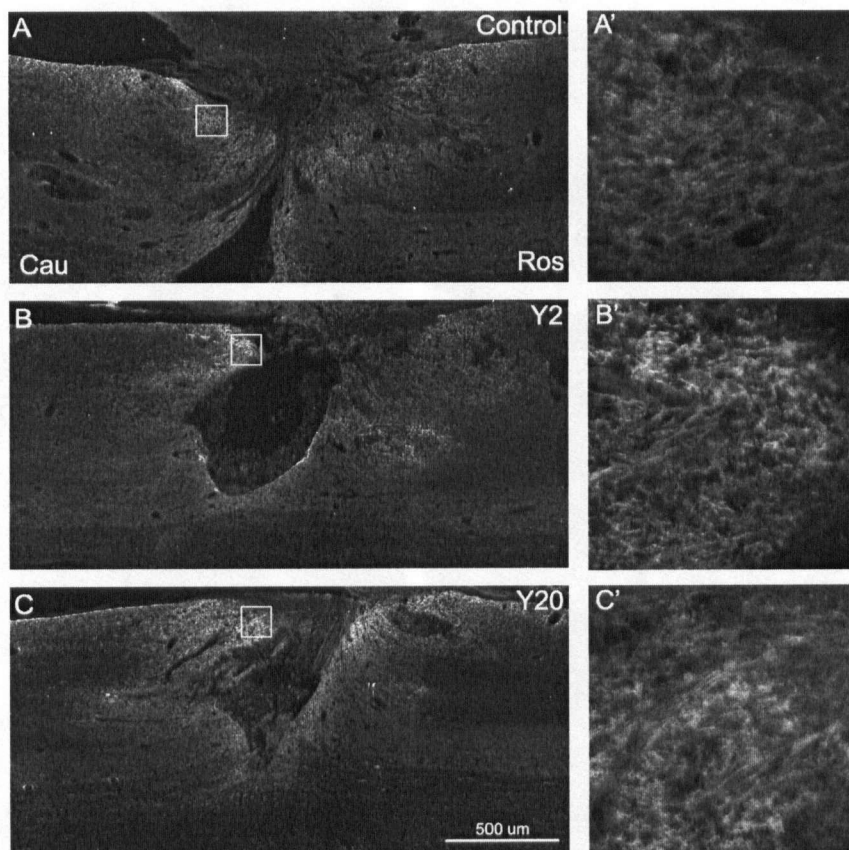
Figure 4.4

Y27632 induced astrocyte stellation *in vitro*. Astrocytes were obtained from P2/3 rat cortices, and immunostained with anti-GFAP antibodies. (A) Most of the control, untreated astrocytes were flattened and polygonal. (B-F) Addition of Y27632 induced astrocyte stellation and condensation of GFAP immunoreactivity. Increasing concentrations (1 to 50μM) of Y27632 appeared to result in progressively enhanced stellation up to 25 μM (E), at which maximal stellation occurred. Increasing Y27632 concentration to 50 μM (F) did not appear to result in any higher degree of stellation. (G) Western blots using cell lysates from control and Y27632-treated astrocytes (24hr treatment) showed that both treated and untreated astrocytes expressed a major GFAP band at 50kDa.
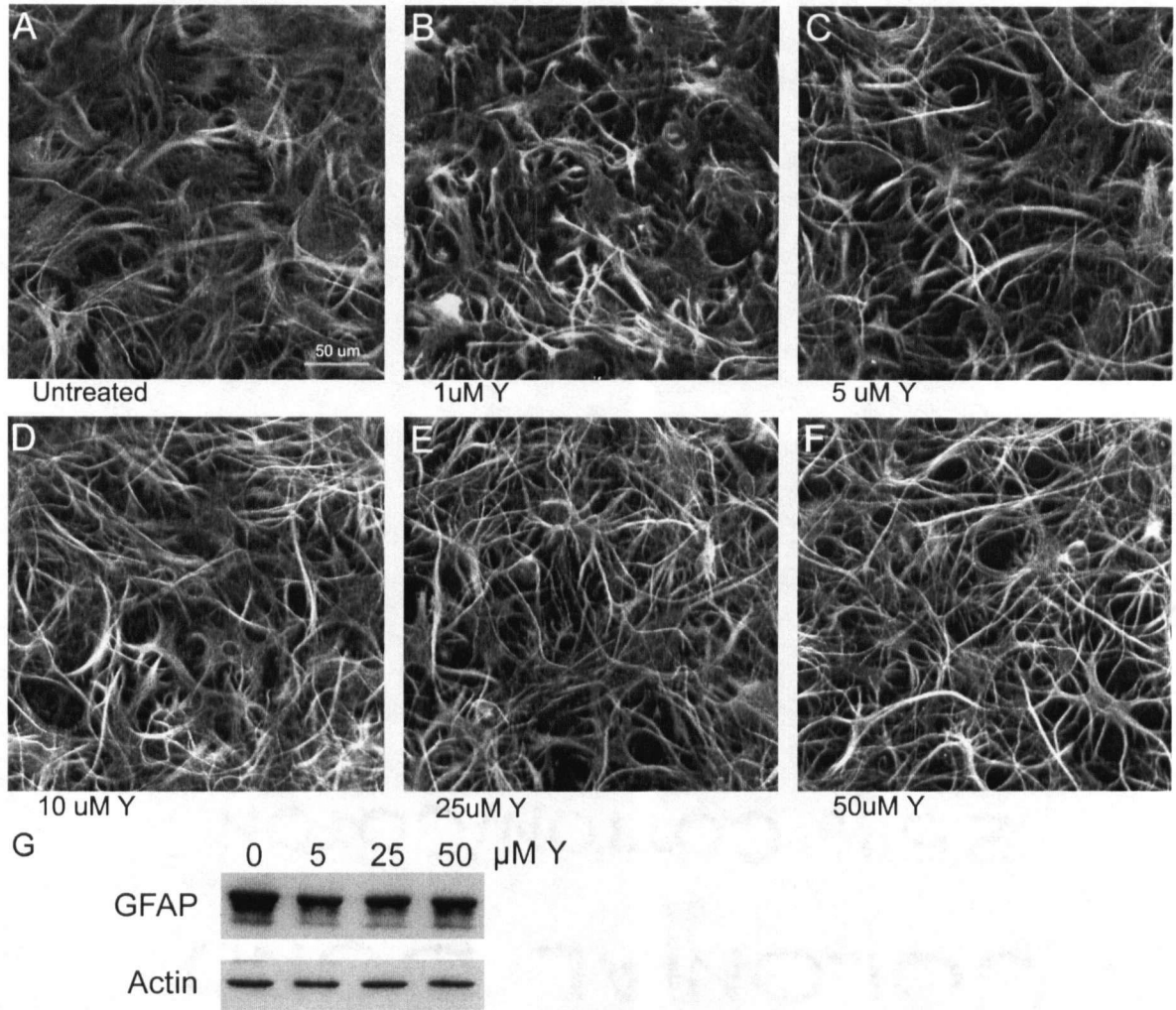
A — Untreated

B — 1uM Y

C — 5 uM Y

D — 10 uM Y

E — 25uM Y

F — 50uM Y

G

0   5   25   50   μM Y

GFAP

Actin

50 um

Figure 4.5

The expression of fibronectin (A,B) and laminin (C,D) by untreated (A,C) and Y27632-treated (B,D) astrocytes. In B and D, cells were treated with 25 μM Y27632 for 24-hr. (E) Quantification of immunoreactivities showed that the expression of laminin by Y27632-treated astrocytes was significantly higher. *, *p<0.005.*

untreated   25µM Y
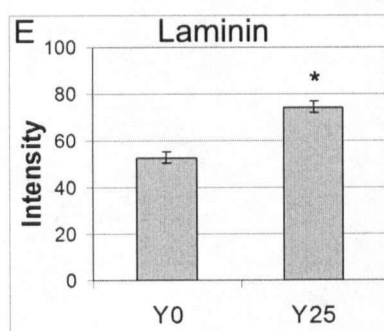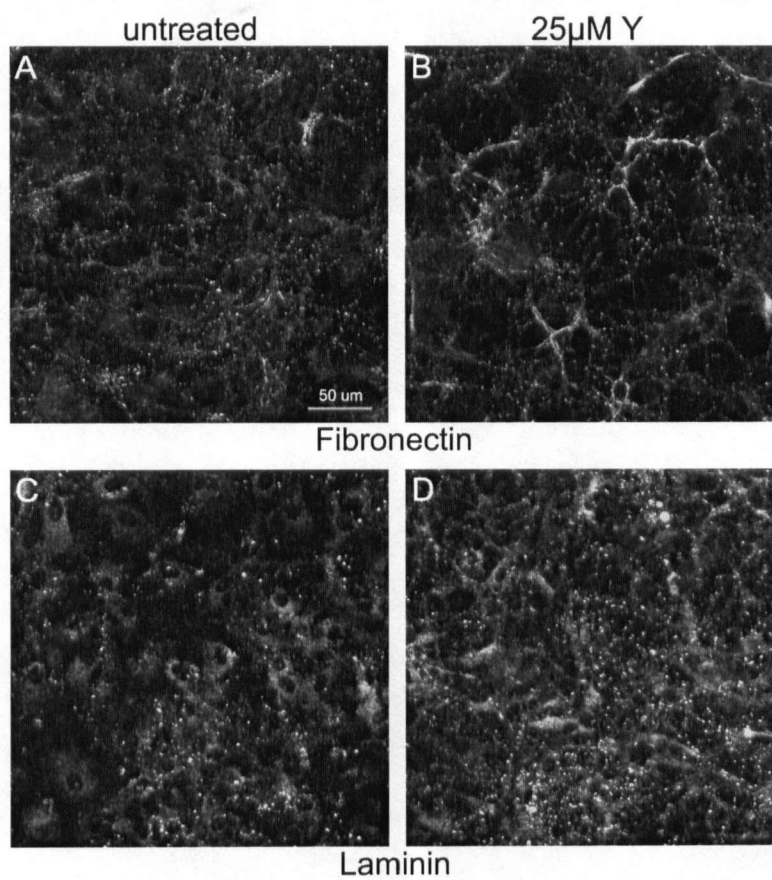
Fibronectin

Laminin

Figure 4.6

Y27632 treatment dramatically altered CSPG expression. (A) In unstimulated astrocyte cultures, CSPG expression (immunostained with the CS56 antibodies) was mainly found in the ECM, and hardly any CSPG was found associated with the cells. (B) In astrocyte cultures treated with 25μM Y27632 for 24 hours, CSPG expression was increased, and was found both in the ECM and associated with the cells. (C) Quantification of CSPG immunoreactivities showed a significant increase in expression by Y27632-treated astrocytes. (D) Western blot was performed using cell lysates treated with ChABC prior to loading onto the SDS-polyacrylamide gels. The 1F6 antibody for neurocan was used in western blots. Two bands at approximately 245 and 130 kDa were detected, corresponding to full length and cleaved neurocan (neurocan-N) respectively. (E) Treated astrocytes displayed increases in the expression of the 245 and 130 kDa bands. Data were collected from 3 separate western analyses. *, $p<0.005$.
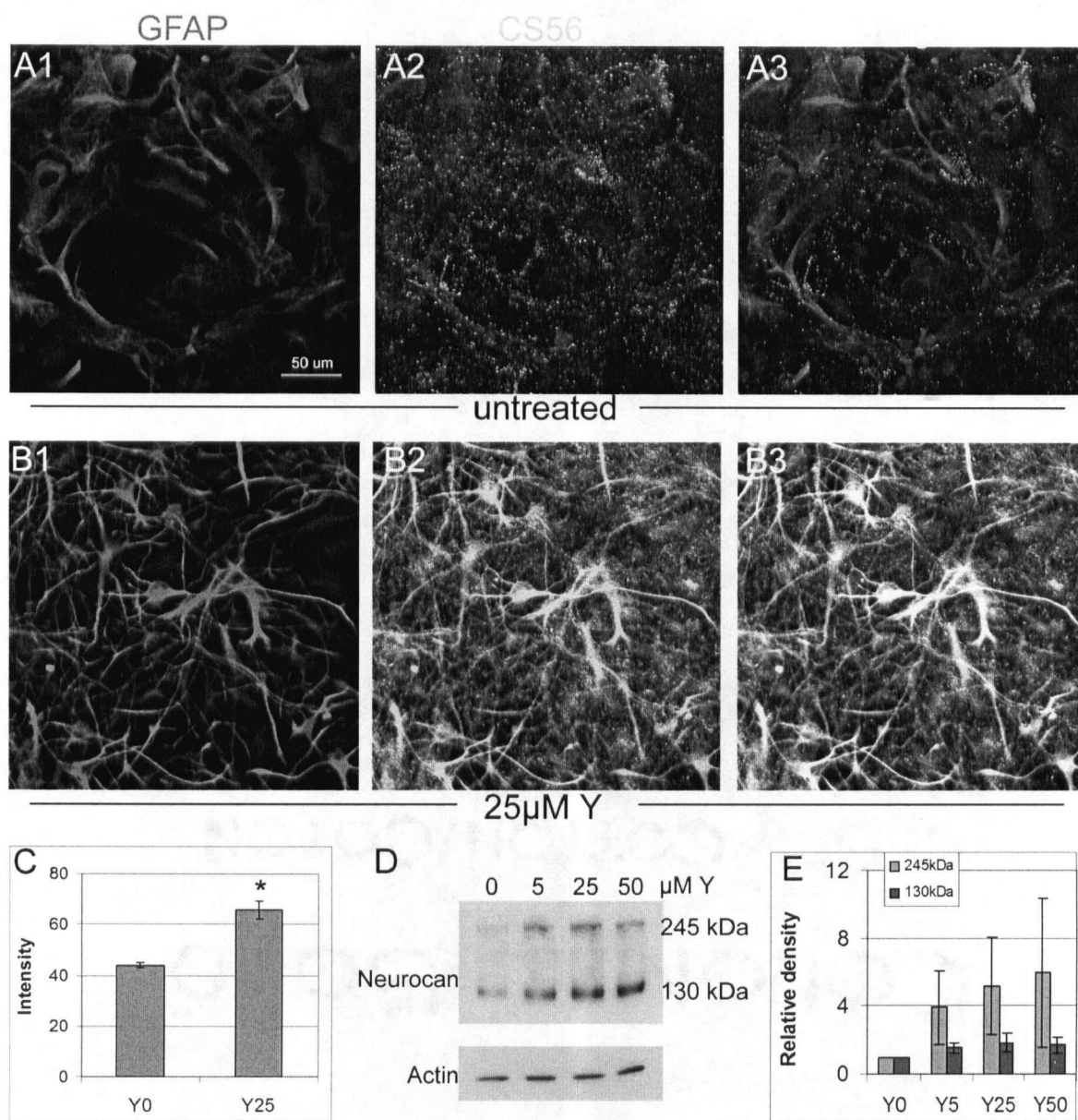
GFAP   CS56

A1   A2   A3

—————————— untreated ——————————

B1   B2   B3

—————————— 25µM Y ——————————

C   D   E

Intensity

Y0   Y25

Neurocan   Actin

0 5 25 50 µM Y

245 kDa
130 kDa

Relative density

245kDa
130kDa

Y0 Y5 Y25 Y50

Figure 4.7.

Neuron-astrocyte cocultures. After cortical neurons (from P5/6 rat pups) were seeded onto the astrocyte monolayer, they were incubated overnight before fixing in 4% formalin. Neurites were identified by immunostaining for βIII-tubulin. Neurite lengths were normalized to the average neurite length on untreated (Y0) astrocytes. (A-C) When the ROCK inhibitor was added at the same time as the cortical neurons are seeded onto the astrocyte monolayer, there was no difference in neurite length compared to growth on untreated astrocytes, i.e. neurite growth was equally robust on these cells. (D-F) Astrocytes pre-treated with 25μM Y27632 were inhibitory to neurite growth. The astrocytes were incubated with various concentrations of Y27632 for 24 hours. On the next day, the astrocytes were washed with PBS, and medium was exchanged with no Y27632 present when the neurons were seeded. At least 350 neurons from 3 independent experiments were included in the quantification. *, $p<0.01$; *Scale bar, 50μm.*

Y0   Y50

A   B
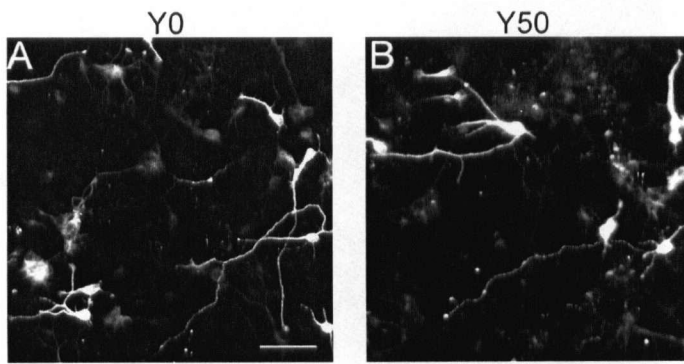
Y added at the same time as neurons

C
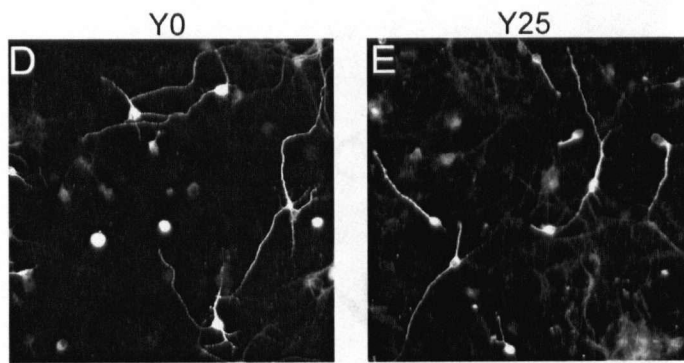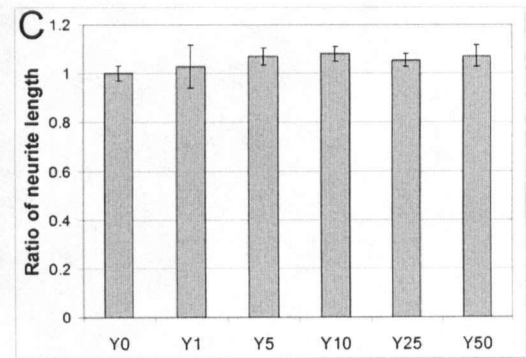
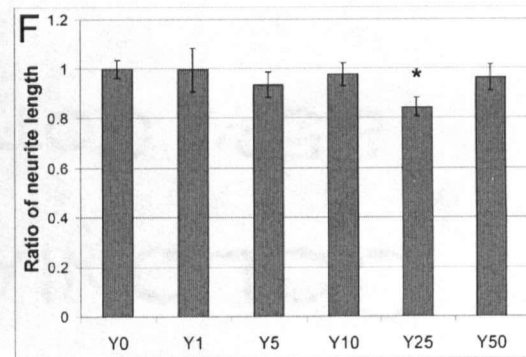Neurons added 1 day later than Y

Y0   Y25

D   E

F

Figure 4.8

Neurite growth from cortical neurons on astrocyte ECM. The astrocytes were lysed with sterile water and 0.2% triton after 24hr treatment with Y27632. The ECM was left behind on the PDL-treated glass slides, and cortical neurons were grown on these slides. (A-C) ECM produced by Y27632-treated astrocytes, at all concentrations tested (Y1 to Y50), was inhibitory to neurite growth compared to ECM produced by untreated astrocytes. (D,E) Neurite growth on ChABC-digested astrocyte ECM. (F) Neurite length on ChABC-digested ECM derived from untreated or Y27632-treated astrocytes (dark bars) was longer than that on control ECM (derived from untreated astrocytes, and not ChABC-digested; 'ratio of neurite length' = 1). For ECM produced by Y27632-treated astrocytes (Y25), ChABC digestion resulted in neurite lengths that were similar to that on ECM derived from untreated astrocytes (Y0), indicating that the growth-inhibitory effects of the ECM were mediated by carbohydrate side chains from CSPGs. At least 350 neurons from 3 independent experiments were included in the quantification. *, $p<0.01$ compared to neurite length on control ECM. Scale bar, $50\mu m$.
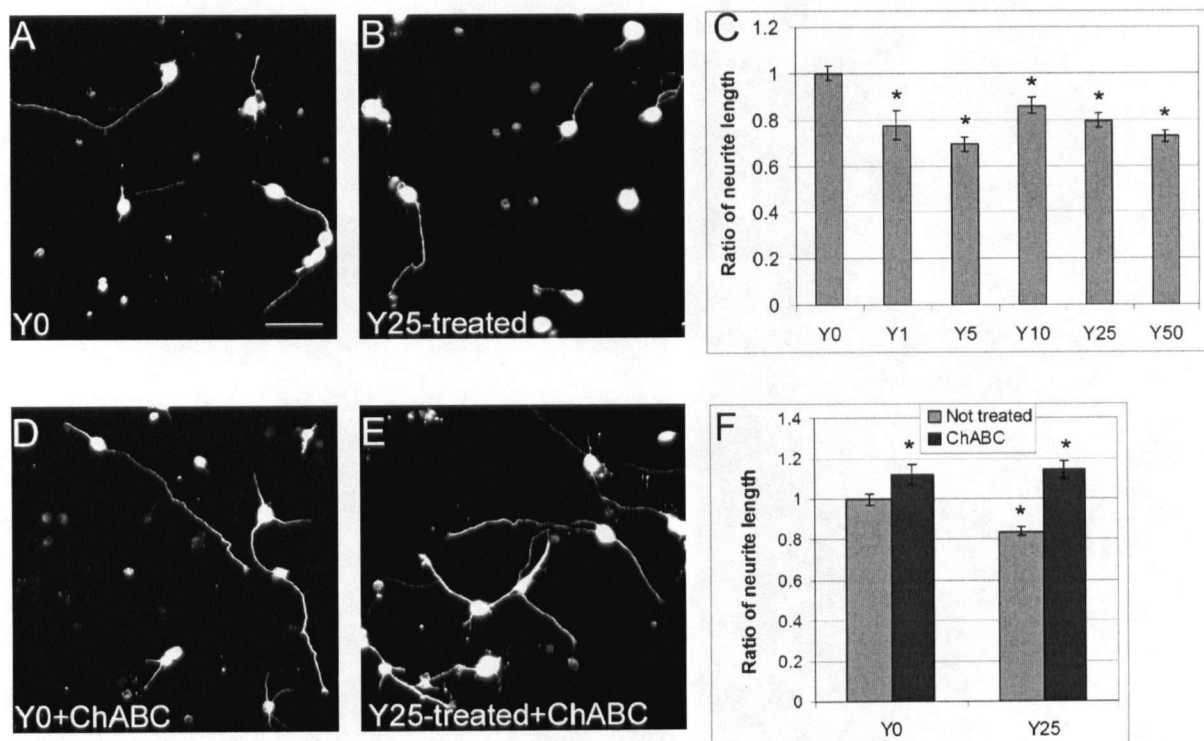
Figure 4.9

Neurite growth from cortical neurons in astrocyte-CM. Cortical neurons were grown on PDL-treated glass slides in medium conditioned by untreated (A,D) or Y27632-treated astrocytes (B,E). For the latter, astrocytes were treated with 25μM Y27632 for 24hr, and this medium was collected to be used in neuronal cultures. (A-C) Neurite length was longer in Y27632-treated astrocyte-CM (Y1 to Y50). (D,E) Astrocyte-CM was incubated with ChABC, which was heat inactivated 2 hours later, before growing the neurons in this CM. ChABC digestion of CM from untreated astrocytes (Y0) almost doubled neurite length, indicating that CSPGs in the astrocyte-CM were inhibiting neurite growth. CM from Y27632-treated astrocytes (Y25) did not show any further increase in neurite length after ChABC digestion. (G) Western blot of the astrocyte CM showed a decrease in the amount of the 130 kDa neurocan (neurocan-N) with Y27632 treatment. *, P<0.001 compared to neurite length in undigested CM produced by untreated astrocytes. Scale bar, 50μm.
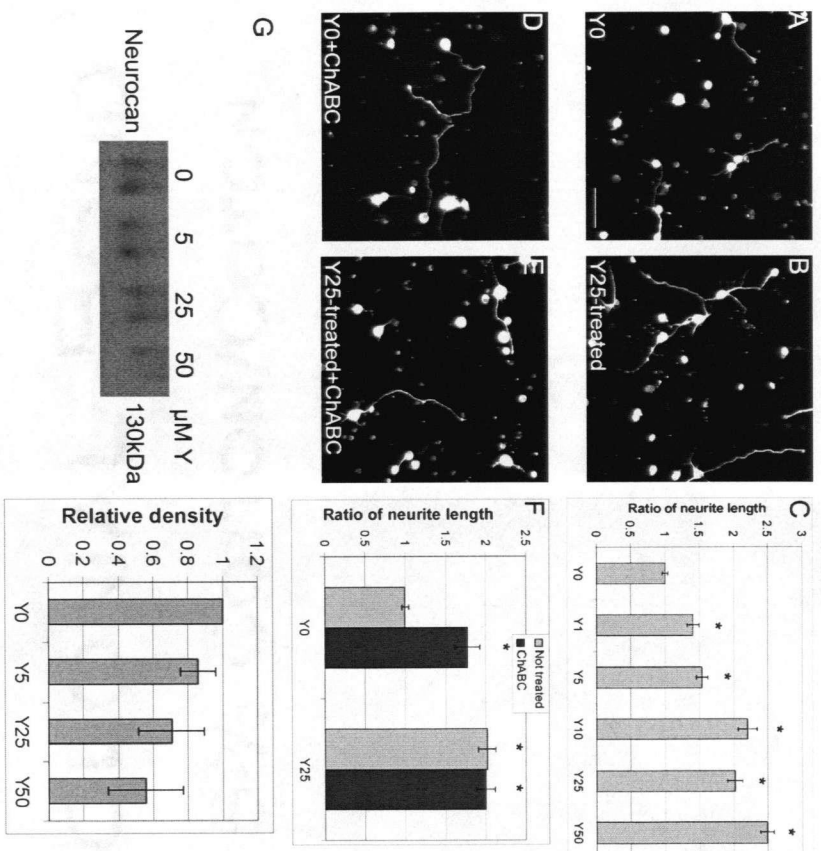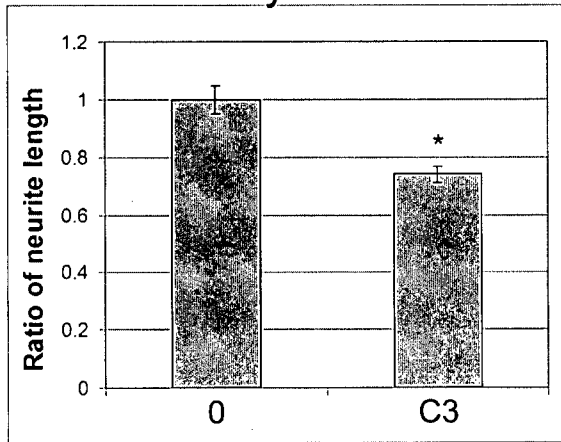
Figure 4.10

C3 treatment of the astrocytes mimicked the effects of Y27632. (A) ECM produced by C3-treated astrocytes inhibited neurite growth from cortical neurons. (B) Neurite length in C3-treated astrocyte-CM was longer than in untreated astrocyte-CM. *, $p<0.001$.

Astrocyte ECM

Astrocyte CM
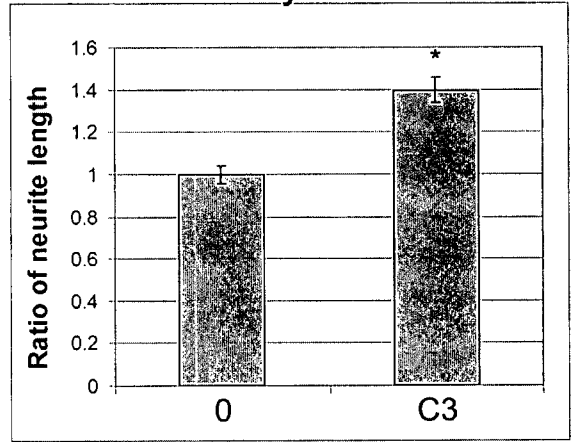
Figure 4.11

Proposed model of Y27632 effects on CSPG (neurocan) processing *in vitro*. (A) Astrocytes produce CSPGs, such as neurocan, and MMPs. Most of the CSPGs are incorporated into the ECM rather than expressed on the astrocytes themselves. MMPs digest CSPGs, and in the case of neurocan, digestion results in the N- and C-terminal fragments being released into the medium or incorporated into the ECM. (B) ROCK inhibition with Y27632 activates astrocytes, and at the same time decreases the activities of MMPs. The CSPGs stay intact, and they remain in the ECM or become associated with the astrocytes. Therefore, there is a net increase in the amount of CSPGs in the ECM, but a net decrease in the medium.
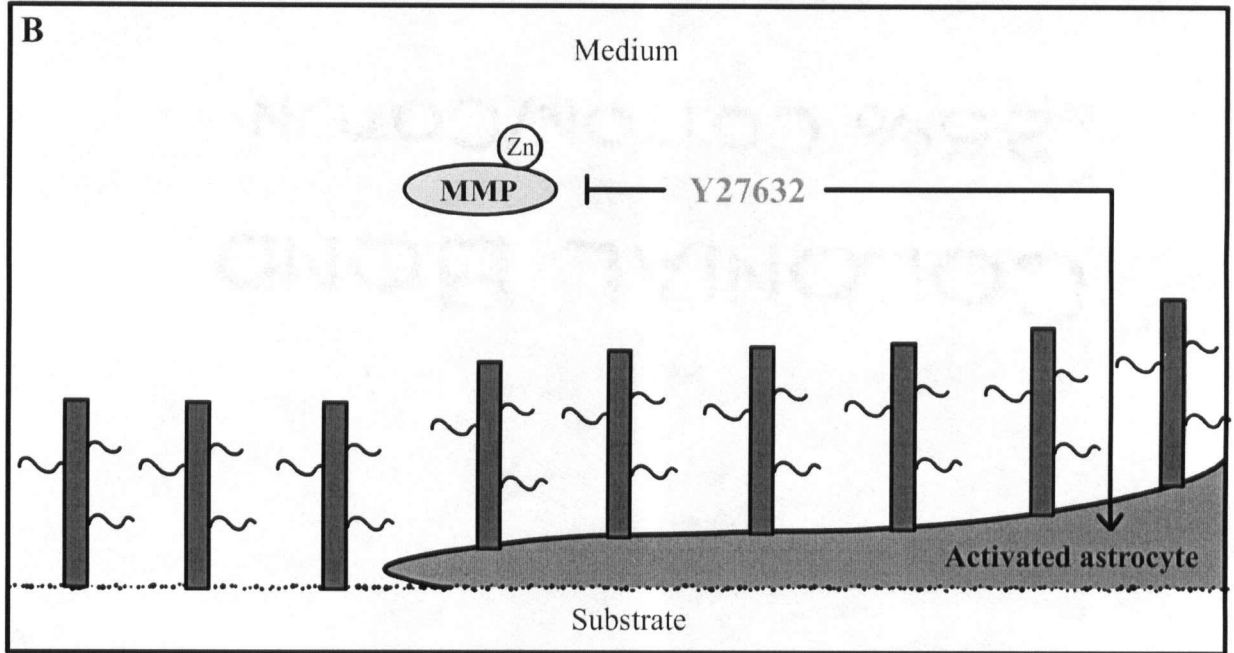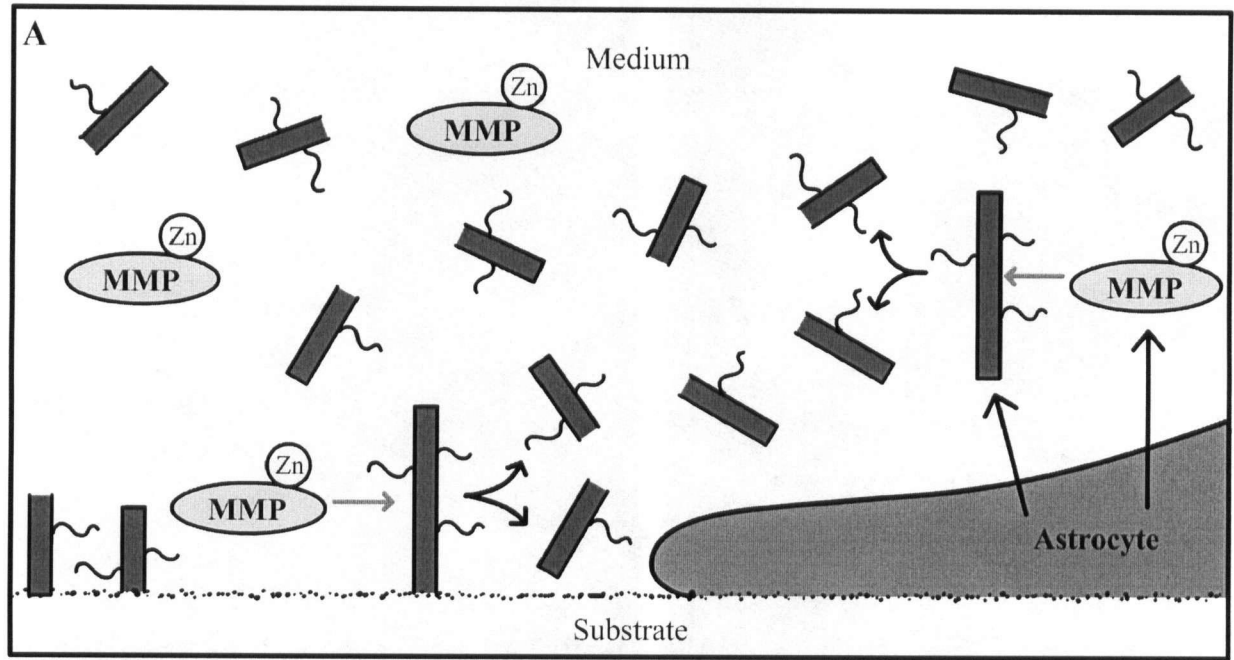
Neurocan

MMP digestion

References

Abe K, Misawa M (2003) Astrocyte stellation induced by Rho kinase inhibitors in culture. Brain Res Dev Brain Res 143:99-104.

Ahmed Z, Dent RG, Leadbeater WE, Smith C, Berry M, Logan A (2005) Matrix metalloproteases: degradation of the inhibitory environment of the transected optic nerve and the scar by regenerating axons. Mol Cell Neurosci 28:64-78.

Amano M, Ito M, Kimura K, Fukata Y, Chihara K, Nakano T, Matsuura Y, Kaibuchi K (1996) Phosphorylation and activation of myosin by Rho-associated kinase (Rho- kinase). J Biol Chem 271:20246-20249.

Asher RA, Morgenstern DA, Fidler PS, Adcock KH, Oohira A, Braistead JE, Levine JM, Margolis RU, Rogers JH, Fawcett JW (2000) Neurocan is upregulated in injured brain and in cytokine-treated astrocytes. J Neurosci 20:2427-2438.

Asher RA, Morgenstern DA, Properzi F, Nishiyama A, Levine JM, Fawcett JW (2005) Two separate metalloproteinase activities are responsible for the shedding and processing of the NG2 proteoglycan in vitro. Mol Cell Neurosci 29:82-96.

Avalos AM, Arthur WT, Schneider P, Quest AF, Burridge K, Leyton L (2004) Aggregation of integrins and RhoA activation are required for Thy-1-induced morphological changes in astrocytes. J Biol Chem 279:39139-39145.

Banerji A, Chakraborti J, Mitra A, Chatterjee A (2005) Cell membrane-associated MT1-MMP-dependent activation of pro-MMP-2 in A375 melanoma cells. J Environ Pathol Toxicol Oncol 24:3-17.

Bartolome RA, Molina-Ortiz I, Samaniego R, Sanchez-Mateos P, Bustelo XR, Teixido J (2006) Activation of Vav/Rho GTPase signaling by CXCL12 controls membrane-type matrix metalloproteinase-dependent melanoma cell invasion. Cancer Res 66:248-258.

Bignami A, Eng LF, Dahl D, Uyeda CT (1972) Localization of the glial fibrillary acidic protein in astrocytes by immunofluorescence. Brain Res 43:429-435.

Borisoff JF, Chan CC, Hiebert GW, Oschipok L, Robertson GS, Zamboni R, Steeves JD, Tetzlaff W (2003) Suppression of Rho-kinase activity promotes axonal growth on inhibitory CNS substrates. Mol Cell Neurosci 22:405-416.

Bradbury EJ, Moon LD, Popat RJ, King VR, Bennett GS, Patel PN, Fawcett JW, McMahon SB (2002) Chondroitinase ABC promotes functional recovery after spinal cord injury. Nature 416:636-640.

Brewer GJ (1997a) Isolation and culture of adult rat hippocampal neurons. J Neurosci Methods 71:143-155.

Brewer GJ (1997b) Isolation and culture of adult rat hippocampal neurons. J Neurosci Methods 71:143-155.

Canning DR, Hoke A, Malemud CJ, Silver J (1996) A potent inhibitor of neurite outgrowth that predominates in the extracellular matrix of reactive astrocytes. Int J Dev Neurosci 14:153-175.

Chan CC, Khodarahmi K, Liu J, Sutherland D, Oschipok LW, Steeves JD, Tetzlaff W (2005) Dose-dependent beneficial and detrimental effects of ROCK inhibitor Y27632 on axonal sprouting and functional recovery after rat spinal cord injury. Exp Neurol 196:352-364.

Chen CJ, Liao SL, Huang YS, Chiang AN (2005) RhoA inactivation is crucial to manganese-induced astrocyte stellation. Biochem Biophys Res Commun 326:873-879.

Costa S, Planchenault T, Charriere-Bertrand C, Mouchel Y, Fages C, Juliano S, Lefrancois T, Barlovatz-Meimon G, Tardy M (2002) Astroglial permissivity for neuritic outgrowth in neuron-astrocyte cocultures depends on regulation of laminin bioavailability. Glia 37:105-113.

Davies SJ, Fitch MT, Memberg SP, Hall AK, Raisman G, Silver J (1997) Regeneration of adult axons in white matter tracts of the central nervous system. Nature 390:680-683.

Davies SP, Reddy H, Caivano M, Cohen P (2000) Specificity and mechanism of action of some commonly used protein kinase inhibitors. Biochem J 351:95-105.

Dergham P, Ellezam B, Essagian C, Avedissian H, Lubell WD, McKerracher L (2002) Rho signaling pathway targeted to promote spinal cord repair. J Neurosci 22:6570-6577.

Dillon ST, Feig LA (1995) Purification and assay of recombinant C3 transferase. Methods Enzymol 256:174-184.

Eng LF, Ghirnikar RS (1994) GFAP and astrogliosis. Brain Pathol 4:229-237.

Fawcett JW, Housden E, Smith-Thomas L, Meyer RL (1989) The growth of axons in three-dimensional astrocyte cultures. Dev Biol 135:449-458.

Feng J, Ito M, Ichikawa K, Isaka N, Nishikawa M, Hartshorne DJ, Nakano T (1999) Inhibitory phosphorylation site for Rho-associated kinase on smooth muscle myosin phosphatase. J Biol Chem 274:37385-37390.

Ferguson TA, Muir D (2000) MMP-2 and MMP-9 increase the neurite-promoting potential of schwann cell basal laminae and are upregulated in degenerated nerve. Mol Cell Neurosci 16:157-167.

Fitch MT, Doller C, Combs CK, Landreth GE, Silver J (1999) Cellular and molecular mechanisms of glial scarring and progressive cavitation: in vivo and in vitro analysis of inflammation-induced secondary injury after CNS trauma. J Neurosci 19:8182-8198.

Fournier AE, Takizawa BT, Strittmatter SM (2003) Rho kinase inhibition enhances axonal regeneration in the injured CNS. J Neurosci 23:1416-1423.

Giulian D, Woodward J, Young DG, Krebs JF, Lachman LB (1988) Interleukin-1 injected into mammalian brain stimulates astrogliosis and neovascularization. J Neurosci 8:2485-2490.

Hatten ME (1985) Neuronal regulation of astroglial morphology and proliferation in vitro. J Cell Biol 100:384-396.

Herx LM, Yong VW (2001) Interleukin-1 beta is required for the early evolution of reactive astrogliosis following CNS lesion. J Neuropathol Exp Neurol 60:961-971.

Hsu JY, Stein SA, Xu XM (2005) Temporal and spatial distribution of growth-associated molecules and astroglial cells in the rat corticospinal tract during development. J Neurosci Res 80:330-340.

Jalink K, van Corven EJ, Hengeveld T, Morii N, Narumiya S, Moolenaar WH (1994) Inhibition of lysophosphatidate- and thrombin-induced neurite retraction and neuronal cell rounding by ADP ribosylation of the small GTP-binding protein Rho. J Cell Biol 126:801-810.

John GR, Chen L, Rivieccio MA, Melendez-Vasquez CV, Hartley A, Brosnan CF (2004) Interleukin-1beta induces a reactive astroglial phenotype via deactivation of the Rho GTPase-Rock axis. J Neurosci 24:2837-2845.

Jones LL, Margolis RU, Tuszynski MH (2003) The chondroitin sulfate proteoglycans neurocan, brevican, phosphacan, and versican are differentially regulated following spinal cord injury. Exp Neurol 182:399-411.

Joosten EA, Gribnau AA (1989) Astrocytes and guidance of outgrowing corticospinal tract axons in the rat. An immunocytochemical study using anti-vimentin and anti-glial fibrillary acidic protein. Neuroscience 31:439-452.

Kalman D, Gomperts SN, Hardy S, Kitamura M, Bishop JM (1999) Ras family GTPases control growth of astrocyte processes. Mol Biol Cell 10:1665-1683.

Lefrancois T, Fages C, Peschanski M, Tardy M (1997) Neuritic outgrowth associated with astroglial phenotypic changes induced by antisense glial fibrillary acidic protein (GFAP) mRNA in injured neuron-astrocyte cocultures. J Neurosci 17:4121-4128.

Lehmann M, Fournier A, Selles-Navarro I, Dergham P, Sebok A, Leclerc N, Tigyi G, McKerracher L (1999) Inactivation of Rho signaling pathway promotes CNS axon regeneration. J Neurosci 19:7537-7547.

Liesi P, Dahl D, Vaheri A (1983) Laminin is produced by early rat astrocytes in primary culture. J Cell Biol 96:920-924.

Liesi P, Kirkwood T, Vaheri A (1986) Fibronectin is expressed by astrocytes cultured from embryonic and early postnatal rat brain. Exp Cell Res 163:175-185.

Liuzzi FJ, Lasek RJ (1987) Astrocytes block axonal regeneration in mammals by activating the physiological stop pathway. Science 237:642-645.

Manning TJ, Jr., Rosenfeld SS, Sontheimer H (1998) Lysophosphatidic acid stimulates actomyosin contraction in astrocytes. J Neurosci Res 53:343-352.

McCarthy KD, de Vellis J (1980) Preparation of separate astroglial and oligodendroglial cell cultures from rat cerebral tissue. J Cell Biol 85:890-902.

McGraw J, Hiebert GW, Steeves JD (2001) Modulating astrogliosis after neurotrauma. J Neurosci Res 63:109-115.

McKeon RJ, Jurynec MJ, Buck CR (1999) The chondroitin sulfate proteoglycans neurocan and phosphacan are expressed by reactive astrocytes in the chronic CNS glial scar. J Neurosci 19:10778-10788.

McKeon RJ, Schreiber RC, Rudge JS, Silver J (1991) Reduction of neurite outgrowth in a model of glial scarring following CNS injury is correlated with the expression of inhibitory molecules on reactive astrocytes. J Neurosci 11:3398-3411.

Meyer-Puttlitz B, Milev P, Junker E, Zimmer I, Margolis RU, Margolis RK (1995) Chondroitin sulfate and chondroitin/keratan sulfate proteoglycans of nervous tissue: developmental changes of neurocan and phosphacan. J Neurochem 65:2327-2337.

Monnier PP, Sierra A, Schwab JM, Henke-Fahle S, Mueller BK (2003) The Rho/ROCK pathway mediates neurite growth-inhibitory activity associated with the chondroitin sulfate proteoglycans of the CNS glial scar. Mol Cell Neurosci 22:319-330.

Niederost B, Oertle T, Fritsche J, McKinney RA, Bandtlow CE (2002) Nogo-A and myelin-associated glycoprotein mediate neurite growth inhibition by antagonistic regulation of RhoA and Rac1. J Neurosci 22:10368-10376.

Okada Y, Morodomi T, Enghild JJ, Suzuki K, Yasui A, Nakanishi I, Salvesen G, Nagase H (1990) Matrix metalloproteinase 2 from human rheumatoid synovial fibroblasts. Purification and activation of the precursor and enzymic properties. Eur J Biochem 194:721-730.

Oohira A, Matsui F, Watanabe E, Kushima Y, Maeda N (1994) Developmentally regulated expression of a brain specific species of chondroitin sulfate proteoglycan, neurocan, identified with a monoclonal antibody IG2 in the rat cerebrum. Neuroscience 60:145-157.

Pagenstecher A, Stalder AK, Kincaid CL, Shapiro SD, Campbell IL (1998) Differential expression of matrix metalloproteinase and tissue inhibitor of matrix metalloproteinase genes in the mouse central nervous system in normal and inflammatory states. Am J Pathol 152:729-741.

Pekny M, Nilsson M (2005) Astrocyte activation and reactive gliosis. Glia 50:427-434.

Price J, Hynes RO (1985) Astrocytes in culture synthesize and secrete a variant form of fibronectin. J Neurosci 5:2205-2211.

Ramakers GJ, Moolenaar WH (1998) Regulation of astrocyte morphology by RhoA and lysophosphatidic acid. Exp Cell Res 245:252-262.

Rathke-Hartlieb S, Budde P, Ewert S, Schlomann U, Staege MS, Jockusch H, Bartsch JW, Frey J (2000) Elevated expression of membrane type 1 metalloproteinase (MT1-MMP) in reactive astrocytes following neurodegeneration in mouse central nervous system. FEBS Lett 481:227-234.

Rudge JS, Silver J (1990) Inhibition of neurite outgrowth on astroglial scars in vitro. J Neurosci 10:3594-3603.

Sango K, Oohira A, Ajiki K, Tokashiki A, Horie M, Kawano H (2003) Phosphacan and neurocan are repulsive substrata for adhesion and neurite extension of adult rat dorsal root ganglion neurons in vitro. Exp Neurol 182:1-11.

Shain W, Forman DS, Madelian V, Turner JN (1987) Morphology of astroglial cells is controlled by beta-adrenergic receptors. J Cell Biol 105:2307-2314.

Sivasankaran R, Pei J, Wang KC, Zhang YP, Shields CB, Xu XM, He Z (2004) PKC mediates inhibitory effects of myelin and chondroitin sulfate proteoglycans on axonal regeneration. Nat Neurosci 7:261-268.

Smith GM, Miller RH, Silver J (1986) Changing role of forebrain astrocytes during development, regenerative failure, and induced regeneration upon transplantation. J Comp Neurol 251:23-43.

Smith-Thomas LC, Fok-Seang J, Stevens J, Du JS, Muir E, Faissner A, Geller HM, Rogers JH, Fawcett JW (1994) An inhibitor of neurite outgrowth produced by astrocytes. J Cell Sci 107 (Pt 6):1687-1695.

Steindler DA, O'Brien TF, Cooper NG (1988) Glycoconjugate boundaries during early postnatal development of the neostriatal mosaic. J Comp Neurol 267:357-369.

Tang X, Davies JE, Davies SJ (2003) Changes in distribution, cell associations, and protein expression levels of NG2, neurocan, phosphacan, brevican, versican V2, and tenascin-C during acute to chronic maturation of spinal cord scar tissue. J Neurosci Res 71:427-444.

Turk BE, Huang LL, Piro ET, Cantley LC (2001) Determination of protease cleavage site motifs using mixture-based oriented peptide libraries. Nat Biotechnol 19:661-667.

Turner NA, O'Regan DJ, Ball SG, Porter KE (2005) Simvastatin inhibits MMP-9 secretion from human saphenous vein smooth muscle cells by inhibiting the RhoA/ROCK pathway and reducing MMP-9 mRNA levels. FASEB J 19:804-806.

Uehata M, Ishizaki T, Satoh H, Ono T, Kawahara T, Morishita T, Tamakawa H, Yamagami K, Inui J, Maekawa M, Narumiya S (1997) Calcium sensitization of smooth muscle mediated by a Rho-associated protein kinase in hypertension. Nature 389:990-994.

Zuo J, Ferguson TA, Hernandez YJ, Stetler-Stevenson WG, Muir D (1998) Neuronal matrix metalloproteinase-2 degrades and inactivates a neurite-inhibiting chondroitin sulfate proteoglycan. J Neurosci 18:5203-5211.

Chapter 5: Discussion

Major conclusions

In chapter 2, the inhibition of neurite growth due to aggrecan components including aggrecan aggregate, aggrecan monomer, chondroitin sulfate, hyaluronic acid, and ChABC-treated aggrecan was analyzed *in vitro*. Aggrecan aggregate, aggrecan monomer, and hyaluronic acid inhibited neurite growth from NGF- and NT3-responsive chick DRG neurons. Aggrecan inhibition is dependent on its chondroitin sulfate glycosaminoglycan side chains, but the chondroitin sulfate by itself did not reduce neurite growth. On aggrecan aggregate, hyaluronic acid, and ChABC-treated aggrecan, GC sizes were diminished, suggestive of partial or total GC collapse. ROCK inhibition with Y27632 increased neurite growth on some, but not all of the aggrecan components tested, suggesting that not all aggrecan components activated the Rho/ROCK pathway.

In chapter 3, a dorsal column transection model in rats was used to analyze the efficacy of Y27632 in stimulating axonal regeneration *in vivo*. Acute treatment with the ROCK inhibitor Y27632 stimulated sprouting of CST and DCT axons, and accelerated functional recovery/compensation. However, low doses of ROCK inhibition appeared to be detrimental, as low dose-treated animals had decreased axonal regrowth and impaired functional recovery compared to control (untreated) rats.

In chapter 4, *in vivo* spinal cord tissue and *in vitro* astrocyte cultures were used to test if Y27632 treatment increased axonal growth inhibition by astrocytes. *In vivo*, Y27632 treatment enhanced the upregulation of GFAP and neurocan after SCI. *In vitro*, there was an increase in CSPG levels in the ECM produced by Y27632-treated astrocytes, on which neurite growth from cortical neurons was inhibited. Such decrease in neurite growth was reversed with ChABC digestion of the Y27632 astrocyte-derived ECM, showing that chondroitin sulfate side chains on the CSPGs were responsible for the inhibition. The increase in the expression of inhibitory molecules in the ECM explained, at least partially, why Y27632 treatment caused detrimental side effects in the rat model of SCI (chapter 3).

Growth inhibition due to aggrecan

With the many studies characterizing CSPG signaling, the mechanisms of CSPG inhibition on neurite growth are still not fully understood. Not only can these proteoglycans

activate specific receptors in neurons and result in typical ligand-receptor interactions (Dou and Levine, 1997;Schweigreiter et al., 2004), they can also bind to and alter the signaling of other ECM or cell adhesion molecules (Aspberg et al., 1995;Aspberg et al., 1997;Friedlander et al., 1994;Grumet et al., 1993). In chapter 2, the effects of aggrecan and its components on neurite growth was analysed in the absence of other molecules with which it may interact. In agreement with the initial hypothesis, both the chondroitin sulfate glycosaminoglycan side chains and core protein are important for aggrecan inhibition on neurite growth. When the core protein (ChABC-digested aggrecan) or chondroitin sulfate was present on its own in the substrate, no decrease in DRG outgrowth was observed. At present no receptor for aggrecan has been identified, nonetheless, indirect evidence suggested the existence of such a receptor. Embryonic chick DRG neurons can adapt to the inhibition due to aggrecan if laminin is also present in the substrate (Snow et al., 1990;Snow and Letourneau, 1992). Such adaptation was accomplished by an upregulation of integrin receptors for laminin (Condic et al., 1999), resulting in increased neuronal adhesion and neurite extension on aggrecan. Therefore, aggrecan may interact with a cell surface receptor, which initiates a signaling cascade that inhibits neurite growth and increases gene expression for integrin.

CSPGs also interact with trophic factors via their glycosaminoglycan side chains, and may either present them to or sequester them away from their receptors. Chondroitin sulfate binds to epidermal growth factor (EGF) and fibroblast growth factor (Deepa et al., 2002;Bao et al., 2004). Glycosaminoglycans including chondroitin sulfate and heparin sulfate in culture medium potentiated NGF-induced neurite growth (Damon et al., 1988). Since NGF or NT3 was present in the DRG cultures in chapter 2, it was possible that the aggrecan components affected neurite growth indirectly via the alteration of trophic factor signaling. This could explain why Y27632 treatment differentially affected neurite growth on hyaluronic acid (promoted growth of NT3-responsive neurites but not of NGF-responsive ones). To eliminate the effects due to trophic factors, the experiments can be repeated using cortical neurons or adult DRG neurons, which are not dependent on trophic factor for survival or neurite extension.

Unexpectedly, ROCK suppression with Y27632 did not increase NGF-neurite outgrowth on hyaluronic acid. I speculated that this was due to the need of ROCK activity in NGF growth cones for forming stable point contacts (as covered in the discussion of chapter 2). It would be interesting to pursue this finding. As a start, the C3 exoenzyme can be used to specifically inhibit

Rho in DRG neurons and ascertain that the Rho pathway is involved. Active Rho pull-down assays can be performed to determine if hyaluronic acid activates the Rho/ROCK pathway. In addition, DRG neurons can be cultured on a substrate that contains both hyaluronic acid and another molecule that promote focal adhesion formation. One candidate is laminin, which is highly stimulatory to neurite growth (Manthorpe et al., 1983). Neurite outgrowth in the presence or absence of Y27632 can be compared on this substrate to determine whether ROCK inhibition reverses the decrease in outgrowth on hyaluronic acid. One caveat is that laminin may affect neurite growth via the deactivation of Rho (Brouns et al., 2001), but there is also evidence that neurite growth on laminin is dependent on Cdc42 rather than Rho (Weston et al., 2000)

There appeared to be differences in signaling within NGF- versus NT3-responsive DRG neurites, as Y27632 treatment increased NT3-dependent neurite growth on hyaluronic acid but not NGF-dependent growth on the same substrate. On ChABC-digested aggrecan, NGF-responsive neurite growth was stimulated by Y27632, but there was no stimulation of NT3-dependent growth. Again, whether these aggrecan components differentially activate Rho in the different DRG neurons can be tested by performing Rho-GTP pull-down assays. Their signaling can be further probed with inhibitors of common intracellular second messenger systems such as the PKA and PKC pathways.

ROCK inhibition and axonal regeneration

In chapter 3, *in vivo* application of the Y27632 ROCK inhibitor stimulated local sprouting of the DCT and CST, rather than long distance regeneration. As briefly mentioned in the discussion of chapter 3, the presence of inhibitory molecules that activate signaling pathways other than Rho/ROCK may explain the limited regenerative response. A plethora of known inhibitors has been found and characterized in the SCI area, and most of them signal through Rho. However, new inhibitors of axonal regeneration are still being identified, for example, repulsive guidance molecule (RGM) (Monnier et al., 2002;Rajagopalan et al., 2004), and Wnt (Lyuksyutova et al., 2003;Yoshikawa et al., 2003). The inhibitory signaling activated by these new molecules is not fully understood, and may or may not act through Rho.

Alternatively but not mutually exclusively, counteracting inhibitory signaling within the growth cone without stimulation of cell body response may be insufficient for long distance regeneration. The importance of cell body response is best demonstrated by the sensory system.

DRG neurons regenerate their central axon if the peripheral branches of their axons were previously injured (Richardson and Verge, 1986;Richardson and Issa, 1984), suggesting that peripheral injury induces a cell body reaction that increases regenerative competence. It is now known that peripheral injury stimulated the expression of regeneration associated genes in the DRG cell bodies (Broude et al., 1997;Schreyer and Skene, 1993).

Combinatorial treatments that provide a permissive substrate for regrowing axons and at the same time supply trophic support have produced better outcomes than when only one of these was available. For examples, when supplemented with acidic FGF (aFGF), intercostal nerves implanted into a gap formed by complete spinal cord transection at low thoracic level supported regrowth of CST axons into and across these nerve grafts (Cheng et al., 1996). Similarly, after a complete thoracic spinal cord transection, CST axons did not regrow into a Schwann cell graft alone, but they did when supplemented with aFGF and there was decreased CST axon dieback (Guest et al., 1997). The trophic factors could be retrogradely transported to cell bodies in the brain to augment the normally weak regenerative response of CST neurons. However, trophic factor could also have altered the interactions between host and graft tissues, and could act locally on glial cells which would affect gliosis and further trophic factor release (Guest et al., 1997). Our lab has shown that BDNF infusion into the vicinity of the motoneuron cell bodies in the cortex increased CST sprouting rostral to the lesion site where a pre-degenerated peripheral nerve was implanted (Hiebert et al., 2002). However, no CST axons were found within the graft. Nonetheless, BDNF proves to be an effective trophic factor for enhancing the growth propensity of CST axons (Giehl and Tetzlaff, 1996;Hiebert et al., 2002). In order to achieve a better regenerative response, I propose that Y27632 treatment should be combined with trophic factor infusion into the injured spinal cord. The most efficient way to deliver trophic support would be to infuse it directly into the brain where the cell bodies are, but unfortunately this would be difficult to translate clinically. However, there are less invasive alternatives to increase BDNF levels in the brain such as repetitive Transcranial Magnetic Stimulation (Yukimasa et al., 2006;Zanardini et al., 2006). NGF (Grill et al., 1997b;Oudega and Hagg, 1996;Ramer et al., 2000b), BNDF (Oudega and Hagg, 1999), NT3 (Schnell et al., 1994;Grill et al., 1997a;Bradbury et al., 1999;Blits et al., 2000;Tuszynski et al., 2003;Oudega and Hagg, 1999), and aFGF (Cheng et al., 1996;Guest et al., 1997) stimulate the regrowth of CST and/or DCT

axons when applied locally at the lesion, thus they would be the best choices for combined treatment with Y27632 in a dorsal column transection model of SCI.

ROCK inhibition and astrocytes

The absence of long distance regeneration in all Y27632-treated animals, and decreased axonal sprouting and function recovery associated with low dose Y27632 treatment in the *in vivo* model of SCI (chapter 3) prompted the investigation into the hypothesis that nonspecific ROCK inhibition affects non-neuronal cells in the injured spinal cord, resulting in negative side effects (chapter 4). In agreement with the hypothesis, Y27632 treatment resulted in an increase in the expression of CSPGs *in vivo* and in the level of CSPGs in the ECM produced by cultured astrocytes. It is uncertain how ROCK inhibition causes such changes in CSPG expression, but I speculate that it suppresses CSPG degradation and turnover by metalloproteinases (proposed model discussed in chapter 4). This model can be tested by adding recombinant metalloproteinases (e.g. MMP2) to ECM produced by Y27632-treated astrocytes, before or as neurons are seeded onto the ECM. Neurite growth on the metalloproteinase-digested ECM should be similar to growth on control (not Y27632-treated) astrocyte-derived ECM, and to growth on ChABC-digested ECM produced by Y27632-treated astrocytes (refer to results in chapter 4). Another experiment would be to inhibit the activity of metalloproteinases by phenanthroline. Astrocytes monolayers can be maintained in the presence of this metalloproteinase inhibitor before seeding neurons onto them. Neurite growth should decrease on these monolayers even without Y27632 treatment of the astrocytes.

After SCI, there is a general increase in Rho activation in the spinal cord tissue, and one of the cellular sources of such an increase are astrocytes (Conrad et al., 2005;Sung et al., 2003). However, astrogliosis appears to depend on an inhibition of the Rho pathway (Chapter 4 and; Abe and Misawa, 2003;John et al., 2004). This apparent dilemma may be explained by the timing of astrogliosis and Rho activation. Astrocyte activation, as indicated by increased GFAP expression and hypertrophy, was evident between 3 to 5 days after injury to the CNS (reviewed in McGraw et al., 2001). The increase in Rho activation in astrocytes could not be detected until 7 days after SCI (Conrad et al., 2005). Therefore it appears that astrogliosis requires an initial inactivation of the Rho pathway preceding the later increase in Rho activation.

Results from chapter 4 provoke further investigation into the signaling pathway that leads to astrogliosis. Astrogliosis is a major contributor to glial scar formation, which appears to be the ultimate barrier to regeneration. Therefore it is important to understand the factors that activate astrocytes and to investigate the regulation of Rho activities in these cells. Likely candidates are cytokines released after a CNS injury, such as IL-1β, TNFα and TNFβ. IL-1β induced astrocyte stellation *in vitro* via deactivation of Rho (John et al., 2004). TGFβ-neutralizing antibodies decreased all indicators of CNS scarring investigated, which included a reduction in GFAP immunoreactivity (Logan et al., 1999). *In vitro*, TGFβ increased the expression of neurocan by cultured astrocytes (Asher et al., 2000;Smith and Strunz, 2005). In transgenic mice that overproduce TGFα, there was increased expression of GFAP in the brain and spinal cord as revealed by northern blot analyses, and the astrocytes appeared larger with thicker processes (Rabchevsky et al., 1998). Such astrocytic morphology was reminiscent of reactive astrocytes found in the injured CNS. TGFα increased Rho-GTP levels in endothelial cells (Birukova et al., 2005) and in an epithelial cell line (LLC-PK$_1$) (Masszi et al., 2003), which appeared to contradict the hypothesis that Rho inactivation led to astrogliosis. It is possible that TGFα and TGFβ counteract IL-1β to keep astrogliosis in check. For future experiments, the role of Rho activities in cytokine-mediated astrogliosis can be analyzed by exogenous expression of constitutively active Rho in astrocytes, and then incubating these cells in medium containing cytokines. If cytokine-induced astrogliosis is dependent on Rho inactivation, constitutively active Rho-expressing astrocytes should be resistant to cytokine treatment and retain a fibroblast-like flattened morphology.

Experimental models

In Chapter 2, DRG explants were used to study the effects of an inhibitory molecule on neurite growth and GC behavior. These neurons are well-characterized and commonly used in other studies for similar purposes (Tang et al., 2001;Ughrin et al., 2003;Gilbert et al., 2005;Snow et al., 1991;Snow et al., 2003;Yamashita et al., 2002;Snow and Letourneau, 1992). However, the cell bodies of the DRG neurons reside in the PNS, although they have axons that project centrally to the SC. It would be interesting to repeat the experiments in Chapter 2 to CNS neurons such as cortical or cerebellar granule neurons (CGNs), which are also well-characterized and commonly used *in vitro* (Bito et al., 2000;Dergham et al., 2002;Domeniconi et al.,

2005;Niederost et al., 2002;Sivasankaran et al., 2004). Although there may be differences in neurite and GC behavior between peripheral DRG neuron and central neurons, the same signaling machinery are likely to be activated downstream of inhibitory or guidance molecules. On a neutral substrate (PDL or non-transfected CHO cell monolayer), Rho inhibition by C3 or ROCK inhibition by Y27632 increased neurite length from both DRG neurons (Chapter 2; Fournier et al., 2003) and CGNs (Niederost et al., 2002;Bito et al., 2000). Inhibitory substrates such as myelin, MAG, and Nogo, decreased neurite growth from both kinds of neurons, and C3 or Y27632 treatment reversed the decrease (Fournier et al., 2003;Niederost et al., 2002). Therefore, Rho activation appears to be a common signaling mechanism by which inhibitory molecules exert their effects on neurite growth, and I expect similar results if the experiments were repeated using CNS neurons.

The *in vitro* assays used in the experiments in Chapters 2 and 4 were two dimensional (2D) culture models. They are commonly used in studying neurite growth. However, three dimensional (3D) cultures are more representative of *in vivo* tissue, and may be better ways to characterize neurite growth and GC morphology in a matrix with CSPGs (Chapter 2) or with astrocytes (Chapter 4). In 2D cultures, the GCs are in contact with the substrate or with astrocytes on only one plane. Thus they are exposed to a smaller amount of inhibitory molecules, and their morphology would be different than *in vivo*. In a 3D culture model, the GCs are exposed to inhibitory molecules or cells on all surfaces, and they have to navigate through this potentially more hostile environment. The difference in culture model might be one of the reasons why there was no decrease in neurite length on chondroitin sulfate-treated glass slides (Chapter 2), but in 3D cultures chondroitin sulfate significantly inhibited neurite growth from chick DRGs (Carbonetto et al., 1983;Yu and Bellamkonda, 2001). However, before moving to a 3D culture system, the properties of the matrix must be carefully characterized in case it inadvertently participates in random biological signaling (e.g. the matrix may absorb or bind to the molecule being tested, and prevent the active epitopes from interacting with GCs).

The difference between 2D and 3D culture may critically influence astrocyte-mediated inhibition on neurite growth. Axons grow well on monolayers of primary astrocytes (Chapter 4 and; Fawcett et al., 1992;Lindsay, 1979;Noble et al., 1984;Smith et al., 1990). In a 3D astrocyte culture constructed by packing purified primary astrocytes into cellulose ester tubes, the cells were much less permissive compared to astrocyte monolayers, and displayed similar axon

regeneration-blocking activity as *in vivo* (Fawcett et al., 1989). It will be worthwhile to analyze neurite growth through Y27632-treated astrocytes in a 3D culture system. Since Y27632 treatment increase CSPG expression and the GCs will be exposed to these CSPGs on all surfaces, I hypothesize that neurite growth will be more severely inhibited in a 3D model than in 2D assays.

In vivo, transection models of SCI allow us to analyze the regeneration of specific axonal tracts. However, the disadvantage is that they differ from the blunt traumatic injury more commonly seen in humans. Contusion injury, on the other hand, is more comparable to most cases of human SCI in terms of the temporal pattern of injury maturation, i.e. initial spread of hemorrhagic necrosis and edema, followed by partial repair and tissue reorganization, and chronic formation of cystic cavity (reviewed in Kwon et al., 2002). Thus contusion is a better model for studying secondary tissue damage and assessing neuroprotective strategies. Although the Y27632 ROCK inhibitor is commonly used for overcoming the effects of inhibitory molecules on the GC and stimulating axonal regrowth, others (Fournier et al., 2003) and myself (Chapter 3) have shown that some of its beneficial effects were due to neuroprotection (early recovery of some of the behavioral parameters). In Fournier's and my own studies, the effects of Y27632 on axonal regrowth were assessed after a transection of the spinal cord. In a contusion model, rats that received Y27632 immediately after the injury appeared to have more spared tissue at 5 weeks, and this was estimated by staining post-fixed SC tissues with hematoxylin and eosin (Sung et al., 2003). Unfortunately a more thorough analysis of neuroprotection was lacking and the reader wondered about parameters such as area of spared tissue, and number of dying cells due to apoptosis.

Inhibiting ROCK's upstream regulator, Rho, with C3 might decrease cell death due to apoptosis after SCI (Dergham et al., 2002;Dubreuil et al., 2003). Contrary to this, another group showed that C3 treatment might actually increase tissue damage (Fournier et al., 2003). In yet another study, the C3-treated group had to be euthanized prematurely due to severe side effects (Sung et al., 2003). It remains to be clarified whether inhibition of the Rho pathway is neuroprotective. Therefore, more experiments are needed to analyze the effects of Y27632 in animal contusion models of SCI in order to determine whether this drug possess both neuroprotective and regeneration-stimulating properties.

Other effects of Rho/ROCK inhibition

In SCI, the initial mechanical trauma and secondary injury processes such as metabolic disturbances, excitotoxicity, and immune responses damage axons, resulting in axonal degeneration (Gomes-Leal et al., 2005). One well-characterized axon self-destruct process, Wallerian degeneration (Waller, 1850), occurs in the distal fragment of injured axons. Rho played a role in Wallerian degeneration, possibly through modulating the cytoskeletal reorganization necessary for such an active process (Yamagishi et al., 2005). *In vitro,* Nogo-66 activated Rho and significantly accelerated Wallerian degeneration of transected neurites from DRG explants. Inhibiting ROCK with Y27632 abolished this effect, and *in vivo* it delayed the degeneration of injured CST axons (Yamagishi et al., 2005). Therefore, ROCK inhibition might offer some protection against degeneration after SCI. In addition, since axonal degeneration produces myelin debris, Y27632 treatment may decrease the amount of axonal growth-inhibitory molecules in the injured spinal cord.

Suppression of the Rho pathway is implicated in oligodentrocyte differentiation. Fyn, a Src family kinase, is activated when oligodendrocytes differentiate (Osterhout et al., 1999). One of the downstream effectors of Fyn is p190RhoGAP, which generates GDP-bound, i.e. inactive, Rho. Rho inactivation resulted in hyperextension of oligodendrocyte processes (Liang et al., 2004). Interestingly, the differentiation of oligodendrocyte precursor cells was inhibited by myelin debris (Kotter et al., 2006), which contains numerous myelin-associated proteins that activate Rho (reviewed in Yamashita et al., 2005). Thus inhibition of the Rho pathway may favor oligodendrocyte differentiation and remyelination after SCI.

The Rho/ROCK pathway controls cell migration (reviewed in Ridley, 2001). Inhibiting Rho or ROCK decreased cell migration and tumor metastasis (Nakajima et al., 2003;Sahai and Marshall, 2003). Thus nonspecific inhibition of ROCK may decrease the number of immune cells that migrate into the lesion area after SCI. Indeed, ROCK inhibition decreased leukocyte infiltration (measured by myeloperoxidase activity) into the injured spinal cord (Hara et al., 2000). *In vitro,* the Y27632 ROCK inhibitor decreased the number of macrophages that migrate in a 3D assay (Nakayama et al., 2005). The activities of macrophages after SCI may exacerbate secondary tissue damage (Fitch and Silver, 1997;Fitch et al., 1999;reviewed in Fitch and Silver, 2000;Popovich et al., 2002). In contrast, suppression of macrophages delayed the functional loss due to secondary damage, and increased the number of preserved axons (Blight, 1994).

Therefore, ROCK inhibition may contribute to neuroprotection via its inhibition of immune cell migration.

These other effects of ROCK inhibition than stimulating axonal growth emphasize the need to further test the Y27632 drug in contusion models of SCI, before applying it in a clinical setting.

mDia, another downstream effector of Rho

This thesis focused on one of the Rho downstream effectors, ROCK. There are numerous other molecules which show selective binding to the active, GTP-bound form of Rho, and they have been proposed as putative downstream Rho effectors (reviewed in Bishop and Hall, 2000). Examples of such are mDia, protein kinase N (PKN), citron kinase, and rhotekin. In non-neuronal HeLa cells, Rho activation induces stress fiber formation. The expression of a dominant negative ROCK mutant (kinase-negative and Rho-binding defective) protein inhibited the Rho-induced formation of focal adhesions and stress fibers (Ishizaki et al., 1997). However, the Rho-induced increase in F-actin content persisted, suggesting that other downstream effector(s) stimulated actin polymerization. That Rho effector turned out to be mDia, which was a mammalian homolog of the *Drosophila* protein, diaphanous (Watanabe et al., 1997). It binds to both Rho-GTP and profilin at the inner surface of the plasma membrane, and stimulates the activity of profilin. Profilin is as an actin monomer-binding protein that promotes actin polymerization (Pantaloni and Carlier, 1993). For stress fiber formation, mDia and ROCK cooperate to induce *de novo* production of actin filaments and actin-myosin contraction (Watanabe et al., 1999). Depending on the relative amount of constitutively active ROCK and mDia expressed in the cell, a gradient of F-actin/stress fiber phenotypes results. Normal stress fiber formation requires the coordinated activation of both mDia and ROCK.

Very interestingly, the activities of mDia and ROCK antagonize each other in both neurons and non-neuronal cells (Arakawa et al., 2003;Nusser et al., 2006;Tsuji et al., 2002;Tominaga et al., 2002). In neurons, their relative activities determine the degree of neurite growth. The expression of dominant active Rho (RhoV14) or ROCK (ROCK Δ 3) resulted in short neurites, and in contrast the overexpression of mDia resulted in neurite extension and multibranching in cerebellar granule neurons (CGNs; Tominaga et al., 2002). Neurite shortening due to RhoV14 or ROCK Δ 3 was reversed by the co-expression of mDia. Stromal cell–derived

factor (SDF)-1α, at low concentration, facilitated axon elongation in CGNs via the activation of Rho and mDia (Arakawa et al., 2003). Higher concentrations of SDF-1α repressed axon formation due to the activation of Rho and ROCK. mDia and ROCK were hypothesized to respond to different levels of GTP-bound Rho, and thus the dose-dependent effects of SDF-1α.

ROCK and mDia also differentially interact with PKA-phosphorylated Rho (Nusser et al., 2006). PKA phosphorylates Rho on serine-188, resulting in increased association between Rho and Rho-GDI (Rho guanine nucleotide dissociation inhibitor) and decreased binding of Rho with GTP (Lang et al., 1996). NGF stimulates the activity of PKA (Cremins et al., 1986;Yao et al., 1998), although the exact mechanism is unclear. In PC12 cells, NGF induced neurite outgrowth, but such growth was inhibited by the expression of a dominant active Rho mutant that could not be phosphorylated by PKA (Nusser et al., 2006). This Rho mutant constitutively activated both mDia and ROCK. PKA-phosphorylated Rho was unable to activate ROCK, however it appeared to retain its ability to activate other Rho targets including mDia (Nusser et al., 2006). The expression of another Rho mutant that mimicked the phosphorylation by PKA (phosphomimetic mutant Rho that activated mDia but not ROCK; Ellerbroek et al., 2003) promoted neurite outgrowth, and overcame the inhibitory effect of the dominant active Rho mutant (Nusser et al., 2006). Therefore, the activation of mDia favored neurite growth, but activation of ROCK inhibited growth.

Based on the above studies, ROCK appears to be the major Rho effector responsible for inhibiting neurite growth and other effectors such as mDia may counteract such inhibitory influence. Therefore the selective inhibition of Rho-ROCK interaction or of ROCK, rather than a general suppression of Rho activity, would be most favorable for neurite growth. Along this line of logic, Y27632 would be a better therapeutic agent for stimulating axonal regrowth than C3. However, there may be other unidentified downstream effectors of Rho, and for the known effectors, there may be as yet undiscovered functions in neurite growth. Therefore, more research is needed in delineating the signaling from Rho to its downstream effectors and the functions of each effector in neurite growth.

Feasibility of using Y27632 to treat human SCI

In vitro, our laboratory and others have shown that Y27632 effectively counteracts the inhibitory effects on neurite growth of multiple molecules, such as myelin-associated

glycoprotein (MAG), Nogo, oligodendrocyte myelin, and CSPG, (Chapter 2 and; Borisoff et al., 2003;Dergham et al., 2002;Fournier et al., 2003;Monnier et al., 2003;Niederost et al., 2002;Sivasankaran et al., 2004;Schweigreiter et al., 2004). *In vivo*, there are positive results with Y27632 treatment in animal models of SCI (Chapter 3, Chan et al., 2005;Fournier et al., 2003). It stimulates axon sprouting and accelerated function recovery. However, Y27632 treatment also caused negative side effects. In chapter 3, low dose-treated rats had decreased axonal sprouting/regeneration, and impaired functional recovery as indicated by footprint analysis and skilled forepaw reaching test. In another study, Y27632 given immediately after a weight-drop contusion injury and continued for 10 days onward resulted in a significant reduction in the BBB (Basso, Beattie, and Bresnahan; Basso et al., 1996) score for open field locomotion on the last day of drug administration (Sung et al., 2003). Since an oral route of drug delivery was used, it was difficult to determine drug concentration in the CSF and at the lesion area. Nonetheless, the dosage they used might be similar to the low dose (2 mM, 12 μL/day for 14 days) paradigm in my experiment (Chapter 3). Alternatively, the ROCK inhibitor could be detrimental to axonal regeneration and functional recovery at any dosage when used in a contusion injury model, which is a more suitable model for assessing secondary damage.

Another ROCK inhibitor, fasudil (or HA1077), also has positive effects on axonal regeneration and functional recovery (Hara et al., 2000;Sung et al., 2003; Nishio et al., in press). When fasudil was applied immediatly at the injury site after contusion of the thoracic spinal cord in rats, it stimulated axonal sprouting and recovery of hindlimb function (Nishio et al., in press). It also decreased neutrophil infiltration, and reduced tissue damage (Hara et al., 2000;Sung et al., 2003). So far there has been no evidence that this drug causes any negative side effects. One major difference between fasudil and Y27632 is that fasudil is a less specific inhibitor for ROCK, and fasudil inhibits other kinases such as PKA, PKC, myosin light chain kinase (MLCK) at lower concentrations than Y27632 (Uehata et al., 1997). Its general inhibition of multiple kinases, rather than just ROCK, may be responsible for its neuroprotective properties (Hara et al., 2000).

The question arises: whether a more potent and selective inhibitor for ROCK such as Y27632, or a more general inhibitor for multiple kinases is a better option for treating SCI. As discussed in the previous section, selective inhibition of ROCK while leaving the other downstream effectors of Rho unaffected was a logical choice for stimulating axonal growth. In addition, ROCK inhibition with Y27632 may have other beneficial effects such as suppression of

Wallerian degeneration and deposition of myelin debris, promotion of remyelination, and decreasing macrophage migration into the injury site (discussed in earlier sections). However, there are side effects associated with using Y27632, and one of them is an increase in the expression of CSPGs by astrocytes (Chapter 4). Results from using fasudil in animal models of SCI suggested that a more general kinase inhibitor was neuroprotective, perhaps even more so than Y27632 (Sung et al., 2003). Because both neuroprotection and stimulation of axonal regrowth was important for recovery from SCI, a new drug that does both and without adverse side effects will be ideal.

Alternatively, the use of Y27632 can be combined with intervention protocols that reduce secondary damage (e.g. agents that suppress inflammation), and minimize the formation of a nonpermissive glial scar. In any case, an effective strategy to promote axonal regeneration likely require combinatorial treatment paradigm that encompasses neuroprotective, neurorestaurative (e.g. promoting remyelination) and neuroregenerative approaches (for reviews, see Ramer et al., 2000a;Schwab et al., 2006). Because Y27632 increase CSPG deposition, ChABC can be one option in the combination therapy. Also, cells (e.g. Schwann cells, genetically engineered fibroblasts that secrete trophic factors) or tissue (e.g. peripheral nerve, embryonic SC) grafts are commonly used to bridge a lesion site and minimize local damage (Blits et al., 2000;Bregman et al., 2002;Cheng et al., 1996;David and Aguayo, 1981;Grill et al., 1997b;Li and Raisman, 1994). Transplanting olfactory ensheathing cells (OECs) into the spinal cord after a dorsolateral funiculus crush injury reduced the formation of an astroglial barrier (Ramer et al., 2004). Therefore, combining OEC transplants with Y27632 treatment may be effective in promoting regeneration. Taking into account the importance of cell body response (discussed earlier), future therapeutic paradigm may consist of Y27632 and trophic factor infusion and OEC transplant into the injured spinal cord.

Timing is also an important consideration in designing a therapeutic paradigm. Y27632 treatment has resulted in beneficial effects in the acute setting. Delaying the start of therapeutic treatment may significantly affect outcome. This was demonstrated by Nishio's study (in press), in which fasudil treatment was delayed for 4 weeks, and there was no positive effect. This outcome was in contrast to the stimulated axonal sprouting and functional recovery seen after immediate treatment. Such decline in growth-promoting abilities as the post-injury interval

increases is also observed with other therapeutic interventions (Houle, 1991;Decherchi and Gauthier, 2000;Jin et al., 2000;von Meyenburg et al., 1998).

Unexpected negative side effects with the low dose Y27632 ROCK inhibitor amid widely reported beneficial outcomes with this drug demonstrate the need for a more thorough understanding of the neuronal and glial responses to injury, and their responses to the various experimental interventions. Over the years, evidence on the promoting effects of ROCK inhibition on neurite growth is abundant, especially from *in vitro* studies. Based on this knowledge, the Y27632 drug should in theory stimulate axonal regeneration after SCI. On the contrary, studies about its effects on non-neuronal cells are lacking, and the experiments in chapter 4 are the first to explore such relationship between ROCK inhibition and glial cell responses. On route to develop an effective therapeutic paradigm for the promotion of axonal regeneration after SCI, more research into the signaling involved in the inhibition of regeneration and methods of targeting such inhibitory signaling is critical. At the same time, glial cell responses to these therapeutic manipulations should be monitored as closely as for signs of axonal sprouting/regeneration, in case the manipulations cause undesirable effects on the glial cells and hinder regeneration.

References

Abe K, Misawa M (2003) Astrocyte stellation induced by Rho kinase inhibitors in culture. Brain Res Dev Brain Res 143:99-104.

Arakawa Y, Bito H, Furuyashiki T, Tsuji T, Takemoto-Kimura S, Kimura K, Nozaki K, Hashimoto N, Narumiya S (2003) Control of axon elongation via an SDF-1alpha/Rho/mDia pathway in cultured cerebellar granule neurons. J Cell Biol 161:381-391.

Asher RA, Morgenstern DA, Fidler PS, Adcock KH, Oohira A, Braistead JE, Levine JM, Margolis RU, Rogers JH, Fawcett JW (2000) Neurocan is upregulated in injured brain and in cytokine-treated astrocytes. J Neurosci 20:2427-2438.

Aspberg A, Binkert C, Ruoslahti E (1995) The versican C-type lectin domain recognizes the adhesion protein tenascin-R. Proc Natl Acad Sci U S A 92:10590-10594.

Aspberg A, Miura R, Bourdoulous S, Shimonaka M, Heinegard D, Schachner M, Ruoslahti E, Yamaguchi Y (1997) The C-type lectin domains of lecticans, a family of aggregating chondroitin sulfate proteoglycans, bind tenascin-R by protein-protein interactions independent of carbohydrate moiety. Proc Natl Acad Sci U S A 94:10116-10121.

Bao X, Nishimura S, Mikami T, Yamada S, Itoh N, Sugahara K (2004) Chondroitin sulfate/dermatan sulfate hybrid chains from embryonic pig brain, which contain a higher proportion of L-iduronic acid than those from adult pig brain, exhibit neuritogenic and growth factor binding activities. J Biol Chem 279:9765-9776.

Basso DM, Beattie MS, Bresnahan JC, Anderson DK, Faden AI, Gruner JA, Holford TR, Hsu CY, Noble LJ, Nockels R, Perot PL, Salzman SK, Young W (1996) MASCIS evaluation of open field locomotor scores: effects of experience and teamwork on reliability. Multicenter Animal Spinal Cord Injury Study. J Neurotrauma 13:343-359.

Birukova AA, Birukov KG, Adyshev D, Usatyuk P, Natarajan V, Garcia JG, Verin AD (2005) Involvement of microtubules and Rho pathway in TGF-beta1-induced lung vascular barrier dysfunction. J Cell Physiol 204:934-947.

Bishop AL, Hall A (2000) Rho GTPases and their effector proteins. Biochem J 348 Pt 2:241-255.

Bito H, Furuyashiki T, Ishihara H, Shibasaki Y, Ohashi K, Mizuno K, Maekawa M, Ishizaki T, Narumiya S (2000) A critical role for a Rho-associated kinase, p160ROCK, in determining axon outgrowth in mammalian CNS neurons. Neuron 26:431-441.

Blight AR (1994) Effects of silica on the outcome from experimental spinal cord injury: implication of macrophages in secondary tissue damage. Neuroscience 60:263-273.

Blits B, Dijkhuizen PA, Boer GJ, Verhaagen J (2000) Intercostal nerve implants transduced with an adenoviral vector encoding neurotrophin-3 promote regrowth of injured rat corticospinal tract fibers and improve hindlimb function. Exp Neurol 164:25-37.

Borisoff JF, Chan CC, Hiebert GW, Oschipok L, Robertson GS, Zamboni R, Steeves JD, Tetzlaff W (2003) Suppression of Rho-kinase activity promotes axonal growth on inhibitory CNS substrates. Mol Cell Neurosci 22:405-416.

Bradbury EJ, Khemani S, Von R, King, Priestley JV, McMahon SB (1999) NT-3 promotes growth of lesioned adult rat sensory axons ascending in the dorsal columns of the spinal cord. Eur J Neurosci 11:3873-3883.

Bregman BS, Coumans JV, Dai HN, Kuhn PL, Lynskey J, McAtee M, Sandhu F (2002) Transplants and neurotrophic factors increase regeneration and recovery of function after spinal cord injury. Prog Brain Res 137:257-273.

Broude E, McAtee M, Kelley MS, Bregman BS (1997) c-Jun expression in adult rat dorsal root ganglion neurons: differential response after central or peripheral axotomy. Exp Neurol 148:367-377.

Brouns MR, Matheson SF, Settleman J (2001) p190 RhoGAP is the principal Src substrate in brain and regulates axon outgrowth, guidance and fasciculation. Nat Cell Biol 3:361-367.

Carbonetto S, Gruver MM, Turner DC (1983) Nerve fiber growth in culture on fibronectin, collagen, and glycosaminoglycan substrates. J Neurosci 3:2324-2335.

Chan CC, Khodarahmi K, Liu J, Sutherland D, Oschipok LW, Steeves JD, Tetzlaff W (2005) Dose-dependent beneficial and detrimental effects of ROCK inhibitor Y27632 on axonal sprouting and functional recovery after rat spinal cord injury. Exp Neurol 196:352-364.

Cheng H, Cao Y, Olson L (1996) Spinal cord repair in adult paraplegic rats: partial restoration of hind limb function. Science 273:510-513.

Condic ML, Snow DM, Letourneau PC (1999) Embryonic neurons adapt to the inhibitory proteoglycan aggrecan by increasing integrin expression. J Neurosci 19:10036-10043.

Conrad S, Schluesener HJ, Trautmann K, Joannin N, Meyermann R, Schwab JM (2005) Prolonged lesional expression of RhoA and RhoB following spinal cord injury. J Comp Neurol 487:166-175.

Cremins J, Wagner JA, Halegoua S (1986) Nerve growth factor action is mediated by cyclic AMP- and Ca+2/phospholipid-dependent protein kinases. J Cell Biol 103:887-893.

Damon DH, D'Amore PA, Wagner JA (1988) Sulfated glycosaminoglycans modify growth factor-induced neurite outgrowth in PC12 cells. J Cell Physiol 135:293-300.

David S, Aguayo AJ (1981) Axonal elongation into peripheral nervous system "bridges" after central nervous system injury in adult rats. Science 214:931-933.

Decherchi P, Gauthier P (2000) Regrowth of acute and chronic injured spinal pathways within supra-lesional post-traumatic nerve grafts. Neuroscience 101:197-210.

Deepa SS, Umehara Y, Higashiyama S, Itoh N, Sugahara K (2002) Specific molecular interactions of oversulfated chondroitin sulfate E with various heparin-binding growth factors. Implications as a physiological binding partner in the brain and other tissues. J Biol Chem 277:43707-43716.

Dergham P, Ellezam B, Essagian C, Avedissian H, Lubell WD, McKerracher L (2002) Rho signaling pathway targeted to promote spinal cord repair. J Neurosci 22:6570-6577.

Domeniconi M, Zampieri N, Spencer T, Hilaire M, Mellado W, Chao MV, Filbin MT (2005) MAG Induces Regulated Intramembrane Proteolysis of the p75 Neurotrophin Receptor to Inhibit Neurite Outgrowth. Neuron 46:849-855.

Dou CL, Levine JM (1997) Identification of a neuronal cell surface receptor for a growth inhibitory chondroitin sulfate proteoglycan (NG2). J Neurochem 68:1021-1030.

Dubreuil CI, Winton MJ, McKerracher L (2003) Rho activation patterns after spinal cord injury and the role of activated Rho in apoptosis in the central nervous system. J Cell Biol 162:233-243.

Ellerbroek SM, Wennerberg K, Burridge K (2003) Serine phosphorylation negatively regulates RhoA in vivo. J Biol Chem 278:19023-19031.

Fawcett JW, Fersht N, Housden L, Schachner M, Pesheva P (1992) Axonal growth on astrocytes is not inhibited by oligodendrocytes. J Cell Sci 103 (Pt 2):571-579.

Fawcett JW, Housden E, Smith-Thomas L, Meyer RL (1989) The growth of axons in three-dimensional astrocyte cultures. Dev Biol 135:449-458.

Fitch MT, Doller C, Combs CK, Landreth GE, Silver J (1999) Cellular and molecular mechanisms of glial scarring and progressive cavitation: in vivo and in vitro analysis of inflammation-induced secondary injury after CNS trauma. J Neurosci 19:8182-8198.

Fitch MT, Silver J (2000) Inflammation and the glial scar: factors at the site of injury that influence regeneration in the central nervous system. In: Degeneration and Regeneration in the Nervous System (Saunders NR, Dziegielewska KM, eds), Amsterdam, Harwood.

Fitch MT, Silver J (1997) Activated macrophages and the blood-brain barrier: inflammation after CNS injury leads to increases in putative inhibitory molecules. Exp Neurol 148:587-603.

Fournier AE, Takizawa BT, Strittmatter SM (2003) Rho kinase inhibition enhances axonal regeneration in the injured CNS. J Neurosci 23:1416-1423.

Friedlander DR, Milev P, Karthikeyan L, Margolis RK, Margolis RU, Grumet M (1994) The neuronal chondroitin sulfate proteoglycan neurocan binds to the neural cell adhesion molecules Ng-CAM/L1/NILE and N-CAM, and inhibits neuronal adhesion and neurite outgrowth. J Cell Biol 125:669-680.

Giehl KM, Tetzlaff W (1996) BDNF and NT-3, but not NGF, prevent axotomy-induced death of rat corticospinal neurons in vivo. Eur J Neurosci 8:1167-1175.

Gilbert RJ, McKeon RJ, Darr A, Calabro A, Hascall VC, Bellamkonda RV (2005) CS-4,6 is differentially upregulated in glial scar and is a potent inhibitor of neurite extension. Mol Cell Neurosci.

Gomes-Leal W, Corkill DJ, Picanco-Diniz CW (2005) Systematic analysis of axonal damage and inflammatory response in different white matter tracts of acutely injured rat spinal cord. Brain Res 1066:57-70.

Grill R, Murai K, Blesch A, Gage FH, Tuszynski MH (1997a) Cellular delivery of neurotrophin-3 promotes corticospinal axonal growth and partial functional recovery after spinal cord injury. J Neurosci 17:5560-5572.

Grill RJ, Blesch A, Tuszynski MH (1997b) Robust growth of chronically injured spinal cord axons induced by grafts of genetically modified NGF-secreting cells. Exp Neurol 148:444-452.

Grumet M, Flaccus A, Margolis RU (1993) Functional characterization of chondroitin sulfate proteoglycans of brain: interactions with neurons and neural cell adhesion molecules. J Cell Biol 120:815-824.

Guest JD, Hesse D, Schnell L, Schwab ME, Bunge MB, Bunge RP (1997) Influence of IN-1 antibody and acidic FGF-fibrin glue on the response of injured corticospinal tract axons to human Schwann cell grafts. J Neurosci Res 50:888-905.

Hara M, Takayasu M, Watanabe K, Noda A, Takagi T, Suzuki Y, Yoshida J (2000) Protein kinase inhibition by fasudil hydrochloride promotes neurological recovery after spinal cord injury in rats. J Neurosurg 93:94-101.

Hiebert GW, Khodarahmi K, McGraw J, Steeves JD, Tetzlaff W (2002) Brain-derived neurotrophic factor applied to the motor cortex promotes sprouting of corticospinal fibers but not regeneration into a peripheral nerve transplant. J Neurosci Res 69:160-168.

Houle JD (1991) Demonstration of the potential for chronically injured neurons to regenerate axons into intraspinal peripheral nerve grafts. Exp Neurol 113:1-9.

Ishizaki T, Naito M, Fujisawa K, Maekawa M, Watanabe N, Saito Y, Narumiya S (1997) p160ROCK, a Rho-associated coiled-coil forming protein kinase, works downstream of Rho and induces focal adhesions. FEBS Lett 404:118-124.

Jin Y, Tessler A, Fischer I, Houle JD (2000) Fibroblasts genetically modified to produce BDNF support regrowth of chronically injured serotonergic axons. Neurorehabil Neural Repair 14:311-317.

John GR, Chen L, Rivieccio MA, Melendez-Vasquez CV, Hartley A, Brosnan CF (2004) Interleukin-1beta induces a reactive astroglial phenotype via deactivation of the Rho GTPase-Rock axis. J Neurosci 24:2837-2845.

Kotter MR, Li WW, Zhao C, Franklin RJ (2006) Myelin impairs CNS remyelination by inhibiting oligodendrocyte precursor cell differentiation. J Neurosci 26:328-332.

Kwon BK, Oxland TR, Tetzlaff W (2002) Animal models used in spinal cord regeneration research. Spine 27:1504-1510.

Lang P, Gesbert F, espine-Carmagnat M, Stancou R, Pouchelet M, Bertoglio J (1996) Protein kinase A phosphorylation of RhoA mediates the morphological and functional effects of cyclic AMP in cytotoxic lymphocytes. EMBO J 15:510-519.

Li Y, Raisman G (1994) Schwann cells induce sprouting in motor and sensory axons in the adult rat spinal cord. J Neurosci 14:4050-4063.

Liang X, Draghi NA, Resh MD (2004) Signaling from integrins to Fyn to Rho family GTPases regulates morphologic differentiation of oligodendrocytes. J Neurosci 24:7140-7149.

Lindsay RM (1979) Adult rat brain astrocytes support survival of both NGF-dependent and NGF-insensitive neurones. Nature 282:80-82.

Logan A, Green J, Hunter A, Jackson R, Berry M (1999) Inhibition of glial scarring in the injured rat brain by a recombinant human monoclonal antibody to transforming growth factor-beta2. Eur J Neurosci 11:2367-2374.

Lyuksyutova AI, Lu CC, Milanesio N, King LA, Guo N, Wang Y, Nathans J, Tessier-Lavigne M, Zou Y (2003) Anterior-posterior guidance of commissural axons by Wnt-frizzled signaling. Science 302:1984-1988.

Manthorpe M, Engvall E, Ruoslahti E, Longo FM, Davis GE, Varon S (1983) Laminin promotes neuritic regeneration from cultured peripheral and central neurons. J Cell Biol 97:1882-1890.

Masszi A, Di CC, Sirokmany G, Arthur WT, Rotstein OD, Wang J, McCulloch CA, Rosivall L, Mucsi I, Kapus A (2003) Central role for Rho in TGF-beta1-induced alpha-smooth muscle actin expression during epithelial-mesenchymal transition. Am J Physiol Renal Physiol 284:F911-F924.

McGraw J, Hiebert GW, Steeves JD (2001) Modulating astrogliosis after neurotrauma. J Neurosci Res 63:109-115.

Monnier PP, Sierra A, Macchi P, Deitinghoff L, Andersen JS, Mann M, Flad M, Hornberger MR, Stahl B, Bonhoeffer F, Mueller BK (2002) RGM is a repulsive guidance molecule for retinal axons. Nature 419:392-395.

Monnier PP, Sierra A, Schwab JM, Henke-Fahle S, Mueller BK (2003) The Rho/ROCK pathway mediates neurite growth-inhibitory activity associated with the chondroitin sulfate proteoglycans of the CNS glial scar. Mol Cell Neurosci 22:319-330.

Nakajima M, Hayashi K, Egi Y, Katayama K, Amano Y, Uehata M, Ohtsuki M, Fujii A, Oshita K, Kataoka H, Chiba K, Goto N, Kondo T (2003) Effect of Wf-536, a novel ROCK inhibitor, against metastasis of B16 melanoma. Cancer Chemother Pharmacol 52:319-324.

Nakayama M, Amano M, Katsumi A, Kaneko T, Kawabata S, Takefuji M, Kaibuchi K (2005) Rho-kinase and myosin II activities are required for cell type and environment specific migration. Genes Cells 10:107-117.

Niederost B, Oertle T, Fritsche J, McKinney RA, Bandtlow CE (2002) Nogo-A and myelin-associated glycoprotein mediate neurite growth inhibition by antagonistic regulation of RhoA and Rac1. J Neurosci 22:10368-10376.

Nishio, Y., Koda, M., Kitajo, K., Seto, M., Hata, K., Taniguchi, J., Moriya, H., Fujitani, M., Kubo, T. and Yamashita, T. (2006) Delayed treatment with Rho-kinase inhibitor does not enhance axonal regeneration or functional recovery after spinal cord injury in rats. Exp. Neurol. (in press)

Noble M, Fok-Seang J, Cohen J (1984) Glia are a unique substrate for the in vitro growth of central nervous system neurons. J Neurosci 4:1892-1903.

Nusser N, Gosmanova E, Makarova N, Fujiwara Y, Yang L, Guo F, Luo Y, Zheng Y, Tigyi G (2006) Serine phosphorylation differentially affects RhoA binding to effectors: implications to NGF-induced neurite outgrowth. Cell Signal 18:704-714.

Osterhout DJ, Wolven A, Wolf RM, Resh MD, Chao MV (1999) Morphological differentiation of oligodendrocytes requires activation of Fyn tyrosine kinase. J Cell Biol 145:1209-1218.

Oudega M, Hagg T (1996) Nerve growth factor promotes regeneration of sensory axons into adult rat spinal cord. Exp Neurol 140:218-229.

Oudega M, Hagg T (1999) Neurotrophins promote regeneration of sensory axons in the adult rat spinal cord. Brain Res 818:431-438.

Pantaloni D, Carlier MF (1993) How profilin promotes actin filament assembly in the presence of thymosin beta 4. Cell 75:1007-1014.

Popovich PG, Guan Z, McGaughy V, Fisher L, Hickey WF, Basso DM (2002) The neuropathological and behavioral consequences of intraspinal microglial/macrophage activation. J Neuropathol Exp Neurol 61:623-633.

Rabchevsky AG, Weinitz JM, Coulpier M, Fages C, Tinel M, Junier MP (1998) A role for transforming growth factor alpha as an inducer of astrogliosis. J Neurosci 18:10541-10552.

Rajagopalan S, Deitinghoff L, Davis D, Conrad S, Skutella T, Chedotal A, Mueller BK, Strittmatter SM (2004) Neogenin mediates the action of repulsive guidance molecule. Nat Cell Biol 6:756-762.

Ramer LM, Au E, Richter MW, Liu J, Tetzlaff W, Roskams AJ (2004) Peripheral olfactory ensheathing cells reduce scar and cavity formation and promote regeneration after spinal cord injury. J Comp Neurol 473:1-15.

Ramer MS, Harper GP, Bradbury EJ (2000a) Progress in spinal cord research - a refined strategy for the International Spinal Research Trust. Spinal Cord 38:449-472.

Ramer MS, Priestley JV, McMahon SB (2000b) Functional regeneration of sensory axons into the adult spinal cord. Nature 403:312-316.

Richardson PM, Issa VM (1984) Peripheral injury enhances central regeneration of primary sensory neurones. Nature 309:791-793.

Richardson PM, Verge VM (1986) The induction of a regenerative propensity in sensory neurons following peripheral axonal injury. J Neurocytol 15:585-594.

Ridley AJ (2001) Rho GTPases and cell migration. J Cell Sci 114:2713-2722.

Sahai E, Marshall CJ (2003) Differing modes of tumour cell invasion have distinct requirements for Rho/ROCK signalling and extracellular proteolysis. Nat Cell Biol 5:711-719.

Schnell L, Schneider R, Kolbeck R, Barde YA, Schwab ME (1994) Neurotrophin-3 enhances sprouting of corticospinal tract during development and after adult spinal cord lesion. Nature 367:170-173.

Schreyer DJ, Skene JH (1993) Injury-associated induction of GAP-43 expression displays axon branch specificity in rat dorsal root ganglion neurons. J Neurobiol 24:959-970.

Schwab JM, Brechtel K, Mueller CA, Failli V, Kaps HP, Tuli SK, Schluesener HJ (2006) Experimental strategies to promote spinal cord regeneration-an integrative perspective. Prog Neurobiol 78:91-116.

Schweigreiter R, Walmsley AR, Niederost B, Zimmermann DR, Oertle T, Casademunt E, Frentzel S, Dechant G, Mir A, Bandtlow CE (2004) Versican V2 and the central inhibitory domain of Nogo-A inhibit neurite growth via p75NTR/NgR-independent pathways that converge at RhoA. Mol Cell Neurosci 27:163-174.

Sivasankaran R, Pei J, Wang KC, Zhang YP, Shields CB, Xu XM, He Z (2004) PKC mediates inhibitory effects of myelin and chondroitin sulfate proteoglycans on axonal regeneration. Nat Neurosci 7:261-268.

Smith GM, Rutishauser U, Silver J, Miller RH (1990) Maturation of astrocytes in vitro alters the extent and molecular basis of neurite outgrowth. Dev Biol 138:377-390.

Smith GM, Strunz C (2005) Growth factor and cytokine regulation of chondroitin sulfate proteoglycans by astrocytes. Glia 52:209-218.

Snow DM, Lemmon V, Carrino DA, Caplan AI, Silver J (1990) Sulfated proteoglycans in astroglial barriers inhibit neurite outgrowth in vitro. Exp Neurol 109:111-130.

Snow DM, Letourneau PC (1992) Neurite outgrowth on a step gradient of chondroitin sulfate proteoglycan (CS-PG). J Neurobiol 23:322-336.

Snow DM, Smith JD, Cunningham AT, McFarlin J, Goshorn EC (2003) Neurite elongation on chondroitin sulfate proteoglycans is characterized by axonal fasciculation. Exp Neurol 182:310-321.

Snow DM, Watanabe M, Letourneau PC, Silver J (1991) A chondroitin sulfate proteoglycan may influence the direction of retinal ganglion cell outgrowth. Development 113:1473-1485.

Sung JK, Miao L, Calvert JW, Huang L, Louis HH, Zhang JH (2003) A possible role of RhoA/Rho-kinase in experimental spinal cord injury in rat. Brain Res 959:29-38.

Tang S, Qiu J, Nikulina E, Filbin MT (2001) Soluble myelin-associated glycoprotein released from damaged white matter inhibits axonal regeneration. Mol Cell Neurosci 18:259-269.

Tominaga T, Meng W, Togashi K, Urano H, Alberts AS, Tominaga M (2002) The Rho GTPase effector protein, mDia, inhibits the DNA binding ability of the transcription factor Pax6 and changes the pattern of neurite extension in cerebellar granule cells through its binding to Pax6. J Biol Chem 277:47686-47691.

Tsuji T, Ishizaki T, Okamoto M, Higashida C, Kimura K, Furuyashiki T, Arakawa Y, Birge RB, Nakamoto T, Hirai H, Narumiya S (2002) ROCK and mDia1 antagonize in Rho-dependent Rac activation in Swiss 3T3 fibroblasts. J Cell Biol 157:819-830.

Tuszynski MH, Grill R, Jones LL, Brant A, Blesch A, Low K, Lacroix S, Lu P (2003) NT-3 gene delivery elicits growth of chronically injured corticospinal axons and modestly improves functional deficits after chronic scar resection. Exp Neurol 181:47-56.

Uehata M, Ishizaki T, Satoh H, Ono T, Kawahara T, Morishita T, Tamakawa H, Yamagami K, Inui J, Maekawa M, Narumiya S (1997) Calcium sensitization of smooth muscle mediated by a Rho-associated protein kinase in hypertension. Nature 389:990-994.

Ughrin YM, Chen ZJ, Levine JM (2003) Multiple regions of the NG2 proteoglycan inhibit neurite growth and induce growth cone collapse. J Neurosci 23:175-186.

von Meyenburg J, Brosamle C, Metz GA, Schwab ME (1998) Regeneration and sprouting of chronically injured corticospinal tract fibers in adult rats promoted by NT-3 and the mAb IN-1, which neutralizes myelin-associated neurite growth inhibitors. Exp Neurol 154:583-594.

Waller A (1850) Experiments on the section of glossopharyngeal and hypoglossal nerves of the frog and observations of the alternatives produced thereby in the structure of their primitive fibres. Phil Trans R Soc Lond 140:423.

Watanabe N, Kato T, Fujita A, Ishizaki T, Narumiya S (1999) Cooperation between mDia1 and ROCK in Rho-induced actin reorganization. Nat Cell Biol 1:136-143.

Watanabe N, Madaule P, Reid T, Ishizaki T, Watanabe G, Kakizuka A, Saito Y, Nakao K, Jockusch BM, Narumiya S (1997) p140mDia, a mammalian homolog of Drosophila diaphanous, is a target protein for Rho small GTPase and is a ligand for profilin. EMBO J 16:3044-3056.

Weston CA, Anova L, Rialas C, Prives JM, Weeks BS (2000) Laminin-1 activates Cdc42 in the mechanism of laminin-1-mediated neurite outgrowth. Exp Cell Res 260:374-378.

Yamagishi S, Fujitani M, Hata K, Kitajo K, Mimura F, Abe H, Yamashita T (2005) Wallerian degeneration involves RHO/RHO-kinase signaling. J Biol Chem.

Yamashita T, Fujitani M, Yamagishi S, Hata K, Mimura F (2005) Multiple signals regulate axon regeneration through the nogo receptor complex. Mol Neurobiol 32:105-111.

Yamashita T, Higuchi H, Tohyama M (2002) The p75 receptor transduces the signal from myelin-associated glycoprotein to Rho. J Cell Biol 157:565-570.

Yao H, York RD, Misra-Press A, Carr DW, Stork PJ (1998) The cyclic adenosine monophosphate-dependent protein kinase (PKA) is required for the sustained activation of mitogen-activated kinases and gene expression by nerve growth factor. J Biol Chem 273:8240-8247.

Yoshikawa S, McKinnon RD, Kokel M, Thomas JB (2003) Wnt-mediated axon guidance via the Drosophila Derailed receptor. Nature 422:583-588.

Yu X, Bellamkonda RV (2001) Dorsal root ganglia neurite extension is inhibited by mechanical and chondroitin sulfate-rich interfaces. J Neurosci Res 66:303-310.

Yukimasa T, Yoshimura R, Tamagawa A, Uozumi T, Shinkai K, Ueda N, Tsuji S, Nakamura J (2006) High-frequency repetitive transcranial magnetic stimulation improves refractory depression by influencing catecholamine and brain-derived neurotrophic factors. Pharmacopsychiatry 39:52-59.

Zanardini R, Gazzoli A, Ventriglia M, Perez J, Bignotti S, Rossini PM, Gennarelli M, Bocchio-Chiavetto L (2006) Effect of repetitive transcranial magnetic stimulation on serum brain derived neurotrophic factor in drug resistant depressed patients. J Affect Disord 91:83-86.

Appendix

UBC

THE UNIVERSITY OF BRITISH COLUMBIA

Carmen Chan

has successfully completed the online training requirements of the Canadian Council on Animal Care (CCAC) / National Institutional Animal User Training (NIAUT) Program

_____
Chair, Animal Care Committee

_____
Veterinarian

Certificate #: 0421

Date Issued: July 22, 2005